EFFECTS OF ACADIAN KYANITE-ZONE METAMORPHISM ON RELICT GRANULITE-FACIES ASSEMBLAGES, MOUNT MINERAL FORMATION, PELHAM DOME, MASSACHUSETTS

BY MARGARET A. ROLL

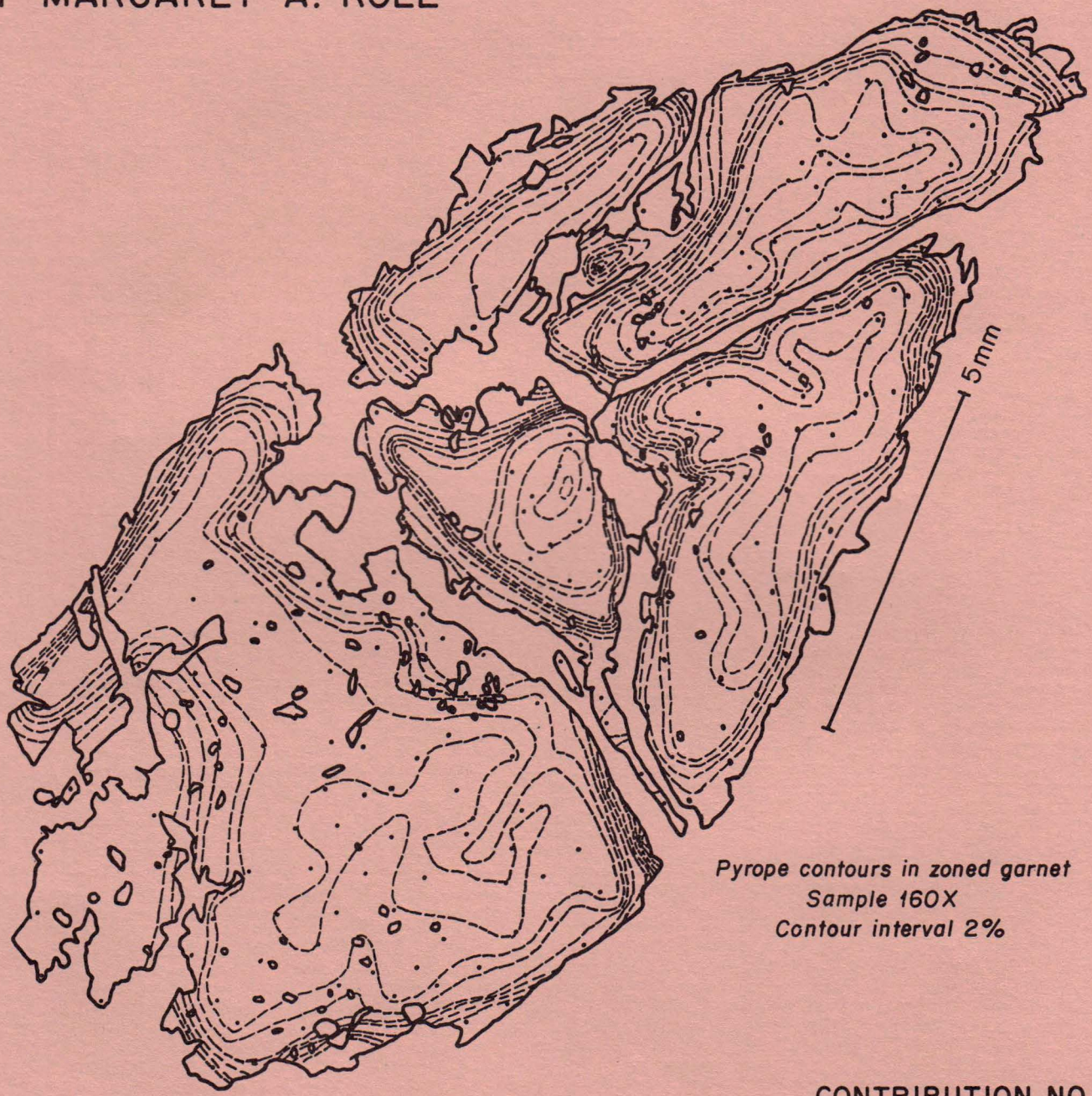

Pyrope contours in zoned garnet
Sample 160X
Contour interval 2%

CONTRIBUTION NO. 60
DEPARTMENT OF GEOLOGY & GEOGRAPHY
UNIVERSITY OF MASSACHUSETTS
AMHERST, MASSACHUSETTS

EFFECTS OF ACADIAN KYANITE-ZONE METAMORPHISM ON RELICT GRANULITE-FACIES ASSEMBLAGES, MT. MINERAL FORMATION, PELHAM DOME, MASSACHUSETTS

By

Margaret A. Roll

Contribution No. 60

Department of Geology and Geography

University of Massachusetts

Amherst, Massachusetts

May, 1987

TABLE OF CONTENTS

LIST OF TABLES

APPENDIX

ILLUSTRATIONS

Figure Page

APPENDIX

ABSTRACT

The late Precambrian Mt. Mineral Formation within the Pelham dome, contains pelitic layers with strongly sheared relics of an original assemblage of sillimanite, orthoclase, pyrope-rich garnet, biotite, and rutile in well foliated schist dominated by kyanite, muscovite, pyrope-poor garnet, biotite, and ilmenite, consistent with assemblages in nearby outcrops of metamorphosed Paleozoic strata.

Garnets from different locations have been chemically mapped by electron microprobe. Patterns of zoning in Fe, Mg, Mn, and Ca are consistent either 1) with extensive volume diffusion resulting from garnet-consuming hydration reactions taking place both during cooling from early high-grade metamorphism and during Acadian reheating or 2) with garnet-producing retrograde reactions following complete Acadian reconstitution. In garnets showing relict compositions, local patches in cores are $Alm_{61}Py_{35}Sp_{1}Gr_{3}$ with complete gradation to $Alm_{81}Py_{11}Sp_{4}Gr_{4}$ at the rim, a composition approximately the same as Acadian prograde garnets in nearby Paleozoic strata.

Localized areas of low activity of water were responsible for preserving the relict assemblages. In relict assemblages, the hydration reaction, GAR + KSP + H_2O = BIO + SILL + QTZ, was limited by low activity of water, and garnet and K-feldspar were not completely consumed. Muscovite probably became stable with increased activity of water during Acadian reheating. Muscovite was produced by the reaction KSP + Al-sil. + H_2O = MUSC + QTZ, GAR + KSP + H_2O = MUSC + BIO + QTZ, or both. Reconstituted assemblages experienced sufficient activity of water to largely destroy relict garnet, and new garnet probably grew by the reaction BIO + Al-sil. = GAR + MUSC.

Relict garnet megacrysts may contain cracks filled with green or brown biotite. Green biotites have very low Ti content, suggesting inhibited transport of Ti along cracks compared to other major constituents. Extreme variations in almandine-pyrope content along different garnet margins suggest tectonic disruption and reorientation late in the hydration that produced the gradients. In one location, a 3 mm oblong garnet grain containing Py_{36} is bounded by biotite, 0.5 mm from the garnet "core".

Paired analyses of garnet core and retrograde, matrix biotite yield false estimates of temperature as high as 1000°C (Thompson, 1976). Estimates based on ion-exchanged biotite inclusions paired with a garnet core yields an estimated temperature of 630°C, giving minimum pressure of 7.3 kbar (Tracy and others, 1976), within the kyanite zone. Since the actual assemblage contains sillimanite, this estimate must be lower than the true peak temperature. When a higher temperature of 700°C is chosen, yielding a corresponding pressure of 6.8 kbar, back-calculation gives the approximate "original" biotite composition. Pairs consisting of garnet rim and reconstituted biotite give approximately 580°C for the peak of Acadian reheating.

INTRODUCTION

Location

The Mount Mineral Formation crops out in the southern part of the Pelham dome, west-central Massachusetts (Figure 1), within the Millers Falls, Shutesbury, and Belchertown 7.5-minute quadrangles. The outcrop area is included within the townships of Wendell, Shutesbury, Pelham, and Belchertown. The outcrop pattern is an irregular U-shape approximately 30 km in length and 8 km in width, reflecting the shape of the southern part of the Pelham dome. The exposed width of the Mt. Mineral Formation forming this "U" ranges from 60 to 600 meters.

Regional and Local Setting

The Pelham dome is one of a series of north or northeast trending domes within the Bronson Hill anticlinorium in central New England. These domes were formed during late stages of Acadian deformation following the formation of regional nappes (Thompson and others, 1968). The inner part of the Pelham dome contains 600 my. old gneisses and related rocks (Zartman and others, 1984) with an inner mantle of plagioclase gneisses of uncertain age (OZ?) and an outer mantle of metamorphosed Ordovician, Silurian, and Devonian sedimentary and volcanic rocks (Robinson and others, 1975). All of the rocks of the Pelham dome are within the kyanite zone of Acadian regional metamorphism (Zen and others, 1983).

The Pelham dome is unique among the gneiss domes of the Bronson Hill anticlinorium in Massachusetts in that it is the only dome containing abundant rocks of obviously sedimentary derivation in its interior (Thompson and others, 1968). Emerson (1898, 1917) and Balk (1956) were the first to note that the granitic rocks of the Pelham dome differ from those of other Bronson Hill domes, being less massive and more in sheet-like masses relative to the latter. The actual sequence of stratified units below the Middle Ordovician cover rocks (Figure 2) was first worked out by Ashenden (1973) and subsequently extended by Onasch (1973), Laird (1974), Robinson and others (1975), and Zen and others (1983).

The Mount Mineral Formation is underlain by the Precambrian Dry Hill Gneiss (Zen and others, 1983), a massive, well foliated, light-gray to pink, two-feldspar biotite ± hornblende gneiss (Ashenden, 1973). Overlying the Mt. Mineral Formation is the Fourmile Gneiss of uncertain age, a yellow- to gray-weathering biotite-feldspar±hornblende gneiss with local amphibolite and quartzite beds (Ashenden, 1973; Laird, 1974). The exact nature of the contacts between these units and the Mt. Mineral Formation have not been clearly determined. The Middle Ordovician Ammonoosuc Volcanics and Partridge Formation are thought by Robinson (1979) to overlie the Fourmile Gneiss unconformably.

The Poplar Mountain Gneiss, a biotite gneiss containing white microcline megacrysts and beds of quartzite, crops out in the northern part of the dome (Zen and others, 1983). Locally this has a basal quartzite member, commonly containing biotite and actinolite or

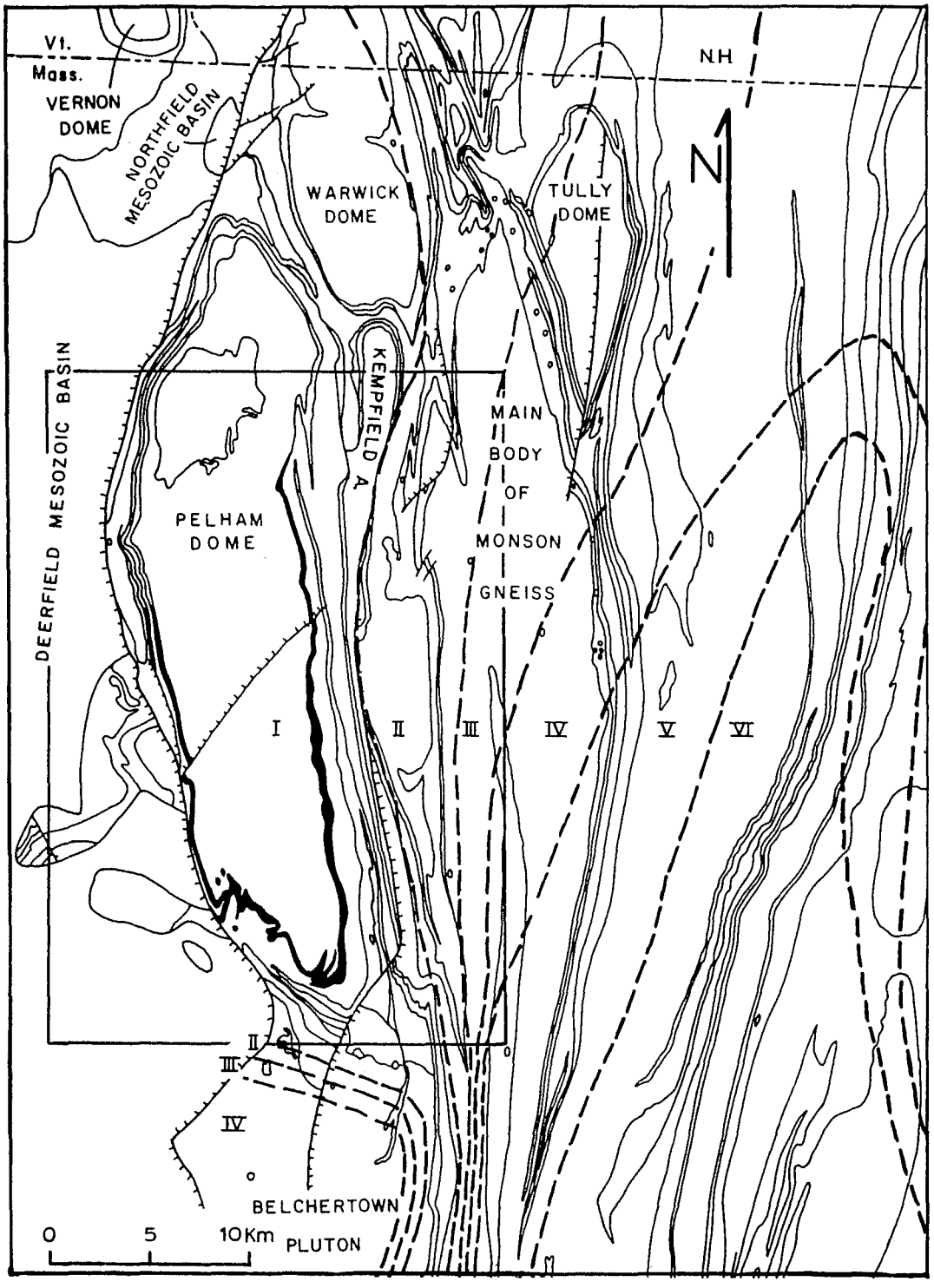

Figure 1. Location of Mt. Mineral Formation (black). Dashed lines are boundaries of Acadian metamorphic zones: I) Ky-Staur Zone; II) Sill-Staur-Musc Zone; III) Sill-Musc Zone; IV) Sill-Musc-Ksp Zone; V) Sill-Ksp Zone; VI) Sill-Ksp-Gar-Cord Zone. Area of Figure 3 shown in rectangle. (After Zen and others, 1983)

Figure 2. Pre-Middle Ordovician Rocks of the Pelham Dome.

Fourmile Gneiss(Ordovician, Cambrian, or Proterozoic Z)

OZfm	Layered to massive biotite-feldspar gneiss and amphibolite
OZfmu	Ultramafic hornblendite
OZfmg	Muscovite quartzite

Poplar Mountain Gneiss(Proterozoic Z)--(Probably correlates with Mt. Mineral Formation but is more feldspathic)

Zpm	Dark biotite gneiss containing white microcline megacrysts and beds of quartzite
Zpmg	Biotite gneiss where mapped separately
Zpmq	Basal quartzite, where thick enough to map; commonly feldspathic, containing biotite and actinolite or muscovite

Mt. Mineral Formation(Proterozoic Z)--(Probably correlates with Poplar Mtn. Gneiss but is more aluminous)

Zmm	Aluminous schist, amphibolite, and quartzite, undifferentiated; locally rich in garnet and kyanite, and with relict sillimanite and orthoclase from pre-Middle Ordovician metamorphism
Zmmu	Lenses of partially serpentinized harzburgite containing abundant veins of anthophyllite

Dry Hill Gneiss(Proterozoic Z)

Zdh	Pink microcline-biotite and microcline-hornblende gneiss containing pink microcline megacrysts and minor quartzite
Zdhs	Biotite-tourmaline schist and quartzite
Zdpq	Pelham Quartzite Member. White to buff quartzite and feldspathic quartzite commonly with biotite and/or actinolite

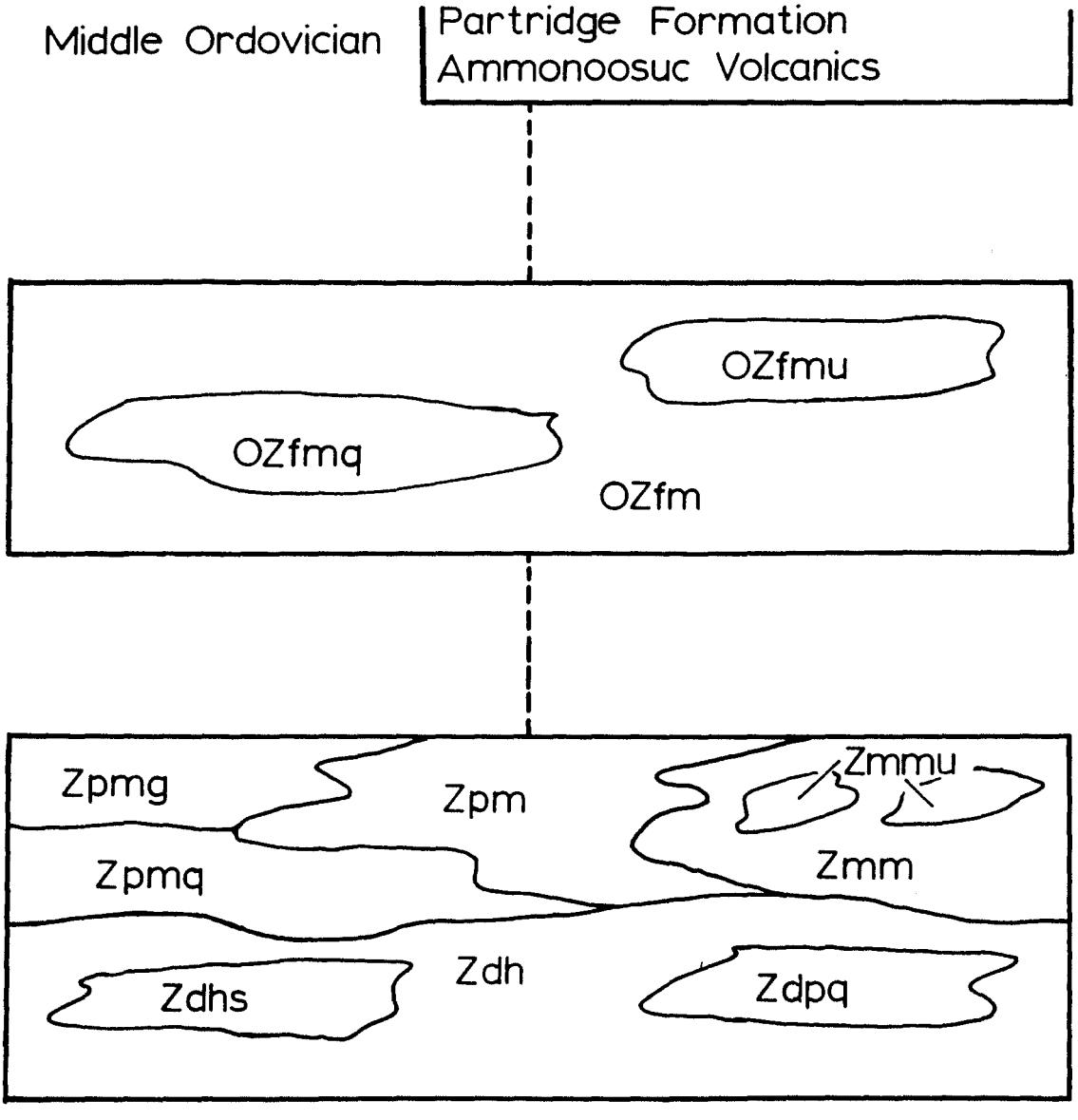
Middle Ordovician
Partridge Formation
Ammonoosuc Volcanics
OZfmu
OZfmq
OZfm
Zpmg
Zpm
Zmmu
Zpmq
Zmm
Zdh
Zdhs
Zdpq

muscovite. The Poplar Mountain Gneiss is thought to be a more feldspathic facies of the Mt. Mineral Formation (Zen and others, 1983).

The Mt. Mineral Formation has been subdivided into several rock units (Robinson, and others, 1973). The dominant rock is mica-garnet schist that may or may not contain aluminosilicate, potassium feldspar, plagioclase, staurolite, tourmaline, rutile, ilmenite, and graphite. The texture of the schist ranges from well foliated to strongly sheared. Other rock units include an actinolite or muscovite quartzite with calc-silicate interbeds, recognized locally as a basal member, and amphibolite, an important rock type in the lower part of the formation (Robinson and others, 1973). Pods of hornblendite and harzburgite within the formation crop out in a few areas (Tracy and others, 1984). A mica-garnet quartzite has been recognized locally as the uppermost member of the formation.

Large potassium feldspar megacrysts are common in the Mt. Mineral Formation and also occur in the Dry Hill Gneiss and the Poplar Mountain Gneiss. Their association with sillimanite in the Mt. Mineral Formation suggests that these rocks have experienced metamorphism at a much higher grade than the Acadian kyanite zone. The potassium feldspar megacrysts and the sillimanite-orthoclase assemblage is not found in the Fourmile Gneiss or in the overlying rocks of Middle Ordovician age. For this reason, it is believed that this high grade metamorphism probably took place before the Middle Ordovician and possibly before deposition of the Fourmile Gneiss.

Major deformation took place to the west of the study area during the Middle-Ordovician Taconic orogeny. Evidence for Taconian deformation and metamorphism have not been observed in nearby Middle-Ordovician cover rocks. The Precambrian gneiss es of the Pelham dome are believed to have been structurally high during this deformation and therefore probably were <u>not</u> under metamorphic conditions during the Middle Ordovician (Stanley and Ratcliffe, 1985; Zen and others, 1983).

All of the rocks of the Pelham dome are within the kyanite zone of Acadian metamorphism. The apparent thermal history of the Mt. Mineral Formation, then, is metamorphism to sillimanite-orthoclase conditions, followed by cooling to below metamorphic conditions, followed by reheating during Devonian Acadian metamorphism to the kyanite zone.

The pelitic rocks of the Mt. Mineral Formation exhibit a wide variety of mineral assemblages and textures. Some of the rocks contain high-grade mineral assemblages and are mylonitic in texture whereas others contain typical Acadian kyanite-zone (Zone I) assemblages and exhibit recrystallized, foliated textures. These rocks probably experienced similar conditions of pressure and temperature through time, and therefore some other factor must be responsible for the petrologic variation within the rocks.

Previous Work

More recent structural and reconnaissance studies of the northern

portions of the Pelham dome began in the late 1960's (Ashenden, 1973; Onasch, 1973; Laird, 1974). The central and southern portions of the dome have been mapped by Advanced Geologic Mapping classes at the University of Massachusetts, Amherst under Peter Robinson and Donald Wise during the 1970's. Michener (1983) studied the bedrock geology of the Pelham-Shutesbury syncline along the eastern flank of the Pelham dome. Hodgkins (1985) has investigated some geochemical aspects of various gneissic units in the north part of the dome.

Robinson and others (1975) reported the occurrence of pelitic schist within the Mt. Mineral Formation, locally containing relics of an original assemblage of coarsely crystalline sillimanite, high orthoclase, pyrope-rich garnet, and rutile. In other areas, the schist is dominated by pyrope-poorer garnet, kyanite, muscovite, brown biotite, ilmenite, and graphite, with or without staurolite and tourmaline, consistent with assemblages of Acadian kyanite-zone metamorphism in the region.

Potassium feldspar from this locality, analysed by X-ray diffraction techniques, shows high orthoclase structure state (Laird, 1974; Tracy, 1975). Laird (1974) presented X-ray diffraction analyses of nine potassium feldspar samples from the Dry Hill Gneiss and the Poplar Mountain Gneiss, all showing maximum microcline structure state.

Robinson and others (1975, 1982) discussed one sample of garnet from the Mt. Mineral Formation which is rich in pyrope at the core and steeply zoned to a pyrope-poor, spessartine-almandine-enriched rim. Spessartine-enriched rims were attributed to a continuous retrograde hydration reaction (Robinson and others, 1982). Garnet zoning in this sample was not directly influenced by bounding mineral phases, suggesting that a water-rich intergranular fluid was present during the hydration reaction.

Purpose

The purpose of this study is to: 1) provide petrographic descriptions of selected samples of pelitic schists from the Mount Mineral Formation; 2) examine variations in essential mineral chemistry within these samples; and 3) determine some constraints on the metamorphic evolution of the unit based on phase equilibria, and suggest possible pressure-temperature-aH_2O paths of metamorphism.

Methods

Field work was carried out from September, 1984 to November, 1985. Pelitic samples containing sillimanite and/or kyanite were collected from 13 localities in Shutesbury, Pelham, and Belchertown for hand specimen and thin section study (Figure 3). Collection localities were selected from field data of Robinson (personal communication, 1984). Thin sections were made and polished at the University of Massachusetts. Thirty-three polished thin sections were studied using transmitted and reflected light microscope techniques. Selected samples were studied using X-ray powder diffraction and electron microprobe techniques.

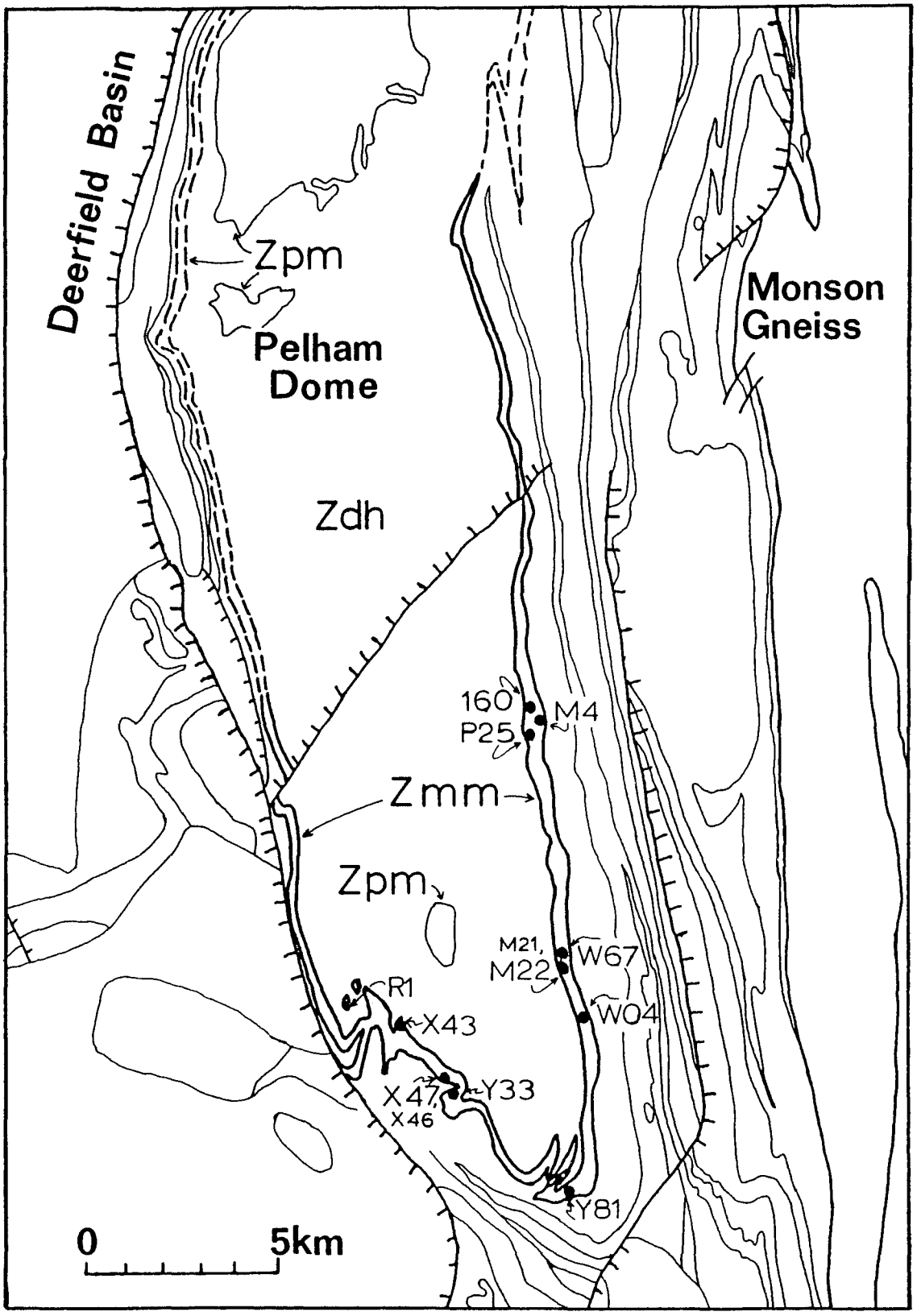

Figure 3. Sample collection localities within Mt. Mineral Fm. (Zmm). Also shown are Poplar Mountain Gneiss (Zpm) and Dry Hill Gneiss(Zdh).

The electron microprobe was used to determine the mineral chemistry of garnet, biotite, staurolite, muscovite, feldspar, tourmaline, aluminosilicate, rutile, and ilmenite. Based on freshness of sample, mineral assemblage, and texture, seven thin sections were chosen for electron microprobe study. Mineral texture maps showing grain size and shape, inclusions, microfractures, and bounding minerals were used to locate microprobe spot analyses. Maps were made by projecting the thin section with a microfiche viewer and tracing the texture of the area onto paper. These maps were then used to illustrate the pattern of garnet composition isopleths for each analysed sample.

The three-spectrometer, wavelength dispersive ETEC Autoprobe at the University of Massachusetts, Amherst was used to analyse five of the samples. Standard operating parameters included: a beam current of 0.02 microamperes, an accelerating potential of 15,000 volts, and a chamber vacuum of about $1x10^{-5}$ Torr. The electron beam diameter was about 2 micrometers for oxides and garnets and approximately 10 micrometers for all other minerals. Countin g time for all elements and backgrounds was 15 seconds. Raw count rates were corrected using the procedures of Bence and Albee (1968) and using the alpha correction factors of Albee and Ray (1970).

Three samples were analysed using the Yale University CAMECA MS-64 microprobe using a Tracor Northern TN-2000 energy-dispersion analyzer. Counting time for all standards and analyses was 200 seconds. Accelerating potential was 15,000 volts and sample current was 5 nanoamperes measured on brass. Raw concentration data were corrected using the method of Bence and Albee (1968) with the alpha factors of Albee and Ray (1970).

Composition and structure state of many potassium feldspars may be estimated by using the three peak method of Wright (1968). Feldspars with anomalous cell dimensions may be identified by this method and "apparent" structure state may be estimated. Therefore, thirteen samples of potassium feldspar were chosen from a variety of sheared pelitic samples for X-ray powder diffraction analysis at the University of Massachusetts to determine structure state. Pure silicon powder was used as an internal standard. Charts were run at 1/2 degree per minute from 56 degrees to 13 degrees two theta.

Acknowledgements

This study is submitted in partial fulfillment of the requirements for the degree of Master of Science in Geology, University of Massachusetts, Amherst. I would like to thank Peter Robinson, chairman of the Thesis Committee, whose enthusiasm, k nowledge, and thoughtful advice made invaluable contributions to this work. Jack Cheney and Steve Haggerty provided careful review and critical commentary during the final stages of writing. Steve Field contributed patient instruction and guidance from thin section polishing to electron microprobe analysis to reflected light microscopy, which is greatly appreciated. Peter Crowley assisted greatly in computer modelling of garnet diffusion. Robert Tracy assisted with microprobe analyses at Yale University. John Roll, Suzanne McEnroe, and Angela Hyjek assisted

in field work. John Roll assisted in preparation and coloring of illustrations. These contributions as well as the prayers and support of family and friends have been greatly appreciated.

Summer field and laboratory work, preparation of thin sections, electron microprobe analyses, X-ray diffraction analyses, preparation of illustrations, and publication of results were supported by NSF Grants EAR 84-10370 and EAR 86-08762 (to Robinson).

DESCRIPTION OF ROCK TYPES

For the purposes of description and discussion, the thirty-three thin sections have been grouped according to observed rock texture and bulk composition. The four groups are: 1) strongly sheared pelitic schist; 2) reconstituted pelitic schist; 3) sheared pegmatite; and 4) sheared quartzite. Attention is given to the pelitic units, where striking differences in texture, mineral assemblage, and mineral chemistry are apparent between groups (1) and (2). These differences will be discussed petrographically and chemically and finally will be used to suggest some constraints on the metamorphic evolution of the Mt. Mineral Formation. The following section contains modes and descriptions of mineral texture and summaries of petrographic evidence for mineral reactions.

Strongly Sheared Pelitic Schist

In hand sample, these rocks are highly sheared and commonly have classic mylonitic fabrics. Megacrysts of garnet and potassium feldspar are common in the relatively fine-grained schist matrix. The matrix foliation, defined by biotite, ribbon-quartz, granulated feldspar, and sillimanite, when present, commonly gives the rock a laminated appearance (Figure 4). These rocks are typically slabby and break easily along the mylonitic foliation. Several samples have a weakly developed mica foliation, crosscutting the mylonitic foliation.

Twenty-three thin sections of the strongly sheared pelitic schist from eight different localities have been studied (Table 1). Each thin section contains variable amounts of quartz, plagioclase, biotite, garnet, and rutile and may contain variable amounts of potassium feldspar, muscovite, aluminosilicate, ilmenite, graphite, sulfide, zircon, or chlorite.

Mineral occurrence and texture. Quartz varies in both grain size and shape, and varies in abundance from 22 to 70 modal percent. Several samples contain polycrystalline ribbons of quartz, subparallel to foliation, which transect the entire thin section. Single grains within these ribbons are elongate in shape, and are up to 4-5 mm in length. Equant grains of quartz are common throughout the matrix and range in diameter from 0.5 to 3 mm. Undulatory extinction is common. Several samples contain areas of fine-grained quartz with average grain size of less than 0.25 mm. Quartz also forms symplectites with muscovite and plagioclase, probably as a replacement of sodium-bearing K-feldspar, or occurs as inclusions in garnet or kyanite.

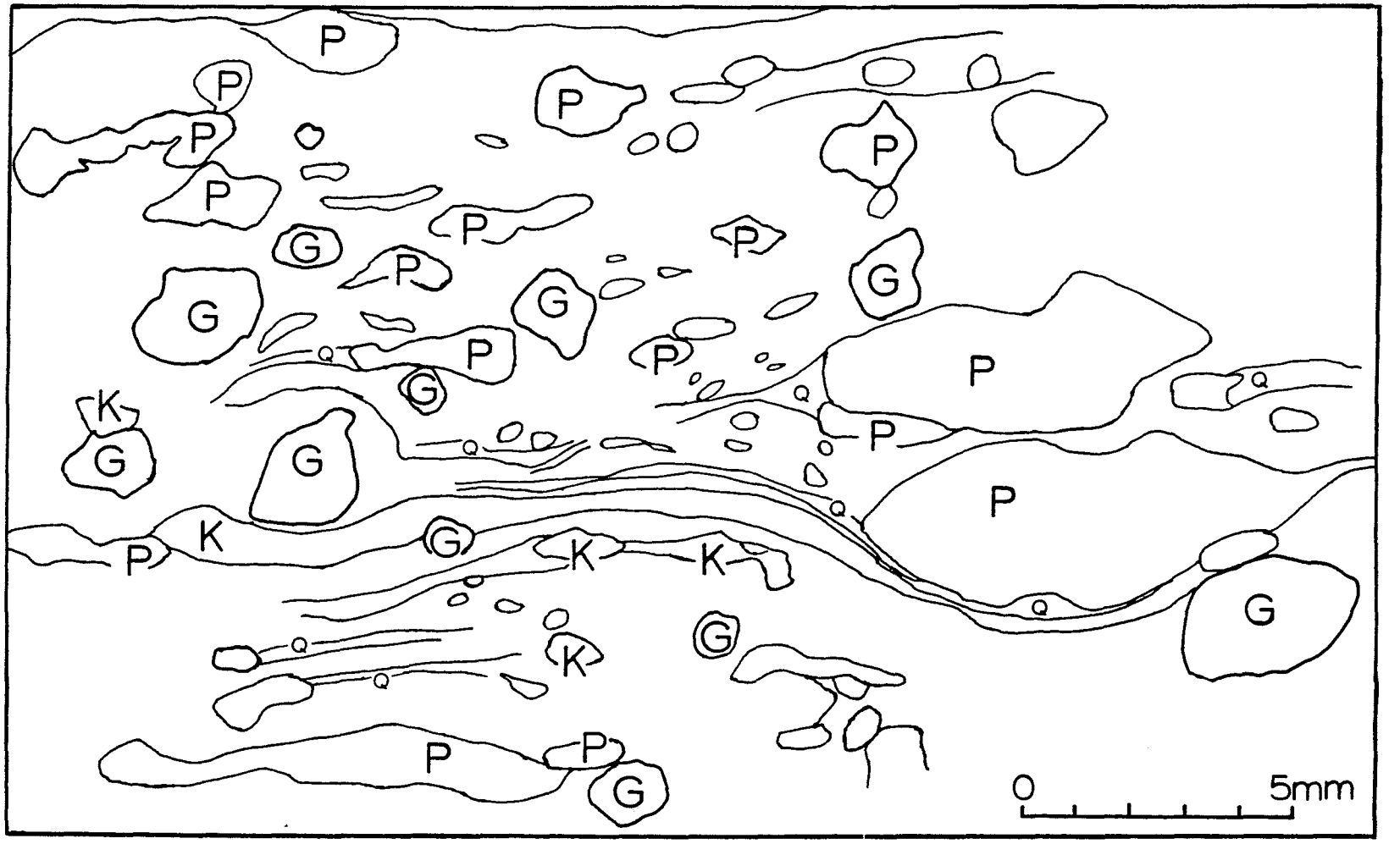

Figure 4. Sketch of texture of sheared pelitic schist in hand sample W67. Megacrysts are garnet (G), plagioclase and plagioclase plus quartz (P), potassium feldspar (K), and quartz (Q). Matrix minerals are fine-grained quartz, biotite, kyanite, feldspar, and muscovite.

Table 1. Estimated modes of twenty-three samples of strongly-sheared pelitic schist. Many, if not all, of these samples were originally sulfide-bearing sillimanite-garnet-biotite-potassium feldspar schists. UM indicates microprobe analyses done at the University of Massachusetts; YU indicates microprobe analyses done at Yale University. Where no modal sillimanite is given, # or + indicates presence only as inclusions.

X = present in trace amounts.
# = included in garnet. * indicates kyanite rimmed by
+ = included in K-feldspar. fine-grained muscovite

Sect #	160W	UM 160X	160X	160Y	160Z	X46	X47	M22V	M22W	M22X	M22Y	M22Z	Y81A	Y81C
Quartz	40	35	22	40	25	40	40	50	55	50	51	50	45	50
Ksp		X		X	X	1		8	8	30	6	6	12	
Plag	3	8	5	7	12	6	10	4	X	3	3	7	5	6
Musc	25	X	6	3	20	30	35		X	5	14	2	1	1
Bio	7	12	12	10	8	8	9	8	7	2	8	7	12	11
Gar	15	30	45	30	25	10	6	12	7	2	8	10	10	16
Sill	10 #	15 #	10 #	10 #	10 #		#	4 #	15 #	X #	#	3	X +#	#
Ky						*5		15	8	8	10	15	15	16
Rut	X	X	X	X	X	X	X	X	X	X	X	X	X	X
Ilm	X	X	X	X	X	X	X	X	X	X	X	X	X	X
Graph	X	X	X	X	X			X	X	X	X	X	X	
Sulf			X			X		X	X	X	X	X	X	X
Zirc	X	X	X	X		X			X				X	X
Chl						X	X	X		X				

Table 1, continued.

Sect #	Y81E	W67A	UM W67B	W67C	R1A	R1B	P25K	YU X43A	X43B
Quartz	50	41	41	40	60	70	60	50	60
Ksp	30	17	10	13	12	2	11		1
Plag	5	5	5	4	5	10	5	10	20
Musc	1	5	2	6	12	11	1	X	X
Bio	6	12	15	16	5	5	3	11	5
Gar	3	5	11	6	6	2	5	20	8
Sill		+	1	#			#	1 #	1 #
Ky	5	*15	*15	*15			15	8	5
Rut	X	X	X	X	X	X	X	X	X
Ilm					X	X	X	X	X
Graph							X		
Sulf		X				X		X	X
Zirc		X	X	X	X				
Chl								X	X

Plagioclase occurs in at least trace amounts in all of the strongly sheared pelitic rocks and ranges up to 20 modal percent in some. The grains are generally equant and anhedral and the average size is 1-2 mm, although some grains are 6 mm long. Plagioclase commonly forms polycrystalline ribbons parallel to foliation. Albite twinning is common and grains may show slight zoning. Undulatory extinction is common, especially in the larger grains. Plagioclase commonly contains minor sericite along rims and cracks and may be associated with quartz and muscovite as a rim or symplectite around potassium feldspar. Plagioclase has been observed as irregular exsolution lamellae within porphyroblasts of potassium feldspar and may have fully replaced some of these.

Megacrysts of potassium feldspar, 4-6 cm in diameter, are characteristic of the sheared pelitic schist. Potassic feldspar occurs in samples from all but one of the eight sheared-schist localities, ranging in abundance from trace amounts to 30 modal percent. In hand specimen, the K-feldspar has two well developed cleavages, is milky-white to bluish in color and is commonly translucent. One sample contains an 8 x 12 cm K-feldspar megacryst, probably within a thin pegmatite unit at this locality. Graphite may be more abundant adjacent to grains of K-feldspar.

In thin section, potassium feldspar occurs as large colorless porphyroclasts, commonly irregular in shape. The K-feldspar commonly has undulatory extinction, grid twinning, and low birefringence. The larger grains are commonly highly strained and have irregular extinction. The potassium feldspars are optically negative with 2V ranging from 40 to 70 degrees and have dispersion of r greater than v. Some samples contain exsolved albite lamellae which are tenths of a millimeter thick.

Much smaller, equant grains of potassium feldspar also occur in several samples. These are 2-3 mm in size and commonly show undulatory extinction and more rarely, grid or irregular twinning. They occur in close proximity to larger feldspar grains or as polycrystalline ribbons parallel to foliation and probably represent granulated porphyroclasts of what once were larger porphyroblasts of K-feldspar.

Potassium feldspar grains may contain inclusions of biotite or prismatic sillimanite, up to 0.4 mm long, though commonly they are inclusion-free. In several samples, K-feldspar contains crystallographically oriented rutile needles. The larger potassium feldspar grains are commonly largely surrounded by rims of small grains or a symplectite of muscovite and quartz or muscovite, quartz, and plagioclase.

Sample W67A contains a 1-2 mm diameter anhedral grain that is optically zoned at the rim under crossed-polarized light and is surrounded by a rim of polycrystalline quartz. This may be due to the diffusion of potassium into the matrix leaving sodium-richer feldspar at the rim. These rims were not chemically analysed and interpretation based on texture is purely speculative.

Several of the strongly sheared pelitic rocks contain little or no muscovite. Where muscovite is present in greater than trace amounts, it has variable habit. In several samples, muscovite occurs as fine-grained rims on partially resorbed kyanite grains. Grain size of muscovite in these rims is less than 0.5 mm. Rims on kyanite vary from barely discernable to (almost) complete replacement of kyanite by muscovite. Slightly larger muscovite grains, 1-3 mm in size, are also associated with resorbed kyanite, but they do not form a well defined rim.

Muscovite is also closely associated with potassium feldspar in the form of a symplectite rim together with plagioclase and quartz around the K-feldspar. Muscovite may be present as small subhedral grains, 1-3 mm in size, in close proximity to partially resorbed potassium feldspar and abundant quartz.

In one sample, fine-grained muscovite makes up about 25 % of the rock and forms rims on garnet, kyanite, and potassium feldspar. The muscovite here is intergrown with ilmenite and is in close proximity to biotite (Figure 5).

These textures suggest that muscovite was not a stable phase during the early sillimanite-orthoclase metamorphism. Muscovite appears to have become stable locally at the expense of K-feldspar, alumino-silicate, and/or garnet at some later time.

Biotite in these sheared pelitic rocks is black in hand sample. Biotite is present in all of these rocks, ranging from 2 to 16 percent. In a few samples it forms concentrated rims, together with sillimanite, quartz , and rutile, around garnet megacrysts. In others, biotite may be adjacent to garnet megacrysts together with other matrix minerals, with no evidence of concentration or rimming relationships.

In thin section, both inclusion and matrix biotite is typically red-brown to orange-brown in the Z ≅ Y direction and tan in the X direction. Biotite is anhedral in shape and average grain length is 1-2 mm. Trace amounts of green biotite occur in several samples at garnet edges or occupying cracks within garnets. Brown biotite is commonly included in garnet, potassium feldspar, kyanite, and more rarely, plagioclase. Zircon is commonly observed as inclusions, with pleochroic halos, in biotite. Brown biotite also contains inclusions of rutile or ilmenite.

Several samples appear to have a second generation of brown biotite, oriented at an angle to the dominant foliation. These biotites are commonly proximal to kyanite.

Garnet ranges from less than 2-3 mm to 6 cm in length as oblong porphyroclasts or irregular shapes. The hand specimen color of garnet throughout these rocks is typically a translucent violet-red. Garnet is present in all of these rocks and ranges from 2 to 45 modal percent in various thin sections. Euhedral grains or pieces of grains are rare but may occur in the strongly sheared rocks. In a few samples, cracks in garnet interiors are filled with green biotite. Pressure shadows around

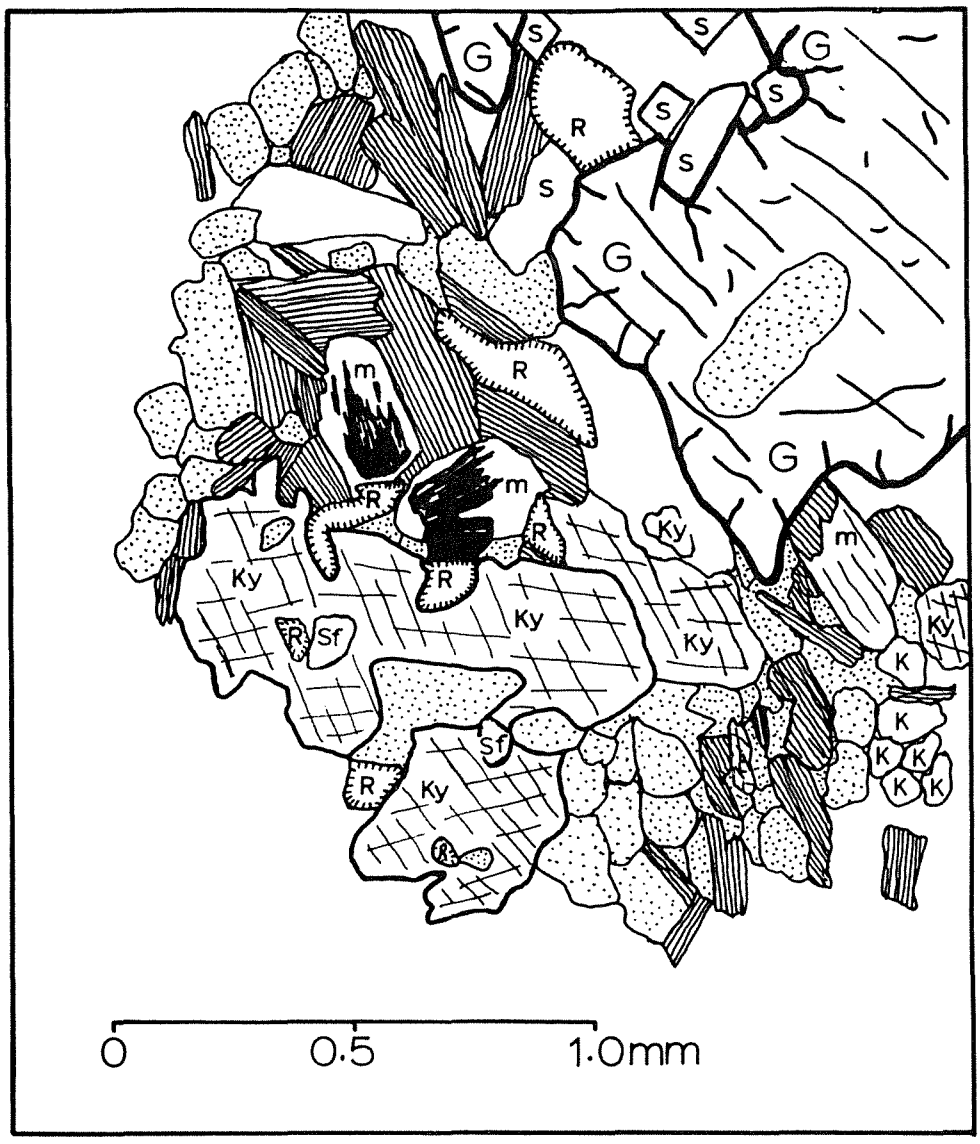

Figure 5. Sketch of muscovite-ilmenite intergrowth in sheared pelitic schist sample P25K. Minerals are muscovite (m), ilmenite (black), rutile (R), biotite (ruled), kyanite (Ky), quartz (stippled), garnet (G), sillimanite (S), K-feldspar (K), and sulfide (Sf). Sulfide is marcasite rimmed by goethite.

garnet, where present, may contain biotite, quartz, kyanite, or muscovite.

In some samples, large oblong garnet megacrysts, 1-4 cm long, are immediately surrounded by ribbon-quartz, elongate masses of brown biotite up to 2 mm thick, and locally sillimanite or kyanite (Figure 6). This texture suggests that garnet has been consumed at the rims to produce biotite and sillimanite or biotite and kyanite. Garnets in these pods commonly contain cracks, with pieces of garnet separated from one another by brown biotite masses. In other samples, there is virtually no concentration of biotite near garnet grains. Garnet from 160W is locally rimmed by fine-grained muscovite (Figure 7).

Garnet commonly contains one or more sets of subparallel fractures. The orientation of the fractures is subparallel in all garnet grains throughout a given hand sample. These were probably produced during late-stage brittle deformation. Grains containing more than one set of fractures suggest that the sample experienced at least two different stress orientations under brittle deformation of garnet. These fractures may have formed during shearing if garnet behaved brittlely, however chemical evidence discussed below suggests that these fractures were not present while volume diffusion within garnet was progressing.

Inclusions of quartz, biotite, and crystallographically oriented needles of rutile are common in garnet cores. This suggests that biotite and quartz were stable matrix phases during garnet growth. The rutile probably exsolved from the garnet with decreasing temperature. There are generally more inclusions of quartz, biotite, and rutile in the cores than near the rims, but this transition is normally gradational.

Garnet from several localities contains inclusions of small needles of sillimanite in the outer margins of the garnet, normally at an angle to matrix foliation. Sillimanite must have been stable as a matrix phase during the later stages of garnet growth, before any garnet consuming hydration reactions were active.

Within the strongly sheared pelitic rocks, sillimanite occurs as a matrix phase with variable abundance, or only as inclusions in garnet or potassium feldspar, or may not be present. Where observable in hand sample, it is generally parallel to foliation.

Where sillimanite occurs as a matrix phase, it is prismatic in habit, and ranges in size from less than 0.5 mm to several cm in length. In end section, sillimanite may be up to 2 mm in width. Its abundance ranges from trace amounts up to 10 percent. At locality 160, polycrystalline ribbons of prismatic sillimanite up to 3-4 mm thick are concentrated with biotite around large garnet porphyroclasts (samples 160X,160Z). Several other samples contain only very small prismatic grains, easily overlooked under low magnification (samples X43A, X43A, W67B).

Sillimanite is commonly found as inclusions in garnet and more rarely as inclusions in potassium feldspar. The inclusions are

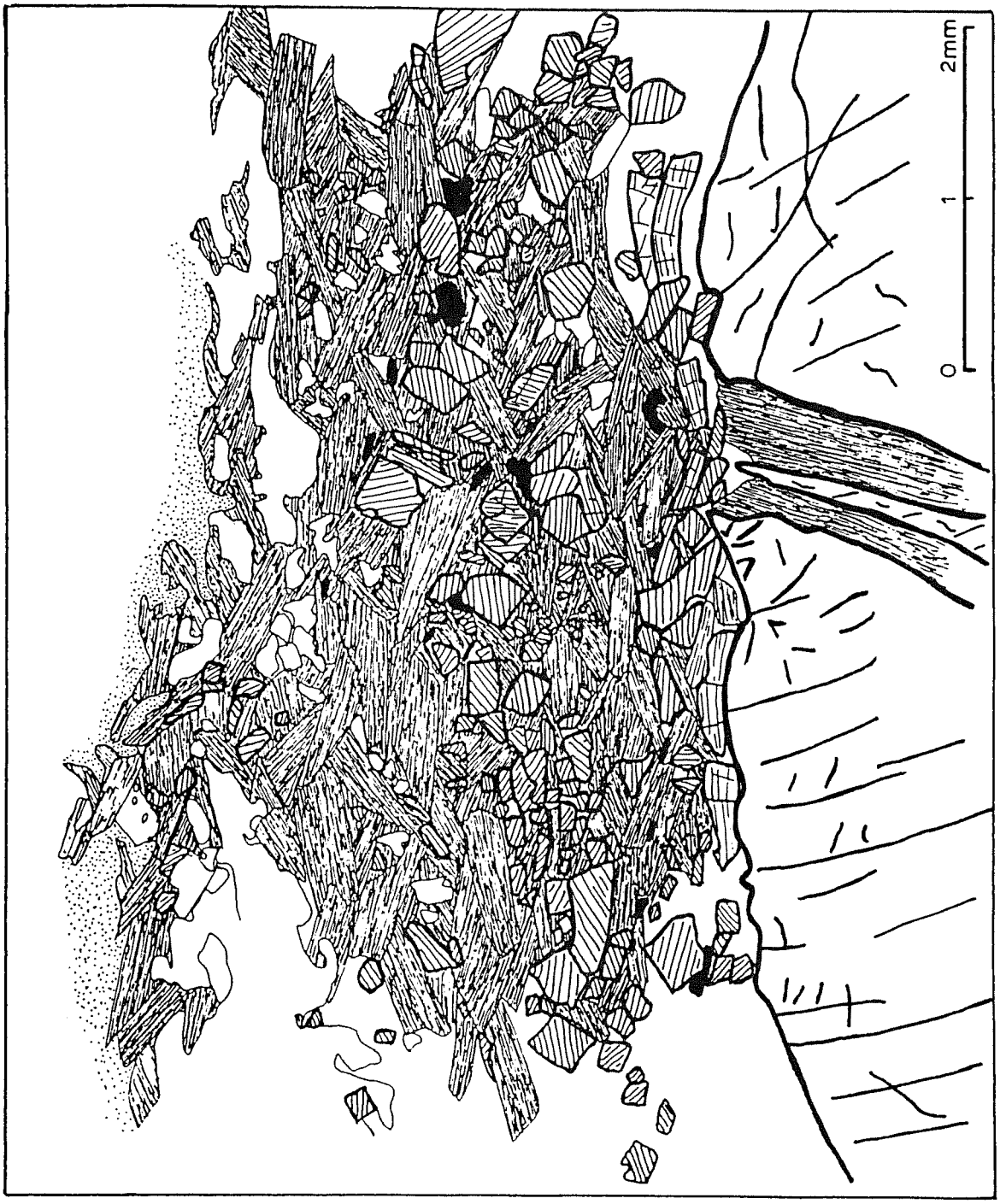

Figure 6. Sketch of biotite-sillimanite rim on garnet porphyroblast from sheared pelitic schist sample 160X. Minerals are garnet (high relief with fractured texture), sillimanite (moderate relief with coarse rule), biotite (low relief with fine rule), rutile (black), quartz (unpatterned), and muscovite-quartz-plagioclase symplectite (stippled).

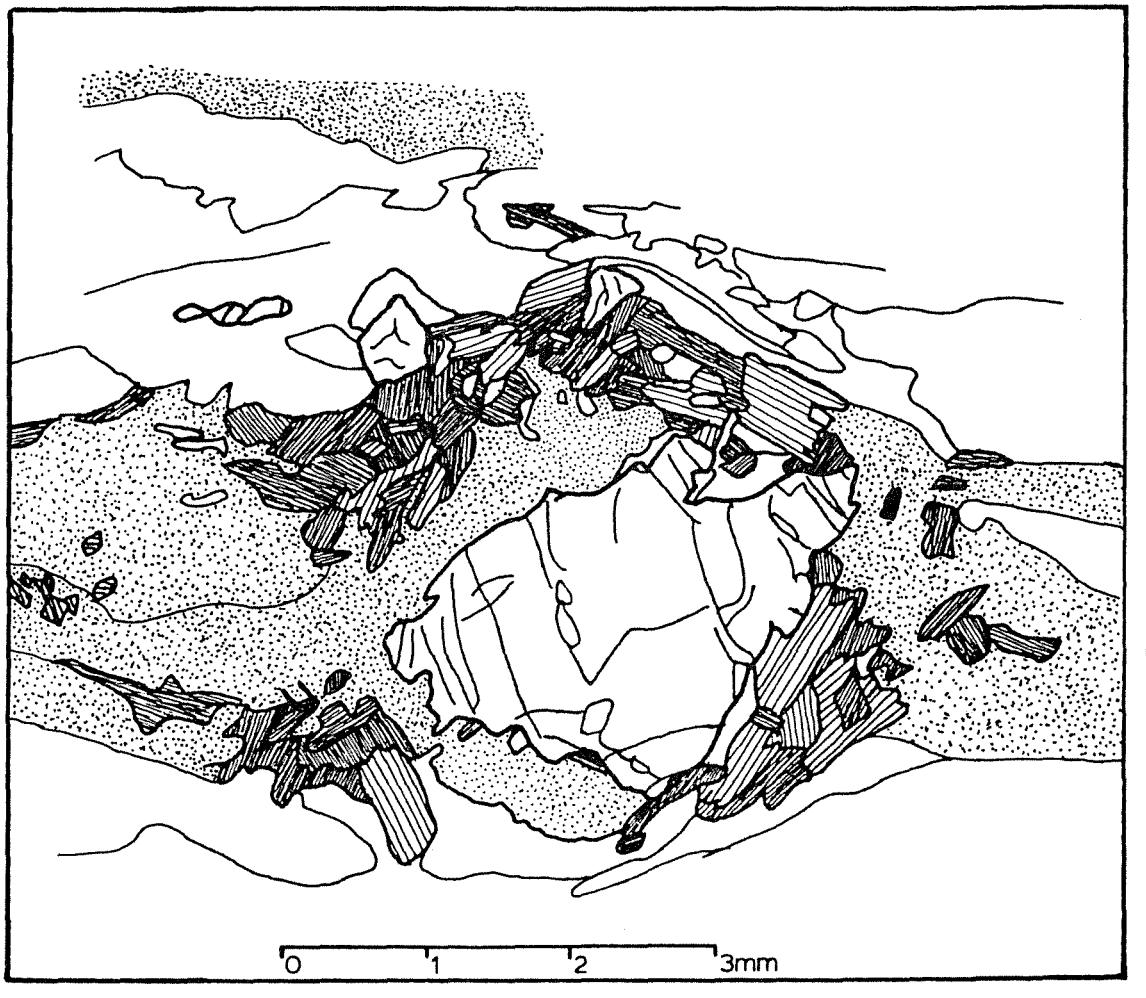

Figure 7. Sketch of partial muscovite rim on garnet from sample 160W of sheared pelitic schist. Minerals are garnet (high relief with fractured texture), fine-grained muscovite (stippled), coarse-grained muscovite (coarse ruled), biotite (fine ruled), and quartz (unpatterned).

typically fine needles, less than 1 mm long, though prismatic, equant grains less than 1 mm in diameter have been observed. Where sillimanite is included in garnet, it does not occur near the core. The needle-like sillimanite inclusions are commonly oriented subparallel to one another within the garnet, and are generally at an angle to the foliation in the matrix. The outer part of the garnet may have grown parallel to some pre-existing foliation when sillimanite was a stable matrix phase or may have been rotated after growth.

Comprising up to 16 modal percent of some of these rocks, kyanite is observable in hand specimen as 1-3 mm long, translucent-blue tablets with two cleavage directions. Pale blue kyanite is especially obvious on sawed surfaces. In thin section, kyanite commonly occurs as equant to elongate grains with well defined cleavage, parting, and common twinning. Kyanite is commonly bent adjacent to large garnet or feldspar megacrysts together with the matrix foliation producing undulatory extinc tion in the grains.

Kyanite from three localities is rimmed by fine-grained muscovite (Figure 8). Kyanite from these samples is embayed and resorbed, in a fashion generally proportional to the thickness of the surrounding muscovite rim. Where muscovite rims are absent, partially resorbed kyanite is commonly surrounded by abundant biotite and quartz. Kyanite may be intergrown with biotite adjacent to garnet grains, perhaps as a product of garnet consumption. Common mineral inclusions in kyanite are biotite, quartz, rutile, and ilmenite.

Kyanite and sillimanite occur together as matrix phases at several localities (M22, Y81, W67, X43). Where sillimanite is present in the rock, the kyanite is not rimmed by fine-grained muscovite. The kyanite and sillimanite may be immediately adjacent to one another or may be separated by quartz or biotite grains. Replacement textures between these two minerals have not been observed. One sample contains only one grain (less than 0.5 mm diameter) of sillimanite in a garnet pressure shadow, with kyanite throughout the remainder of the matrix.

Rutile has been observed in at least trace amounts in the matrix of all samples of strongly sheared pelitic schist. It is commonly slightly elongate and rounded in shape, ranging in length from less than 0.5 mm to 1 mm. Ilmenite may partially or completely rim rutile, although rutile also occurs independent of ilmenite in the matrix. Garnet or kyanite commonly contain inclusions of rutile. Crystallographically oriented needles of rutile are commonly present in garnet cores and less commonly in potassium feldspar. These needles probably exsolved from the host mineral during cooling.

Ilmenite is present in many of the strongly sheared pelitic rocks. It occurs as inclusions in garnet and/or kyanite and as a matrix phase. Where present, it has irregular shapes and is 1-2 mm long.

Graphite, where present, occurs as elongate, irregular plates up to 3 mm long. Graphite has not been observed as an included phase in any other mineral, although it may be intergrown with biotite.

Figure 8. Sketch of muscovite rims on kyanite from sample X46 of sheared pelitic schist. Minerals are garnet (high relief with fractured texture), biotite (fine ruled), fine-grained muscovite (stippled), coarse-grained muscovite (coarse ruled), kyanite (moderate relief with two cleavages), rutile (black), and quartz (unpatterned).

Chlorite occurs in trace amounts in 6 thin sections of sheared pelitic schist. It is associated with biotite and is pleochroic from colorless to light green. The chlorite has abnormal blue interference colors indicating a relatively iron-rich composition.

Zircon is present in trace amounts in all of the strongly sheared rocks. It may be present in the matrix or included in biotite. Grains are anhedral and generally less than 0.5 mm in size.

One or more of the sulfides, pyrite, pyrrhotite, and chalcopyrite, are present in trace amounts at each of the eight localities of strongly sheared pelitic rocks. They are commonly rimmed by goethite in the sheared matrix, due to weathering. Where included in kyanite, the goethite rim may be lacking. The sulfides are irregular in shape, equant to oblong, and are less than 1 mm in size. One sample contains a garnet grain with an inclusion of goethite-rimmed pyrrhotite approximately 0.5 mm in length.

Petrographic evidence for mineral reactions. Evidence for several reactions has been observed during petrographic study of these samples. The original assemblage stable during early sillimanite-orthoclase metamorphism probably contained garnet, sillimanite, orthoclase, biotite, rutile, quartz, plagioclase, and sulfide. Muscovite was probably not present in the early high-grade assemblage.

Embayed garnet and various garnet rim textures suggest that one or more garnet-consuming reactions have taken place. Garnet is commonly rimmed by biotite, quartz, and kyanite or sillimanite, suggesting that these minerals were produced as garnet was consumed. These textures suggest partial progress of the reaction,

$$GAR + KSP + H_2O = KY/SILL + BIO + QTZ, \qquad (1)$$

This reaction probably took place before muscovite was stable in the rocks. Since the garnet has not been fully consumed in these rocks, some factor must be responsible for limiting this reaction. Possible factors include limited time, unfavorable temperature-pressure conditions, or limited activity of one or more reactants.

Rims of quartz, plagioclase, and/or muscovite on K-feldspar suggest that the K-feldspar has been partially consumed in these rocks. Several samples also contain kyanite rimmed by fine-grained muscovite. One sample contains an embayed grain of sillimanite rimmed by muscovite and quartz. The hydration reaction,

$$KY/SILL + KSP + H_2O = MUSC + QTZ, \qquad (2)$$

appears to have been responsible for the formation of these textures. This reaction could not have occurred until muscovite was a stable phase in these rocks. In some samples, garnet is rimmed primarily by biotite and quartz, further suggesting that aluminosilicate has since been consumed.

The net reaction of these two hydration reactions is

$$GAR + 2\ KSP + 2\ H_2O = BIO + MUSC + 3\ QTZ. \qquad (3)$$

Garnet has been observed with rims of biotite and muscovite, although this is less common.

The kyanite-zone conditions experienced by these rocks during the Acadian metamorphism should have been favorable for these hydration reactions to have taken place. Garnet and K-feldspar are still present in most of these rocks, and would not have limited these reactions. Therefore, assuming that these rocks had enough time to react, the activity of water must have been the limiting factor preventing the completion of the above reactions.

The relationships between kyanite and sillimanite remain somewhat ambiguous. The writer believes that only sillimanite was present in the early high grade assemblage based on the following reasons. Sillimanite is included in both garnet and potassium feldspar and therefore must have been stable in the original assemblage. When kyanite is present in rocks showing minimal hydration, it seems to be largely associated with garnet rims. This suggests that kyanite grew at the expense of minerals stable during the early garnet-sillimanite-orthoclase equilibrium.

However, there may have been two generations of sillimanite growth in these rocks. Sillimanite was present in the early assemblage. Sillimanite was also produced with biotite as garnet was consumed. This growth may have taken place either during initial cooling from high-grade metamorphism or during reheating of these rocks during Acadian metamorphism.

Reconstituted Pelitic Schist

This group of 6 rocks from 5 localities (Table 2) are well foliated and recrystallized in texture. The foliation is defined by the coplanar orientation of muscovite and biotite and locally, by oblong plagioclase grains. The coarse megacrysts of garnet and potassium feldspar, characteristic of the strongly sheared samples, are lacking and potassium feldspar and sillimanite do not occur as matrix phases. These pelitic samples have been grouped together for descriptive purposes on the basis of similar texture and mineral assemblage.

Mineral occurrence and texture. Quartz is abundant and may be equant to tabular in shape. Tabular quartz may be up to 4-5 mm long and the long dimension lies in the plane of schistosity. Polycrystalline quartz ribbons may be present, but they are not extensive. Undulatory extinction is common.

Plagioclase is present in at least trace amounts in each of the reconstituted rocks. In thin section, it is equant or oblong and normally less than 3 mm in diameter, although grains may exceed 7 mm in length. It commonly has albite twins and is optically positive with 2V of about 88 degrees. Plagioclase is commonly found in polycrystalline layers up to 4 x 1 mm, in the plane of foliation.

Muscovite is present in all of the reconstituted rocks and ranges in amount from 2 to 30 modal percent. It is typically colorless, is subhedral in shape, has an average grain size of 1-3 mm, and commonly includes or is intergrown with graphite or ilmenite. Muscovite is generally parallel to foliation, except in sample 160M, where 1-2 % of

Table 2. Estimated modes in thin section of reconstituted pelitic schist, sheared quartzite, and sheared pegmatite. Matrix phases in each rock type are interpreted as equilibrium assemblages with the exception of chlorite, which probably formed at a later stage. UM indicates microprobe analyses done at the University of Massachusetts; YU indicates microprobe analyses done at Yale University.

X = present in trace amounts
# = included in garnet
* = fine-grained muscovite rims around kyanite

Rock Type	Reconstituted Pelitic Schist						Quartzite	Sheared Pegmatite		
		UM			YU		UM	YU		
Sect #	W04	160M	160N	Y33	M4A	M4B	M21	M22A	M22B	M22C
Quartz	65	40	40	58	70	80	93	65	70	60
Ksp							2	10	4	6
Plag	5	3	5	5	21	2		6	15	15
Musc	18	29	20	20	2	12	2	2	X	
Bio	7	5	10	5	3	3	2	3	1	1
Gar	5	15	10	5	4	3	1	10	2	15
Sill		#	#					3 #	5 #	3 #
Ky		5	15	6				1	X	
Staur		2	X	1						
Tourm	X	X	X	X	X					
Rut			X		X			X		X
Ilm	X	X	X	X	X	X	#	X		X
Graph		X	X			X				
Zirc	X	X	X	X	X	X				
Chl	X								3	

the muscovite crosscuts the muscovite in the plane of foliation, indicating a late phase of deformation has taken place.

Biotite is present in all of these rocks, but is generally less abundant than muscovite. Subhedral biotite grains are less than 2 mm in size. In plane light, biotite may be dark brown, brown, or orange-brown in the Z = Y direction and light tan to colorless in the X direction. Biotite may be included in garnet or kyanite or may form beards on garnet grains.

Garnet forms equant, rounded to irregular grains and is present in all six of the reconstituted rocks examined. The grains are generally anhedral except in one sample (Y33) where the garnet may be euhedral or anhedral. Grain size is less than 1 cm, with an average size of 3-4 mm. Adjacent mineral phases include muscovite, biotite, staurolite, and quartz, which appear to be in textural equilibrium with garnet.

Garnet contains inclusions of quartz, biotite, ilmenite, or rutile. Three thin sections contain rutile within garnet: two have fine, crystallographically oriented needles while the other contains a 0.2 mm long inclusion. One sample (160M) contains fibrous sillimanite inclusions within garnet. The rutile and sillimanite within the some garnets suggest that these garnets grew during high-grade conditions. In contrast, garnet from sample Y33 is commonly euhedral and does not contain rutile or sillimanite, suggesting lower grade conditions of formation.

Three of the six rocks contain light blue kyanite. Kyanite from these samples is subhedral to anhedral in bladed shapes, ranging from 4 to 8 mm long. Kyanite may be twinned and may contain irregularly-shaped inclusions of quartz, biotite, ilmenite, or, in one case, rutile. Extinction is commonly undulatory and kyanite orientation is parallel to foliation. Two of the three sections containing kyanite (160M,160N) exhibit muscovite replacement textures after kyanite.

Staurolite occurs in trace amounts only in the three sections containing kyanite. Where present, it is subhedral to irregular in shape and is generally less than 3 mm in size. It commonly contains abundant inclusions of quartz. In plane light, it is pleochroic from colorless to pale yellow and does not exhibit optical zoning. It is optically positive and has a 2V of 85 degrees.

In sample 160M, staurolite appears to be an inclusion at the outer rim of a garnet. It is possible, however, that what appears to be staurolite included in garnet in two dimensions, may be a grain of staurolite adjacent to an irregular rim on garnet in the third dimension. No other such inclusions have been observed, and irregular rims on garnets are common in these rocks, therefore the writer prefers this explanation.

Tourmaline is present in trace amounts in 5 of these 6 thin sections. It is euhedral to irregular in shape and normally less than 1 mm in size. Tourmaline is pleochroic from a light tan or pink to green or olive green in plane light. Tourmaline may be optically zoned.

Grain interiors may or may not contain Becke lines, suggesting that the zoning may result from continuous growth or from overgrowths on pre-existing grains. Inclusions of ilmenite are common.

Rutile, when present in these rocks, has variable habit. Two samples (160M,160N) contain fine crystallographically oriented inclusions in several garnets. One of these samples also has a 0.2 mm long rutile grain included in kyanite. Only one section contains rutile as a matrix phase, where it is less than 0.2 mm in size and irregular in shape. Here rutile is also found as 1 mm inclusions in garnet and muscovite.

The scarcity of rutile in the reconstituted rocks relative to the sheared pelitic rocks suggests that rutile was probably stable during the early high-grade metamorphism, and may have been largely consumed following the peak of the early metamorphism.

Ilmenite is found in all of these rocks as irregular grains less then 2 mm in size. It may be included in garnet or kyanite. It is commonly intergrown with muscovite (160M). Ilmenite is in textural equilibrium with matrix minerals and was probably produced in these rocks following cooling from early high-grade conditions.

Graphite occurs in trace amounts in some of these rocks. Grains are commonly elongate and irregular.

Petrographic evidence for mineral reactions. The six samples of reconstituted rocks may exhibit one or more disequilibrium textures. Three samples do not contain aluminosilicate or staurolite, probably due to their quartz-rich bulk composition. In two of these three samples, concentrations of muscovite, biotite, and quartz may occur adjacent to garnet, where the garnet is embayed and irregular, consistent with the reaction,

$$\text{GAR} + 2\ \text{KSP} + 2\ H_2O = \text{BIO} + \text{MUSC} + 3\ \text{QTZ} \quad (3).$$

Relict oblong shapes, 1-2 mm in length, now occupied by coarse muscovite in one of these two samples may once have been kyanite (WO4). The third of these samples contains relict shapes now containing plagioclase, muscovite, and quartz. These were probably originally potassium feldspar, although this has not been demonstrated. These textures are consistent with above reaction,

$$\text{KY/SILL} + \text{KSP} + H_2O = \text{MUSC} + \text{QTZ}. \quad (2)$$

The three kyanite- and staurolite-bearing rocks contain corroded kyanite and garnet surrounded by concentrations of muscovite, biotite, quartz, and plagioclase with or without staurolite. Sample 160N contains much more kyanite than the other two kyanite-bearing samples and it contains almost no staurolite. Only one of these samples (Y33) contains euhedral garnets as well as embayed and rounded garnets.

Sheared Pegmatite

The third group of samples studied includes three samples of sheared pegmatite from locality M22A. The rock is dominantly white in

color, with quartz and feldspar ribbons alternating with thin stringers of biotite to give the rock a laminated appearance. The pegmatite contains quartz, potassium feldspar, and plagioclase with minor amounts of sillimanite, garnet, and biotite. Two of these samples contain trace amounts of muscovite and kyanite. Feldspar porphyroclasts may be up to 4 mm in diameter and irregularly-shaped garnet porphyroclasts may be up to 2 cm long.

Quartz may be present as polycrystalline ribbons extending across the entire thin section, with single grains up to 2 mm in length. It may also be present as small equant grains averaging less than 0.5 mm in the matrix with plagioclase and sillimanite. Quartz is commonly included in garnet, and may itself contain inclusions of fine needles of rutile or sillimanite.

Polycrystalline plagioclase is commonly found in ribbons parallel to the foliation. Grain size is less than 1.5 mm in diameter. It commonly has albite twinning with a maximum extinction angle of 19 degrees. Composition is approximately 34 % anorthite by the Michel-Levy method. Plagioclase in some ribbons may be unaltered, whereas other ribbons show significant sericitization. Plagioclase may replace large potassium feldspar porphyroclasts; in places up to 90 % of the porphyroclast is plagioclase.

Potassic feldspar occurs either as large, irregular porphyroclasts, up to 4 cm in length, or as smaller equant grains, 1-2 mm in diameter, in polycrystalline ribbons parallel to foliation. Under crossed-polars, it has first-order gray birefringence with undulatory extinction, and commonly displays grid twinning. Potassic feldspar may exhibit micro-perthitic exsolution of plagioclase in its interior. The potassium feldspar is optically negative with 2V of 50-60 degrees, suggesting a disordered structure state. Crystallographically oriented needles of rutile and prismatic sillimanite, less than 0.5 mm in length, are commonly present in potassium feldspar.

Muscovite occurs either as sericite, associated with plagioclase grains, or as coarse subhedral grains, less than 2 mm in length, associated with sericite and kyanite.

Biotite is present in trace amounts in the sheared pegmatite matrix. Biotite color is orange-brown in the Y and Z directions and tan to colorless in the X direction. It is irregular to subhedral in shape and less than 0.5 mm in size.

Chlorite is found in close association with garnet as colorless to light brownish-green, fine-grained mats. It shows anomalous blue interference colors, indicating iron-rich composition.

Garnet is generally less than 1 cm in size, though porphyroclasts are up to 2 cm long. Shapes are irregular and embayed and may be equant to oblong. The garnet grains are locally rimmed by biotite or chlorite.

Sillimanite occurs in the pegmatite matrix as prismatic grains less than 2 mm long. It may also be included as needles, less than 0.5 mm

long, in garnet, quartz, or potassium feldspar.

Kyanite occurs in two of the samples as elongate blades less than 2 mm in length. Kyanite only occurs in ribbons that also contain muscovite and sericitized plagioclase.

Rutile and ilmenite are found in the matrix as small, irregular grains less than 0.5 mm long.

Sheared Quartzite

One sample of micaceous quartzite from locality M21 exhibits sheared texture. Grains of quartz may be as large as 8 mm in length, and are slightly elongate to tabular in shape. Quartz commonly contains inclusions of mica or small garnet grains, oriented parallel to matrix foliation.

Potassic feldspar is present as large porphyroclasts up to 8 mm in length. It may be largely replaced by plagioclase.

Muscovite occurs as subhedral grains, less than 3 mm in length, throughout the matrix or included in quartz. It generally lies parallel to the foliation.

Biotite occurs as subhedral grains, less than 1.5 mm in length, throughout the matrix or included in garnet or quartz. Matrix biotite color is almost-opaque brown in the Z and Y directions and olive-tan in the X direction. Biotites included in garnet are more orange-brown in color and commonly rounded in shape.

Garnet may be present as irregularly shaped porphyroclasts, up to 3-5 mm in length, or as tiny blebs, less than 1 mm in length, in the matrix. Garnet color in plane light is light pink and may show optical zoning. Garnet commonly contains abundant inclusions of quartz, biotite, ilmenite, and tiny, unidentified, cube-shaped grains less than 0.05 mm long. There are no obvious rimming or replacement textures associated with these garnets.

Ilmenite has been observed only as small inclusions in garnet.

Summary of Petrographic Evidence from Pelites

The pelitic samples have been divided into sheared schist and reconstituted schist on the basis of texture and mineral assemblage. The sheared schists are commonly mylonitized and may contain garnet and K-feldspar megacrysts, rutile, and prismatic sillimanite as matrix phases. Muscovite from sheared schists, where present, appears to be a secondary mineral, in local equilibrium with other matrix phases. In contrast, reconstituted schists are recrystallized and foliated, containing minerals typical of the biotite-staurolite-kyanite zone and muscovite is in textural equilibrium in all of these samples.

All of the rocks of the Mt. Mineral Formation would have experienced the early high-grade metamorphism and therefore all of the aluminous rocks should have contained high-grade mineral assemblages

similar to those observed in the sheared pelitic schists. However, not all of the rocks preserve evidence of this event. It is believed that many of the rocks re-equilibrated during the lower-grade Acadian metamorphism and now contain little or no evidence of earlier textures and assemblages. Petrographic evidence within the sheared schists suggests that many of these reactions were hydration reactions, such as

GAR + KSP + H_2O = KY/SILL + BIO + QTZ, (1)
KY/SILL + KSP + H_2O = MUSC + QTZ, (2)
GAR + 2 KSP + 2 H_2O = BIO + MUSC + 3 QTZ (3).

Some factor other than pressure and temperature must have been responsible for producing the wide range in mineral assemblages and textures occurring in these rocks on such a localized scale. Each of the above reactions, which probably were active in the sheared pelitic schists, are hydration reactions, and it is believed that a low activity of water prevented these reactions from going to completion in the sheared pelitic schists. In this way the sheared textures and high-grade mineral assemblages have been preserved from re-equilibration during low-grade Acadian metamorphism.

The reconstituted schists probably once contained mineral assemblages similar to the sheared schists, but have been recrystallized and now contain biotite-staurolite-kyanite zone mineral assemblages. Disequilibrium textures have been found in these schists, some of which are consistent with the above reactions. Staurolite and tourmaline were produced in some of these schists but evidence for specific mineral reactions have not been demonstrated. It is probable that the reconstituted schists formerly contained K-feldspar and that the K-feldspar was completely consumed via hydration reactions as the rocks experienced lower temperature conditions.

MINERAL CHEMISTRY

Seven polished thin sections were chosen for chemical analysis using the electron microprobe. Chemical compositions of major mineral phases, based on electron microprobe analyses from these samples, are discussed in this section. Analytical methods are discussed in the Introduction.

Compositions of plagioclase, muscovite, and biotite within sheared pelitic schists from the Mt. Mineral Formation resemble those within nearby K-feldspar-sillimanite-muscovite zone rocks (Acadian zone IV) which record chemical conditions in rocks near the Acadian prograde muscovite breakdown reaction (Tracy, 1975, 1978). Compositions of plagioclase, muscovite, and biotite within reconstituted pelitic schists resemble those within nearby Acadian kyanite zone cover rocks (Hollocher, 1981). Comparisons of chemical data from these studies are included where appropriate.

Plagioclase

Microprobe analyses of plagioclase feldspars from sheared pelitic schist and reconstituted pelitic schist are given in Table 3. Cation

Table 3. Electron microprobe analyses of plagioclase. Analyses are from two samples of sheared pelitic schist and from one sample of reconstituted pelitic schist. Cation proportions are calculated on the basis of the formula, $Ca_xNa_{1-x}Al_{1+x}Si_{3-x}O_8$, containing 8 oxygens. Feldspar data are plotted on An-Or-Ab ternary diagram in Figure 27.

Sample W67A

Alys#	1	2	3	4	5
SiO_2	62.20	61.61	61.79	63.19	60.13
TiO_2	0.0	0.0	0.0	0.0	0.02
Al_2O_3	23.96	24.45	24.36	22.35	23.98
Cr_2O_3				0.03	0.01
FeO	0.05	0.0	0.0	0.09	0.02
MgO	0.0	0.0	0.02	0.02	0.01
CaO	4.84	5.31	5.12	4.87	5.01
Na_2O	8.70	8.72	8.60	8.16	8.32
K_2O	0.21	0.25	0.23	0.24	0.27
Total	99.96	100.34	100.12	98.95	97.77

Formulae based on 8 oxygens

Si	2.755	2.727	2.736	2.819	2.727
Al	1.152	1.276	1.272	1.176	1.283
Total	3.907	4.003	4.008	3.995	4.010
Ti					.001
Cr				.001	
Fe	.002			.003	.001
Mg				.001	.001
Ca	.230	.252	.243	.233	.244
Na	.748	.749	.739	.706	.732
K	.012	.014	.013	.014	.015
Total	.992	1.015	.995	.958	.994
Ab	75.56	73.79	74.27	74.08	73.86
An	23.23	24.83	24.42	24.45	24.63
Or	1.21	1.38	1.31	1.47	1.51

Table 3, continued.

Sample X43A

Alys#	1	2	3	4	5	6	7	8	9	10
SiO_2	60.28	61.47	62.32	61.66	60.98	61.42	61.85	60.93	61.09	60.84
TiO_2	0.02	0.0	0.0	0.0	0.01	0.01	0.0	0.01	0.03	0.0
Al_2O_3	23.57	23.00	24.07	23.46	23.91	23.76	23.49	24.91	24.32	24.54
FeO	0.02	0.0	0.0	0.0	0.01	0.01	0.04	0.0	0.0	0.02
MnO	0.01	0.0	0.01	0.0	0.01	0.0	0.01	0.0	0.0	0.0
MgO	0.01	0.04	0.02	0.03	0.03	0.02	0.02	0.03	0.01	0.06
CaO	6.40	6.48	6.26	6.30	6.31	6.20	6.11	6.18	5.77	5.76
Na_2O	8.48	7.83	8.00	7.93	8.05	7.97	8.33	7.81	8.23	7.98
K_2O	0.13	0.14	0.14	0.13	0.13	0.13	0.11	0.15	0.16	0.13
Total	98.92	98.96	100.82	99.51	99.44	99.52	99.96	100.02	99.61	99.33

Formulae based on 8 oxygens

Si	2.717	2.758	2.742	2.750	2.726	2.739	2.749	2.704	2.722	2.716
Al	1.253	1.217	1.249	1.234	1.260	1.250	1.231	1.303	1.278	1.292
Total	3.970	3.975	3.991	3.984	3.986	3.989	3.980	4.007	4.000	4.008
Ti	0.001								0.001	
Fe	0.001				0.001		0.002			0.001
Mg	0.001	0.002	0.001	0.002	0.002	0.001	0.002	0.002		0.004
Ca	0.309	0.312	0.295	0.301	0.302	0.296	0.291	0.294	0.276	0.276
Na	0.742	0.681	0.683	0.686	0.698	0.689	0.718	0.672	0.712	0.691
K	0.007	0.008	0.008	0.007	0.007	0.008	0.006	0.009	0.009	0.008
Total	1.061	1.003	0.987	0.996	1.010	0.994	1.019	0.977	0.998	0.980
Ab	70.13	68.03	69.27	69.01	69.31	69.39	70.74	68.93	71.42	70.87
An	29.21	31.17	29.92	30.28	29.99	29.81	28.67	30.15	27.68	28.31
Or	0.66	0.80	0.81	0.70	0.70	0.80	0.59	0.92	0.90	0.82

Table 3, continued.

Sample 160M

Alys#	1	2	3	4	5
SiO_2	63.35	65.10	65.29	65.19	65.70
TiO_2	0.0	0.0	0.0	0.0	0.0
Al_2O_3	21.02	21.32	21.32	20.41	21.72
FeO	0.0	0.0	0.07	0.0	0.02
MgO	0.0	0.02	0.03	0.01	0.0
CaO	2.85	2.95	2.97	2.78	3.05
Na_2O	11.54	11.34	11.37	11.28	11.04
K_2O	0.07	0.09	0.08	0.10	0.11
Total	98.83	100.82	101.13	99.77	101.64

Formulae based on 8 oxygens

Si	2.835	2.856	2.858	2.888	2.858
Al	1.109	1.103	1.101	1.066	1.114
Total	3.944	3.959	3.959	3.954	3.972
Ti					
Fe				0.003	0.001
Mg	0.001	0.001		0.002	
Ca	0.137	0.139	0.139	0.132	0.143
Na	1.002	0.965	0.965	0.970	0.932
K	0.004	0.005	0.004	0.006	0.006
Total	1.144	1.110	1.108	1.113	1.082
Ab	87.66	87.02	87.09	87.55	86.22
An	11.99	12.53	12.55	11.91	13.23
Or	0.35	0.45	0.36	0.54	0.55

proportions have been calculated on the basis of the formula $Ca_xNa_{1-x}Al_{1+x}Si_{3-x}O_8$ containing 8 oxygens. Normal or irregular zoning is rare in plagioclase.

Plagioclase from sample X43A contains the most calcic composition of those analysed from pelitic schist (An_{29} to An_{31}), whereas plagioclase from reconstituted schist is the most sodic (An_{12} to An_{13}). Plagioclase from sheared schist is similar in composition to plagioclase from similar Acadian Zone VI rocks (Tracy and others, 1976; Chamberlain and Lyons, 1983). Plagioclase from sample M22 of sheared pegmatite is approximately An_{34}, by the Michel-Levy method.

Potassium Feldspar

Electron microprobe analyses of potassium feldspar from sheared pelitic schist are given in Table 4. Cation proportions have been calculated based on the ideal formula $(K,Na)AlSi_3O_8$, containing 8 oxygens. The average composition is Or_{86}. This composition is similar to that reported by Tracy (1978) from nearby Zone VI cover rocks.

Thirteen potassium feldspars have been analysed by X-ray powder diffraction techniques to determine structure state. All samples are from single large grains of potassium feldspar with two well eveloped cleavages and commonly with translucent appearance.

All of the samples analysed are considered to have "anomalous" cell dimensions according to the three peak method of Wright (1968). The (131) peak appears as a single peak in all but three of the analysed samples, indicating monoclinic structure state in most samples. Petrographic evidence for exsolution of plagioclase from these megacrysts may explain anomalous X-ray results. "Apparent" structure state is illustrated in Figure 9, where two theta (060) is plotted against two theta (204). These samples plot between the orthoclase series of Wright and Stewart (1968) and the maximum microcline series of Orville (1967).

Muscovite

Cation proportions for analysed muscovites have been calculated on the basis of the ideal formula, $KAl_2AlSi_3O_{10}(OH)_2$, containing 11 oxygens and one H_2O. Full tetrahedral sites are assumed. Sodium may substitute for potassium in th e A-site and Ti, Cr, Fe, Mn, Mg may substitute for Al in the octahedral site.

Muscovite from sample W67B has been analysed by electron microprobe (Table 5). These muscovites contain a wide range in Ti contents from between 0.058 and 0.099 Ti per 11 oxygens (Figure 10). Analysed muscovites adjacent to potassium feldspar from this sample have a higher Ti content than analysed muscovites adjacent to garnet. The average Fe/(Fe+Mg) ratio is 0.479, ranging from 0.406 to 0.565.

Analysed muscovites from samples 160M and Y33 of reconstituted pelitic schist (Table 6) contain between 0.037 and 0.074 Ti per 11 oxygens, a lower range in Ti content than in the sheared rocks. The

Table 4. Electron microprobe analyses of potassium feldspar. Three analyses are from sample W67B. Cation proportions are calculated on the basis of the formula, $(K,Na)AlSi_3O_8$, containing 8 oxygens. Feldspar data are plotted on An-Or-Ab ternary diagram in Figure 27.

Alys #	W67-1	W67-2	W67-3
SiO_2	63.46	64.08	63.97
TiO_2	0.04	0.01	0.0
Al_2O_3	19.1	18.8	19.07
FeO	0.0	0.02	0.0
MgO	0.01	0.02	0.02
CaO	0.0	0.0	0.0
Na_2O	1.59	1.52	1.65
K_2O	14.63	14.71	14.49
Total	98.83	99.16	99.20

Formulae based on 8 oxygens

Si	2.958	2.974	2.966
Al	1.050	1.029	1.043
Total	4.008	4.003	4.009
Ti	0.002	0.001	
Fe		0.001	
Mg		0.001	0.001
Ca			
Na	0.144	0.137	0.148
K	0.870	0.871	0.858
Total	1.016	1.011	1.007
Or	85.80	86.40	85.30
Ab	14.20	13.60	14.70

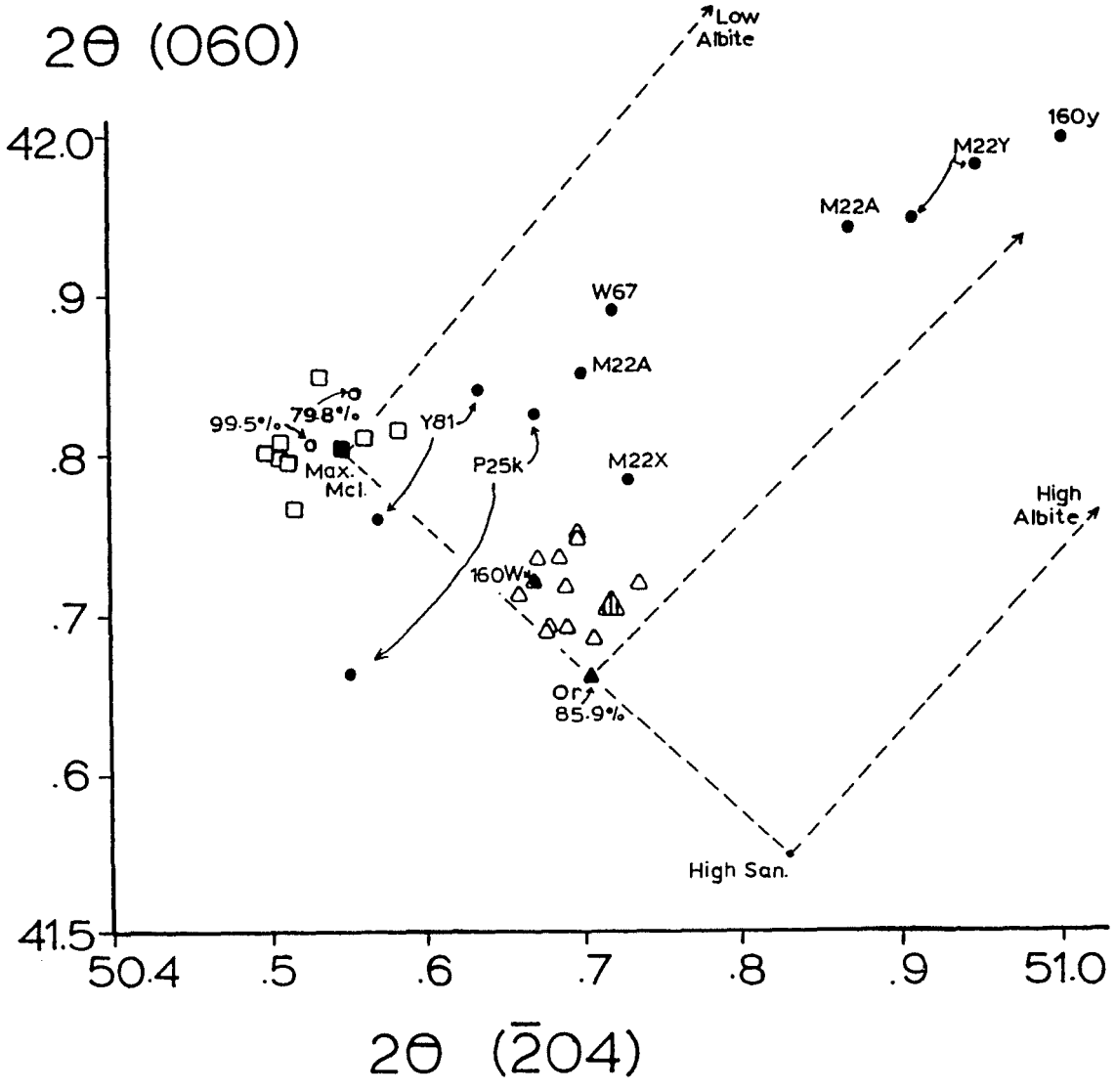

Figure 9. Apparent structure state of potassium feldspars. 2θ (060) plotted aganist 2θ ($\bar{2}$04) after Wright(1968). Mt. Mineral Fm. samples shown as solid circles. Maximum microcline data Or 99.5% and Or 79.8% (open circles) from Orville (1967). High orthoclase Or 85.9% from Wright & Stewart (1968). Irregularity of Mt. Mineral Fm. data indicate abnormal structure state, probably due to exsolution of plagioclase. Open squares indicate data of Laird (1974) and open triangles indicate data of Tracy (1975).

Table 5. Electron microprobe analyses of muscovite from sheared pelitic schist. Eight analyses are from sample W67B. Cation proportions are calculated on the basis of the formula, $(K,Na)Al_2Si_3AlO_{10}(OH)_2$, containing 11 oxygens plus one H_2O. Muscovite data are plotted on Figure 10.

Alys#	1	2	3	4	5	6	7	8
SiO_2	47.08	46.76	47.31	45.92	45.56	46.88	48.82	47.61
TiO_2	1.28	1.49	1.39	1.15	1.90	2.00	1.38	1.39
Al_2O_3	34.99	35.41	36.07	34.90	33.66	34.46	35.54	34.54
Cr_2O_3	0.04	0.05	0.0	0.01	0.02	0.01	0.03	0.0
FeO	1.26	1.23	1.20	1.26	1.18	1.06	1.26	1.91
MnO	0.03	0.0	0.0	0.02	0.02	0.02	0.0	0.02
MgO	0.74	0.76	0.75	0.69	0.85	0.87	0.78	0.83
CaO	0.0	0.0	0.0	0.0	0.0	0.0	0.0	0.0
Na_2O	0.38	0.39	0.39	0.37	0.38	0.36	0.36	0.36
K_2O	10.68	10.47	10.58	10.71	10.50	10.39	10.67	10.39
Total	96.48	96.56	97.69	95.03	94.07	96.05	98.84	97.05
Formulae based on 11 oxygens								
Si	3.094	3.067	3.065	3.069	3.077	3.089	3.122	3.113
Al	0.906	0.933	0.935	0.931	0.923	0.911	0.878	0.887
Total	4.000	4.000	4.000	4.000	4.000	4.000	4.000	4.000
Al	1.806	1.807	1.821	1.819	1.758	1.767	1.803	1.776
Ti	0.063	0.073	0.068	0.058	0.096	0.099	0.066	0.068
Cr	0.002	0.003		0.001	0.001		0.001	
Fe	0.069	0.068	0.065	0.071	0.066	0.058	0.067	0.105
Mn	0.002			0.001	0.001	0.001		0.001
Mg	0.072	0.074	0.073	0.069	0.085	0.085	0.074	0.081
Total	2.014	2.025	2.027	2.019	2.007	2.010	2.011	2.031
Ca								
Na	0.049	0.050	0.049	0.048	0.050	0.046	0.045	0.045
K	0.897	0.876	0.875	0.914	0.905	0.874	0.871	0.867
Total	0.946	0.926	0.924	0.962	0.955	0.920	0.916	0.912
$\frac{Fe}{(Fe+Mg)}$	0.489	0.479	0.471	0.507	0.437	0.406	0.475	0.565
$\frac{K}{(K+Na)}$	0.948	0.946	0.947	0.950	0.948	0.950	0.951	0.951

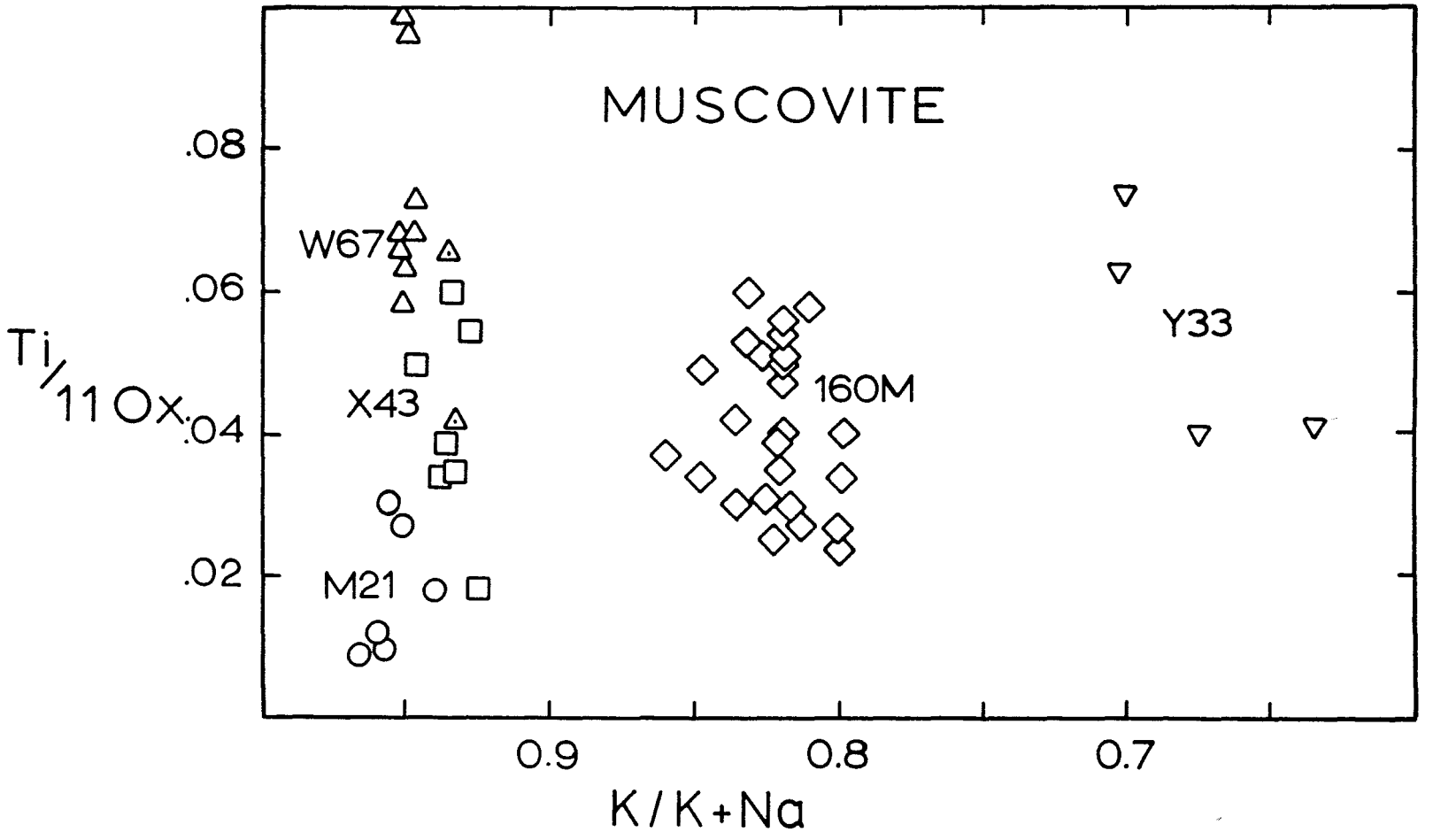

Figure 10. Ti per 11 oxygens plotted against K/(K+Na) ratios for analyzed muscovites from various samples. Samples are Y33 (inverted triangles), 160M (diamonds), X43A (squares), W67B (triangles), M21 (circles). Dotted triangles represent data from Tracy (1975).

Table 6. Selected electron microprobe analyses of muscovite from reconstituted pelitic schist. Cation proportions are calculated on the basis of the formula, $(K,Na)Al_2Si_3AlO_{10}(OH)_2$, containing 11 oxygens plus one H_2O. Muscovite data are plotted on Figure 10.

Sample	M160 (Reconstituted schist)					Y33 (Reconstituted schist)			
Alys#	1	2	3	4	5	1	2	3	4
SiO_2	45.74	47.74	48.87	46.79	46.36	45.00	44.81	45.15	45.05
TiO_2	1.02	1.20	1.05	0.82	1.14	0.78	0.79	1.45	1.25
Al_2O_3	35.53	35.51	33.54	34.15	33.35	34.99	34.62	34.44	35.30
Cr_2O_3				0.0	0.02				
FeO	1.26	1.12	1.27	1.18	1.14	1.26	0.76	1.10	1.14
MnO	0.0	0.05	0.03	0.0	0.0	0.0	0.26	0.29	0.0
MgO	0.70	0.65	0.73	0.57	0.63	0.64	0.47	0.40	0.89
CaO	0.03	0.0	0.0						
Na_2O	0.91	0.96	0.97	1.32	1.45	2.43	3.02	2.36	2.21
K_2O	7.94	7.85	7.91	9.06	9.42	7.69	7.95	8.43	8.07
Total	93.13	95.08	94.37	93.89	93.51	92.79	92.68	93.62	93.91
Formulae based on 11 oxygens									
Si	3.070	3.127	3.224	3.136	3.133	3.050	3.050	3.051	3.023
Al	0.930	0.873	0.776	0.864	0.867	0.950	0.950	0.949	0.977
Total	4.000	4.000	4.000	4.000	4.000	4.000	4.000	4.000	4.000
Al	1.880	1.868	1.831	1.835	1.791	1.845	1.828	1.794	1.814
Ti	0.051	0.059	0.052	0.041	0.058	0.040	0.041	0.074	0.063
Cr					0.001				
Fe	0.071	0.061	0.070	0.066	0.065	0.071	0.043	0.062	0.064
Mn		0.003	0.002				0.015	0.017	
Mg	0.070	0.063	0.072	0.057	0.063	0.065	0.048	0.040	0.089
Total	2.072	2.054	2.027	1.999	1.978	2.021	1.975	1.987	2.030
Ca									
Na	0.118	0.122	0.124	0.171	0.190	0.320	0.399	0.309	0.287
K	0.680	0.656	0.665	0.775	0.813	0.665	0.691	0.726	0.690
Total	0.798	0.778	0.789	0.946	1.003	0.985	1.090	1.035	0.977
$\frac{Fe}{(Fe+Mg)}$	0.504	0.492	0.493	0.537	0.508	0.522	0.473	0.608	0.418
$\frac{K}{(K+Na)}$	0.852	0.843	0.842	0.819	0.811	0.675	0.634	0.701	0.706

Fe/(Fe+Mg) ratio in muscovite from reconstituted pelitic rocks ranges from 0.41 to 0.61, averaging 0.504.

Muscovite from sample M21 of sheared quartzite (Table 7) contains between 0.009 and 0.031 Ti per 11 oxygens. The Fe/(Fe+Mg) ratio is between 0.645 and 0.712, with an average of 0.684, making these muscovites considerably more iron rich than those in pelitic assemblages.

Average alkali content of muscovites (Figure 10) shows systematic variation in K/(K+Na) ratios. Each of the pelitic samples represented here contains aluminosilicate and plagioclase. Potassium feldspar is absent from the reconstituted schist, and the sheared quartzite contains neither plagioclase nor aluminosilicate.

Muscovites from strongly sheared schist are rich in potassium whereas those from reconstituted schist are substantially more paragonitic. Chatterjee and Flux (1986) have demonstrated that a lower activity of water effectively lowers the composition curve of equilibrium muscovites (T-X diagram) toward lower temperatures. Therefore, for a given temperature, muscovite coexisting with fluid of low activity of water would be more potassic than that coexisting with fluid of higher activity of water. Assuming that all of the Mt. Mineral rocks experienced the same temperatures during the Acadian metamorphism, the variation in the K/(K+Na) ratio in muscovites may be explained by variable activity of water. The sheared schists must experienced a lower activity of water, probably less than 0.5, and muscovite remained richer in potassium whereas the reconstituted schists must have experienced a higher activity of water, probably between 0.5 and 1.0, and muscovite became more sodic during the Acadian metamorphism.

The potassium-rich composition of muscovites in sheared schist resembles that of muscovite just prior to prograde muscovite breakdown observed in Acadian Zone IV rocks (Tracy, 1978). Since the reaction, KSP + Al-sil. + H_2O = MUSC + QTZ (2) also takes place at lower temperatures with decreasing activity of water (Chatterjee and Flux, 1986), forward progress of this reaction may occur with either decreasing temperature or with isothermal increase of activity of water. This suggests that muscovites from the sheared schists here are close to the first muscovites produced in the muscovite-in reaction approached from "above", by isothermal increase of activity of water. This reaction has gone to completion in the reconstituted schists such that K-feldspar is no longer present, and sodic muscovite coexists with plagioclase and aluminosilicate.

Muscovite from sample 160M contains an intermediate paragonite content whereas that from sample Y33 is the most paragonitic, with 0.67 K/K+Na. The latter value is similar to that observed by Hollocher (1981) for relatively fresh muscovite from nearby Devonian schists within the Acadian kyanite zone, in equilibrium with kyanite, staurolite, garnet, and biotite.

The phengite component (Fe+Mg+Mn per 11 oxygens) of muscovites analysed here apparently decreases with increasing hydration state.

Table 7. Electron microprobe analyses of muscovite from sheared quartzite. Six muscovite analyses are from sample M21. Cation proportions are calculated on the basis of the formula $(K,Na)Al_2Si_3AlO_{10}(OH)_2$, containing 11 oxygens plus one H_2O. Muscovite data are plotted in Figure 10.

Alys#	1	2	3	4	5	6
SiO_2	49.99	49.94	48.23	48.26	49.27	48.84
TiO_2	0.64	0.21	0.17	0.24	0.36	0.55
Al_2O_3	34.89	35.47	34.15	34.13	35.29	34.21
Cr_2O_3						
FeO	2.60	2.95	2.87	2.68	2.64	2.39
MnO	0.0	0.0	0.0	0.0	0.0	0.0
MgO	0.64	0.68	0.71	0.72	0.68	0.73
CaO	0.0	0.0	0.0	0.0	0.0	0.0
Na_2O	0.29	0.27	0.20	0.24	0.37	0.29
K_2O	9.14	9.02	8.86	8.62	8.53	8.42
Total	98.19	98.54	95.19	94.89	97.14	95.43
Formulae based on 11 oxygens						
Si	3.199	3.186	3.187	3.192	3.178	3.202
Al	0.801	0.814	0.813	0.808	0.822	0.798
Total	4.000	4.000	4.000	4.000	4.000	4.000
Al	1.832	1.854	1.849	1.855	1.862	1.847
Ti	0.031	0.010	0.009	0.012	0.018	0.027
Cr						
Fe	0.139	0.158	0.159	0.148	0.143	0.131
Mn						
Mg	0.061	0.064	0.070	0.071	0.066	0.072
Total	2.063	2.086	2.087	2.086	2.089	2.077
Ca						
Na	0.035	0.033	0.026	0.031	0.046	0.036
K	0.746	0.735	0.747	0.728	0.703	0.705
Total	0.781	0.768	0.773	0.759	0.749	0.741
$\frac{Fe}{(Fe+Mg)}$	0.695	0.712	0.694	0.676	0.684	0.645
$\frac{K}{(K+Na)}$	0.955	0.957	0.966	0.959	0.939	0.951

Muscovites from sample W67B of sheared schist contain an average of 0.148 per 11 oxygens. Analysed muscovites from nearby Ordovician Partridge Formation within Zone IV of Acadian metamorphism, in equilibrium with sillimanite, orthoclase, garnet, and biotite, contain a similarly high phengite component, averaging 0.144 per 11 oxygens (Tracy, 1975). Analysed muscovites from sheared quartzite sample M21 have a higher average phengite content of 0.214 per 11 oxygens.

The phengite content of analysed muscovites from samples 160M and Y33 of reconstituted schist average 0.134 and 0.118 per 11 oxygens, respectively. These values are significantly lower than those of muscovites from sheared pelitic schist. Analysed muscovites from nearby Devonian cover rocks contain slightly lower average phengite contents of 0.086 per 11 oxygens (Hollocher, 1981).

The strong similarities between muscovite from sheared rocks and higher grade rocks studied by Tracy (1975) and between reconstituted rocks and nearby cover rocks within the Acadian kyanite zone of Hollocher (1981) present strong evidence that the sheared rocks coexisted with fluid of much lower activity of water than that of the reconstituted rocks.

Biotite

Cation proportions of analysed biotites are calculated on the basis of the formula $KFe_3Si_3AlO_{10}(OH)_2$, containing 11 oxygens and one H_2O. Full tetrahedral sites are assumed. Sodium may substitute for potassium in the A-site and Al, Ti, Cr, Mg, and Mn may substitute for iron in the octahedral sites.

The biotite analyses show that there is no sodium in a number of biotites from sheared schist and sheared pegmatite. However, there is very likely measurable sodium in all of the biotites analysed, and the discrepancy may be due to volatilization of sodium during analysis. The analyses included here are interpreted to be valid chemical compositions of biotites, excepting sodium.

In sheared pelitic rock. Microprobe analyses of biotites from three samples of sheared pelitic rock (Table 8) include biotite from the matrix, biotite adjacent to garnet rim, brown or green biotite infilling cracks in garnet, and biotite included in garnet. Matrix biotites in the sheared pelitic rocks have Fe/(Mg+Fe) ratios between 0.47 and 0.53 (Figure 11). Biotites adjacent to garnet are on the Mg-rich end of this range. Biotites included in garnet are lower in Fe with an Fe/(Mg+Fe) ratio of up to 0.29 to 0.39. The lower iron content of the included biotites is probably due to localized ion exchange with garnet as temperature decreased.

Both matrix and included biotites from sheared rocks show a wide range of Ti contents from 0.10 to 0.25 Ti per 11 oxygens. The dominant factor controlling the variation in Ti content has not yet been determined. Green biotite filling garnet cracks are extremely low in Ti with less than 0.01 Ti per 11 oxygens. Ti content of these green biotites decreases from the outer parts of the garnet toward the garnet

Table 8. Some electron microprobe analyses of biotite from sheared pelitic schist. Eighteen analyses from three samples representing biotites from matrix, adjacent to garnet rim, infilling crack in garnet, and included in garnet are given. Cation proportions are calculated on the basis of the formula, $(K,Na)(Fe,Mg)_3Si_3AlO_{10}(OH)_2$, containing 11 oxygens plus one H_2O. Biotite data are plotted in Figure 11.

Sample	160X						W67				
	brown rim			brown crack	green crack		brown matrx		brown rim		
Alys#	1	26	27	24	18	21	1	28	2	3	22
SiO_2	37.39	37.01	35.64	36.03	37.62	37.80	34.20	35.66	33.12	34.73	34.95
TiO_2	1.78	1.85	2.87	2.18	0.09	0.17	4.08	3.92	4.07	3.53	3.34
Al_2O_3	19.08	20.36	20.33	20.82	21.06	21.03	18.50	18.79	18.93	18.69	18.06
Cr_2O_3		0.05	0.03	0.01	0.02	0.03	0.0	0.05	0.02	0.04	0.05
FeO	17.03	16.75	17.71	16.20	15.32	14.89	18.02	18.25	18.05	17.76	18.94
MnO	0.05	0.05	0.06	0.02	0.02	0.03	0.01	0.11	0.04	0.05	0.07
MgO	11.07	10.99	10.67	12.51	12.74	13.06	8.91	10.04	9.72	9.35	9.54
CaO	0.0	0.0	0.0	0.0	0.0	0.0	0.0	0.0	0.0	0.0	0.0
Na_2O	0.25	0.18	0.04	0.15	0.08	0.07	0.02	0.05	0.03	0.06	0.0
K_2O	9.58	9.13	9.47	9.28	9.16	8.76	9.87	9.61	9.90	9.73	9.63
Total	96.23	96.37	96.82	97.20	96.11	95.84	93.61	96.48	93.88	93.94	94.58
Formulae based on 11 oxygens											
Si	2.773	2.727	2.640	2.634	2.751	2.759	2.650	2.668	2.568	2.672	2.684
Al	1.227	1.273	1.360	1.366	1.249	1.241	1.350	1.332	1.432	1.328	1.316
Total	4.000	4.000	4.000	4.000	4.000	4.000	4.000	4.000	4.000	4.000	4.000
Al	0.441	0.496	0.416	0.429	0.568	0.569	0.340	0.326	0.300	0.368	0.320
Ti	0.099	0.102	0.160	0.120	0.005	0.009	0.238	0.220	0.237	0.204	0.193
Cr		0.003	0.002	0.001	0.001	0.002		0.003	0.001	0.003	0.003
Fe	1.056	1.032	1.098	0.991	0.938	0.909	1.168	1.143	1.171	1.143	1.217
Mn	0.003	0.003	0.004	0.001	0.002	0.002	0.001	0.007	0.003	0.003	0.005
Mg	1.224	1.207	1.179	1.364	1.390	1.422	1.030	1.121	1.124	1.073	1.093
Total	2.823	2.843	2.859	2.906	2.904	2.913	2.777	2.820	2.836	2.794	2.831
Ca											
Na	0.037	0.025	0.006	0.021	0.011	0.010	0.003	0.007	0.004	0.009	
K	0.906	0.859	0.896	0.866	0.855	0.816	0.976	0.918	0.980	0.956	0.944
Total	0.943	0.884	0.902	0.887	0.866	0.876	0.979	0.925	0.984	0.965	0.944
$\frac{Fe}{(Fe+Mg)}$	0.463	0.461	0.482	0.420	0.402	0.390	0.531	0.505	0.510	0.516	0.527
$\frac{K}{(K+Na)}$	0.961	0.972	0.993	0.976	0.987	0.988	0.997	0.992	0.996	0.991	1.000

Table 8, continued.

Sample	W67		X43				
	brown inclusion		brown matrx	brown rim			browm inclusion
Alys#	17	19	27	16	22	30	17
SiO_2	36.15	36.03	36.47	35.84	35.24	36.04	38.58
TiO_2	3.23	2.69	2.98	2.75	2.98	2.89	1.57
Al_2O_3	19.77	18.70	19.13	17.93	18.39	18.64	17.73
Cr_2O_3	0.05	0.0	0.0	0.07	0.0	0.0	0.05
FeO	14.36	12.35	18.39	17.46	19.46	17.24	12.38
MnO	0.04	0.01	0.0	0.05	0.15	0.0	0.05
MgO	12.83	14.53	11.56	11.19	11.20	11.58	16.66
CaO	0.0	0.0	0.0	0.0	0.0	0.0	0.0
Na_2O	0.15	0.41	0.0	0.17	0.0	0.0	0.96
K_2O	9.49	8.83	8.65	8.55	8.65	8.77	7.01
Total	96.07	93.55	97.18	94.01	96.07	95.16	94.99
Formulae based on 11 oxygens							
Si	2.658	2.692	2.686	2.726	2.654	2.704	2.800
Al	1.342	1.308	1.314	1.274	1.346	1.296	1.200
Total	4.000	4.000	4.000	4.000	4.000	4.000	4.000
Al	0.373	0.340	0.356	0.335	0.286	0.352	0.318
Ti	0.179	0.151	0.165	0.158	0.169	0.163	0.086
Cr	0.003			0.004			0.003
Fe	0.884	0.772	1.132	1.112	1.225	1.081	0.752
Mn	0.002	0.001		0.003	0.010		0.002
Mg	1.407	1.619	1.269	1.269	1.257	1.295	1.803
Total	2.848	2.883	2.922	2.881	2.947	2.891	2.964
Ca							
Na	0.021	0.060		0.025			0.135
K	0.891	0.842	0.813	0.830	0.831	0.839	0.649
Total	0.912	0.902	0.813	0.855	0.831	0.839	0.784
$\frac{Fe}{(Fe+Mg)}$	0.386	0.323	0.471	0.467	0.494	0.455	0.294
$\frac{K}{(K+Na)}$	0.977	0.933	1.000	0.971	1.000	1.000	0.828

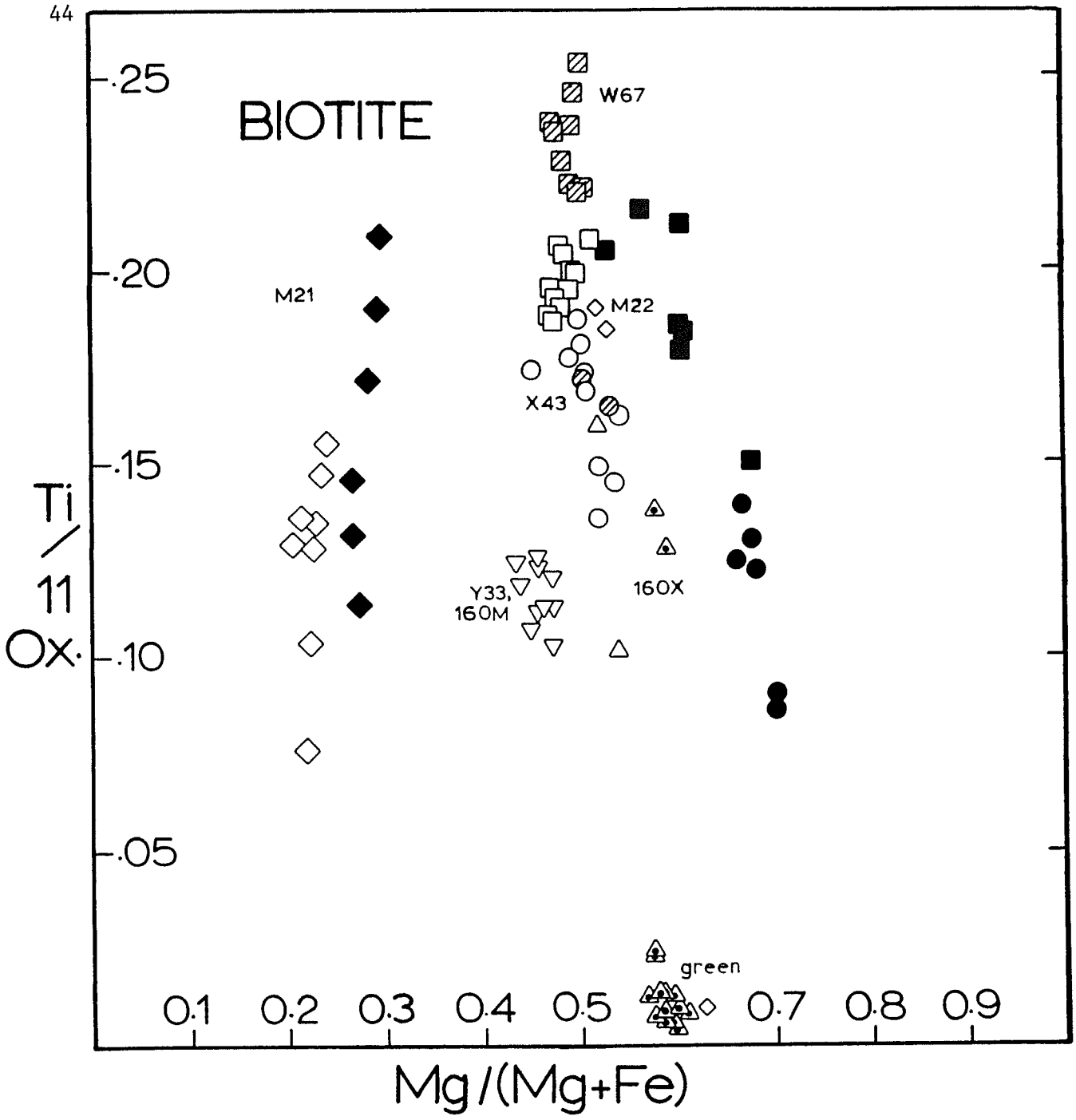

Figure 11. Ti per 11 oxygens versus Mg/(Mg+Fe) ratios for analysed biotites from various samples. Samples shown are W67 (squares), X43 (circles), 160X (triangles), Y33 and 160M (inverted triangles), M22A (small diamonds), M21 (large diamonds). Included biotites (solid) are more magnesian than corresponding rim (open) or matrix (ruled) biotites. Dot in some 160X triangles indicates biotite infilling crack in garnet. Green biotites are extremely low in Ti.

interiors. There appears to be a gap in Ti content between the very low-Ti green biotites and the higher-Ti brown biotites.

The average A-site occupancy is 0.885 and the octahedral site occupancy is only 2.870, assuming full tetrahedral sites. No evidence has been found for compositional zoning within individual grains.

In reconstituted pelitic rock. Matrix biotites from two samples of reconstituted pelitic rocks (Table 9) have Fe/(Mg+Fe) ratios of 0.50-0.60. A more limited range in Ti contents of 0.10-0.13 Ti per 11 oxygens suggests a lower temperature of formation or equilibration of these biotites relative to biotites in the sheared schists. Average A-site occupancy in these biotites is 0.868 and octahedral site occupancy averages 2.290, assuming full tetrahedral sites.

In sheared pegmatite. Three analyses of biotite from one sample of sheared pegmatite appear to be similar in composition to biotite in the sheared pelitic rocks (Table 10). These biotites are adjacent to garnet rim and may be brown or green in color. The Fe/(Mg+Fe) ratio ranges from 0.373 to 0.481, and Ti contents range from 0.010 (green) to 0.191 (brown) Ti per 11 oxygens (Figure 11).

In sheared quartzite. Both matrix and included boitites from sample M21 of sheared quartzite have been analysed (Table 11). Fe/(Fe+Mg) ratio ranges from 0.708 to 0.796 with matrix biotites being slightly more iron rich. Average Ti content of included biotites is 0.158 per 11 oxygens whereas matrix biotites are lower in Ti, averaging 0.124 Ti per 11 oxygens (Figure 11). Average K/(K+Na) ratio is 0.972, being slightly higher in matrix biotites. Average A-site occupancy is 0.989 and average octahedral site occupancy is 2.820.

Reaction controlling biotite composition. The Al-Ti-FM site occupancy of biotite could be controlled by the reaction: (Mg_2Al)biotite + ilmenite + quartz = $(Mg_2Fe_{.5}Ti_{.5})$biotite + sillimanite. Biotite end members are illustrated in K-feldspar projection in Figure 12 together with a plot of all analysed biotites. As the reaction proceeds forward, ilmenite is consumed and biotite compositions become more Fe-Ti rich. In the reverse direction, sillimanite is consumed and biotite composition becomes more aluminous at the expense of Fe-Ti. This is a water-independent reaction, though entropy probably increases slightly in the forward direction with octahedral aluminum going to tetrahedral aluminum.

Biotites from samples analysed here do not show this particular variation trend, but rather a trend towards increasing Al and Ti with decreasing Fe and Mg. This variation trend must involve both tetrahedral and octahedral sites. As seen in Figures 11 and 12, matrix biotites from sheared pelitic schist contain the most titanium whereas biotites included in garnet contain the least titanium.

Garnet

Garnets from this study are composed largely of almandine with significant variations in pyrope, spessartine, and grossular. These

Table 9. Electron microprobe analyses of biotite from reconstituted pelitic schist. Eleven analyses are given of matrix biotites from two samples. Cation proportions are calculated on the basis of the formula, $(K,Na)(Fe,Mg)_3Si_3AlO_{10}(OH)_2$, containing 11 oxygens plus one H_2O. Data are plotted on Figure 11.

Sample	M160							Y33			
Alys#	1	2	3	4	5	6	7	1	2	3	4
SiO_2	35.26	35.57	36.51	36.91	36.52	35.61	34.61	34.83	34.15	33.85	34.51
TiO_2	1.94	1.90	2.16	1.84	2.00	1.98	2.13	2.19	2.04	2.11	1.87
Al_2O_3	17.84	18.01	18.91	18.69	18.16	19.17	19.15	19.16	18.99	18.06	18.89
FeO	20.16	22.50	20.49	20.24	20.16	21.46	20.40	20.59	21.32	21.40	20.99
MnO	0.03	0.09	0.0	0.04	0.0	0.01	0.03	0.0	0.0	0.0	0.0
MgO	9.66	10.37	10.15	10.13	10.12	10.11	9.60	9.64	9.32	9.19	9.57
ZnO	0.25	0.22	0.24	0.18	0.12	0.0	0.0				
CaO	0.05	0.04	0.05	0.0	0.0	0.0	0.0	0.0	0.0	0.0	0.0
Na_2O	0.23	0.18	0.29	0.24	0.32	0.22	0.23	0.0	0.76	0.88	1.41
K_2O	8.68	8.29	8.89	8.48	8.62	7.48	8.57	8.11	7.99	7.80	8.01
Total	94.10	97.17	97.69	96.75	96.02	96.04	94.72	94.52	94.57	93.29	95.25
Formulae based on 11 oxygens											
Si	2.727	2.683	2.711	2.754	2.752	2.681	2.656	2.668	2.636	2.655	2.645
Al	1.273	1.317	1.289	1.246	1.248	1.319	1.344	1.332	1.364	1.345	1.355
Total	4.000	4.000	4.000	4.000	4.000	4.000	4.000	4.000	4.000	4.000	4.000
Al	0.352	0.284	0.366	0.397	0.364	0.382	0.387	0.397	0.364	0.325	0.351
Ti	0.113	0.108	0.121	0.103	0.113	0.112	0.123	0.126	0.118	0.124	0.107
Fe	1.304	1.419	1.272	1.262	1.270	1.351	1.309	1.319	1.376	1.404	1.346
Mn	0.002	0.006		0.003		0.001	0.002				
Mg	1.113	1.166	1.123	1.126	1.136	1.134	1.098	1.101	1.073	1.075	1.093
Total	2.884	2.983	2.882	2.891	2.883	2.980	2.919	2.943	2.931	2.928	2.897
Ca											
Na	0.036	0.026	0.042	0.035	0.047	0.032	0.034		0.113	0.134	0.210
K	0.856	0.797	0.842	0.807	0.828	0.718	0.839	0.793	0.786	0.780	0.783
Total	0.892	0.826	0.884	0.842	0.875	0.750	0.873	0.793	0.899	0.914	0.993
$\frac{Fe}{(Fe+Mg)}$	0.539	0.549	0.531	0.529	0.528	0.544	0.544	0.545	0.562	0.566	0.552
$\frac{K}{(K+Na)}$	0.956	0.965	0.948	0.958	0.946	0.957	0.961	1.000	0.874	0.853	0.789

Table 10. Electron microprobe analyses of biotite from sheared pegmatite. Three analyses are of biotites rimming garnet, both brown and green, from sample M22A. Cation proportions are calculated on the basis of the formula, $(K,Na)(Fe,Mg)_3Si_3AlO_{10}(OH)_2$, containing 11 oxygens plus one H_2O. Biotite data are plotted in Figure 11.

Color	brown		green
Alys#	1	2	3
SiO_2	36.04	34.45	35.98
TiO_2	3.44	3.24	0.18
Al_2O_3	19.24	18.70	19.91
FeO	18.39	17.26	15.22
MnO	0.0	0.0	0.33
MgO	11.15	11.08	14.32
CaO	0.0	0.0	0.0
Na_2O	0.0	1.58	0.0
K_2O	8.78	8.60	8.63
Total	97.04	94.91	94.57
Formulae based on 11 oxygens			
Si	2.663	2.617	2.687
Al	1.337	1.383	1.313
Total	4.000	4.000	4.000
Al	0.338	0.291	0.439
Ti	0.191	0.185	0.010
Fe	1.137	1.097	0.950
Mn			0.021
Mg	1.228	1.255	1.594
Total	2.894	2.838	3.014
Ca			
Na		0.233	
K	0.828	0.834	0.822
Total	0.828	1.067	0.822
$\frac{Fe}{(Fe+Mg)}$	0.481	0.472	0.373
$\frac{K}{(K+Na)}$	1.000	0.782	1.000

Table 11. Electron microprobe analyses of biotite from sheared quartzite, sample 21. Fifteen analyses are given of biotite included in (I) and rimming (R) garnet as well as matrix biotite (M). Cation proportions are calculated on the basis of the formula, $(K,Na)(Fe,Mg)_3Si_3AlO_{10}(OH)_2$, containing 11 oxygens plus one H_2O. Biotite data are plotted on Figure 11.

Relative Position	(R)	(I)	(I)	(I)	(I)	(I)	(I)	(I)	(R)	(R)	(R)	(R)
Alys#	2	3	4	5	6	7	8	9	10	11	12	13
SiO_2	34.98	35.32	35.24	34.79	35.05	35.42	35.06	34.73	33.85	32.94	33.13	33.86
TiO_2	2.31	3.63	1.95	2.82	2.96	2.34	2.50	3.27	1.28	1.71	2.11	2.15
Al_2O_3	17.72	18.27	18.69	18.00	18.48	19.78	18.56	18.63	18.23	18.27	17.77	17.74
FeO	27.72	24.33	25.31	24.54	24.52	24.86	25.25	24.03	26.85	27.41	26.91	27.36
MnO	0.40	0.02	0.07	0.03	0.11	0.17	0.01	0.10	0.37	0.39	0.47	0.46
MgO	4.18	5.64	5.29	5.74	5.38	5.06	5.10	5.51	4.20	4.42	4.38	3.94
CaO	0.0	0.0	0.0	0.0	0.0	0.0	0.0	0.0	0.0	0.0	0.0	0.0
Na_2O	0.22	0.20	0.21	0.34	0.21	0.21	0.26	0.22	0.11	0.16	0.09	0.05
K_2O	9.64	9.57	9.83	9.51	9.38	9.69	9.64	9.52	9.74	9.70	9.43	9.74
Total	97.17	96.98	96.59	95.77	96.09	97.53	96.38	96.01	94.63	95.00	94.29	95.30
Formulae based on 11 oxygens												
Si	2.731	2.707	2.728	2.711	2.714	2.701	2.718	2.690	2.713	2.645	2.671	2.703
Al	1.269	1.293	1.272	1.289	1.286	1.299	1.282	1.310	1.287	1.355	1.329	1.297
Total	4.000	4.000	4.000	4.000	4.000	4.000	4.000	4.000	4.000	4.000	4.000	4.000
Al	0.363	0.359	0.435	0.365	0.402	0.480	0.415	0.392	0.436	0.375	0.361	0.373
Ti	0.136	0.209	0.114	0.165	0.172	0.134	0.146	0.190	0.077	0.104	0.128	0.129
Fe	1.811	1.561	1.639	1.600	1.589	1.587	1.638	1.557	1.801	1.842	1.816	1.828
Mn	0.026	0.001	0.005	0.002	0.007	0.011	0.001	0.007	0.025	0.027	0.032	0.031
Mg	0.487	0.645	0.611	0.667	0.621	0.575	0.590	0.637	0.502	0.529	0.526	0.469
Total	2.823	2.775	2.804	2.799	2.791	2.787	2.790	2.783	2.841	2.877	2.863	2.830
Ca												
Na	0.033	0.029	0.031	0.052	0.032	0.031	0.039	0.033	0.018	0.025	0.015	0.008
K	0.960	0.937	0.971	0.946	0.927	0.943	0.954	0.941	0.996	0.994	0.971	0.993
Total	0.993	0.966	1.002	0.998	0.959	0.974	0.993	0.974	1.014	1.019	0.986	1.001
$\frac{Fe}{(Fe+Mg)}$	0.788	0.708	0.728	0.706	0.719	0.734	0.735	0.710	0.782	0.777	0.775	0.796
$\frac{K}{(K+Na)}$	0.967	0.970	0.969	0.948	0.967	0.968	0.961	0.966	0.982	0.975	0.985	0.992

Table 11, continued.

	(M)	(R)	(R)
Alys#	14	15	16
SiO_2	34.22	33.15	33.88
TiO_2	2.60	2.42	2.22
Al_2O_3	17.61	17.70	17.48
FeO	26.64	27.00	27.47
MnO	0.24	0.20	0.27
MgO	4.66	4.60	4.54
CaO	0.0	0.0	0.0
Na_2O	0.18	0.06	0.18
K_2O	9.76	9.41	9.23
Total	95.91	94.54	95.27
Formulae based on 11 oxygens			
Si	2.701	2.663	2.699
Al	1.299	1.337	1.301
Total	4.000	4.000	4.000
Al	0.340	0.340	0.341
Ti	0.154	0.146	0.133
Fe	1.759	1.814	1.832
Mn	0.016	0.013	0.018
Mg	0.549	0.551	0.540
Total	2.818	2.864	2.864
Ca			
Na	0.027	0.010	0.028
K	0.983	0.965	0.938
Total	1.010	0.975	0.966
$\frac{Fe}{(Fe+Mg)}$	0.762	0.767	0.772
$\frac{K}{(K+Na)}$	0.973	0.990	0.971

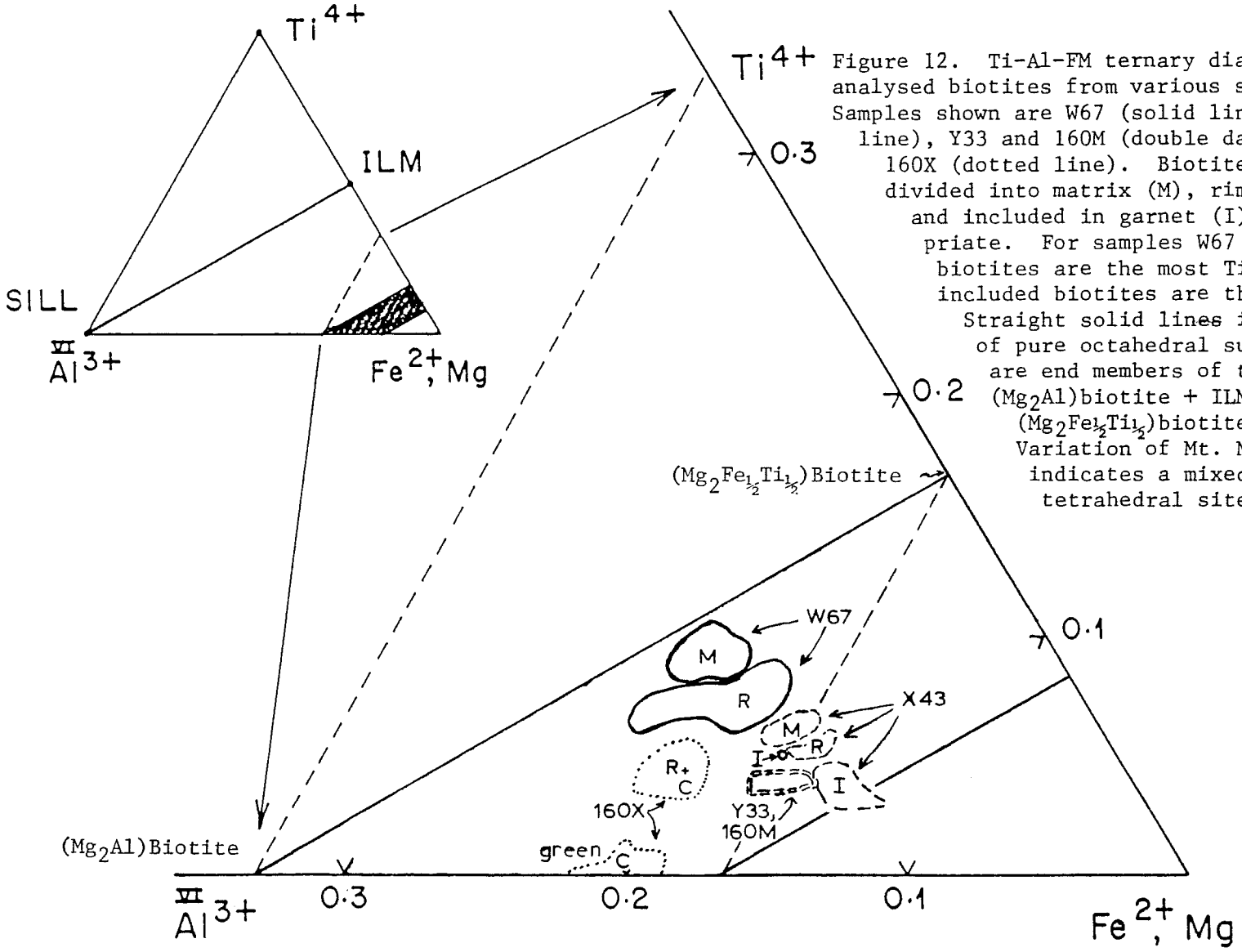

Figure 12. Ti-Al-FM ternary diagram showing analysed biotites from various samples. Samples shown are W67 (solid line), X43 (dashed line), Y33 and 160M (double dashed line), and 160X (dotted line). Biotites have been divided into matrix (M), rimming garnet (R), and included in garnet (I) where appropriate. For samples W67 and X43, matrix biotites are the most Ti-rich while included biotites are the least Ti-rich. Straight solid lines indicate direction of pure octahedral substitutions and are end members of the reaction: (Mg_2Al)biotite + ILM + QTZ = $(Mg_2Fe_{\frac{1}{2}}Ti_{\frac{1}{2}})$biotite + SILL. Variation of Mt. Mineral biotites indicates a mixed octahedral and tetrahedral site substitution.

variations within single grains are discussed according to rock type for each sample analysed. Zoning in almandine component is not shown on chemical maps of individual grains, however the change in almandine component from core to rim may be seen easily on ternary diagrams of individual grains.

Several analyses from sample 160M of reconstituted pelitic schist give ferric iron corrections for andradite component. This component was judged insignificant and the correction was discontinued through the remaining garnet analyses. Garnet structural formulae have been calculated based on the formula $(Fe,Mg,Mn,Ca)_3Al_2Si_3O_{12}$, containing 12 oxygens.

Interpretation of garnet zoning. Patterns of zoning in Mn and Ca can give useful information about garnet growth and resorption. Under normal prograde growth conditions, Mn and Ca are expected to decrease toward garnet rims (Hollister, 1966; Harte and Henley, 1966; Atherton, 1968; Crawford, 1977; Woodsworth, 1977; Yardley, 1977; Karabinos, 1984; and others).

In general, Ca and Mn are expected to increase along garnet rims if almandine-pyrope-rich garnet is being consumed (Chinner, 1962; Grant and Weiblen, 1971; Hess, 1971; deBethune and others, 1975; Hollister, 1977; Woodsworth, 1977; and others). This increase in Mn and/or Ca at garnet rims necessarily involves volume diffusion of these species within the remaining garnet structure. Volume diffusion within a cooling garnet appears to become ineffective below temperatures of about 500°C (Dempster, 1985). When consumption of garnet occurs below this temperature, an increase in Mn at garnet rims is not expected as garnet is consumed (Hollocher, 1981), because measurable diffusion would have ceased and Mn would necessarily have to have been incorporated in product phases.

If Ca and Mn content show different zoning patterns, the interpretation is more complex and must be considered in relation to other Ca or Mn-bearing mineral phases in the assemblage. If Ca increases as Mn decreases toward garnet rims, the garnet may have grown as plagioclase was consumed by the reaction 3 Anorthite = Grossular + 2 Sillimanite + Quartz (6) (Crawford, 1977; Hollister, 1977; Thompson, 1985). Thus, the Ca from the dissolving plagioclase is incorporated into the growing garnet and the normal decrease in Mn continues with growth. This phenomenon has been observed in garnet from the Monadnock, NH region (Thompson, 1985) and is produced by garnet growth rather than by volume diffusion within garnet. Zoning in grossular content may be controlled by other Ca-bearing minerals, such as epidote (Banno and Kurata, 1972; McAteer, 1976).

Empirical evidence suggests that pyrope-rich garnet is most stable at moderate to high metamorphic grades (Miyashiro, 1953). As metamorphic grade increases in rocks with the same assemblage, T(Mg) is greater than T(Fe) and both are greater than T(Mn) (Tracy and others, 1976; Loomis and Nimick, 1982). Therefore, low-grade garnet which is produced in a prograde sense is expected to have Fe-richer cores and Mg-richer rims.

Volume diffusion of Mn, Ca, Fe, and Mg within garnet becomes an important process at moderate to high metamorphic temperatures. Original growth zoning within garnet is expected to homogenize throughout individual grains as the rocks are heated to higher metamorphic grades (Atherton, 1968; Blackburn, 1969; Grant and Weiblen, 1971; Hess, 1971; Kretz, 1973; deBethune and others, 1975; Tracy and others, 1976; Anderson and Olimpio, 1977; Woodsworth, 1977; Yardley, 1977; Tracy and Deitsch, 1982; Karabinos, 1984; Dempster, 1985), beginning within the staurolite-sillimanite transition zone (Yardley, 1977), and should remain unzoned if not exposed to retrograde metamorphism and hydration.

When high-grade pelitic rocks containing this assemblage experience retrograde metamorphism with hydration, the matrix Fe-Mg minerals normally re-equilibrate to Fe-richer compositions with decreasing temperatures. If volume diffusion is still active within pyrope-rich garnet during retrograde metamorphism, the garnet rim should achieve equilibrium with the Fe-richer matrix assemblage. The chemical gradient produced near the garnet rim by re-equilibration with matrix minerals would initiate continued diffusion of Fe-inward and Mg-outward within the garnet to eliminate this gradient. Furthermore, if garnet is consumed during moderate- to high-temperature retrograde metamorphism where volume diffusion is active, garnet rims should also become enriched in Mn. This pattern has been reported by several authors (Grant and Weiblen, 1971; Kerr, 1981; Robinson and others, 1982) and has been attributed to volume diffusion during garnet-consumption and to re-equilibration of garnet rims with matrix minerals with decreasing temperature.

In sheared pelitic rock. One garnet from each of three thin sections of strongly sheared pelitic rock has been chemically mapped using electron microprobe analyses. Representative analyses of garnet core, intermediate, and rim composition s are given in Table 12 (see Appendix for complete listing of analyses). Each of these garnets contains a pyrope-rich core. Of these garnets, two contain maximum pyrope contents of 34 and 35 mole percent. Pyrope decreases in these garnets from core to rim as almandine and spessartine increase.

Garnet from sample 160XA (Figure 13) is 2 cm in length and is oblong in shape. Biotite, sillimanite, and quartz are concentrated in the matrix in the 2-3 mm surrounding this grain. It contains several cracks about 1 mm wide filled with green to brown biotite and it has abundant inclusions of quartz. A detailed chemical map of this grain was made with over 300 analyses. Thus careful study of garnet composition may be made regarding core and rim relations as well as the influence of bounding minerals. (See Figure 16 for chemical compositions plotted on an Fe-Mg-Mn ternary diagram).

Zoning in pyrope is dramatic from a maximum of 35% at the core to an average rim composition of 16 to 18 mole %. Decrease in pyrope content in garnet interiors appears to be controlled by position of biotite- and quartz-filled cracks, where composition may be as low as 8% pyrope. This produces extremely steep gradients in pyrope content, for

Table 12. Some electron microprobe analyses of garnet from sheared pelitic schist. Six analyses from each of three samples are given, representing core (Core), intermediate (Int), and rim (Rim) compositions. For sample 160X, garnet adjacent to brown (br) and green (gr) biotite occupying cracks within the garnet are also given. For samples W67B and X43A, garnet composition adjacent to a brown biotite inclusion are given. Cation proportions are calculated on the basis of the formula $Fe_3Al_2Si_3O_{12}$, containing 12 oxygens. Garnet data are plotted on an Fe-Mg-Mn ternary diagram in Figure 16.

Sample	160X						W67		
Relative Position	Core	Core	Int	Rim	adj gr bio	adj br bio	Core	Core	Int
Alys#	28	29	246	178	31	125	28	53	50
SiO_2	38.60	37.94	38.87	37.84	37.12	37.36	38.63	38.56	38.51
TiO_2	0.10	0.0	0.01	0.0	0.0	0.0	0.0	0.0	0.02
Al_2O_3	20.97	21.95	22.13	21.56	21.67	21.04	21.75	21.71	21.97
Cr_2O_3	0.09	0.0		0.0	0.0	0.02	0.04	0.01	0.04
FeO	30.28	29.68	29.61	34.03	35.11	35.20	31.05	31.49	32.11
MnO	0.57	0.55	0.59	0.93	1.16	0.98	1.65	1.50	1.38
MgO	9.82	8.18	7.53	4.57	3.58	3.87	5.87	5.90	5.54
CaO	1.14	1.20	1.20	1.27	1.40	1.41	1.17	1.17	1.19
Total	101.57	99.50	99.94	100.20	100.04	99.91	100.16	100.34	100.76
Formulae based on 12 oxygens									
Si	2.965	2.966	3.015	3.008	2.974	2.996	3.026	3.020	3.010
Al	1.899	2.023	2.024	2.020	2.047	1.990	2.009	2.005	2.025
Cr	0.005					0.001	0.002	0.001	0.002
Total	1.904					1.991	2.011	2.006	2.027
Ti	0.006		0.001						0.001
Fe	1.946	1.942	1.922	2.262	2.354	2.363	2.036	2.064	2.100
Mg	1.125	0.954	0.871	0.541	0.428	0.462	0.686	0.689	0.646
Mn	0.037	0.037	0.039	0.062	0.078	0.066	0.110	0.100	0.091
Ca	0.094	0.101	0.100	0.108	0.120	0.122	0.098	0.099	0.100
Total	3.208	3.034	2.933	2.973	2.980	3.013	2.930	2.952	2.938
Alm	60.77	64.01	65.55	76.08	78.99	78.43	69.49	69.92	71.50
Pyr	35.13	31.44	29.71	18.20	14.36	15.33	23.41	23.34	22.00
Spes	1.16	1.22	1.33	2.09	2.62	2.19	3.75	3.39	3.10
Gros	2.94	3.33	3.41	3.63	4.03	4.05	3.35	3.35	3.40
$\frac{Fe}{(Fe+Mg)}$	0.634	0.671	0.688	0.807	0.845	0.836	0.748	0.750	0.765

Table 12, continued.

Sample	W67			X43					
Relative Position	Rim	Rim	adj bio incl	Core	Core	Int	Rim	Rim	adj bio incl
Alys#	1A	22	13B	305	325C	315	306	328A	312
SiO_2	38.09	37.30	38.13	37.46	37.81	36.62	37.09	36.62	37.50
TiO_2	0.0	0.01	0.0						
Al_2O_3	21.60	21.07	21.80	20.88	21.39	20.69	20.40	21.35	20.82
Cr_2O_3	0.02	0.01	0.01						
FeO	32.93	33.29	32.33	31.35	30.16	35.47	34.81	34.28	33.70
MnO	2.21	2.61	1.50	0.25	0.66	1.42	1.43	1.73	0.57
MgO	3.83	3.69	5.45	8.57	9.26	5.13	5.88	4.87	7.16
CaO	1.39	1.69	1.28	0.30	0.20	0.24	0.73	1.46	0.41
Total	100.07	99.67	100.50	98.81	99.48	99.57	100.34	100.31	100.16
Formulae based on 12 oxygens									
Si	3.026	2.998	2.997	2.970	2.961	2.957	2.965	2.931	2.968
Al	2.023	1.998	2.021	1.951	1.974	1.970	1.922	2.014	1.942
Cr	0.001	0.001							
Total	2.024	1.999							
Ti		0.001							
Fe	2.189	2.239	2.127	2.078	1.975	2.396	2.327	2.294	2.231
Mg	0.454	0.442	0.639	1.013	1.081	0.618	0.701	0.581	0.845
Mn	0.149	0.178	0.100	0.017	0.044	0.097	0.097	0.117	0.038
Ca	0.118	0.146	0.108	0.026	0.017	0.020	0.062	0.125	0.059
Total	2.910	3.006	2.974	3.134	3.117	3.131	3.187	3.117	3.173
Alm	75.22	74.51	71.52	66.31	63.36	76.52	73.01	73.60	70.85
Pyr	15.60	14.71	21.49	32.32	34.68	19.74	22.00	18.64	26.83
Spes	5.12	5.92	3.36	0.54	1.41	3.10	3.04	3.75	1.21
Gros	4.06	4.86	3.63	0.83	0.55	0.64	1.95	4.01	1.21
$\frac{Fe}{(Fe+Mg)}$	0.828	0.835	0.769	0.672	0.646	0.795	0.768	0.798	0.725

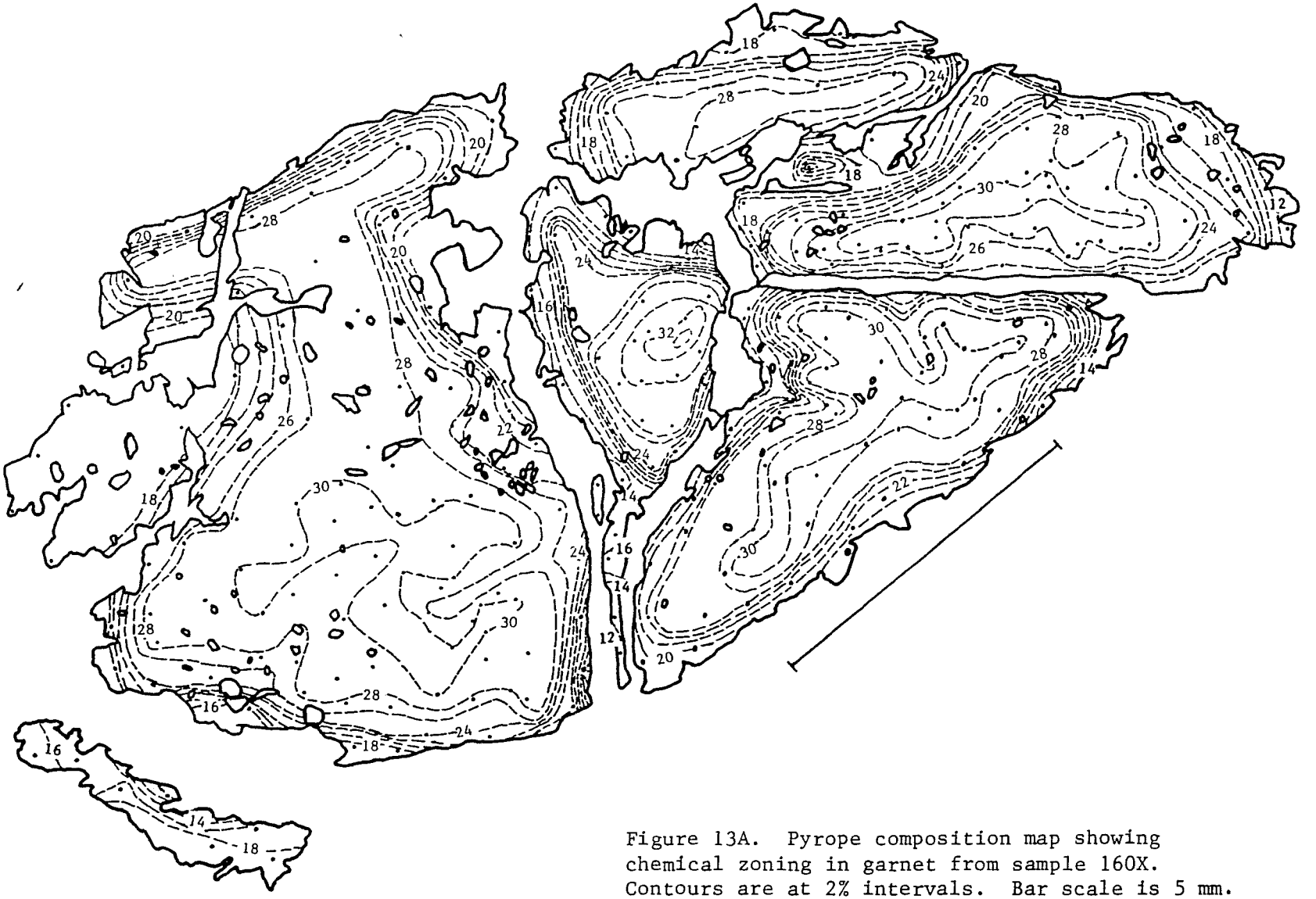

Figure 13A. Pyrope composition map showing chemical zoning in garnet from sample 160X. Contours are at 2% intervals. Bar scale is 5 mm.

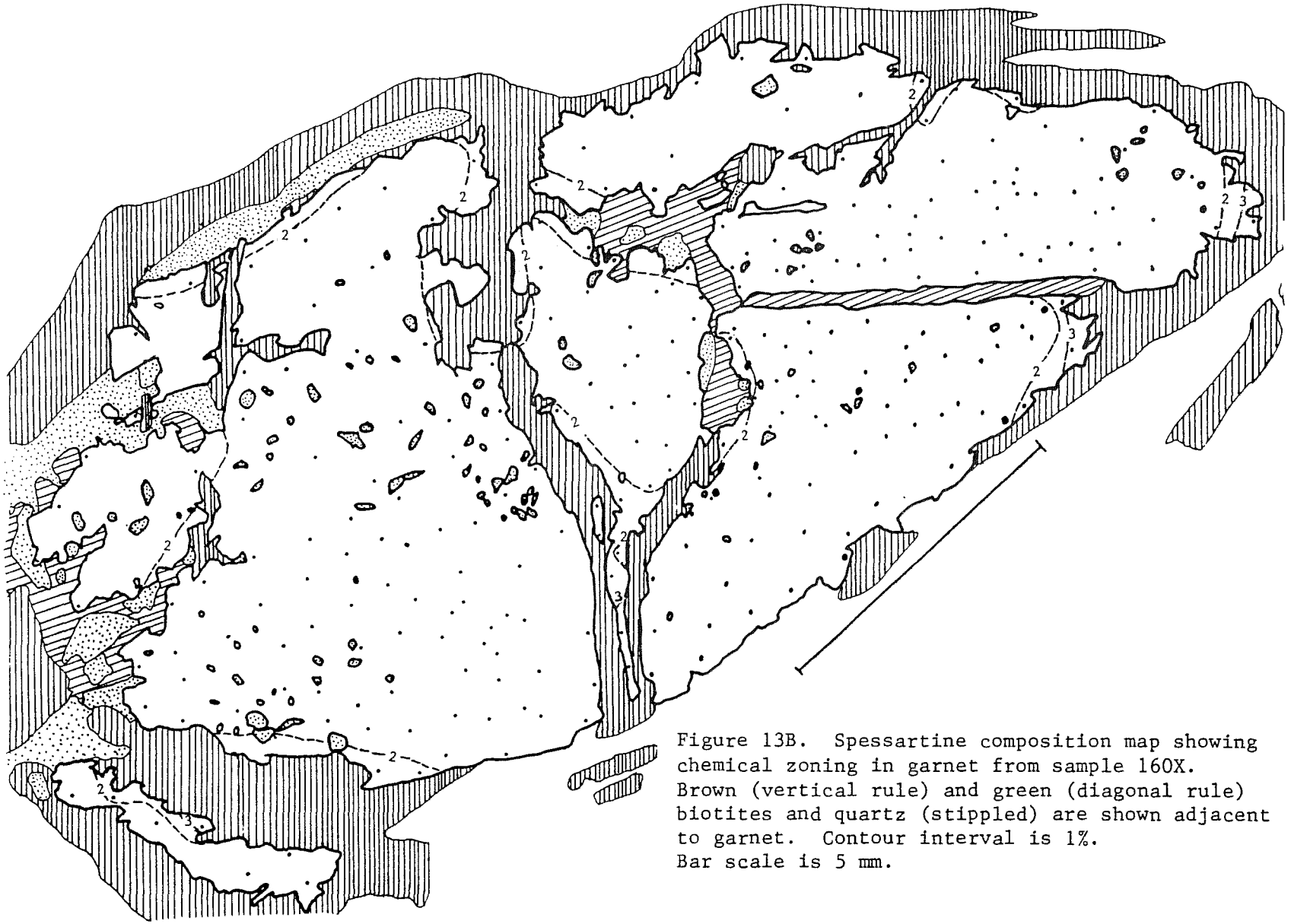

Figure 13B. Spessartine composition map showing chemical zoning in garnet from sample 160X. Brown (vertical rule) and green (diagonal rule) biotites and quartz (stippled) are shown adjacent to garnet. Contour interval is 1%. Bar scale is 5 mm.

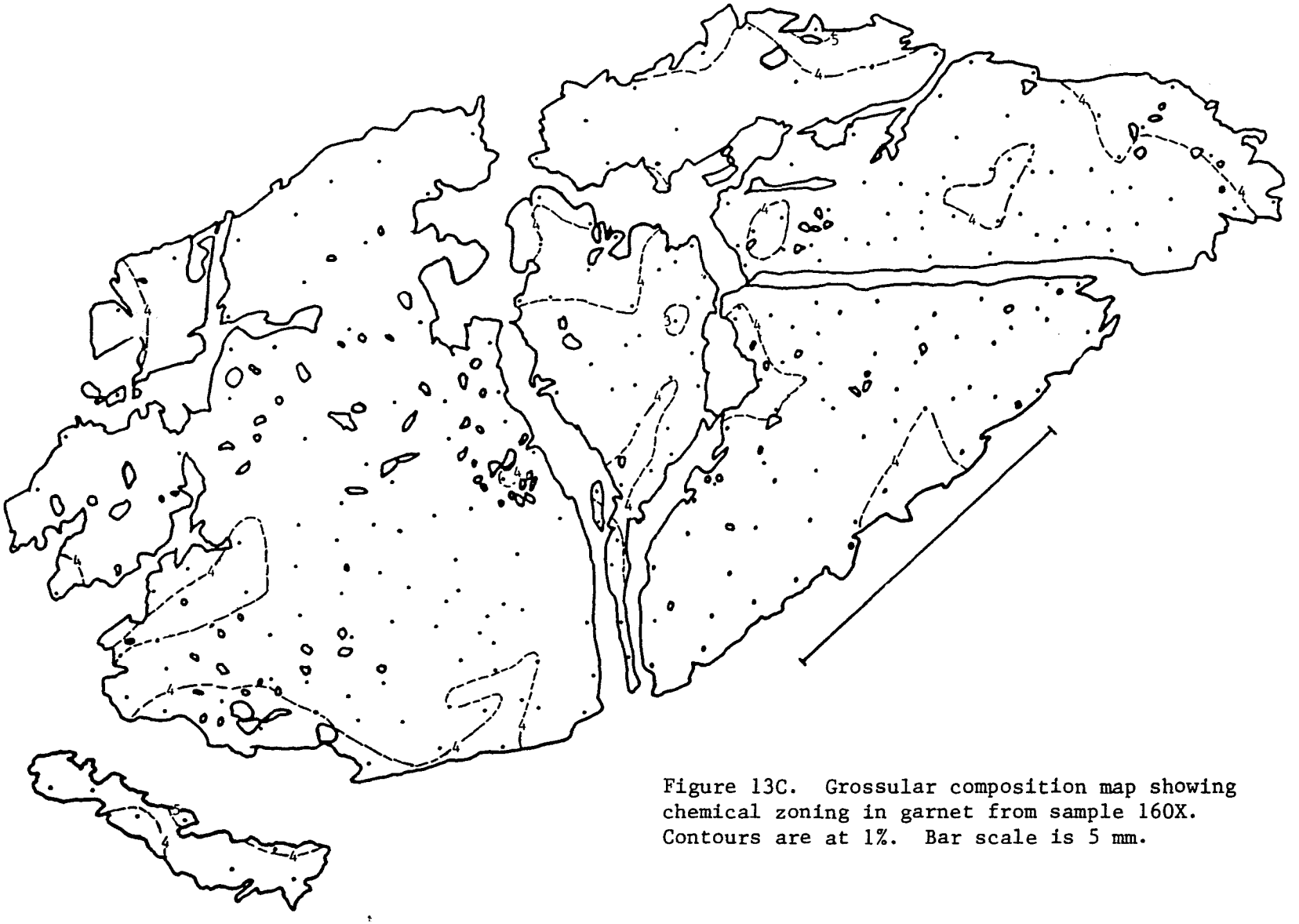

Figure 13C. Grossular composition map showing chemical zoning in garnet from sample 160X. Contours are at 1%. Bar scale is 5 mm.

example from 35% at the core to 8% adjacent to a biotite-filled crack, a distance of 0.5 mm. Several other areas in the interior of this grain achieve 30% pyrope, where composition may be nearly constant across 5 mm. Spessartine is constant at about 1% throughout most of the garnet with an increase to 2-3% along the rims and biotite-filled cracks, over a distance of about 0.5 mm. Biotite distribution (Figure 13B) at garnet rims and infilling cracks may relate to this increase in spessartine. Grossular content is slightly irregular, ranging from 2 to 3%. The compositional contours are apparently not affected by the presence or absence of brown biotite at garnet rims.

Garnet from sample W67B (Figure 14) is 7 mm in length and shows a classic porphyroclast shape. This grain is bordered by biotite, kyanite, quartz, and potassium feldspar. More than 80 analysis points yield good control on composition isopleths. The maximum pyrope content in this grain is 23% at the core which decreases to 14% pyrope at the rim. The interior of the grain is nearly constant in composition, creating a flat profile across the diameter. Spessartine and grossular are both constant at 4% in the core and both increase to 6% and 5%, respectively, along the outer 0.5 mm of the grain. The compositional contours are not influenced by bounding biotite grains. Several biotites are included in the interior of the garnet, but none are located within the maximum pyrope core.

The garnet contours are apparently not deflected with proximity to included biotites. Since no effort was made to cut exactly through centers of garnet grains, it is possible that this garnet gra in contains regions of higher pyrope content than observed. However, another garnet from the same rock sample studied by R.J. Tracy reflects a similar pattern of garnet compositions (Robinson and others, 1982).

Garnet from sample X43B (Figure 15) is 3 mm long and very irregular in shape. Abundant biotite with minor quartz surround this grain. One biotite is included in the garnet. This grain shows a maximum of 34% pyrope in the interior, and pyrope decreases irregularly to 20-16% along different rims. Rim composition does not appear to be affected by biotite proximity. Spessartine and grossular are at a minimum of 1% at the "core", or area of maximum pyrope content, and both increase outward to 3-4% at the rims. Compositional isopleths are not affected by included or bounding biotite.

Compositional maps of garnet from samples 160X and X43A show that chemical zoning does not always follow the shape of the garnet porphyroblast. The network of cracks through the garnet has obviously acted as an important conduit for element transport at a time when Fe-richer garnet was stable. In addition, garnet may have been consumed at temperatures below the limit of measurable diffusion, such that compositional contours are now truncated at garnet edges.

Ternary plots of Fe, Mg, and Mn content of these three garnets are shown in Figure 16. This figure illustrates the increase in Fe and Mn as Mg decreases from core to rim. Since samples 160XA (2 cm) and X43B (3 mm) both have the same range of pyrope zoning, the magnitude and steepness of pyrope zoning cannot be a simple function of garnet size.

Figure 14A. Pyrope composition map showing chemical zoning in garnet from sample W67B. Bounding minerals are biotite (ruled), quartz (unpatterned), and kyanite (two cleavages). Contour interval is 2%. Bar scale is 5 mm.

Figure 14B. Spessartine composition map showing chemical zoning in garnet from sample W67B. Bounding minerals are biotite (ruled), quartz (unpatterned), and kyanite (two cleavages). Contour interval is 1%. Bar scale is 5 mm.

Figure 14C. Grossular composition map showing chemical zoning in garnet from sample W67B. Bounding minerals are biotite (ruled), quartz (unpatterned), and kyanite (two cleavages). Contour interval is 1%. Bar scale is 5 mm.

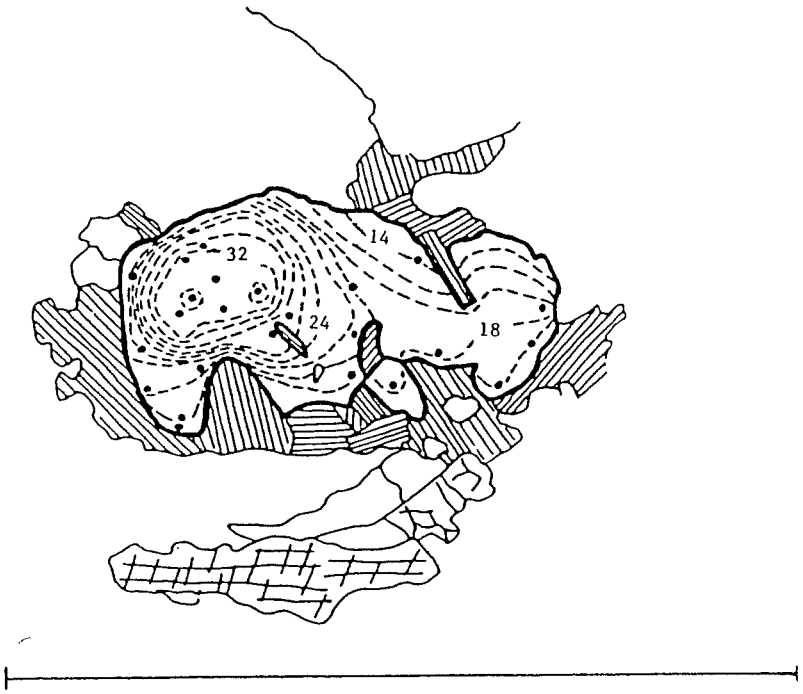

Figure 15A. Pyrope composition map showing chemical zoning in garnet from sample X43A. Bounding minerals are biotite (ruled), quartz (unpatterned), and kyanite (two cleavages). Contour interval is 2%. Bar scale is 5 mm.

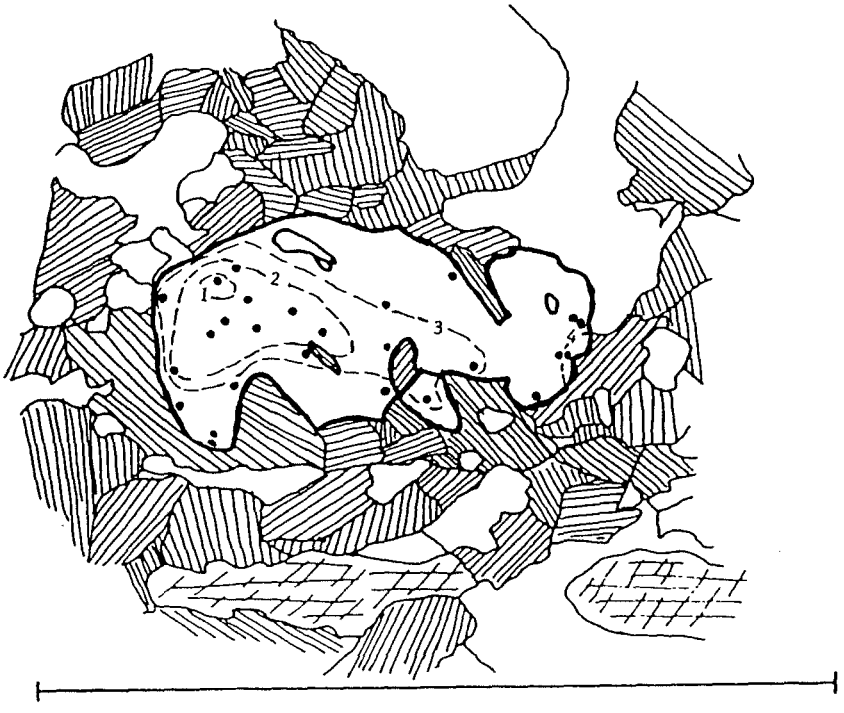

Figure 15B. Spessartine composition map showing chemical zoning in garnet from sample X43A. Bounding minerals are biotite (ruled), quartz (unpatterned), and kyanite (two cleavages). Contour interval is 1%. Bar scale is 5 mm.

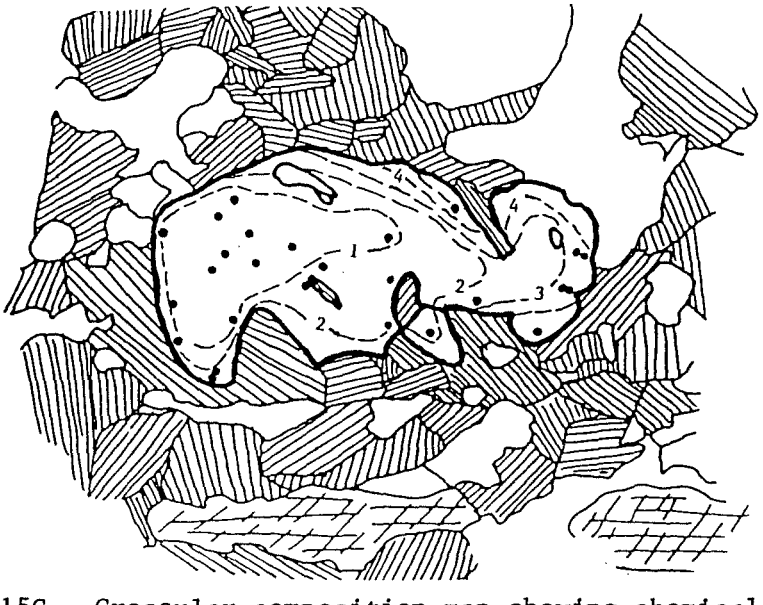

Figure 15C. Grossular composition map showing chemical zoning in garnet from sample X43A. Bounding minerals are biotite (ruled), quartz (unpatterned), and kyanite (two cleavages). Contour interval is 1%.

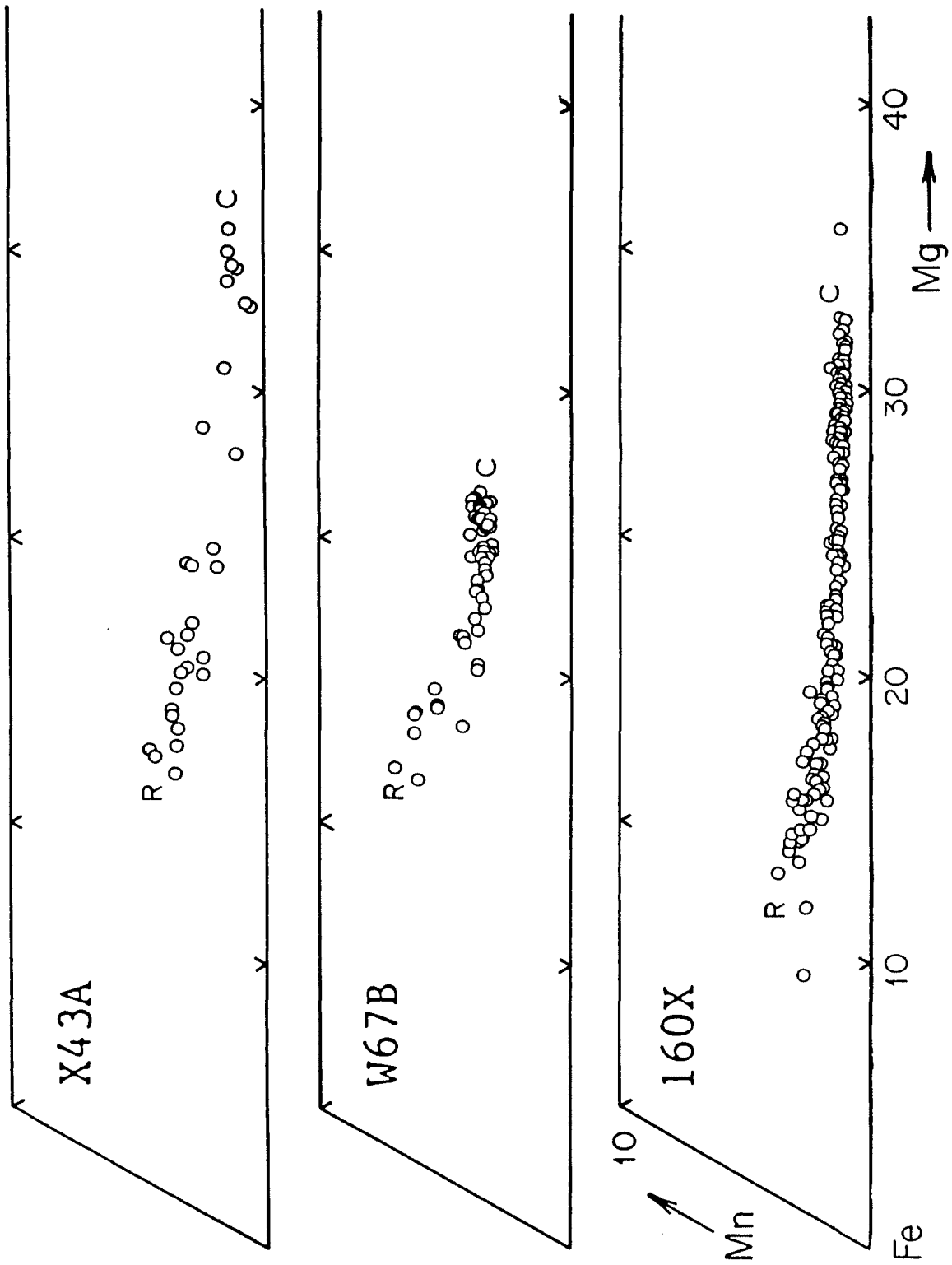

Figure 16. Fe-Mg-Mn ternary diagram showing analysed garnet compositions from sheared pelitic schists. Core (C) to rim (R) trend indicated toward increasing Mn and Fe, decreasing Mg.

Garnet from Mt. Mineral schist was probably pyrope-rich in composition and homogeneous at the peak of early metamorphism, due either to homogenization of original growth zoning or to garnet growth at high grade. Under lower temperature conditions of Acadian metamorphism, garnet rims would have re-equilibrated with the iron-richer matrix assemblage via cation diffusion, producing a pyrope-poorer rim composition. Penetration of the chemical gradient produced by iron-enriched rims, would continue to move toward garnet cores, controlled by the amount of time spent near peak Acadian temperatures and possibly by the magnitude of the chemical gradient at garnet rims. Minimum penetration of diffusion gradients is on the order of 1 mm in sample 160X and 0.5 mm in samples X43A and W67B. The core compositions must represent the minimum possible pyrope content attained during early granulite facies metamorphism.

The increase in both Mn and Ca toward garnet rims in these three grains (Figure 17), demonstrates that garnet-consuming reactions have taken place within the sheared schists at temperatures where measurable diffusion was active.

In reconstituted pelitic rock. Two samples from reconstituted pelitic schist have been selected for garnet compositional analyses (Table 13). Two garnets from sample 160M have been chemically mapped (Figure 18). Both garnets are approximately 3 mm in diameter. One garnet is equant and inclusion-free, whereas the other is very irregular in shape and contains abundant inclusions of quartz and biotite. The irregularly shaped garnet is weakly zoned with contours truncated at high angles to grain boundaries. This garnet is possibly a piece of what was once a much larger concentrically zoned porphyroblast. An example of such a garnet may be seen in sample X47, where a grain is separated into several smaller pieces by green-biotite-filled cracks.

The equant grain shows concentric zoning in which pyrope decreases from 16% at the core to 13% at the rim as almandine increases. Spessartine and grossular are relatively constant at 1% and 1-2%, respectively. Because Mn and Ca remain constant, it is probable that post growth temperatures were high enough to chemically homogenize this grain. The absence of a spessartine-enriched rim suggests that this grain was not involved in a garnet-consuming reaction. The spessartine component in this equant garnet is also noticeably low.

One garnet from sample Y33 has been chemically mapped (Figure 19). This garnet is euhedral and approximately 3 mm in diameter. The pyrope content varies from a maximum of 15% in the core to 11-12% at the rim. Spessartine and grossular also decrease from core to rim from 3% to 1.5% and 4% to 1.5%, respectively.

An Fe-Mg-Mn ternary diagram (Figure 20) illustrates the variation in garnet composition from core to rim for these two samples of reconstituted pelitic schist. Sample 160M has an almost constant spessartine content with increasing almandine from core to rim, whereas the spessartine component decreases from core to rim in the garnet from sample Y33. A further comparison of Fe-Mg-Ca and Fe-Mg-Mn ternary

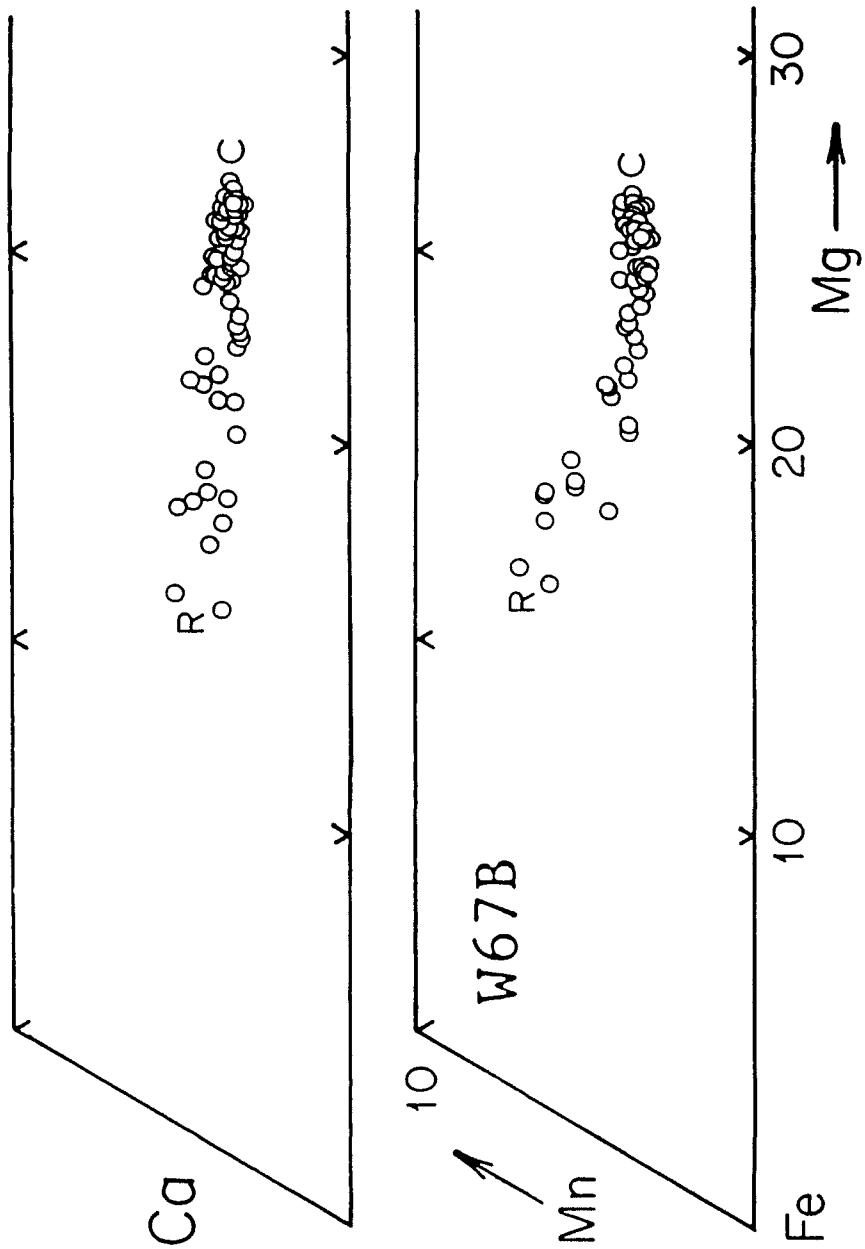

Figure 17. Comparison of Fe-Mg-Ca and Fe-Mg-Mn ternary diagrams for analysed garnet from sample W67B. Core (C) to rim (R) trend indicated. Spessartine and grossular contents both increase from core to rim, suggesting that consumption of almandine-pyrope has taken place.

Table 13. Some electron microprobe analyses of garnet from reconstituted pelitic schist. Five analyses from each sample are given representing core, intermediate (Int), and rim compositions. Cation proportions are calculated on the basis of the formula $Fe_3Al_2Si_3O_{12}$, containing 12 oxygens. Data are plotted in Figure 20.

Sample	160M					Y33				
Position	Core	Core	Int	Rim	Rim	Core	Core	Int	Rim	Rim
Alys#	30	33	38	25	28	22	36	3	1	23
SiO_2	36.76	36.88	37.13	37.35	37.61	37.03	35.87	36.41	35.79	36.48
Al_2O_3	20.25	20.75	20.94	20.89	21.55	20.29	20.94	20.92	20.39	20.13
FeO	36.24	36.53	37.26	37.89	37.46	36.84	36.22	36.85	38.43	39.02
Fe_2O_3	1.60	2.50	0.84							
MgO	3.64	3.67	3.43	3.56	3.32	3.60	3.99	3.89	3.08	2.96
MnO	0.43	0.34	0.39	0.23	0.43	1.11	1.08	1.04	0.98	0.59
CaO	0.59	0.51	0.48	0.55	0.50	0.85	0.67	0.71	0.64	0.48
Total	99.51	101.18	100.47	100.47	100.87	99.72	98.77	99.82	99.31	99.66
Formulae based on 12 oxygens										
Si	2.982	2.947	2.983	2.994	3.002	3.003	2.936	2.951	2.944	2.980
Al	1.937	1.956	1.984	1.975	2.028	1.940	2.020	1.998	1.977	1.938
Fe	2.558	2.593	2.555	2.542	2.502	2.498	2.479	2.497	2.644	2.665
Mg	0.441	0.438	0.410	0.426	0.395	0.435	0.487	0.470	0.378	0.361
Mn	0.030	0.023	0.027	0.016	0.029	0.076	0.075	0.071	0.068	0.041
Ca	0.051	0.044	0.044	0.047	0.043	0.074	0.058	0.062	0.056	0.042
Total	3.080	3.098	3.036	3.031	2.969	3.083	3.099	3.100	3.146	3.109
Alm	83.05	83.70	84.24	83.87	84.27	81.02	79.99	80.55	84.04	85.72
Pyr	14.32	14.14	13.52	14.05	13.30	14.11	15.72	15.16	12.02	11.61
Spes	0.97	0.74	0.89	0.53	0.98	2.47	2.42	2.29	2.16	1.32
Gros	1.66	1.42	1.35	1.55	1.45	2.40	1.87	2.00	1.78	1.35
$\frac{Fe}{(Fe+Mg)}$	0.853	0.855	0.862	0.856	0.864	0.852	0.836	0.842	0.875	0.881

Figure 18A. Pyrope composition map showing chemical zoning in garnet from sample 160M. Bounding minerals are biotite (fine rule), muscovite (coarse rule), quartz (unpatterned), and staurolite (stippled). Contour interval is 1%. Bar scale is 5 mm.

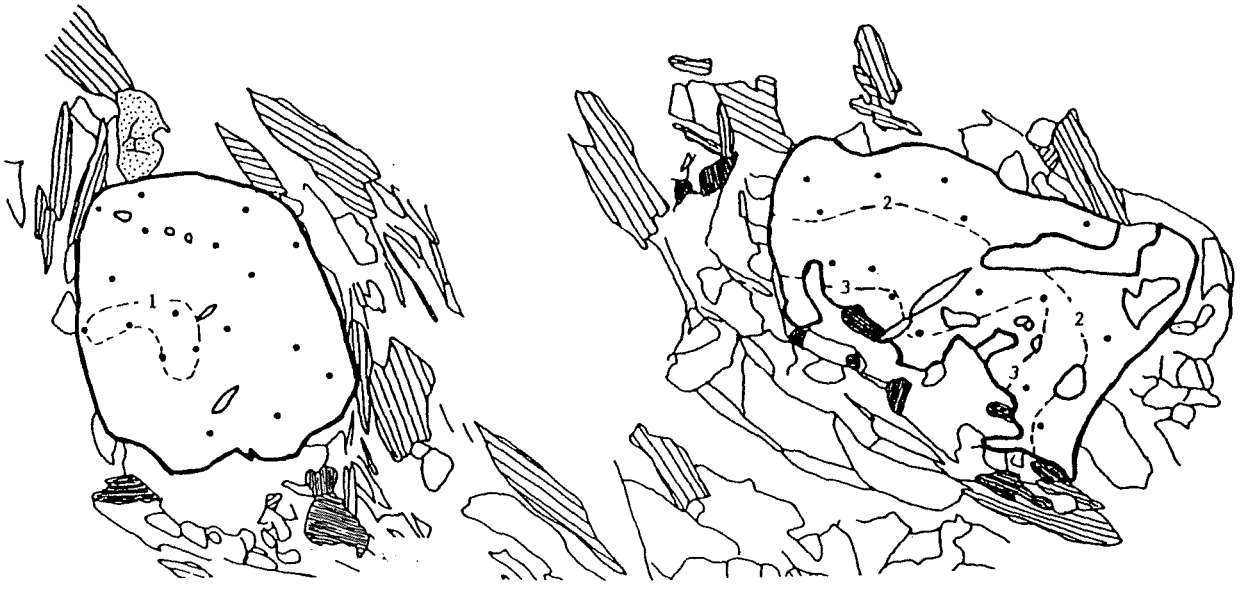

Figure 18B. Spessartine composition map showing chemical zoning in garnet from sample 160M. Bounding minerals are biotite (fine rule), muscovite (coarse rule), quartz (unpatterned), and staurolite (stippled). Contour interval is 1%.

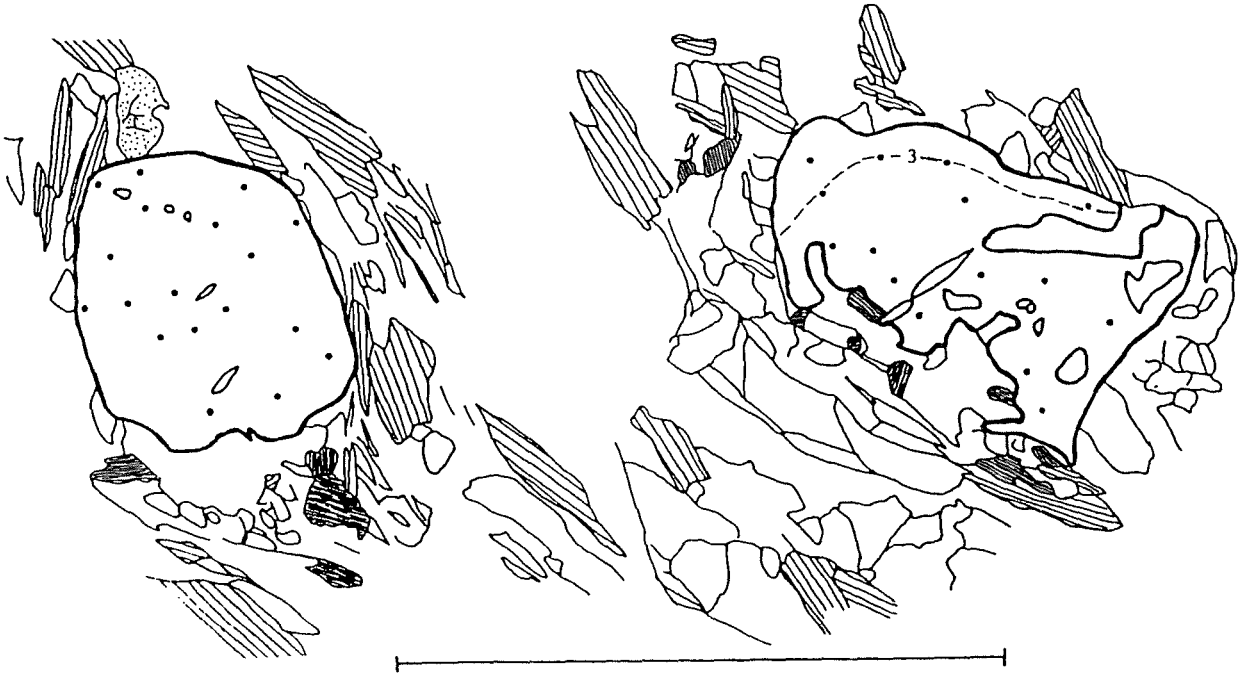

Figure 18C. Grossular composition map showing chemical zoning in garnet from sample 160M. Bounding minerals are biotite (fine rule), muscovite (coarse rule), quartz (unpatterned), and staurolite (stippled). Contour interval is 1%. Bar scale is 5 mm.

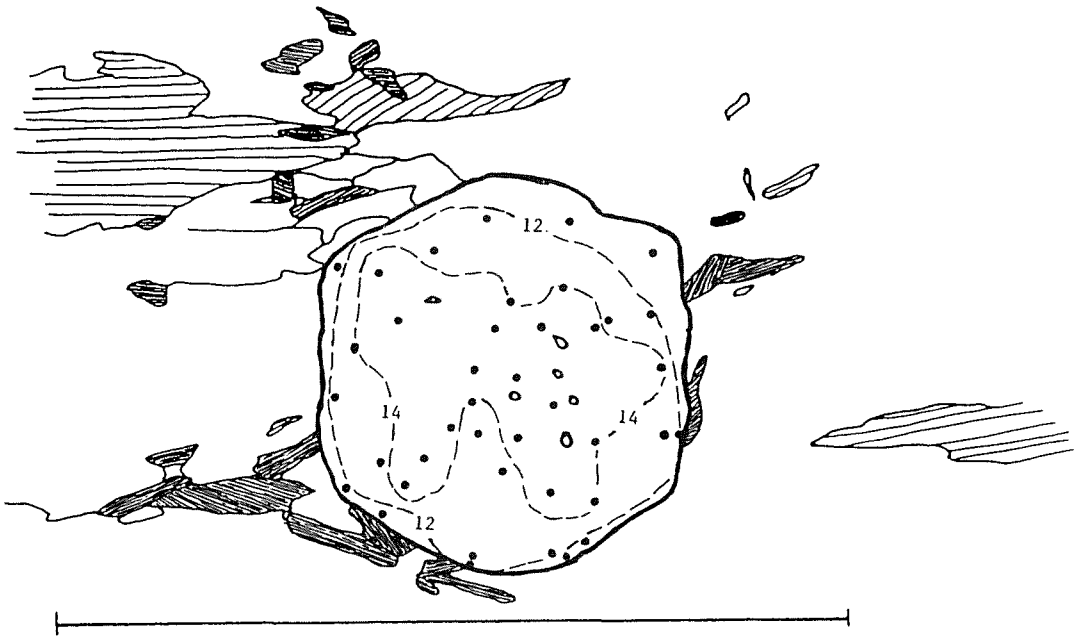

Figure 19A. Pyrope composition map showing chemical zoning in garnet from sample Y33. Bounding minerals are biotite (fine rule), muscovite (coarse rule), quartz (unpatterned). Contour interval is 2%. Bar scale is 5 mm.

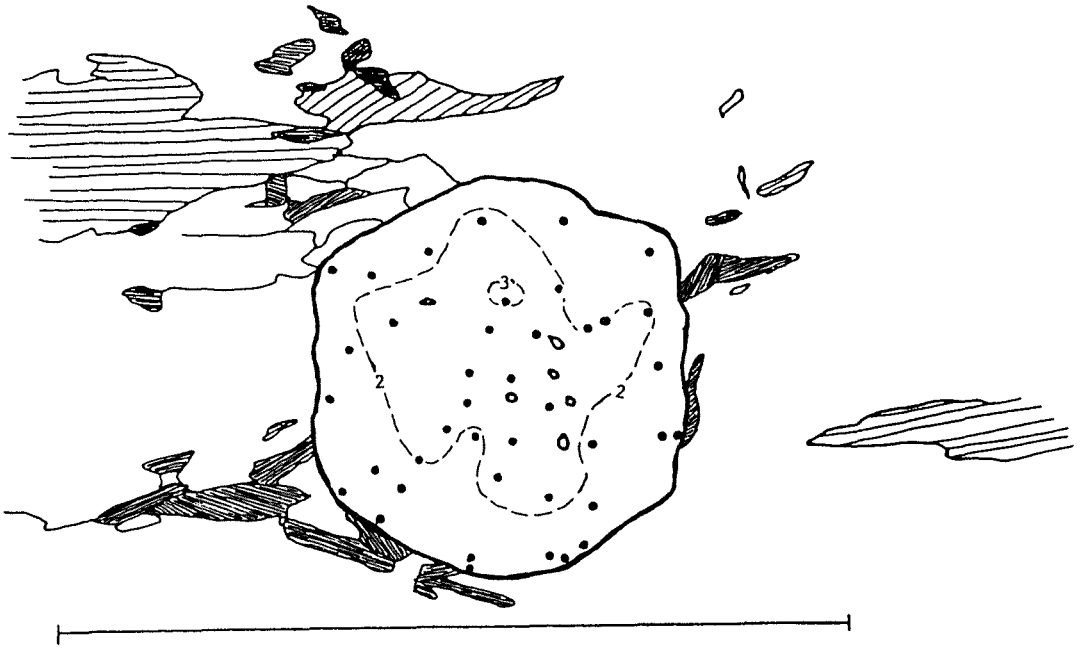

Figure 19B. Spessartine composition map showing chemical zoning in garnet from sample Y33. Bounding minerals are biotite (fine rule), muscovite (coarse rule), and quartz (unpatterned). Contour interval is 1%. Bar scale is 5 mm.

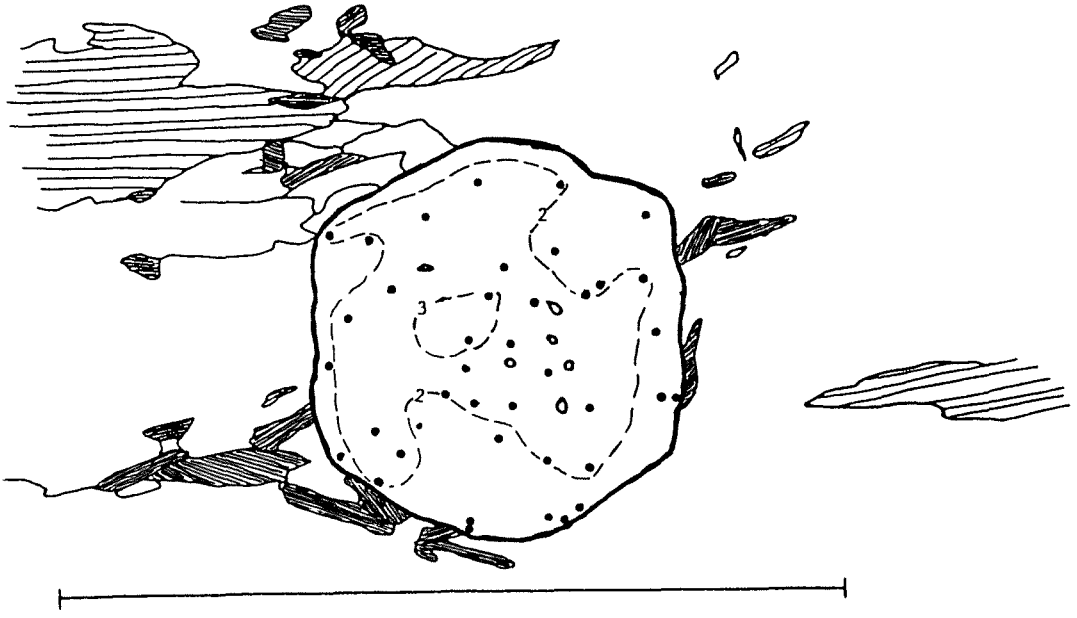

Figure 19C. Grossular composition map showing chemical zoning in garnet from sample Y33. Bounding minerals are biotite (fine rule), muscovite (coarse rule), and quartz (unpatterned). Contour interval is 1%. Bar scale is 5 mm.

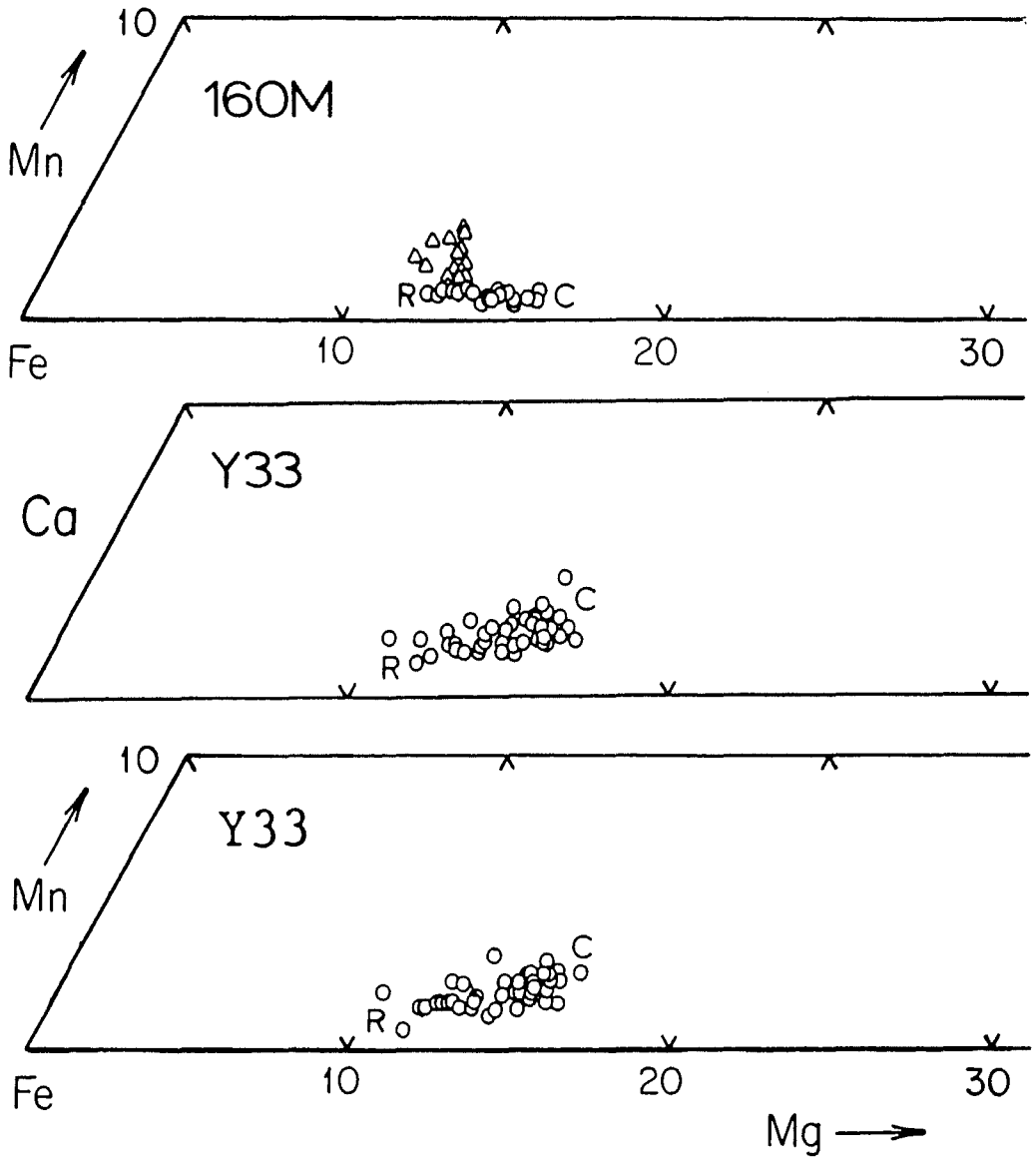

Figure 20. Fe-Mg-Mn and Fe-Mg-Ca ternary diagrams showing analysed garnet from two samples of reconstituted pelitic schist. Core to rim trend indicated.

diagrams (Figure 20) shows that both Ca and Mn decrease from core to rim in sample Y33.

The weakly-zoned garnet from sample 160M probably represents fully re-equilibrated relics from the early metamorphism. Garnet from sample Y33 is the only one of those analysed which decreases in Mn-, Mg-, and Ca- content as the Fe-content increases from core to rim, demonstrating that this garnet grew in the recrystallized rock. Euhedral, growth-zoned garnets from the Mt. Mineral formation were probably produced during Acadian kyanite-zone metamorphism. Zoning within garnets which grew before the early sillimanite-orthoclase metamorphism would have become completely homogenized during this high-grade event. Therefore only garnet which grew at much lower temperatures after this early event could preserve a growth zoning profile.

In sheared pegmatite. One garnet from a sample of sheared pegmatite (M22A) has been chemically mapped (Figure 21). Analyses from this sample are given in Table 14. This garnet is approximately 2 cm in length and oblong in shape with very irregular edges. Brown to green biotite locally rims the grain. Some areas of the grain contain abundant inclusions of sillimanite needles. Except in the outer 0.5 mm, pyrope content of this garnet is relatively constant, varying from 30-33% pyrope. Pyrope decreases variably at the rims to 22-28% pyrope. Although the analysis points are sparse in places, it appears that some of the pyrope contours are truncated at garnet margins.

This grain was probably homogeneous at the peak of early high-grade metamorphism, at 30-33% pyrope. The chemical gradients at the margins of this grain are probably due to volume diffusion of Fe-Mg at the garnet rims during somewhat lower temperature conditions. Under lower temperature conditions, the matrix assemblages probably became more iron-rich, possibly by the continuous reaction GAR + KSP + H_2O = BIO + SILL + QTZ (1). Garnet rims would continually re-equilibrate with matrix minerals toward more iron-rich compositions, promoting Fe-Mg diffusion within the pyrope-richer garnet interior. The truncated compositional contours may be due to continued garnet consumption at temperatures below the limit of effective volume diffusion.

The outer 0.5 mm of the grain is variably zoned with increases in grossular content, at several places up to 6% (Figure 22). This sharp increase in grossular at the rim is probably due to consumption of pyrope. Plagioclase may be involved in a reaction which would produce grossular and sillimanite, for example, 3 Anorthite = Grossular + 2 Sillimanite + Quartz. This reaction could have taken place at the same time that the pyrope component of the garnet was being consumed and either interpretation agrees with the observed pattern of garnet zoning.

The spessartine content of this grain ranges from very low to undetected. No increase in Mn content is observed at garnet rims. Although Mn-enriched rims are expected where garnet-consuming reactions occur, the lack of Mn-enrichment here may be due to the extremely low spessartine content throughout the grain.

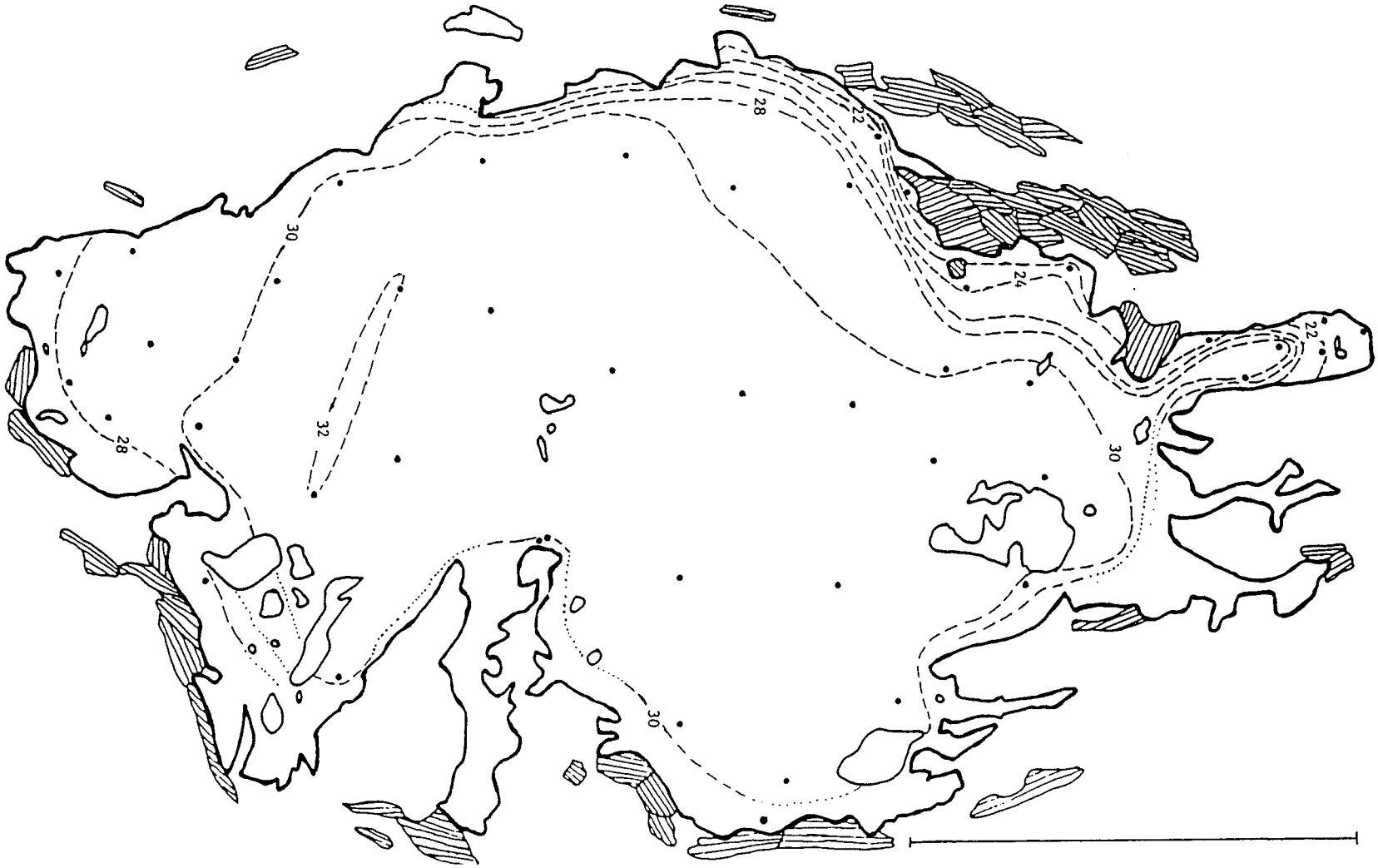

Figure 21A. Pyrope composition map showing chemical zoning in garnet from sample M22A. Bounding mineral is biotite (ruled). Contour interval is 2%. Bar scale is 5 mm.

Figure 21B. Grossular composition map showing chemical zoning in garnet from sample M22A. Bounding biotite is ruled. Contour interval is 1%. Bar scale is 5 mm.

Table 14. Selected electron microprobe analyses of garnet from sheared pegmatite. Eight analyses from sample M22A are given representing core, intermediate (Int), rim, and irregularly-shaped rim (Irreg) compositions. Cation proportions are calculated on the basis of the formula, $Fe_3Al_2Si_3O_{12}$, containing 12 oxygens. Data are plotted in Figure 23.

Position	Core	Core	Int	Int	Rim	Rim	Irreg	Irreg
Alys#	21	28	19	26	11	25	2	5
SiO_2	37.38	37.35	37.84	36.71	37.27	36.68	36.87	37.58
Al_2O_3	21.95	21.82	20.92	21.29	20.67	20.92	21.18	21.15
FeO	30.62	31.21	30.95	30.80	35.67	34.50	35.42	32.22
MnO	0.0	0.0	0.23	0.0	0.0	0.0	0.35	0.27
MgO	8.50	7.98	8.37	8.61	4.94	6.35	4.36	5.96
CaO	1.58	1.27	1.29	1.55	1.40	1.31	1.90	2.13
Total	100.03	99.63	99.60	98.96	99.95	99.76	100.08	99.31
Formulae based on 12 oxygens								
Si	2.921	2.937	2.975	2.912	2.986	2.934	2.957	2.989
Al	2.022	2.022	1.939	1.990	1.952	1.971	2.002	1.982
Fe	2.001	2.052	2.035	2.043	2.390	2.307	2.376	2.142
Mg	0.991	0.936	0.982	1.018	0.590	0.757	0.521	0.707
Mn			0.015				0.024	0.018
Ca	0.132	0.107	0.108	0.131	0.120	0.112	0.164	0.182
Total	3.124	3.095	3.140	3.192	3.100	3.176	3.085	3.049
Alm	64.05	66.30	64.81	64.00	77.10	72.64	77.02	70.25
Pyr	31.72	30.24	31.27	31.89	19.03	23.83	16.90	23.19
Spes			0.48				0.78	0.59
Gros	4.23	3.46	3.44	4.11	3.87	3.53	5.32	5.97
$\frac{Fe}{(Fe+Mg)}$	0.669	0.687	0.675	0.667	0.802	0.753	0.820	0.752

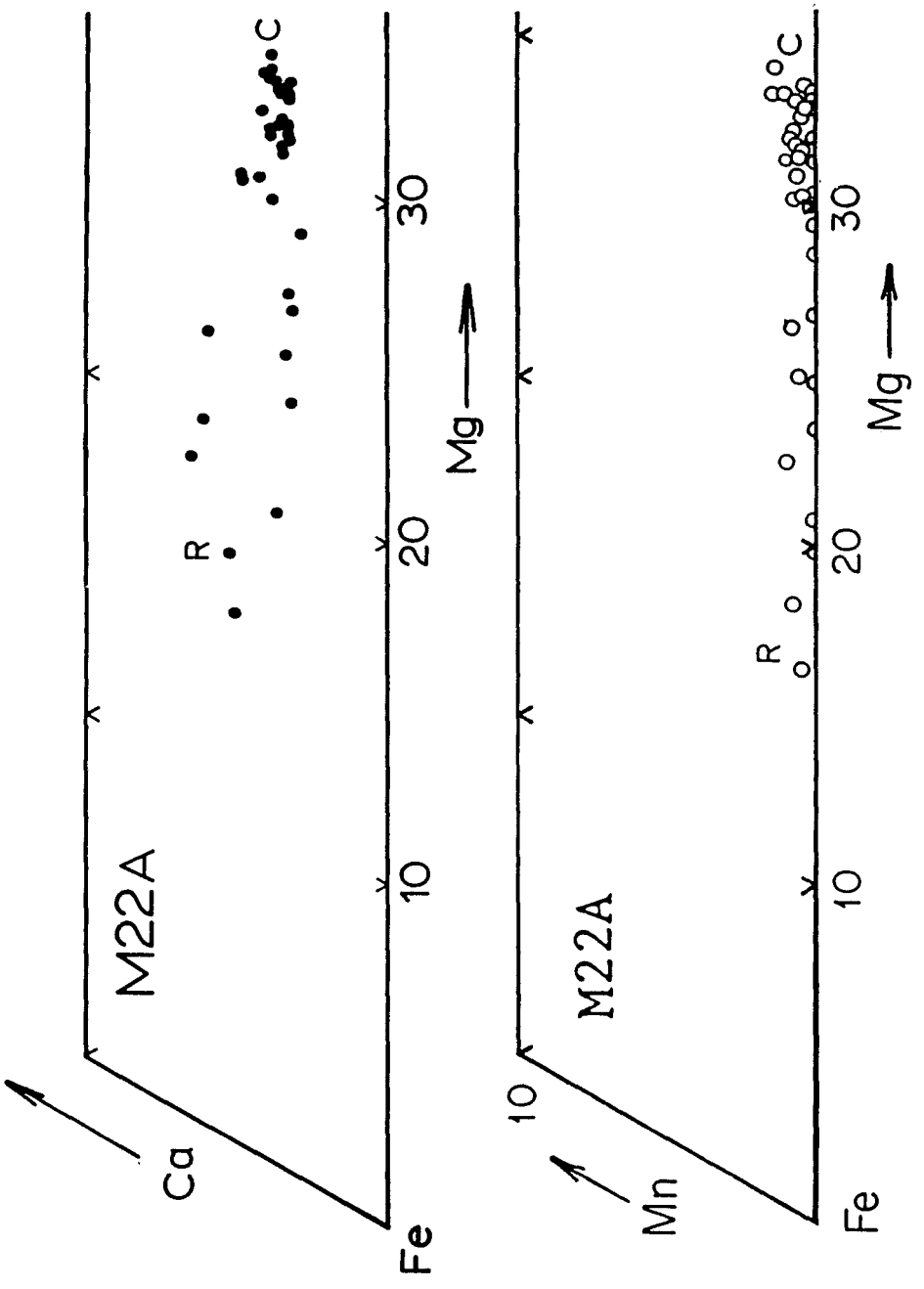

Figure 22. Fe-Mg-Mn and Fe-Mg-Ca ternary diagrams for analysed garnet from sample M22A. Grossular increases from core (C) to rim (R) while spessartine is low throughout the grain.

In sheared quartzite. One garnet from the sheared quartzite sample (M21) has been chemically mapped (Figure 23) and the analyses are given in Table 15. This grain is 3 mm in length, oblong and irregular in shape. Several inclusions of quartz and biotite are present. Bounding phases include quartz, biotite, and muscovite. The almandine and pyrope contents in this grain decrease at nearly constant Fe/(Fe+Mg) ratio from core to rim. The spessartine content increases markedly from 3% at the core to 15% at the rim (Figure 24). Grossular zoning is irregular in this garnet, ranging from 6 to 9%, making any interpretation inconclusive.

The dramatic increase in Mn content from core to rim is interpreted as evidence for a strong garnet-consuming reaction in this sample. Since aluminosilicate is not present in the quartzite assemblage, a garnet-consuming reaction consistent with the observed assemblage is: GAR + KSP + H_2O = BIO + MUSC + QTZ.

Summary of garnet zoning. Analyzed garnets from all seven samples are shown together for comparison on an Fe-Mg-Mn ternary diagram (Figure 25). Zoning within garnets from all samples, except sample Y33 of reconstituted pelitic schist, are interpreted to have been produced by volume diffusion during lower temperature re-equilibration and consumption of garnet following chemical homogenization produced during early high-grade metamorphism. Volume diffusion is believed to have been active only down to about 500 C (Dempster, 1985). Zoning in garnet from sample Y33 of reconstituted schist is believed to result from garnet growth as the rock cooled from Acadian kyanite-zone conditions.

Kyanite and Sillimanite

Several grains of kyanite and sillimanite from sheared pelitic rocks have been analysed (Table 16). Structural formulae have been calculated on the basis of the formula Al_2SiO_5. Iron content in both kyanite and sillimanite does not exceed 0.8 weight percent.

Staurolite

Two grains of staurolite, approximately 1 mm in diameter, from reconstituted schist (160M) have been chemically mapped. Compositional analyses are given in Table 17. Cation proportions have been calculated on the basis of the formula $(Fe,Al,Ti,Zn)_2(Al,Mg)_8(Al,Fe)_{0.7}(Fe,Mn)_{0.12}(Si,Al)_4O_{22}(OH)_2$, using the method of Hollocher (1981). Zinc content ranges from 0.12 to 0.15 Zn per 23 oxygens or 1.1 to 1.5 wt %. Titanium content is less than 0.08 Ti per 23 oxygens. The staurolite does not appear to be chemically zoned. Average Fe/(Fe+Mg) is 0.833, a value typical of other staurolite-kyanite-biotite zone schists in the region (Hollocher, 1981).

Tourmaline

Tourmaline from sample 160M is strongly zoned optically and one might expect to observe analogous zoning in composition. Cation

Table 15. Some electron microprobe analyses of garnet from sheared quartzite. Ten analyses from sample M21 are given representing core, intermediate (Int), and rim compositions. Cation proportions are calculated on the basis of the formula, $Fe_3Al_2Si_3O_{12}$, containing 12 oxygens. Data are plotted in Figure 25.

	Core	Core	Core	Core	Int	Int	Int	Rim	Rim	Rim
Alys#	8	9	21	33	19	27	35	1	6	11
SiO_2	35.53	36.60	35.23	35.99	35.51	37.05	35.56	35.85	36.30	37.88
TiO_2	0.02	0.0	0.0	0.01	0.0	0.0	0.0	0.0	0.0	0.0
Al_2O_3	20.97	21.14	21.00	20.73	21.20	21.04	20.84	20.84	20.99	20.86
FeO	38.18	38.04	37.30	38.42	38.14	36.33	38.24	33.28	35.10	33.39
MnO	1.23	1.19	1.54	1.38	1.90	2.07	1.09	6.04	4.92	5.83
MgO	1.11	1.19	1.13	1.00	1.30	1.33	0.95	1.13	1.09	1.09
CaO	2.73	2.66	3.10	3.17	2.25	2.96	3.17	3.03	2.48	2.74
Total	99.77	100.82	99.30	100.70	100.30	100.78	99.85	100.17	100.88	101.79
Formulae based on 12 oxygens										
Si	2.925	2.966	2.913	2.940	2.911	2.992	2.929	2.937	2.952	3.029
Al	2.036	2.020	2.047	1.998	2.049	2.003	2.024	2.014	2.013	1.967
Ti	0.001			0.001						
Fe	2.631	2.580	2.580	2.627	2.616	2.455	2.635	2.281	2.389	2.234
Mg	0.136	0.143	0.140	0.122	0.158	0.160	0.117	0.138	0.132	0.130
Mn	0.086	0.082	0.108	0.095	0.132	0.142	0.076	0.420	0.339	0.395
Ca	0.241	0.231	0.274	0.278	0.197	0.256	0.280	0.266	0.216	0.235
Total	3.095	3.036	3.102	3.123	3.103	3.013	3.108	3.105	3.076	2.994
Alm	85.04	84.98	83.17	84.15	84.31	81.48	84.78	73.46	77.67	74.62
Pyr	4.39	4.71	4.52	3.91	5.09	5.31	3.76	4.44	4.29	4.34
Spes	2.78	2.70	3.48	3.04	4.25	4.71	2.45	13.53	11.02	13.19
Gros	7.79	7.61	8.83	8.90	6.35	8.50	9.01	8.57	7.02	7.85
$\frac{Fe}{(Fe+Mg)}$	0.951	0.947	0.949	0.956	0.943	0.939	0.957	0.943	0.948	0.945

Figure 23A. Pyrope composition map showing chemical zoning in garnet from sample M21. Bounding minerals are biotite (fine rule), muscovite (coarse rule), and quartz (unpatterned). Contour interval is 1% and hatches point toward higher concentration. Bar scale is 5 mm.

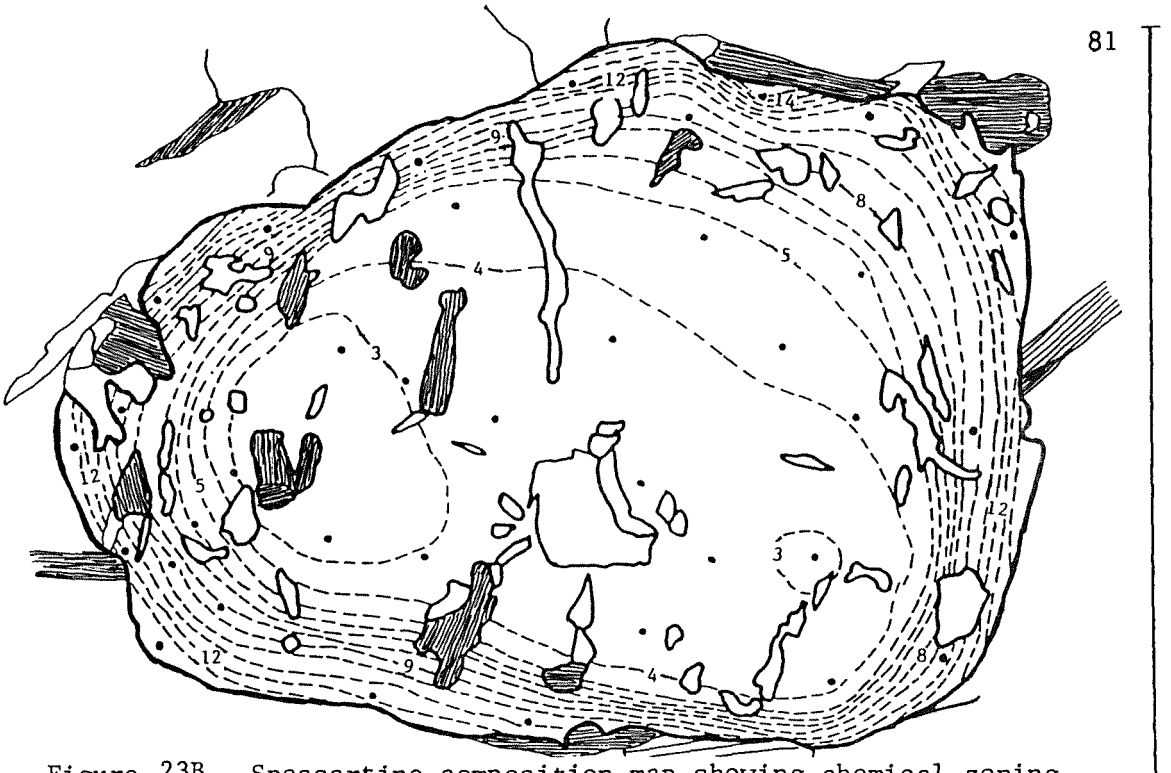

Figure 23B. Spessartine composition map showing chemical zoning in garnet from sample M21. Bounding minerals are biotite (fine rule), muscovite (coarse rule), and quartz (unpatterned). Contour interval is 1%. Bar scale is 5 mm.

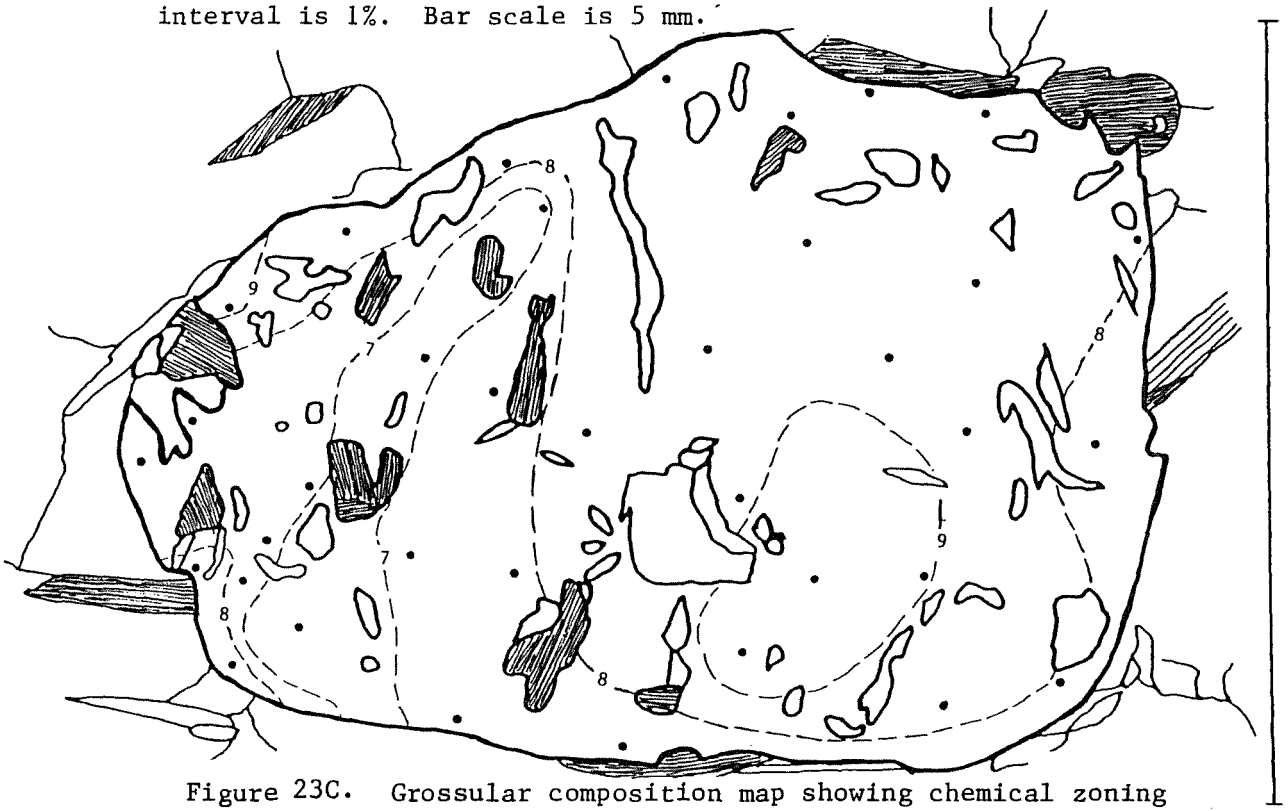

Figure 23C. Grossular composition map showing chemical zoning in garnet from sample M21. Bounding minerals are biotite (fine rule), muscovite (coarse rule), and quartz (unpatterned). Contour interval is 1%. Bar scale is 5 mm.

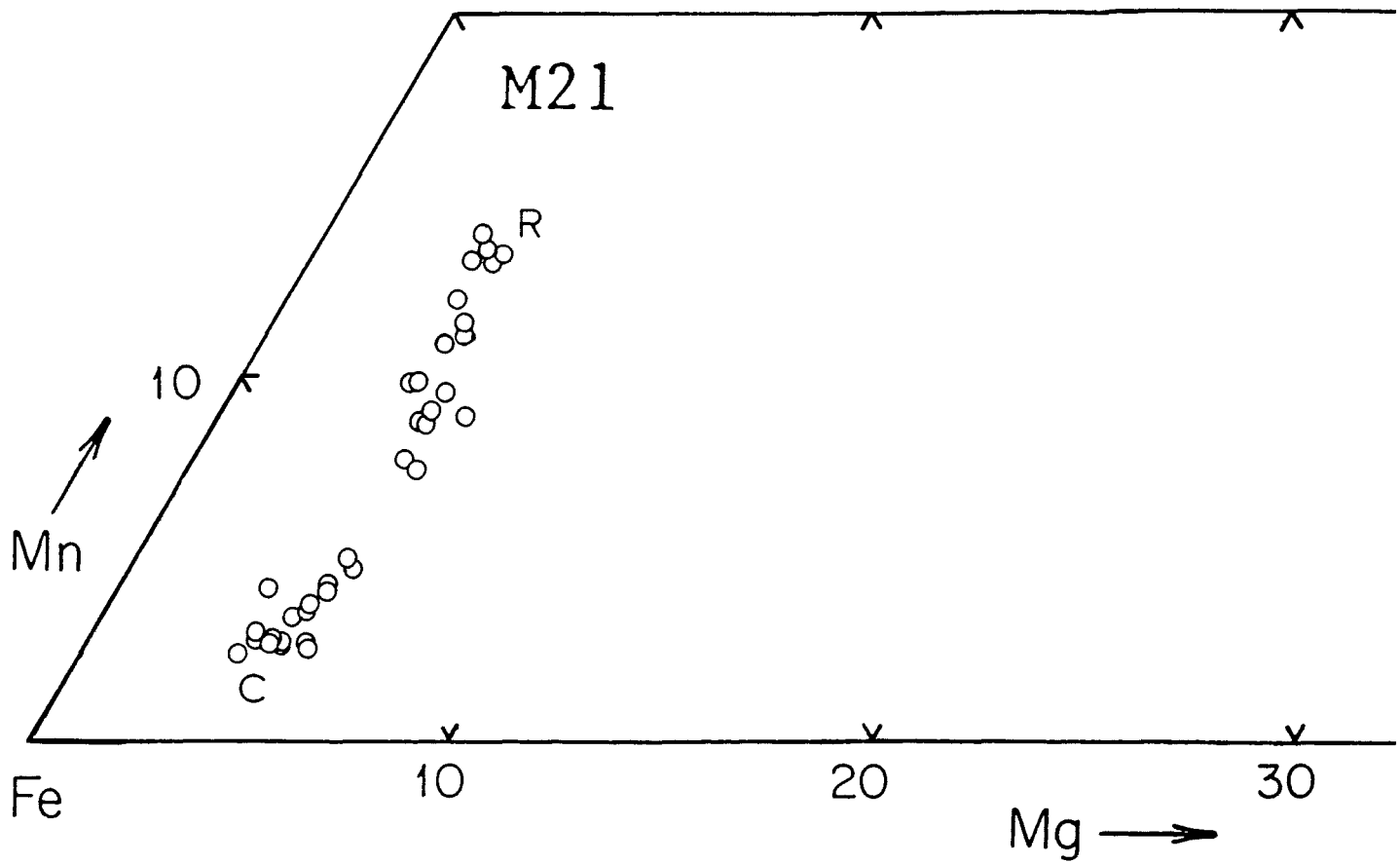

Figure 24. Fe-Mg-Mn ternary diagram for analysed garnet from sample M21. Dramatic increase in spessartine content from core (C) to rim (R) suggests consumption of almandine-pyrope.

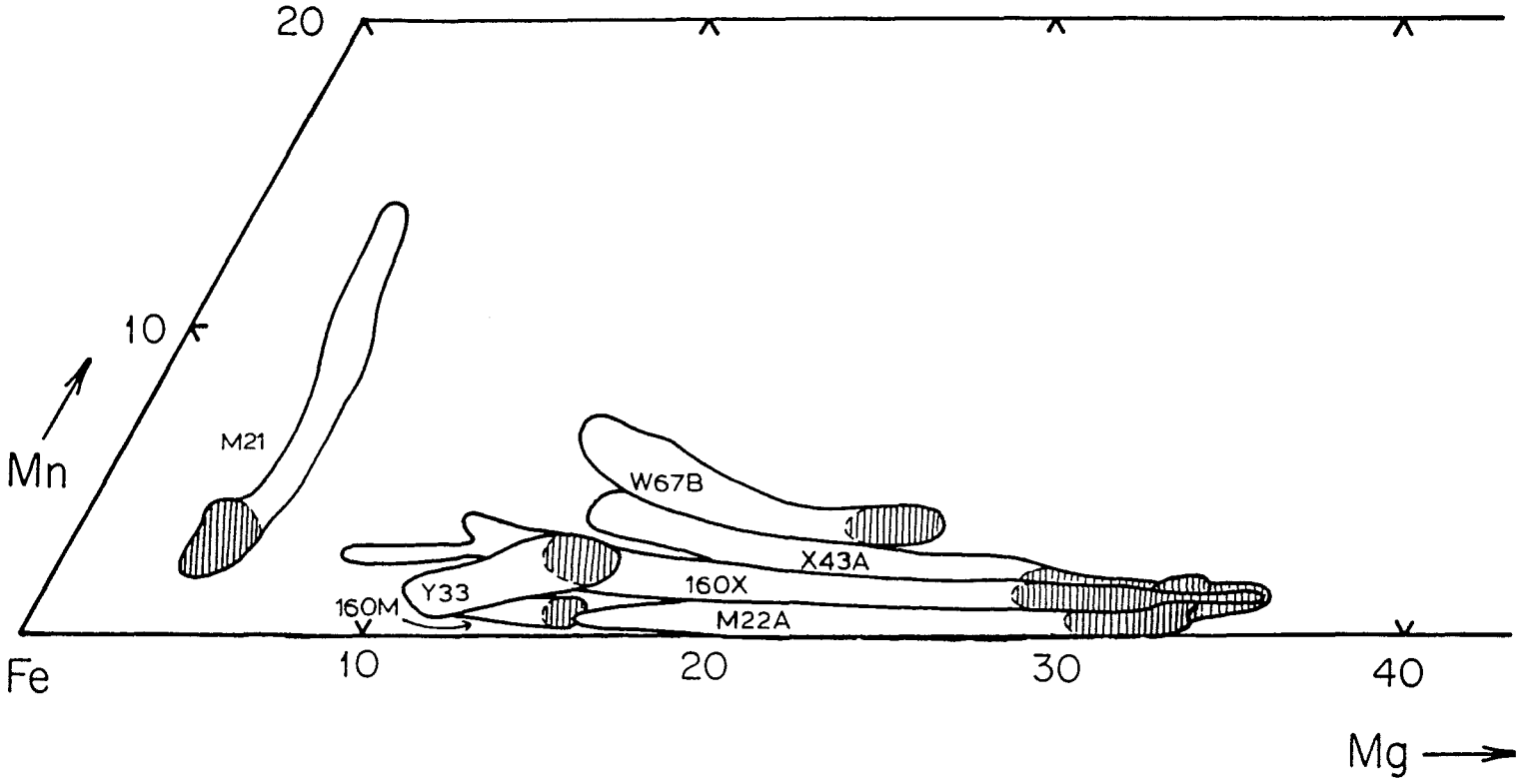

Figure 25. Fe-Mg-Mn summary diagram of garnet zoning from all samples analysed. Core (ruled) to rim trend shown for each sample.

Table 16. Electron microprobe analyses of kyanite and sillimanite. Four kyanite analyses and six sillimanite analyses are from sheared pelitic schist. Cation proportions are calculated on the basis of the formula Al_2SiO_5, containing 5 oxygens.

Sample	W67B	W67B	X43A	X43A	160X	160X	X43A	X43A	160X	160X
Alys#	KY 1	KY 2	KY 3	KY 4	SIL 1	SIL 2	SIL 3	SIL 4	SIL 5	SIL 6
SiO_2	37.38	38.74	38.05	37.69	36.92	37.72	39.04	37.64	37.56	37.26
TiO_2	0.0	0.02	0.0	0.0	0.07	0.06	0.33	0.42	0.0	0.0
Al_2O_3	62.63	61.45	60.89	61.09	62.31	62.63	60.81	60.80	60.08	61.82
Cr_2O_3	0.02	0.07	0.02	0.10	0.10	0.12	0.0	0.0	0.07	0.06
CaO	0.0	0.0	0.0	0.0	0.02	0.02	0.14	0.0	0.01	0.01
MgO	0.0	0.0	0.01	0.02	0.03	0.03	0.01	0.01	0.02	0.0
MnO	0.0	0.03	0.01	0.04	0.01	0.05	0.0	0.0	0.0	0.0
FeO	0.36	0.23	0.77	0.72	0.23	0.19	0.52	0.07	0.25	0.19
Total	100.39	100.54	99.75	99.66	99.69	100.82	100.85	98.94	97.99	99.34
Formulae based on 5 oxygens										
Si	1.005	1.038	1.031	1.023	1.000	1.010	1.045	1.025	1.014	1.012
Ti					0.001	0.001	0.007	0.009		
Al	1.987	1.943	1.946	1.955	1.990	1.978	1.920	1.953	1.976	1.980
Cr	0.001	0.001		0.002	0.002	0.003			0.001	
Ca							0.004			
Mg				0.001	0.001	0.001			0.001	
Mn		0.001		0.001		0.001				
Fe	0.008	0.005	0.018	0.016	0.005	0.005	0.012	0.002	0.006	0.004
Total	1.996	1.950	1.964	1.975	1.999	1.989	1.943	1.964	1.984	1.984

Table 17. Electron microprobe analyses of staurolite. Twelve analyses are from two grains from sample 160M of reconstituted pelitic schist. Cation proportions are calculated on the basis of the formula $(Fe,Al,Ti,Zn)_2(Al,Mg)_8(Al,Fe)_{0.7}(Fe,Mn)_{0.12}(Si,Al)_4O_{22}(OH)_2$, containing 23 oxygens plus one H_2O, after Hollocher (1981). Staurolite-bearing assemblages are plotted on an AFM diagram in muscovite projection in Figure 31B.

Alys#	1	2	3	4	5	6	7	8	9	10	11	12
SiO_2	28.20	27.99	28.07	27.94	28.13	28.44	27.30	27.96	28.15	28.05	27.90	27.06
TiO_2	0.70	0.63	0.64	0.68	0.65	0.64	0.72	0.71	0.73	0.67	0.73	0.70
Al_2O_3	53.69	52.80	53.13	53.02	53.17	53.46	51.62	52.42	52.23	51.89	51.86	52.20
FeO	13.23	13.44	13.40	13.42	13.57	13.46	13.21	13.63	13.88	13.51	13.58	13.73
MnO	0.01	0.03	0.03	0.0	0.01	0.06	0.0	0.0	0.02	0.03	0.01	0.02
MgO	1.52	1.45	1.47	1.52	1.48	1.39	1.50	1.62	1.53	1.59	1.57	1.57
CaO	0.01	0.0	0.0	0.0	0.0	0.01	0.0	0.0	0.0	0.0	0.0	0.0
ZnO	1.34	1.16	1.29	1.39	1.33	1.28	1.39	1.46	1.26	1.29	1.24	1.36
Total	98.70	97.50	98.03	97.97	98.34	98.74	95.74	97.80	97.80	97.03	96.89	96.64
Formulae based on 23 oxygens												
Si site												
Si	3.891	3.913	3.904	3.891	3.903	3.925	3.894	3.908	3.935	3.947	3.932	3.835
Al	0.109	0.087	0.096	0.109	0.097	0.075	0.106	0.092	0.065	0.053	0.068	0.165
Total	4.000	4.000	4.000	4.000	4.000	4.000	4.000	4.000	4.000	4.000	4.000	4.000
Al 1,2 site												
Al	7.687	7.698	7.695	7.685	7.694	7.714	7.681	7.663	7.681	7.667	7.670	7.668
Mg	0.313	0.302	0.305	0.315	0.306	0.286	0.319	0.337	0.319	0.333	0.330	0.332
Total	8.000	8.000	8.000	8.000	8.000	8.000	8.000	8.000	8.000	8.000	8.000	8.000
Al 3 site												
Al	0.287	0.276	0.283	0.295	0.288	0.266	0.296	0.301	0.279	0.280	0.282	0.322
Fe	0.285	0.298	0.294	0.290	0.295	0.299	0.293	0.296	0.307	0.301	0.301	0.302
Total	0.572	0.574	0.577	0.585	0.583	0.565	0.589	0.597	0.586	0.581	0.583	0.624
Fe site												
Fe	1.145	1.178	1.169	1.172	1.181	1.165	1.182	1.195	1.217	1.192	1.200	1.220
Zn	0.136	0.120	0.132	0.143	0.136	0.130	0.146	0.151	0.130	0.134	0.129	0.142
Ti	0.073	0.066	0.067	0.071	0.068	0.066	0.077	0.075	0.077	0.071	0.077	0.075
Al	0.646	0.636	0.632	0.614	0.615	0.638	0.595	0.580	0.577	0.603	0.593	0.563
Total	2.000	2.000	2.000	2.000	2.000	1.999	2.000	2.001	2.001	2.000	1.999	2.000
U site												
Mn	0.001	0.004	0.004		0.001	0.007			0.002	0.004	0.001	0.002
Fe	0.097	0.095	0.095	0.100	0.099	0.099	0.101	0.102	0.098	0.096	0.099	0.105
Total	0.098	0.099	0.099	0.100	0.100	0.106	0.101	0.102	0.100	0.100	0.100	0.107

proportions are based on the formula $(Ca,Na,K)(Al,Ti,Fe,Mg)_3Al_6Si_6O_{18}(BO_3)_3(OH)_4$, after Henry and Guidotti (1985). Thirty compositional analyses from core (C), intermediate (I), and rim (R) areas of a single grain of tourmaline are given in Table 18. Optical zoning was used to determine analysis locations. There are apparently two distinct chemical zones: the interior zone covers roughly 60% of the total area and the outer zone covers about 40% of the area. Although the optical and chemical boundary between these zones is sharp, no Becke line was observed here. Therefore it is interpreted to be a single grain with a small transition area between core and rim zones.

The core of the grain contains less than 0.065 Ti per 29 oxygens and the rims contain 0.093 to 0.123 Ti per 29 oxygens. The Mg/(Mg+Fe) ratio ranges from 0.48 to 0.63, and does not show systematic variation from core to rim. The core area contains between 0.049 and 0.062 Ca per 29 oxygens whereas the rim area contains between 0.070 and 0.091 Ca per 29 oxygens. Aluminum in the Y-site ranges from 0.292 to 0.380 in the core region and a lower value of 0.107 to 0.265 is observed in the rim. The Fe/(Fe+Mg) ratio ranges from 0.37 to 0.45 throughout the grain and does not appear to reflect distinct zones. When compositions are plotted on a ternary of Al-AlFe-AlMg tourmaline end-members (Figure 26), they lie on the Fe-rich border of the region of typical metamorphosed shales and sandstones coexisting with an Al-saturating phase, as defined by Henry and Guidotti (1985). Henry and Guidotti suggest that Fe^{3+} may be a significant component in tourmaline of this general composition, substituting for Al in the Z site.

In summary, the core of this grain is richer in octahedral Al, slightly richer in Na, and poorer in Ti and Ca relative to the rim. Tourmaline zoning has often been overlooked in detailed studies of mineral assemblages and few studies are available for comparison at this point. Correlation of chemical zoning between minerals, for example between tourmaline and garnet, is tenuous. However, it would be very informative if constraints were available for such a correlation.

Rutile and Ilmenite

Several analyses of rutile and ilmenite from the sheared pelitic rocks are given in Table 19. Iron content in rutile is less than 0.7 weight percent and Mn content in ilmenite is less than 1.2 weight percent. Rutile was probably the stable titanian phase during early high-grade metamorphism, whereas ilmenite became stable with hydration and Acadian reheating.

PHASE RELATIONS

In the preceeding section, the chemical compositions of individual minerals in the various rock types have been considered. This section will focus on the interrelationships between two or more minerals as well as on the probable reactions that have occurred in the rocks.

Table 18. Electron microprobe analyses of tourmaline. Thirty analyses are from single zoned tourmaline grain from reconstituted pelitic schist sample 160M. Position of analysis spot with respect to optically zoned grain indicated as follows: core (C), intermediate (I), and rim (R). Cation proportions are calculated on the basis of the formula $(Ca,Na,K)(Al,Ti,Fe,Mg)_3Al_6Si_6(BO_3)_3O_{18}OH_4$, containing 29 oxygens, after Henry and Guidotti (1985). Three boron atoms in the structural formula are assumed. Tourmaline data are plotted in Figure 26.

	(R)	(R)	(I)	(I)	(R)	(R)	(R)	(C)	(C)	(C)	(C)	(C)
Alys#	1	2	3	4	5	6	7	8	9	10	11	12
SiO_2	36.67	33.78	35.68	35.66	33.61	36.31	34.10	34.63	34.83	35.82	35.35	36.20
TiO_2	1.00	0.85	0.58	0.58	0.74	0.75	0.93	0.42	0.43	0.53	0.43	0.42
Al_2O_3	32.22	32.87	32.79	33.12	33.43	33.48	33.30	33.58	33.60	32.99	33.94	33.28
Cr_2O_3	0.01	0.04	0.02	0.0	0.03	0.01	0.0	0.0	0.0	0.0	0.0	0.0
FeO	7.01	6.70	7.64	7.32	7.44	7.20	8.05	6.96	7.33	7.49	7.06	6.96
MnO	0.0	0.66	0.0	0.0	0.0	0.0	0.0	0.96	0.0	0.01	0.0	0.0
MgO	5.87	6.43	5.66	6.01	6.47	6.70	5.98	6.26	6.21	6.05	5.99	6.12
CaO	0.44	0.41	0.37	0.35	0.39	0.43	0.43	0.31	0.29	0.35	0.31	0.29
Na_2O	2.38	2.56	2.59	2.75	2.59	2.46	2.63	2.68	2.64	2.52	2.65	2.69
K_2O	0.03	0.04	0.03	0.02	0.02	0.03	0.04	0.04	0.04	0.03	0.05	0.05
Total	85.63	84.34	85.36	85.81	84.72	87.37	85.46	85.84	85.37	85.79	85.78	86.01
Formulae based on 29 oxygens												
B	3.000	3.000	3.000	3.000	3.000	3.000	3.000	3.000	3.000	3.000	3.000	3.000
Si	6.019	5.679	5.905	5.866	5.627	5.857	5.676	5.725	5.765	5.892	5.806	5.921
Al_t		0.321	0.095	0.134	0.373	0.143	0.324	0.275	0.235	0.108	0.194	0.079
Total	6.019	6.000	6.000	6.000	6.000	6.000	6.000	6.000	6.000	6.000	6.000	6.000
Al_z	6.000	6.000	6.000	6.000	6.000	6.000	6.000	6.000	6.000	6.000	6.000	6.000
Al_y	0.236	0.197	0.305	0.292	0.254	0.227	0.212	0.217	0.323	0.292	0.380	0.341
Ti	0.123	0.107	0.073	0.072	0.093	0.092	0.116	0.052	0.053	0.065	0.054	0.051
Cr	0.002	0.005	0.002		0.004	0.001						
Fe	0.963	0.943	1.058	1.008	1.043	0.972	1.121	0.963	1.015	1.031	0.971	0.952
Mn		0.094						0.134		0.002		
Mg	1.437	1.612	1.398	1.475	1.615	1.613	1.485	1.543	1.533	1.485	1.467	1.492
Y Total	2.761	2.958	2.836	2.847	3.009	2.905	2.934	2.909	2.924	2.875	2.872	2.836
Ca	0.077	0.074	0.066	0.061	0.070	0.075	0.076	0.055	0.051	0.062	0.054	0.050
Na	0.757	0.834	0.831	0.878	0.841	0.771	0.849	0.859	0.849	0.803	0.846	0.854
K	0.006	0.003	0.007	0.004	0.005	0.005	0.008	0.008	0.007	0.007	0.011	0.011
X Total	0.840	0.911	0.904	0.943	0.916	0.851	0.933	0.922	0.907	0.872	0.911	0.915

Table 18, continued.

Alys#	(R) 13	(C) 14	(I) 15	(R) 16	(C) 17	(C) 18	(R) 19	(R) 20	(C) 21	(R) 22	(I) 23	(R) 24
SiO_2	35.61	36.40	35.95	36.66	34.97	34.62	36.30	36.69	36.85	36.61	36.49	36.19
TiO_2	0.92	0.40	0.51	0.86	0.37	0.42	0.99	1.00	0.40	0.95	0.80	0.92
Al_2O_3	32.70	32.29	33.41	32.43	33.37	33.35	32.61	32.35	32.83	31.14	32.61	32.29
Cr_2O_3	0.01	0.02	0.02	0.11	0.0	0.02	0.05	0.02	0.01	0.0	0.0	0.07
FeO	7.85	7.08	7.44	7.92	6.94	6.94	8.14	7.91	7.12	7.45	7.77	7.20
MnO	0.0	0.0	0.27	0.0	0.0	0.0	0.0	0.0	0.01	0.0	0.0	0.0
MgO	5.59	5.86	5.71	5.55	6.15	6.16	5.74	5.78	6.04	5.66	5.93	6.05
CaO	0.48	0.31	0.39	0.41	0.34	0.28	0.52	0.45	0.30	0.43	0.39	0.42
Na_2O	2.32	2.39	2.55	2.48	2.64	2.47	2.62	2.66	2.64	2.51	2.66	2.44
K_2O	0.04	0.04	0.05	0.06	0.02	0.04	0.05	0.02	0.04	0.05	0.04	0.03
Total	85.52	84.79	86.30	86.48	84.80	84.30	87.02	86.88	86.24	84.80	86.69	85.61
Formulae based on 29 oxygens												
Si	5.888	6.030	5.885	5.992	5.811	5.785	5.915	5.975	6.008	6.088	5.950	5.957
Al_t	0.112	____	0.115	0.008	0.189	0.215	0.085	0.025	____	____	0.050	0.043
Total	6.000	6.030	6.000	6.000	6.000	6.000	6.000	6.000	6.008	6.088	6.000	6.000
Al_z	6.000	6.000	6.000	6.000	6.000	6.000	6.000	6.000	6.000	6.000	6.000	6.000
Al_y	0.265	0.308	0.334	0.243	0.351	0.359	0.183	0.187	0.313	0.107	0.222	0.225
Ti	0.115	0.050	0.063	0.106	0.047	0.052	0.122	0.123	0.049	0.118	0.098	0.114
Cr	0.002	0.003	0.002	0.014		0.002	0.007	0.002	0.002			0.009
Fe	1.087	0.981	1.019	1.083	0.964	0.971	1.109	1.078	0.971	1.037	1.060	0.992
Mn			0.037						0.002			
Mg	1.379	1.448	1.393	1.353	1.523	1.534	1.396	1.403	1.468	1.404	1.443	1.484
Y Total	2.848	2.790	2.848	2.799	2.885	2.918	2.817	2.793	2.805	2.666	2.823	2.824
Ca	0.086	0.056	0.068	0.072	0.060	0.049	0.091	0.079	0.052	0.077	0.069	0.074
Na	0.752	0.769	0.810	0.787	0.851	0.801	0.827	0.841	0.834	0.808	0.841	0.780
K	0.009	0.009	0.010	0.013	0.004	0.008	0.011	0.005	0.009	0.010	0.009	0.006
X Total	0.847	0.834	0.888	0.872	0.915	0.858	0.929	0.925	0.895	0.895	0.919	0.860
$\frac{Fe}{(Fe+Mg)}$	0.441	0.404	0.422	0.445	0.388	0.388	0.443	0.435	0.397	0.425	0.423	0.401

Table 18, continued.

Alys#	(R) 25	(R) 26	(C) 27	(C) 28	(C) 29	(C) 30
SiO_2	35.48	35.67	36.08	36.62	36.53	35.34
TiO_2	0.82	0.99	0.45	0.45	0.47	0.53
Al_2O_3	32.86	33.03	33.36	33.03	33.51	33.54
Cr_2O_3	0.01	0.01	0.0	0.01	0.05	0.0
FeO	6.89	8.15	7.31	7.20	7.17	7.37
MnO	0.0	0.0	0.0	0.0	0.0	0.01
MgO	6.48	5.72	6.07	5.93	5.96	6.02
CaO	0.45	0.44	0.32	0.33	0.35	0.28
Na_2O	2.58	2.46	2.67	2.62	2.68	2.57
K_2O	0.03	0.05	0.02	0.04	0.05	0.03
Total	85.60	86.52	86.28	86.23	86.77	85.69

Formulae based on 29 oxygens

Si	5.843	5.845	5.894	5.975	5.927	5.820
Al_t	0.157	0.155	0.106	0.025	0.073	0.180
Total	6.000	6.000	6.000	6.000	6.000	6.000
Al_z	6.000	6.000	6.000	6.000	6.000	6.000
Al_y	0.226	0.228	0.321	0.331	0.338	0.334
Ti	0.102	0.123	0.056	0.058	0.058	0.066
Cr	0.001	0.001		0.001	0.007	
Fe	0.949	1.118	0.999	0.983	0.974	1.016
Mn						0.001
Mg	1.592	1.397	1.480	1.442	1.442	1.479
Y Total	2.870	2.867	2.856	2.815	2.819	2.896
Ca	0.079	0.078	0.056	0.058	0.062	0.050
Na	0.824	0.781	0.845	0.831	0.842	0.820
K	0.006	0.011	0.005	0.009	0.010	0.006
X Total	0.909	0.870	0.906	0.898	0.914	0.876
$\frac{Fe}{(Fe+Mg)}$	0.373	0.445	0.403	0.405	0.403	0.407

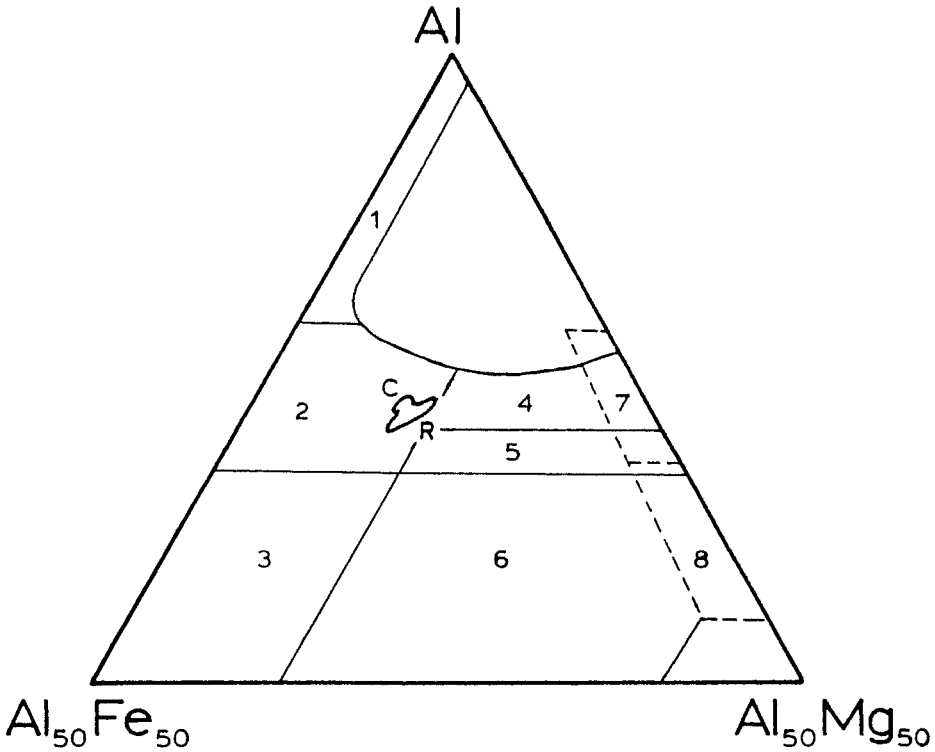

Figure 26. Ternary diagram of Al-Fe(total)-Mg tourmaline end-members (in molecular proportions) showing analysed tourmaline from reconstituted pelitic schist. Solid lines indicate compositional ranges for tourmalines from various rock types. 1) Li-rich granitoids, pegmatites, and aplites; 2) Li-poor granitoids and their associated pegmatites and aplites; 3) Fe(+3)-rich quartz-tourmaline rocks (hydrothermally altered granites); 4) Metamorphosed pelites and psammites co-existing with an Al-saturating phase; 5) Metamorphosed pelites and psammites not co-existing with an Al-saturating phase; 6) Fe(+3)-rich quartz-tourmaline rocks, calc-silicate rocks, and metamorphosed pelitic rocks; 7) Low-Ca metamorphosed ultramafic rocks and Cr, V-rich metamorphosed sedimentary rocks; and 8) Metamorphosed carbonates and pyroxenites. Note: Fields 4 and 5 overlap with field 7. Core (C) to rim (R) trend indicated for tourmaline from Mt. Mineral Fm.

Table 19. Electron microprobe analyses of rutile and ilmenite. Ten grains of rutile and nine grains of ilmenite are from sheared pelitic schist. Fe^{3+} in ilmenites calculated by normalizing totals greater than 2.000.

Sample	160X	160X	160X	160X	W67B	W67B	W67B	W67B	X43A	X43A
Alys#	RUT 1	RUT 2	RUT 3	RUT 4	RUT 5	RUT 6	RUT 7	RUT 8	RUT 9	RUT10
TiO_2	97.76	98.73	99.19	98.42	99.38	99.73	99.42	99.62	97.89	98.70
Al_2O_3	0.12	0.15	0.11	0.09						
Cr_2O_3	0.07	0.08	0.10	0.17	0.04	0.04	0.05	0.06		
CaO	0.03	0.0	0.0	0.01	0.0	0.0	0.0	0.0		
MgO	0.0	0.02	0.0	0.0	0.0	0.0	0.03	0.0	0.0	0.0
MnO	0.0	0.0	0.0	0.0	0.0	0.02	0.01	0.0	0.0	0.0
FeO	0.22	0.23	0.30	0.48	0.54	0.69	0.63	0.39	0.50	0.31
Total	98.20	99.21	99.70	99.17	99.96	100.48	100.14	100.07	98.39	99.01

Formulae based on 2 oxygens

Ti	0.996	0.996	0.995	0.994	0.997	0.996	0.996	0.997	0.997	0.998
Al	0.002	0.002	0.002	0.002						
Cr	0.002	0.002	0.003	0.002	0.001	0.001	0.001	0.002		
Ca	0.001									
Mg		0.001					0.001			
Mn						0.002				
Fe	0.003	0.003	0.003	0.005	0.006	0.008	0.007	0.004	0.005	0.003
Total	1.004	1.004	1.003	1.003	1.004	1.007	1.005	1.003	1.002	1.001

Sample	160X	160X	X43A	X43A	X43A	X43A	X43A	X43A	X43A
Alys#	ILM 1	ILM 2	ILM 3	ILM 4	ILM 5	ILM 6	ILM 7	ILM 8	ILM 9
TiO_2	52.48	52.39	48.57	49.00	49.02	51.60	52.56	51.84	52.81
FeO	46.40	46.35	50.16	50.37	50.71	47.33	46.87	46.51	46.00
Al_2O_3	0.11	0.10				0.04	0.04	0.04	0.01
Cr_2O_3	0.08	0.06				0.04	0.0	0.0	0.0
MgO	0.34	0.10	0.03	0.05	0.0	0.08	0.05	0.04	0.05
MnO	0.40	0.36	0.41	0.40	0.52	1.07	1.08	1.21	0.91
Total	99.81	99.36	99.17	99.82	100.25	100.16	100.60	99.64	99.78

Formulae based on 2 cations and 3 oxygens

Ti	0.994	0.995	0.926	0.928	0.925	0.978	0.992	0.987	1.003
Fe^{2+}	0.972	0.979	0.916	0.917	0.914	0.956	0.969	0.961	0.972
Fe^{3+}	0.006		0.148	0.144	0.150	0.042	0.015	0.025	
Al	0.003	0.003				0.001	0.001	0.001	
Cr	0.003	0.001				0.001			
Mg	0.013	0.013	0.001	0.002					
Mn	0.009	0.008	0.009	0.009	0.011	0.023	0.023	0.026	0.019
Total	2.000	1.999	2.000	2.000	2.000	2.000	2.000	2.000	1.994
Ilm	0.972		0.916	0.917	0.914	0.956	0.969	0.961	
Hem	0.003		0.074	0.072	0.075	0.021	0.0075	0.0125	
Pyph	0.009		0.009	0.009	0.011	0.023	0.023	0.026	
Geik	0.013		0.001	0.002					
Eskl	0.0015					0.0005			
Cor	0.0015					0.0005	0.0005	0.0005	

Petrographic evidence from these rocks suggests that they have experienced hydration to varying degrees at metamorphic temperatures. Three hydration reactions,

GAR + KSP + H_2O = Al-sil. + BIO + QTZ (1),
KSP + Al-sil. + H_2O = MUSC + QTZ (2), and
GAR + KSP + H_2O = MUSC + BIO + QTZ (3),

have been suggested based solely upon petrographic evidence. A closer look at phase relations based on chemical analyses supports this petrographic evidence.

Alkali-Alumina System

Average compositions of plagioclases from sheared and reconstituted pelitic schists and coexisting potassium feldspars from sheared pelitic schist are illustrated in Figure 27. The more calcic plagioclase compositions represent higher grade equilibria and coexist with K-feldspar in sheared schists and pegmatite. The more sodic plagioclase compositions within the reconstituted schists represent typical re-equilibrated compositions of Acadian Zone I.

Potassic muscovite and orthoclase should coexist with calcic plagioclase and more sodic muscovite and orthoclase should coexist with more sodic plagioclase (Tracy, 1975). Within Mt. Mineral pelitic assemblages, paragonitic muscovite coexists with sodic plagioclase and aluminosilicate without K-feldspar in reconstituted schists and potassic muscovite coexists with calcic plagioclase, aluminosilicate, and K-feldspar in sheared schists (Figure 28). Coexisting muscovite, aluminosilicate, and feldspar(s) suggest that the strongly sheared schists have largely preserved early sillimanite-orthoclase grade equilibrium compositions, whereas the reconstituted schists have undergone significant re-equilibration during Acadian hydration and heating. Muscovite from sheared schist is apparently in local equilibrium texturally, and is probably in local equilibrium chemically also.

These relationships may be explained by the discontinuous muscovite-in reaction

Al-sil. + KSP + H_2O = MUSC + QTZ (2)

and by the reaction

Al-sil. + KSP + H_2O = Na-MUSC + Alb + QTZ (4).

Evidence for these reactions have been observed in thin section, especially within sheared schists. Muscovite, plagioclase, and quartz symplectites are associated with K-feldspar and fine-grained muscovite may rim kyanite. Sample W67B may represent a typical assemblage of reactants at the early stages of progress of these reactions whereas samples 160M and Y33 probably represent product assemblages near the completion of the above reactions.

These two reactions may progress either with decreasing temperature or with increasing activity of water. Because these rocks probably experienced the same metamorphic conditions, differences between the sheared and reconstituted schists are best explained by differences in activity of water.

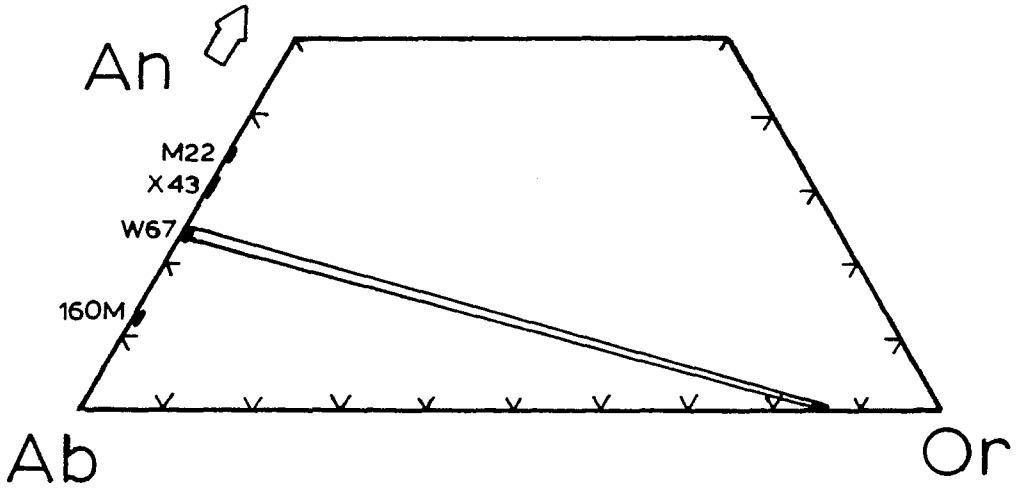

Figure 27. An-Or-Ab ternary diagram showing analysed plagioclase and potassium feldspar compositions. Sample X43 contains K-feldspar, but has not been analysed for it. Sample M22 plagioclase estimate is by Michel-Levy method.

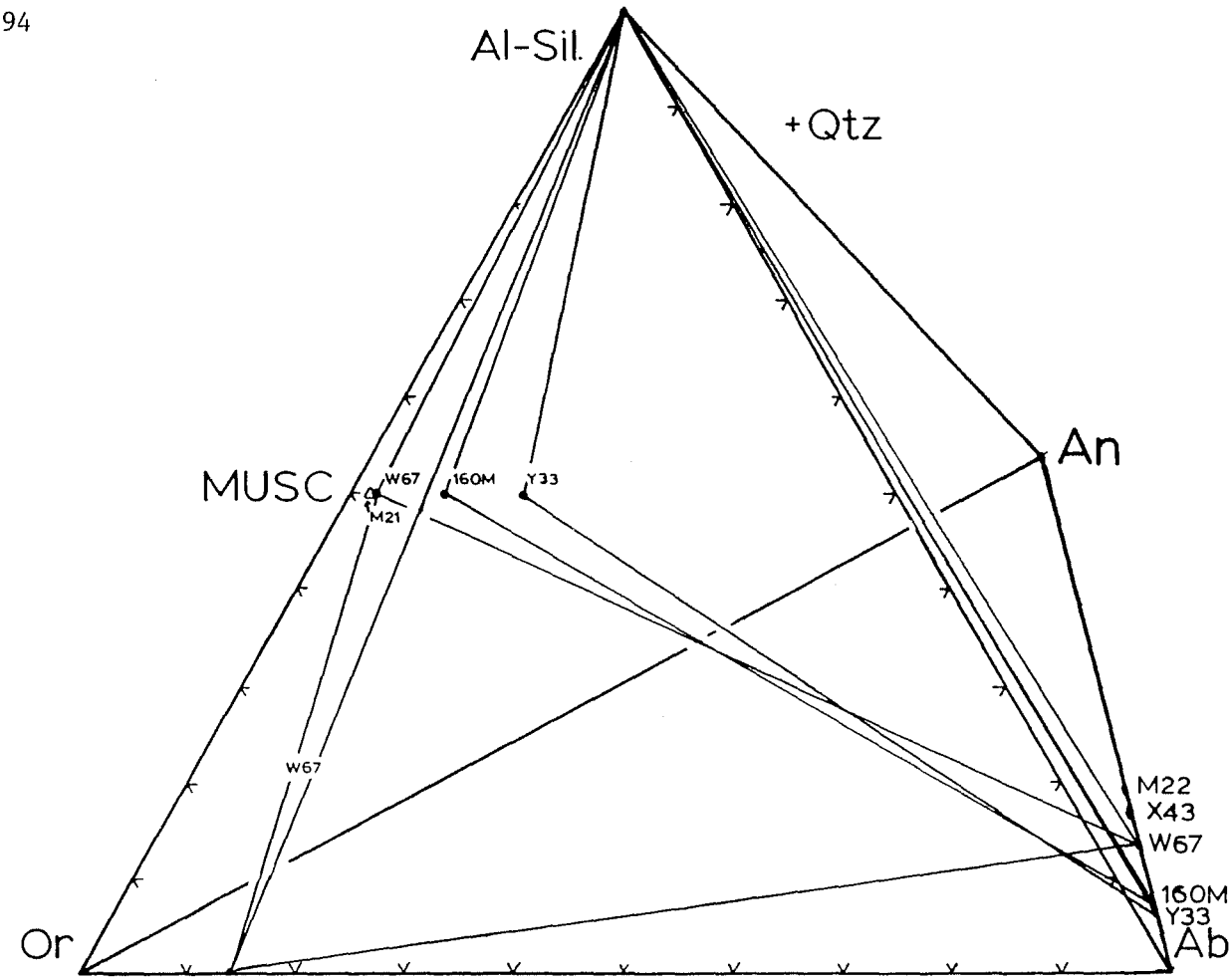

Figure 28A. AKNaCa tetrahedron showing alkali-alumina assemblages (after Evans and Guidotti, 1966).

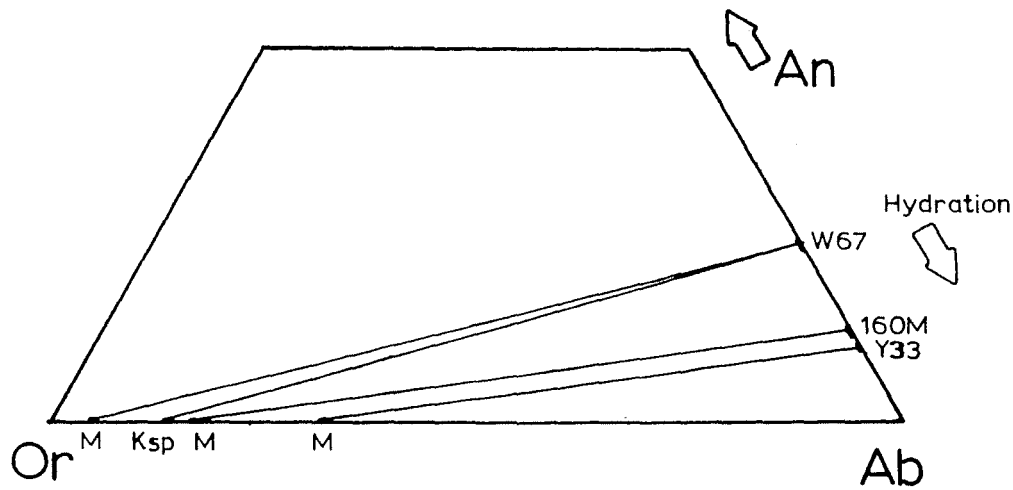

Figure 28B. Al-sil. projection in AKNaCa tetrahedron onto the KNaCa base. 4-phase volume (W67) and 3-phase tie planes (160M and Y33) illustrate changing compositions with hydration.

Sample averages of analysed muscovites and coexisting biotites (Figure 29) show that matrix biotites in reconstituted schists are more sodic than those in sheared schists, where biotite is consistently more potassic than coexisting muscovite. Included biotite in two samples of sheared schist are slightly more sodic than corresponding matrix biotites. Coexisting muscovite and biotite from Zone IV (Tracy, 1978) and Zone II (Hollocher, 1981) are shown for comparison. Hollocher (1981) has demonstrated that within chlorite stability, retrogression drives coexisting muscovites and biotites back toward higher potassium compositions. It is interpreted that hydration in Mt. Mineral schists took place above chlorite stability.

AKFM System

The AKFM tetrahedron (Figure 30) shows the more important silicates of the sheared and reconstituted pelitic schists. Potassium feldspar does not occur in reconstituted schist, and staurolite is present only in reconstituted schist. Muscovite is present in most of the sheared schist samples, though textural evidence suggests that it may only be in local equilibrium here, due to low activity of water.

Muscovite projection onto the AFM plane (after Thompson, 1957) is useful in illustrating garnet-biotite-aluminosilicate relations. Although muscovite is probably only in equilibrium locally in sheared pelitic schists, their assemblages are shown here in muscovite projection for comparison purposes.

Compositions of selected garnet-biotite pairs from aluminosilicate-bearing sheared pelitic schists are shown in Figure 31A. Matrix biotites are paired with garnet rim compositions and included biotites are paired with adjacent garnet interior compositions. Both matrix and included biotites are more magnesian than coexisting garnets. The aluminosilicate may be sillimanite, kyanite, or both.

Included biotites are more magnesian than matrix biotites, most certainly due to localized ion-exchange with progressive cooling. The garnet probably acted as an unlimited reservoir for Fe-Mg exchange and would not have changed measurably in composition.

The pairs of garnet rim and matrix biotite from reconstituted pelitic schist (Figure 31B), coexist with staurolite and kyanite. Both garnet and biotite are more iron-rich than those from sheared pelitic schist. This suggests that the reconstituted rocks are more hydrated than the sheared schists due to progress of continuous hydration reactions.

Compositions of selected garnet-biotite pairs from pegmatite and quartzite are shown in Figure 31C. Biotite in pegmatite is only found adjacent to garnet. Composition pairs resemble those of sheared schist, being magnesian in composition. Garnet-biotite composition pairs from quartzite represent the most iron-rich assemblage of those analysed. Neither staurolite nor aluminosilicate are present in this assemblage, due to bulk composition. Included biotites are more magnesian than

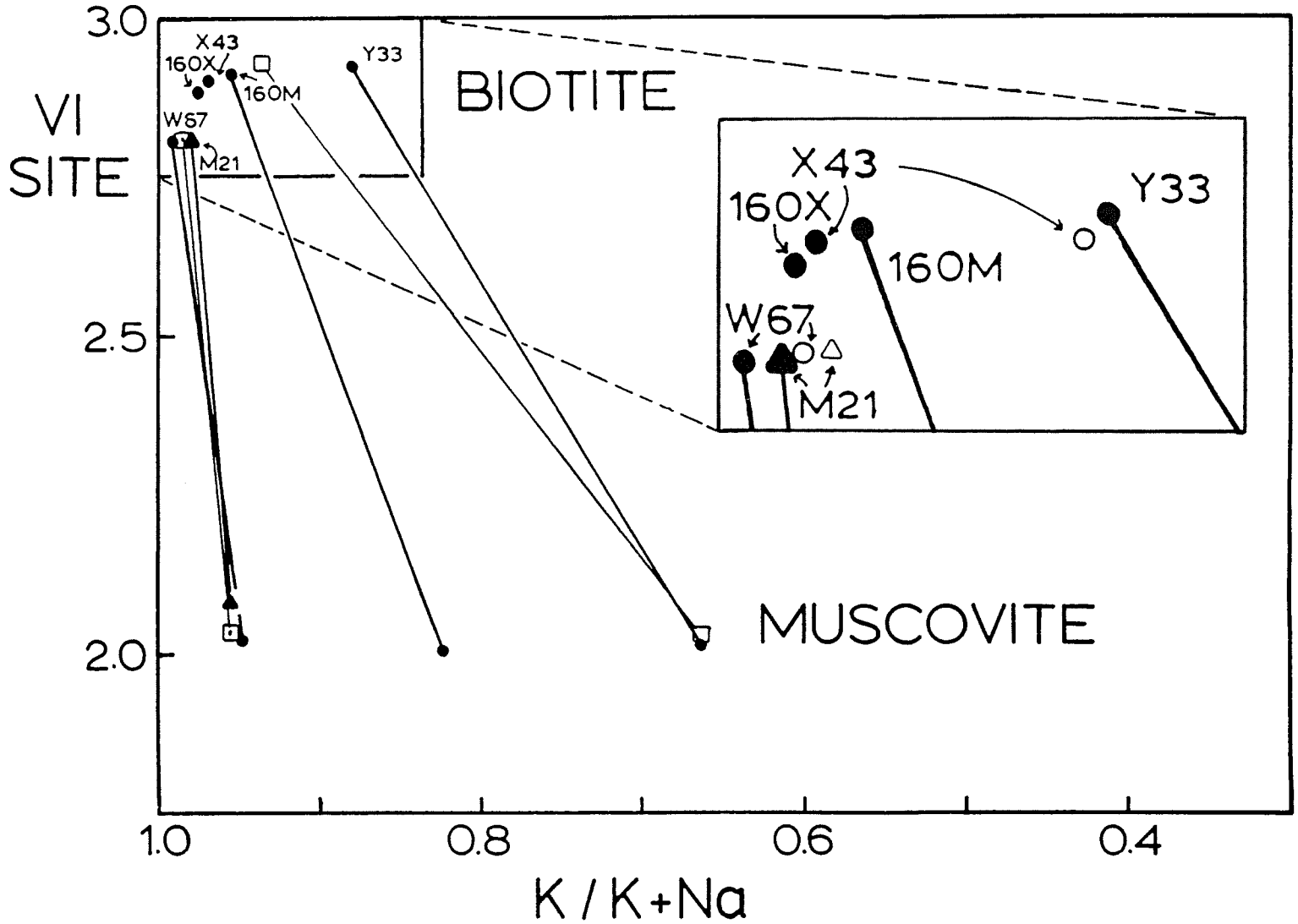

Figure 29. Octahedral site occupancy plotted against K/(K+Na) ratio showing analysed biotites and muscovites. Inset shows included biotites (open symbols). Micas from Tracy (1975) (dotted squares) and Hollocher (1981) (open squares) shown for comparison.

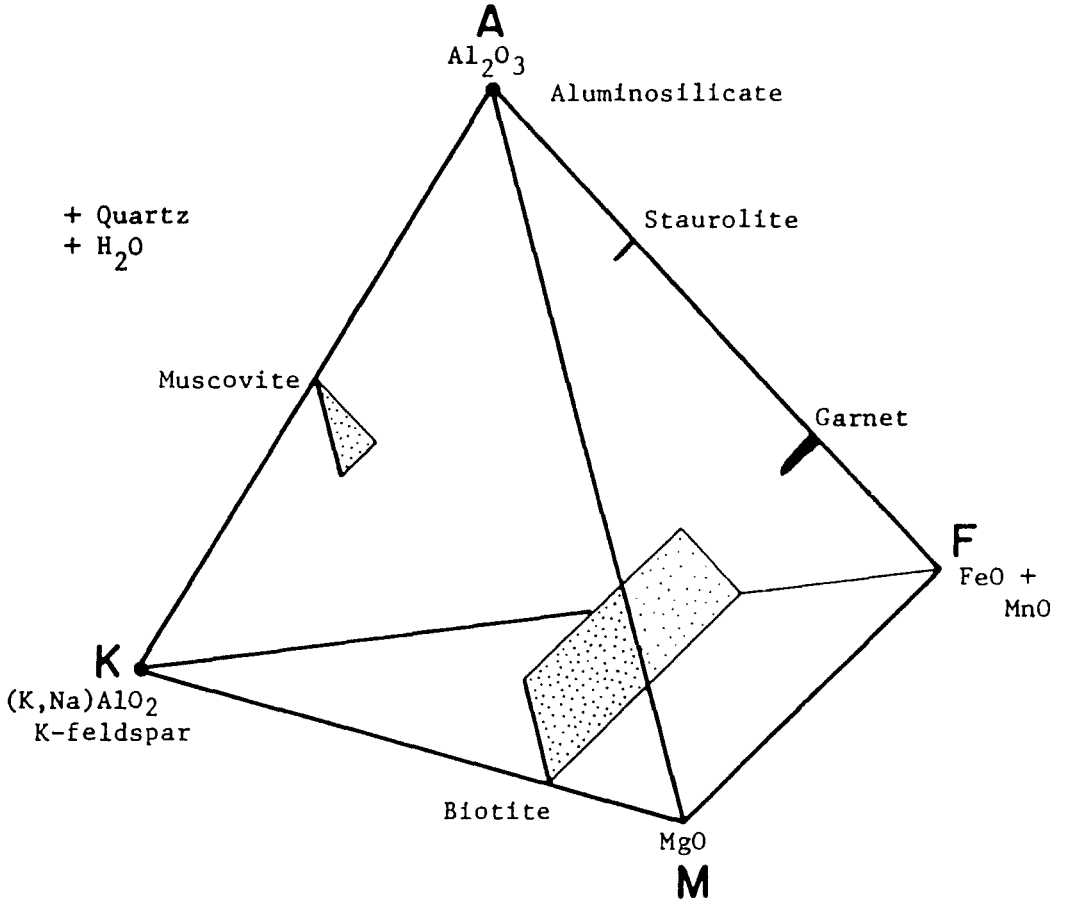

Figure 30. AKFM tetrahedron showing important silicate minerals. The K-apex represents the composition $(K,Na)AlO_2$. (After Hollocher, 1981).

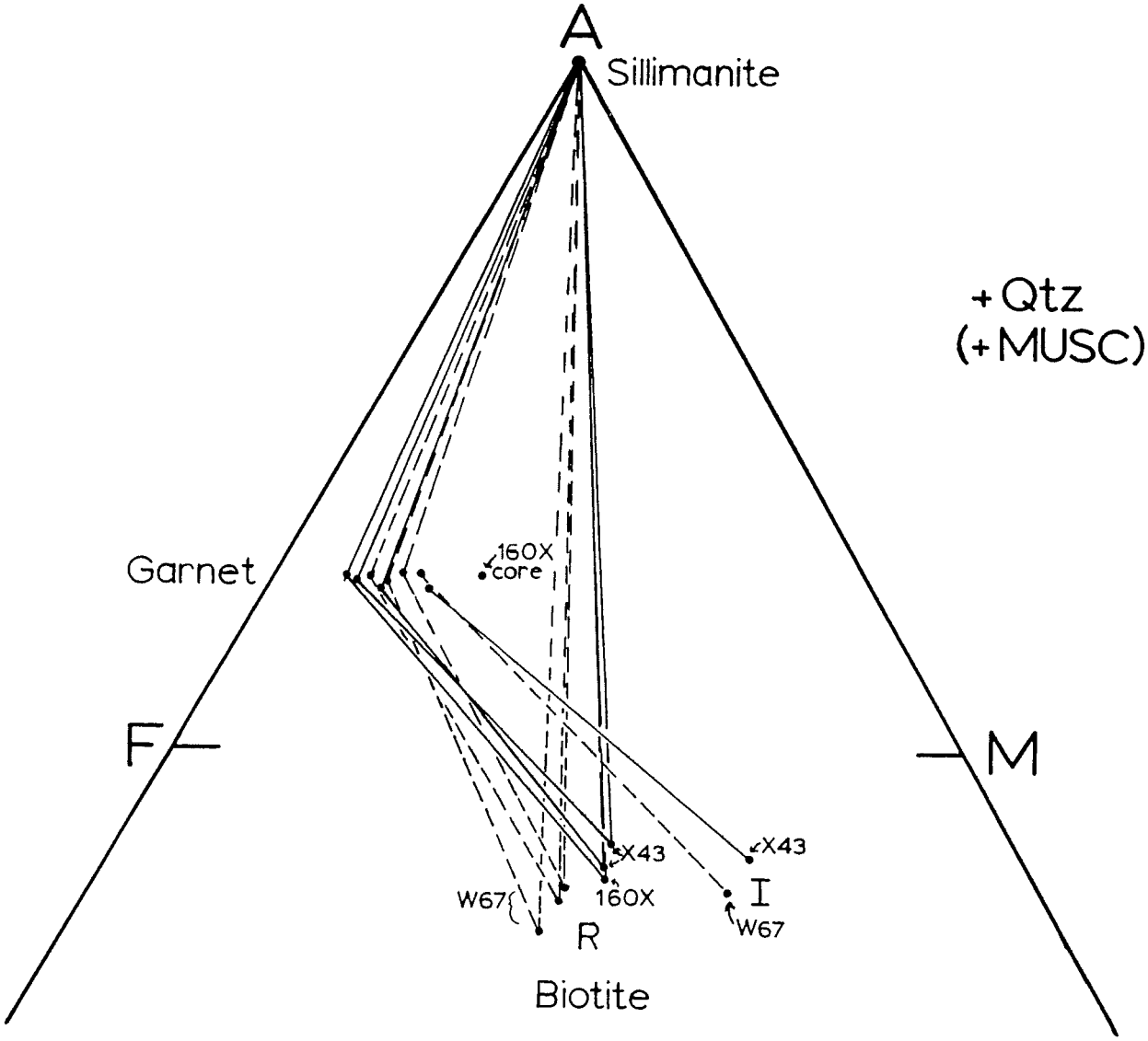

Figure 31A. Muscovite projection onto AFM face showing assemblages of sheared pelitic schist. Biotites rimming garnet (R) and included in garnet (I) are indicated. Included biotites are consistently more magnesian than biotites rimming garnet. Core composition of 160X garnet is given for reference. Muscovite, where present, is in local equilibrium.

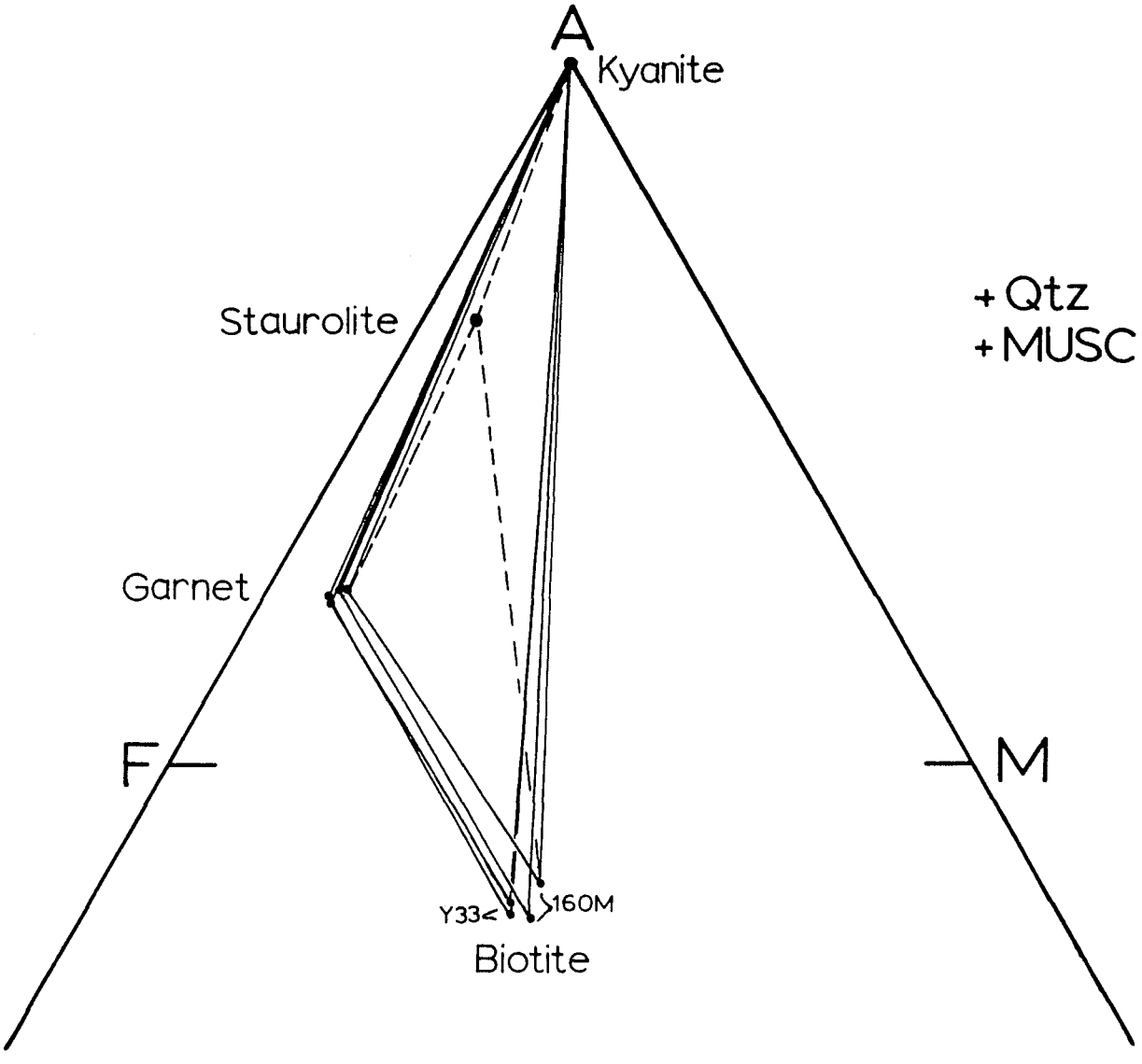

Figure 31B. Muscovite projection onto AFM face showing assemblages of reconstituted pelitic schist. Staurolite coexists with garnet, kyanite, and biotite in all assemblages shown here and many tie lines have been omitted for clarity.

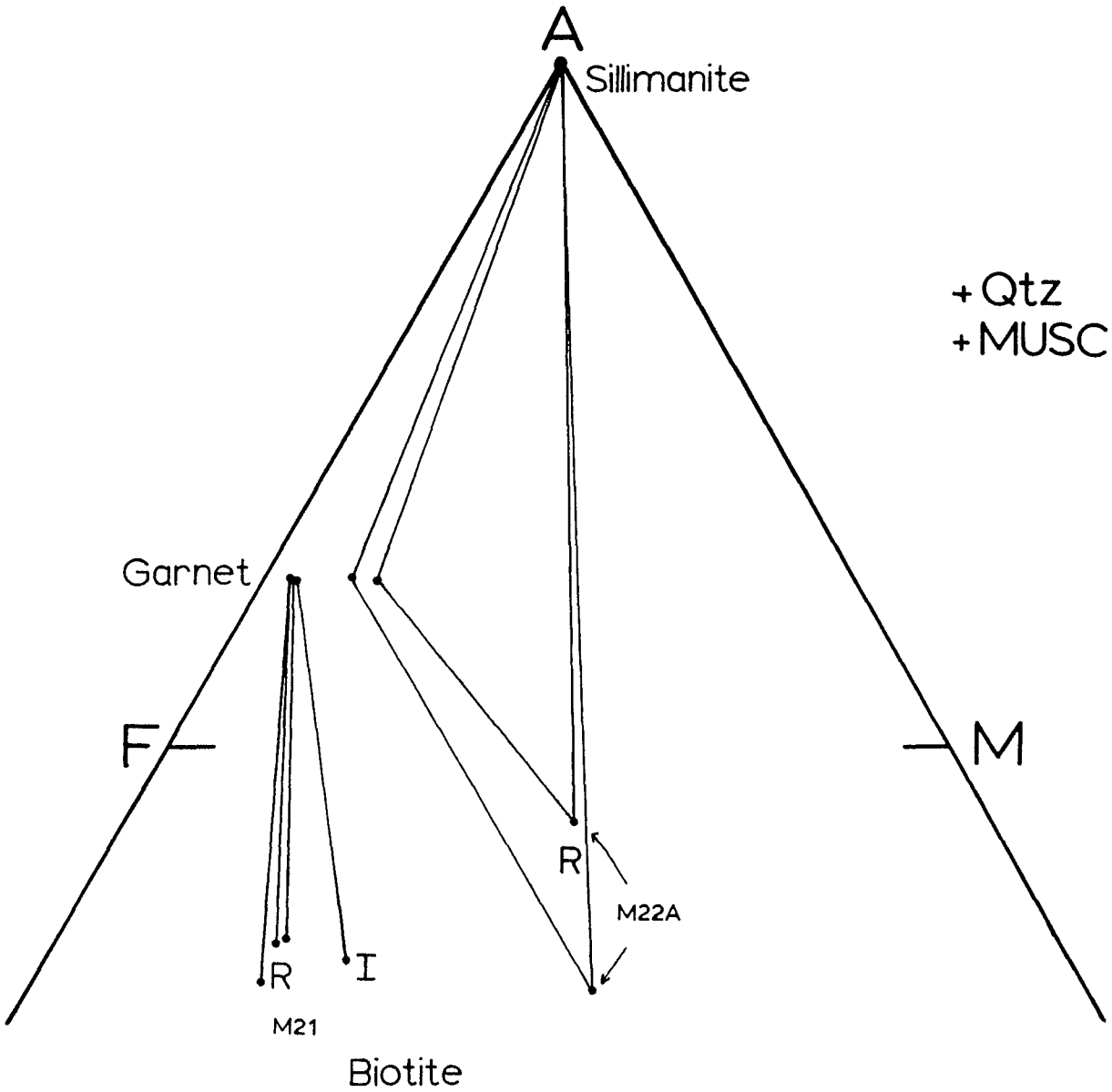

Figure 31C. Muscovite projection onto AFM face showing assemblages of sheared pegmatite and sheared quartzite. Biotites rimming garnet (R) and included in garnet (I) are indicated. Sheared pegmatite does not contain MUSC.

matrix biotites, suggesting that localized ion-exchange occurred with cooling.

Progress of Hydration Reactions

Hydration reaction (1), GAR + KSP + H_2O = Al-sil. + BIO + QTZ, is illustrated chemographically as a continuous reaction on an AFM diagram in K-feldspar projection (Figure 32A). Strong textural evidence suggests that this reaction took place as sheared pelitic schist began to hydrate. As hydration progressed, both biotite and garnet would have become more iron-rich. Assuming that garnet rims were in equilibrium with sheared pelitic matrix, the Fe-Mg zoning pattern in these garnets is consistent with this hydration reaction.

Biotite composition before hydration began would have been more magnesian than biotite in the hydrated matrix. Only those biotites that have been included in other minerals would have been spared re-equilibration (iron enrichment) with the hydrating matrix. Biotite included in garnet is, in fact, more magnesian than matrix biotites. However, biotite included in an iron-magnesian phase such as garnet is also subject to localized ion-exchange with changing temperature. Therefore, biotites included in garnet from these rocks are assumed to be more magnesian than the "original" biotites stable in the high-temperature assemblage.

Either or both kyanite and sillimanite were produced via the hydration reaction GAR + KSP + H_2O = BIO + SILL + QTZ (1). Substantial rims of sillimanite + biotite observed around garnets provide strong evidence for this reaction in several samples of sheared schist. Some samples of sheared schist also have concentrations of biotite and kyanite at garnet rims. Further evidence for the production of aluminosilicate may have been destroyed by progress of the reaction KSP + Al-Sil. + H_2O = MUSC + QTZ (2), which acted on several samples of sheared pelitic schist to consume aluminosilicate.

It is apparent from this interpretation that some hydration must have occurred within the sillimanite stability field. This is an important detail in the determination of the history of metamorphism in these rocks. It indicates either 1) that some hydration occurred before the rocks cooled substantially from high grade conditions or 2) that during a later hydration and heating, at least some of these rocks were heated to sillimanite stability conditions. The former interpretation is preferred here for simplicity, since nearby Siluro-Devonian cover rocks only reached kyanite grade during Acadian metamorphism.

No textural evidence was observed to suggest that muscovite was stable during early high-grade metamorphism. The early peak of metamorphism was obviously above muscovite stability conditions, within the Sill-Ksp zone. Upon cooling, muscovite would have become stable in relation to pressure and temperature conditions, but would also be dependent on the activity of water. Estimates of the activity of water following early high-grade metamorphism are poorly constrained, and one can not be sure whether any muscovite grew at this time. Since muscovite appears to be a secondary phase relative to the early

A.

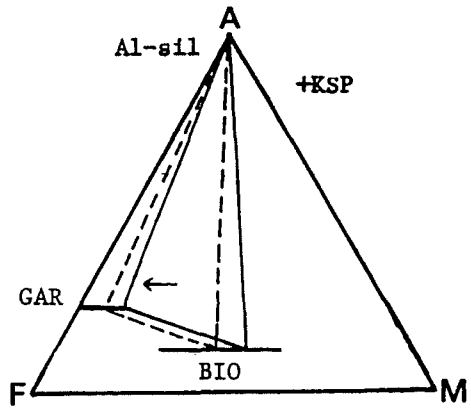

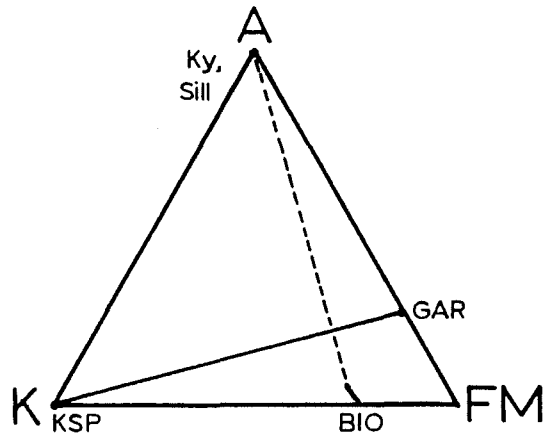

Above: GAR + KSP + H_2O = BIO + Al-sil. + QTZ (1)

Below : KSP + Al-sil. + H_2O = MUSC + QTZ (2)
GAR + KSP + H_2O = BIO + MUSC + QTZ (3)

B.

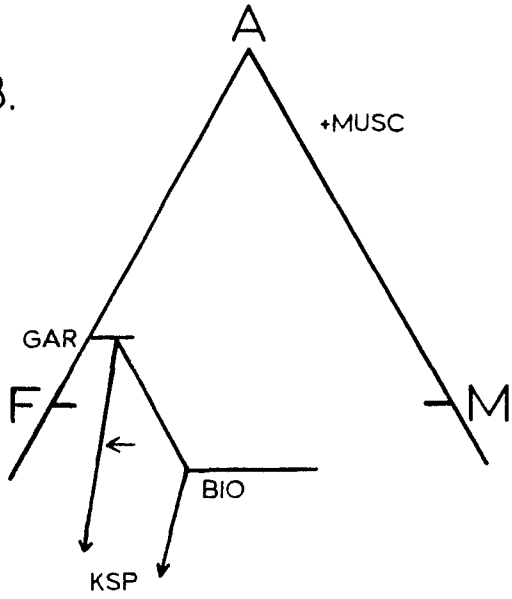

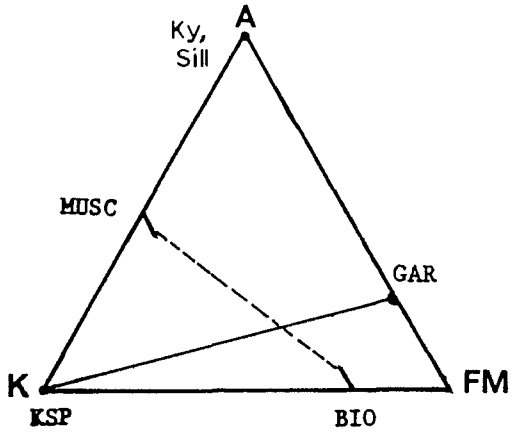

Figure 32. Dominant hydration reactions shown on AFM and A-K-FM ternary projections.

high-grade assemblage, it probably was not produced until the Acadian re-heating.

Muscovite may have been produced by either the reaction KSP + Al-Sil. + H_2O = MUSC + QTZ (2), or the reaction GAR + 2 KSP + 2 H_2O = BIO + MUSC + QTZ (3), or both. These reactions are illustrated chemographically in an A-K-FM diagram (Figure 32B). There is abundant textural evidence for both of these reactions in sheared schist samples (see Description of Rock Types). Symplectites of muscovite, plagioclase, and quartz around potassium feldspar indicate active K-feldspar consumption.

Aluminosilicate is consumed, rather than produced, during hydration within muscovite stability conditions. Rims of fine-grained muscovite around kyanite support this interpretation. Several garnets in sheared schist show rims of only biotite plus quartz, suggesting that aluminosilicate has been consumed from these rims.

Activity of Water in Pelitic Schists

The addition of H_2O as a fourth component to the A-K-FM diagram yields a tetrahedron in which hydration reactions may be illustrated in order of increasing hydration state. Reaction (1) requires the least activity of water in the metamorphic fluid and is "below" muscovite stability (Figure 33A), in terms of available water. Reactions (2) and (3) require higher activities of water, and probably became more active with continued and/or increased hydration (Figure 33B). The sheared schists record the limited progress of reaction (1) where relict garnet and K-feldspar are only partially consumed. The reconstituted schists have (almost) completed the hydration reactions and have produced new equilibrium assemblages consistent with Acadian kyanite-staurolite-biotite zone conditions.

Both analysed samples of reconstituted schist (160M and Y33) contain similar assemblages and have been considered together for discussion purposes to this point. However, petrographic and chemical evidence suggests that there are several significant differences between these samples. Sample Y33 is unique among analysed pelitic samples in several ways: 1) some garnets from this sample are euhedral in shape; 2) these euhedral garnets show normal or growth zoning patterns chemically; and 3) the analysed muscovites and biotites are the most sodic of all pelitic micas analysed.

These lines of evidence suggest that sample Y33 experienced complete hydration and that all relict garnet and K-feldspar porphyroblasts were completely consumed. Sample 160M has been greatly hydrated, but small relics of garnet are still present within the hydrated matrix and H_2O was probably still the limiting factor. Based on chemical analyses of plagioclase, muscovite, and biotite, sample 160M appears to be intermediate between the sheared schists containing preserved relics and the more hydrated sample Y33.

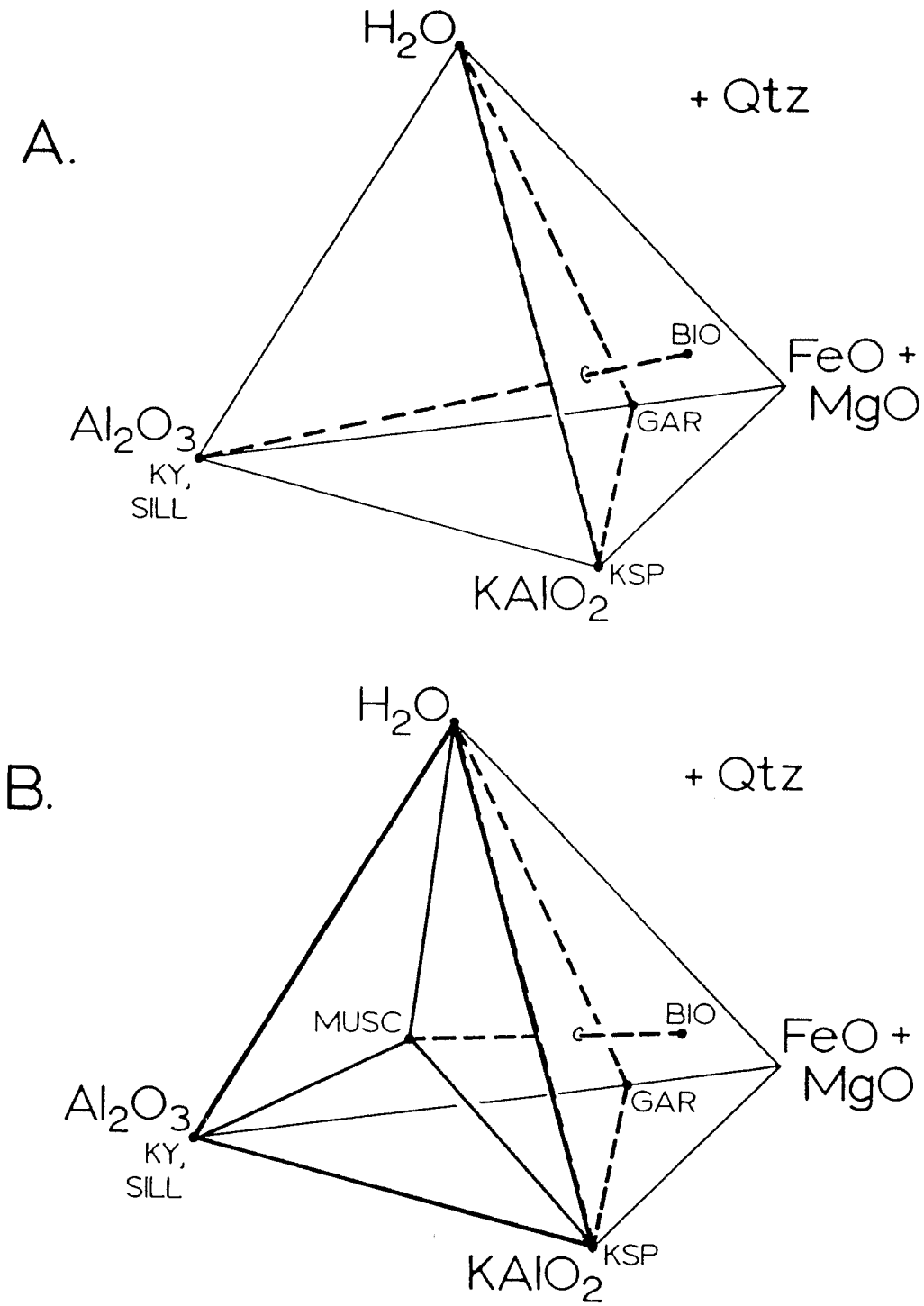

Figure 33. Dominant hydration reactions shown on H_2O-A-K-FM tetrahedron. A) Illustration of reaction (1) GAR + KSP + H_2O = BIO + Al-sil. + QTZ. B) Illustration of reaction (2) KSP + Al-sil. + H_2O = MUSC + QTZ and reaction (3) GAR + KSP + H_2O = MUSC + BIO + QTZ.

A-K-FM-Ti System

Most of the sheared pelitic schist samples contain six phases within the A-K-FM-Ti system. A sillimanite projection onto the K-FM-Ti ternary may be used to show important reactions about an invariant point (Figure 34). The iron end-member of the pressure-sensitive reaction,

GAR + 3 RUT = 3 ILM + SILL + 2 QTZ,

has been experimentally calibrated by Bohlen and others (1983). The reaction takes place at increasingly lower pressures for Mg-richer rocks.

Rutile is present in all of the sheared schists studied here, and is interpreted to have been stable during early high grade metamorphism. The early sillimanite-orthoclase grade assemblage was probably within the GAR-KSP-RUT stability field. Ilmenite appears to be the stable Ti-oxide within the reconstituted schists, suggesting that the rocks crossed the reaction GAR + 3 RUT = 3 ILM + SILL + 2 QTZ at some point after the peak of early high-grade metamorphism.

Rutile or ilmenite would have been consumed together with garnet and K-feldspar during hydration by the reaction

GAR + KSP + RUT + H_2O = BIO + SILL + QTZ

within the garnet-rutile stability field or by the reaction

GAR + KSP + ILM + H_2O = BIO + SILL + QTZ

within the garnet-ilmenite stability field, depending on the pressure and temperature conditions when the hydration took place. Rutile is associated with biotite and sillimanite rims around garnet in some sheared pelitic schists (Figure 6), favoring the former reaction for the production of biotite and sillimanite rims around garnet.

The Mt. Mineral schists would have crossed the reaction, GAR + 3 RUT = 3 ILM + SILL + 2 QTZ, into the ilmenite stability region following the peak of early high-grade metamorphism, and probably remained on the lower pressure side throughout Acadian metamorphism and cooling. The ilmenite-rutile associations in thin section do not show conclusive evidence for specific reactions occuring during mid-Devonian time.

Garnet-Biotite Thermometry and Barometry

Strong petrographic and garnet zoning evidence suggests that reaction (1), involving progressive hydration of garnet in equilibrium with K-feldspar to produce biotite and aluminosilicate, took place in most, if not all, of the strongly sheared pelitic rocks. With hydration and decreasing temperatures, both garnet and biotite compositions would be expected to have become more iron-rich (Figure 32A). Selected garnet--biotite composition pairs are illustrated in Figure 31 from the various rock types.

Biotites included in garnet would have been isolated from interaction with the matrix phases since the time of inclusion. If the included biotites have compositions representative of an early chemical equilibrium, the pairs of garnet core and included biotite should be more magnesian than the pairs of garnet rim and matrix biotite, that represent the product of later hydration reaction. This relationship is

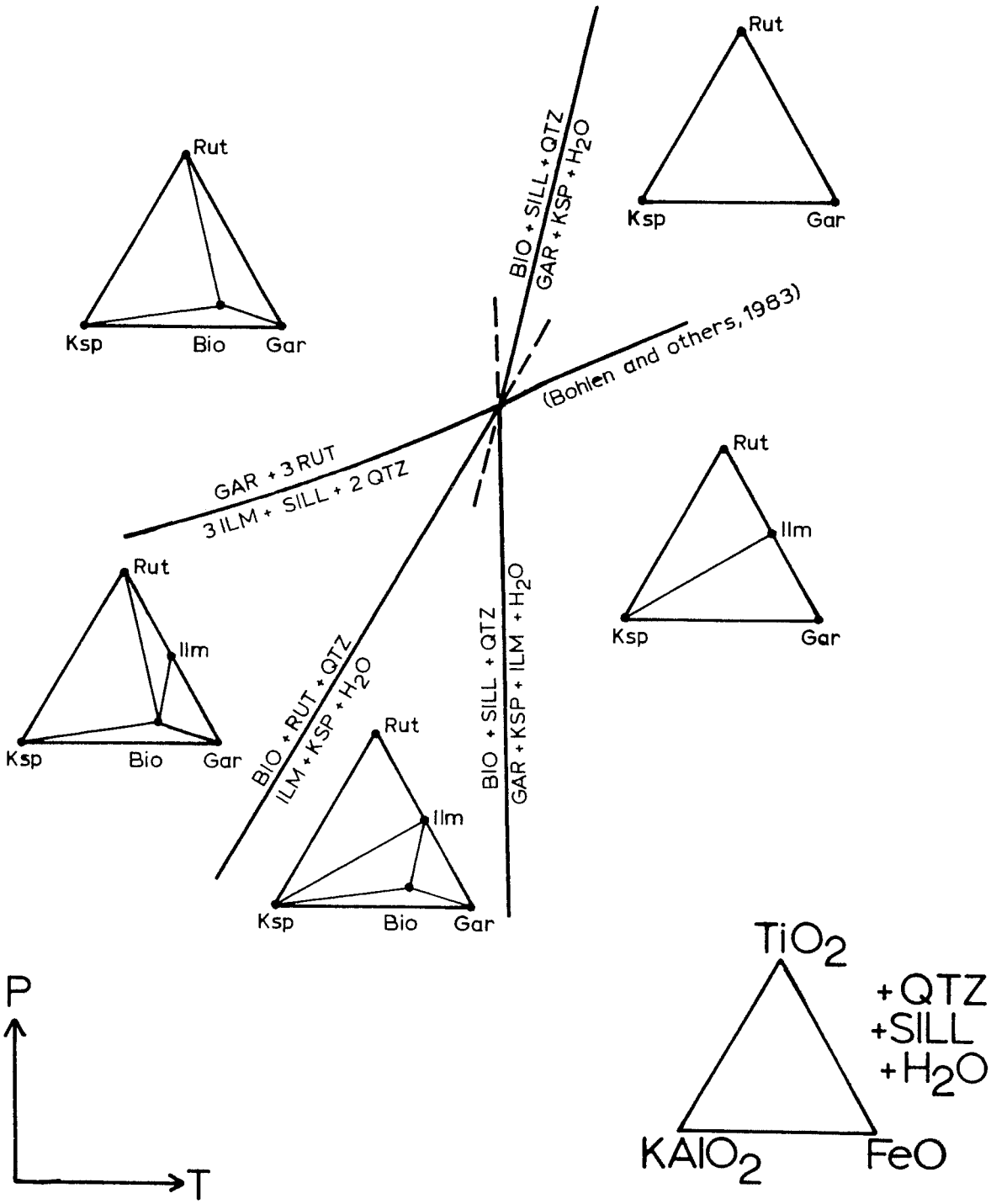

Figure 34. Schematic P-T diagram for reactions involving Rut-Ilm-Ksp-Gar-Bio-Sill-Qtz in the system TiKFASH.

true, as seen in Figure 31, hence it is possible that these pairs of garnet core and included biotite can yield information about early chemical equilibria. It is expected that garnet rims and matrix biotites continued to re-equilibrate with changing temperatures and continued hydration. Therefore the observed pairs of matrix biotite and garnet-rim compositions record chemical information at the time of either 1) the low temperature diffusion limit of the phases, or 2) the limitation of the reaction by one or more phases, perhaps H_2O in this case.

In order for pairs of garnet core and included biotite to give useful information about early equilibria, it must be shown that these phases have not changed chemically since the time of formation. As garnet and biotite are both ferromagnesian phases, it is expected that ion-exchange occurred locally with changing temperature. Because no depletion halos were observed in garnet proximal to biotite inclusions, it is assumed that the garnet host acted as an unlimited reservoir of Fe-Mg for Mg-enrichment of biotite with decreasing temperatures. It is probable, therefore, that the biotites included in garnets in these rocks have undergone localized ion-exchange as they cooled and that the observed biotite compositions are more magnesian than early equilibrium biotite compositions.

The original biotites must have been compositionally intermediate between the more iron-rich, hydrated matrix biotites and the ion-exchanged, magnesium-enriched included biotites. In order for an original biotite composition to have been preserved, the biotite would have to have been isolated from both 1) the re-equilibrating matrix and 2) other iron-magnesium-bearing phases, probably within a non-ferromagnesian phase which has survived from its time of formation to the present.

Sillimanite and potassium feldspar are two possible phases that might have enclosed and preserved original biotite compositions. Biotites have not been found as inclusions in sillimanite, but do occur rarely as inclusions in potassic feldspar porphyroblasts. No satisfactory analyses have been obtained on such biotites to date.

Garnet-biotite pairs may be used to estimate temperature of formation of an assemblage. Table 20 lists estimates made from garnet-biotite pairs from strongly sheared pelitic rocks using the Thompson calibration (Thompson, 1968). The absurd temperatures of over 900-1000 C predicted from pairs of garnet core and matrix biotite illustrate the problem of pairing minerals that never actually coexisted in equilibrium during metamorphism. Since included biotites, yielding XMg= 0.670, have undergone localized ion-exchange, temperature estimates from these pairs, 625-635°C by Thompson calibration (Thompson, 1968), must be lower than actual peak temperatures of the early metamorphism. It is also significant that the analysed included biotites are not located at the maximum-pyrope core of the garnet hosts.

Using temperature estimates of 635°C from pairs of garnet core and included biotite, and using the garnet core composition, this SILL-GAR-QTZ assemblage yields an estimated minimum pressure of 7.3 kbar

Table 20. Temperature estimates from garnet-biotite pairs. Temperature estimates are based on Fe-Mg distribution coefficients of coexisting garnet and biotite from various samples using the Thompson calibration (1976).

Sample	Mineral	XMg	XFe	Kd	ln Kd	Estimated Temperature
160X	Gar rim	.13	.87	9.630	2.265	440°C
	Matr Bio	.59	.41			
160X	Gar core	.35	.65	2.012	0.699	920
	Matr Bio	.52	.48	(Tracy)		
160X	Gar rim (near crack)	.08	.92	17.25	2.848	350
	Green Bio	.60	.40			
Tracy 160	Gar core	.35	.65	3.449	1.238	710
	Estimated Biotite	.65	.35			
X43A	Gar rim	.16	.84	6.163	1.819	540
	Matr Bio	.54	.46			
X43A	Gar core	.35	.65	1.857	0.619	1000
	Matr Bio	.50	.50			
X43A	Gar near inclusion	.27	.73	6.309	1.842	535
	Bio incl	.70	.30			
X43A	Gar core	.35	.65	4.333	1.466	635
	Bio incl	.70	.30			
W67B	Gar rim	.16	.84	5.25	1.658	580
	Matr Bio	.50	.50			
W67B	Gar rim	.16	.84	5.25	1.658	580
	Matr Bio	.50	.50			
W67B	Gar core	.25	.75	2.66	0.978	820
	Matr Bio	.47	.53			
W67B	Gar near inclusion	.22	.78	5.318	1.671	575
	Incl Bio	.60	.40			
W67B	Gar core	.25	.75	4.500	1.504	625
	Incl Bio	.60	.40			
W67B	Gar near	.23	.77	6.797	1.916	520
	Incl Bio	.67	.33			

Table 20, continued.

Sample	Mineral	XMg	XFe	Kd	ln Kd	Estimated Temperature
M22A	Gar rim	.16	.84			
	Matr Bio	.52	.48	5.688	1.738	560°C
	Green Bio	.62	.38	8.566	2.148	470
M22A	Gar core	.35	.65	2.012	0.699	920
	Matr Bio	.52	.48			
Y33	Gar rim	.12	.88	5.762	1.751	560
	Gar core	.16	.84	4.125	1.417	650
	Matr Bio	.44	.56			
M160	Gar rim	.13	.87	5.476	1.700	570
	Gar core	.15	.85	4.636	1.534	615
	Matr Bio	.45	.55			
M21	Gar rim	.05	.95	5.675	1.736	560
	Gar core	.05	.95	5.675	1.736	560
	Matr Bio	.23	.77			
M21	Gar near inclusion	.048	.952	7.336	1.993	500
	Incl Bio	.27	.73			

(Tracy and others, 1976), that is within the kyanite stability field (Holdaway, 1971) (Figure 35). Since the strongly sheared pelitic rocks were certainly within the sillimanite stability field during peak metamorphic conditions, this is a further indication that the ion-exchanged, included biotites give low temperature estimates. Accordingly, a higher temperature of 700°C was chosen as an approximation to early metamorphic temperatures and the original biotite composition was back-calculated from Thompson (1968). This calculated composition of XMg= 0.660, lies between observed matrix and included biotite values, as would be expected. Using the garnet core composition and a temperature approximation of 700°C, the SILL-GAR-QTZ assemblage yields a minimum pressure of 6.8 kbars (Tracy and others, 1976).

Pairs of garnet rim and matrix biotite record a much later equilibrium assemblage, probably the peak temperature of Acadian reheating. This temperature is estimated to have been 540 to 580°C and is in agreement with other estimates from nearby kyanite-zone cover rocks.

In summary, the pairs of garnet core and included biotite give low temperature estimates of 625-635°C and corresponding minimum pressure of 7.3 kbars, suggesting a kyanite assemblage. A higher temperature of 700 was chosen as an approximation, which yields a corresponding minimum pressure of 6.8 kbars. Calculated "original" biotite of XMg= 0.660,

based on the 700 C approximation, lies between observed matrix and included biotite compositions.

Garnet Growth During Acadian Metamorphism

Sample Y33 of reconstituted pelitic schist contains euhedral garnets with growth-zoning profiles, where Fe increases outward from the core as Mg, Mn, and Ca decrease. Decreasing Mn-content from core to rim is formed by garnet production in low- to moderate-grade rocks. This garnet must have been produced after the high temperature conditions of early metamorphism because only garnet which grew at moderate to low grades could preserve growth-zoning profiles.

This sample contains garnet, biotite, staurolite, muscovite, kyanite, plagioclase, quartz, and ilmenite, which appear to be in textural equilibrium with one another. The Acadian-age garnet may have grown by the reaction

BIO + 2 KY + QTZ = GAR + MUSC , (5)

where garnet becomes Fe-richer and biotite becomes Mg-richer. This reaction is water independent and thus not very sensitive to changes in temperature. The topology of this reaction as illustrated in Figure 36A requires that as garnet becomes more iron rich, biotite must become more magnesian so that there can be an increase in modal garnet. This repositioning of garnet-biotite tie lines can only take place with decreasing temperature, demonstrating that garnet production with Fe-enrichment took place during cooling. This is in agreement with the Spear and Selverstone (1984) diagram of calculated garnet and biotite Fe-Mg isopleths in P-T space for the assemblage quartz-garnet-Al-silicate-muscovite-biotite (Figure 37A).

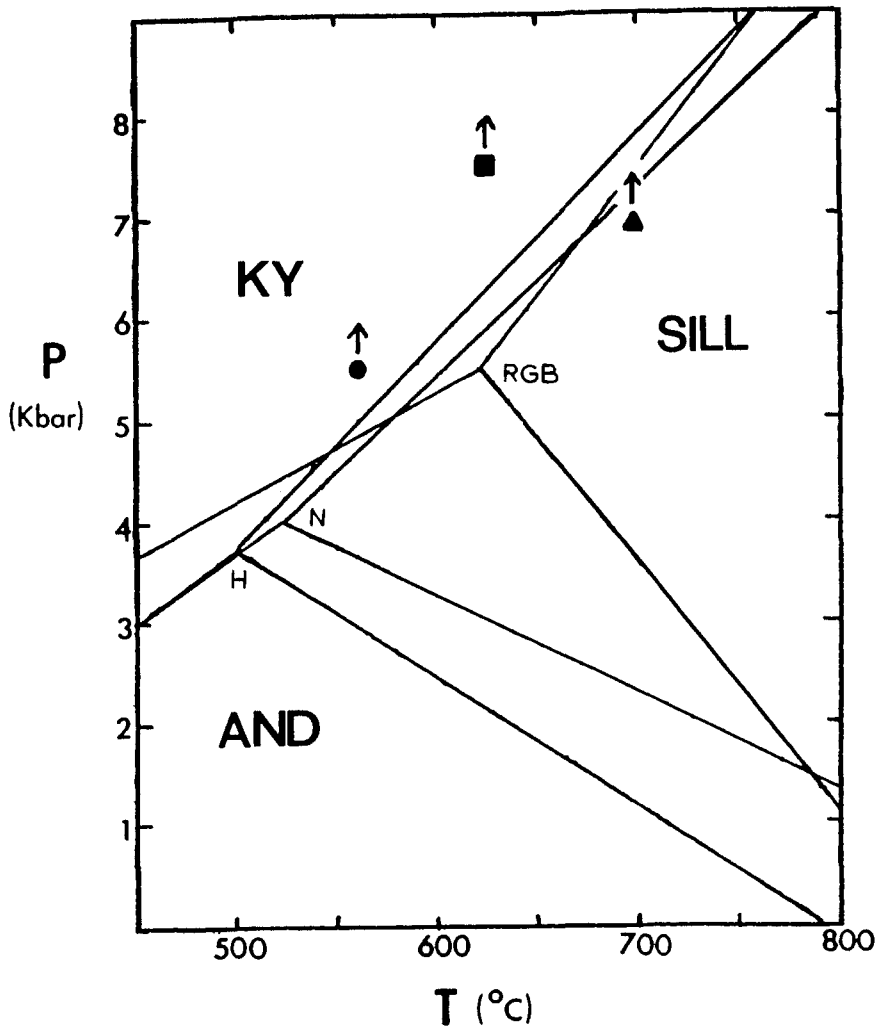

Figure 35. Pressure-temperature diagram illustrating calculated P-T estimates for regional metamorphism. Al_2SiO_5 triple points shown are from N, Newton (1966); RGB, Richardson and others (1969); and H, Holdaway (1971). Square shows estimate based on pair of garnet core with biotite inclusion. Triangle shows approximate pressure based on 700°C. Triangle is believed to be best estimate of conditions of early metamorphism. Circle represents estimate of conditions of peak Acadian metamorphism from reocnstituted samples.

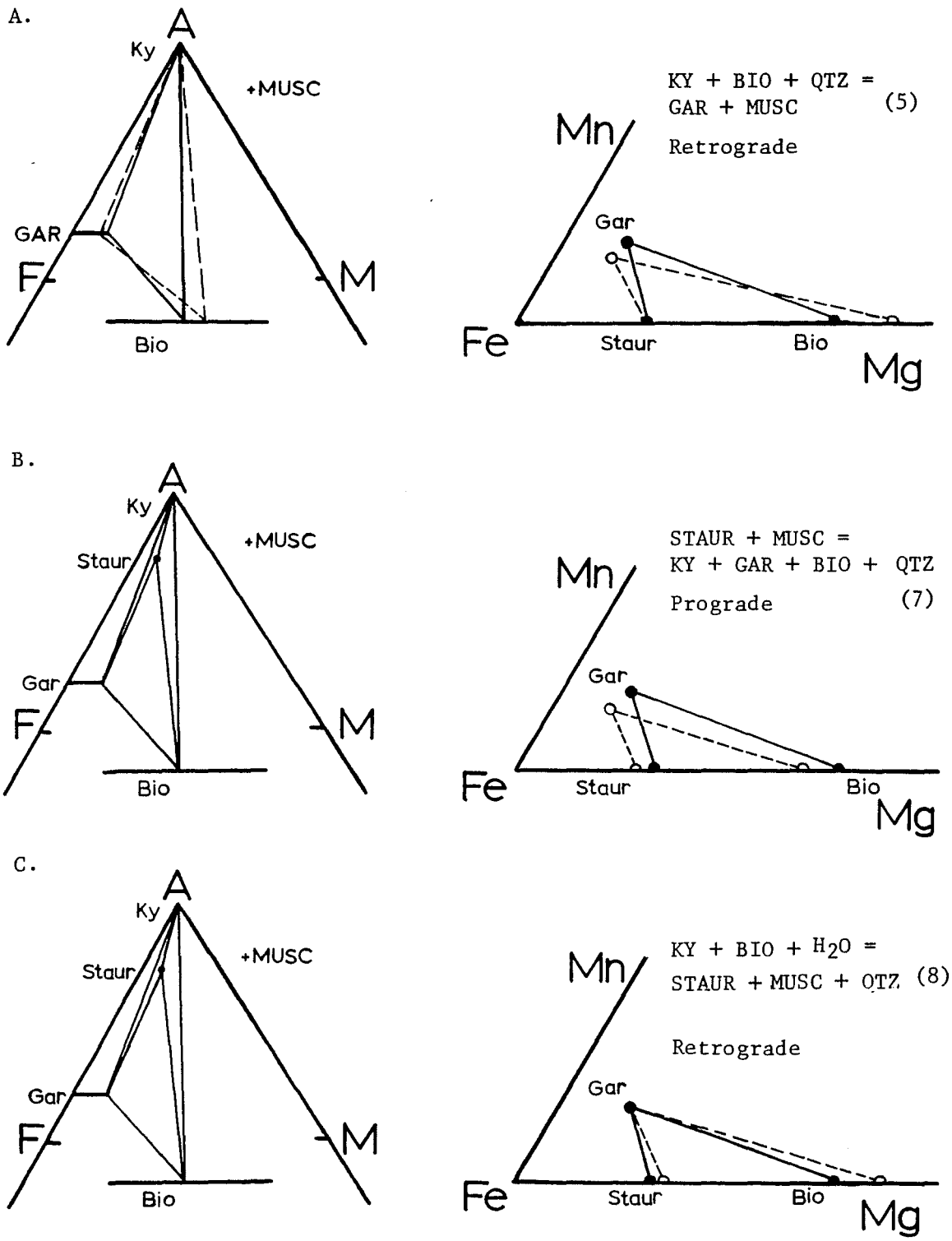

Figure 36. Illustration of possible garnet producing reactions for the assemblage gar-bio-staur-ky-musc-qtz.

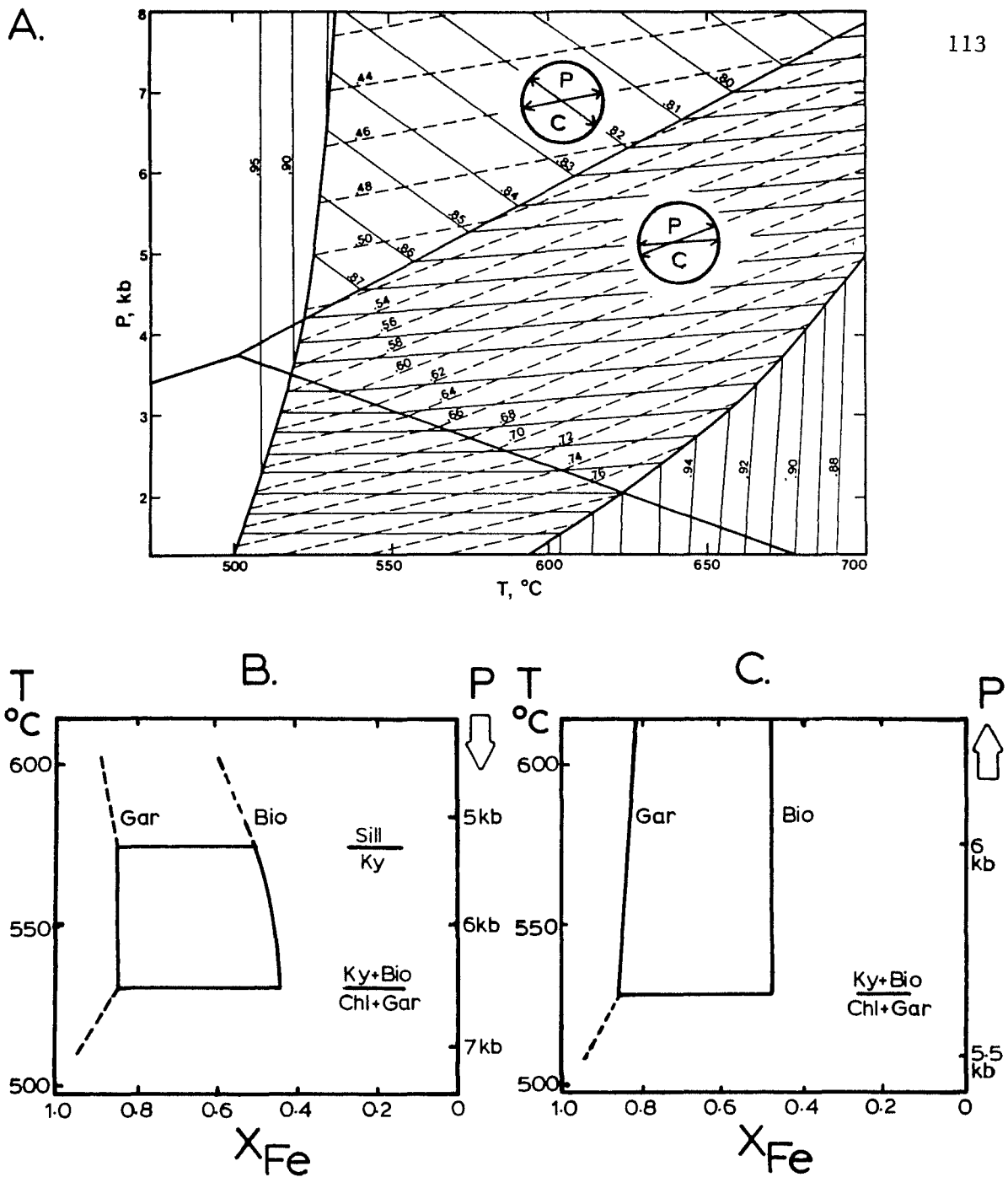

Figure 37. Production and consumption of garnet in P-T space. P-T diagram (37A) illustrating directions of garnet production (P) and consumption (C) trajectories for the assemblage gar-bio-Al_2SiO_5-qtz-musc-H_2O (after Spear & Selverstone, 1984). In kyanite stability, garnet is produced with decreasing T (or consumed with increasing T) along trajectories parallel to garnet isopleths (37B) as biotite becomes enriched in Mg. In kyanite stability, garnet is consumed with decreasing T (or produced with increasing T) along trajectories parallel to biotite isopleths (37C) as garnet becomes enriched in Fe. The boundary between garnet production and consumption must lie within the acute angle between isopleths.

T-X diagrams parallel to constant garnet and constant biotite compositions (Figure 37B) show that modal garnet increases for all trajectories within the "production" region. Likewise, modal garnet decreases for all trajectories within the "consumption" region (Figure 37C). The remaining regions, i.e. in the acute angle between garnet and biotite isopleths, may produce or consume garnet, depending on bulk composition.

If the growth-zoned garnet was produced by the above reaction (5), then garnet from sample Y33 must have grown under decreasing temperature conditions. This is because almandine increases toward the garnet rim and almandine-rich garnet in a quartz-garnet-kyanite-muscovite-biotite assemblage can only be produced with decreasing temperatures (Figure 37A).

However, the above reaction (5) ignores the presence of staurolite in the assemblage. Garnets elsewhere in central Massachusetts within Zone I of Acadian metamorphism show a similar trend of Fe-enrichment and Mn-depletion only at the rims of these garnets (Tracy and others, 1976). The same trend is found in both kyanite-bearing (sample 4F5AY) and kyanite-absent (908) assemblages, suggesting that a kyanite-absent reaction may be responsible for this trend.

Garnet may be produced in a number of ways in an assemblage containing garnet, biotite, staurolite, kyanite, muscovite, plagioclase, and quartz. Reactions which might explain the zoning in sample Y33 and other Acadian Zone I garnet rims must produce Fe-richer and Mn-poorer garnet. The reaction

STAUR + BIO + QTZ = GAR + MUSC + H_2O (6)

produces Mg-richer garnet with increasing temperatures and therefore is not consistent with garnet from sample Y33. With increasing temperature, Fe-richer garnet may be produced by the reaction

STAUR + MUSC + QTZ = KYAN + GAR + BIO + H_2O (7),

where biotite and staurolite also become Fe-richer (Figure 36B). A third reaction (Figure 36C),

KYAN + BIO + H_2O = STAUR + GAR + MUSC + QTZ (8),

which progresses with decreasing temperature is also inconsistent with garnet from sample Y33.

Neither the staurolite nor the biotite are chemically zoned, so it is impossible to determine the early compositions of these phases. If these were known, it might be possible to determine the exact garnet-producing reaction and whether that reaction took place with increasing or decreasing temperature.

MODELLING OF GARNET DIFFUSION

Mineral zoning in metamorphic rocks appears to be largely a function of porphyroblast growth during low to moderate grade continuous reactions, volume diffusion within the porphyroblast at moderate to high metamorphic grades, or both. Growth zoning may only be preserved in rocks of lower metamorphic grades, wherein negligible diffusion has taken place.

Garnets from seven samples have been chemically mapped in this study (see Figure 25). Garnets from three samples of sheared pelitic schist are interpreted as relicts of an early high grade metamorphic assemblage, where the existing zoning was produced by volume diffusion within garnet as rim composition became iron-richer with hydration and lower temperature. Diffusion gradients may have actually reached the "core" or maximum pyrope composition of garnets X43A and 160X, because the Mg-Fe profiles are rounded rather than flat at the cores. The minimum penetration distance of chemical diffusion toward the core of these two garnets is on the order of 0.5 to 1.0 mm. Garnet from sample W67B has a much flatter profile across the interior of the garnet with maximum Fe-Mg diffusion profiles of about 0.5 mm.

Models of volume diffusion within the relict garnets must explain the observed zoning profiles within temperature and time constraints and reasonable estimates of diffusion coefficients. Early in the present study, it was believed that this diffusion occurred entirely during Acadian reheating. However, models of diffusion rates within garnet discussed below suggest that some diffusion may also have taken place as the rocks cooled from the early high-temperature metamorphism.

A computer model to calculate cooling rate from observed zoning profile was adapted for use in this study (P. Crowley, pers.comm.). The model is based on a mathematical solution for Fe-Mg interdiffusion across a planar boundary (Sanford, 1982) and therefore is limited in application to garnets with large diameters relative to the diffusion penetration distance. Therefore, sample W67B is ideal for use here, whereas samples 160X and X43A may yield only qualitative results. Diffusion coefficients of Freer (1981), Elphick, Ganguly, and Loomis (1985), and Cygan and Lasaga (1985) were used as end members of currently available, experimentally calculated coefficients.

The initial garnet was assumed to have been homogeneous and pyrope-rich in composition. In the model, penetration distance is calculated based on input of initial garnet composition, peak metamorphic pressure and temperature, matrix biotite composition, radius of a given garnet grain, and time allowable for volume diffusion to take place.

Chemical compositions from sample 160X of sheared pelitic schist were used to determine maximum penetration distance predicted for a 1 mm radius garnet with Fe/(Fe+Mg) equal to 0.634 (35% pyrope) at 580°C, 5 kbar for 10 million years. Using the three different diffusion coefficients, the range in penetration distance for 10 m.y. at approximate peak Acadian conditions is 0.050 to 0.350 mm (Figure 38A).

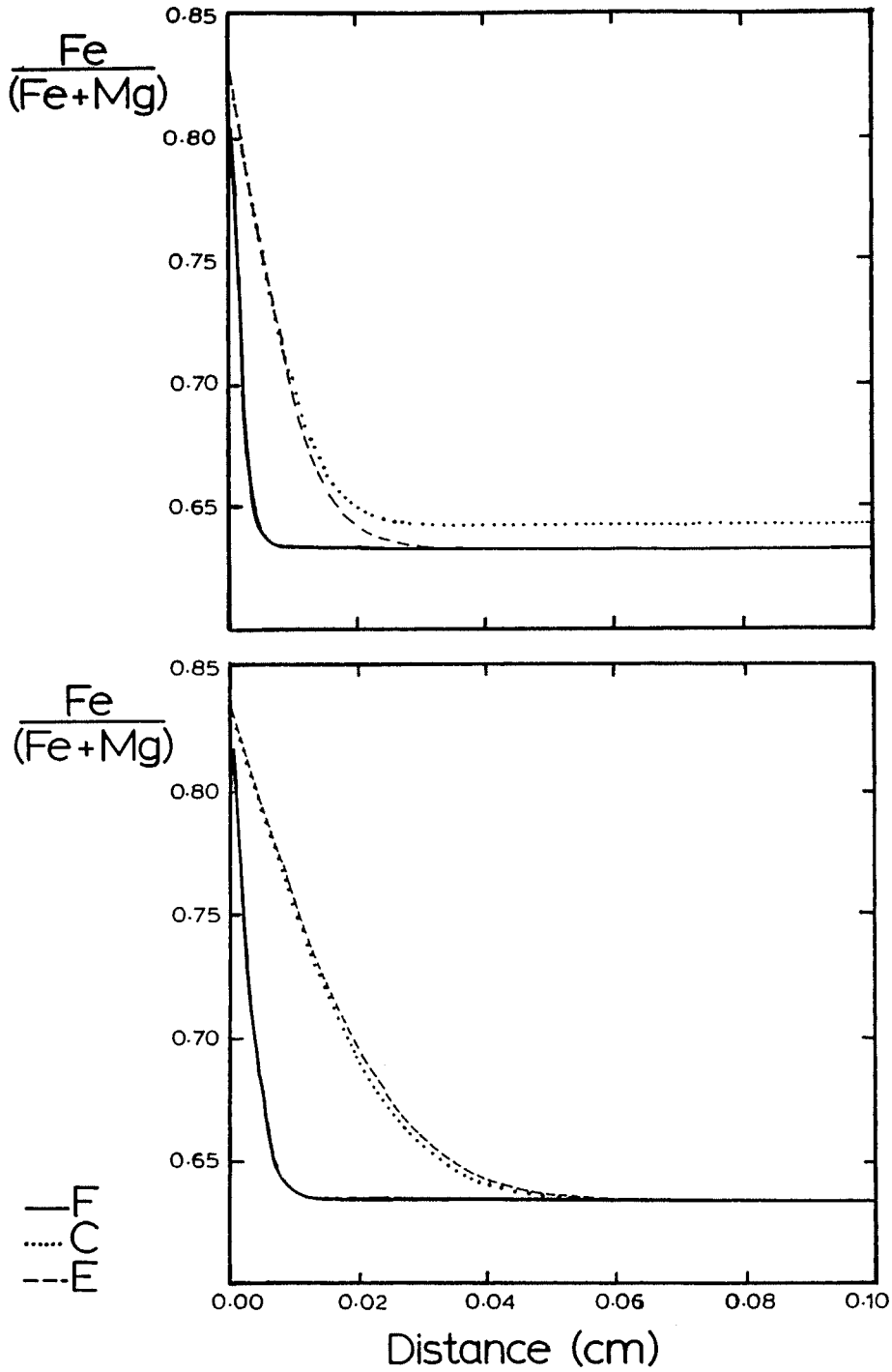

Figure 38. Garnet diffusion profiles for 10my and 40my. Diffusion penetration distance estimated by computer modelling from the following starting parameters: initially homogeneous, 2 mm diameter grain of 35% pyrope composition; constant T of 580°C; 5 kbars; and 10my (A) and 40my (B). Three curves represent diffusion coefficients of Freer (1981)(solid); Cygan and Lasaga (1985)(dotted); and Elphick and Ganguly (1985)(dashed).

Using the same starting conditions, diffusion over 40 m.y. yields penetration distances of 0.350 mm to less than 1 mm (Figure 38B). Because garnet from sample X43A has approximately the same core composition, the results are analogous for both samples.

A second calculation was used to estimate penetration of garnet of the same initial composition during cooling from 700°C to 500°C, the approximate temperatures experienced by garnet after the peak of early high grade metamorphism, assuming that continuous hydration took place. The biotite composition used here was based on back-calculation from initial temperature and garnet core composition, yielding an "original" biotite of Fe/(Fe+Mg) = 0.70. Using a moderate cooling rate of 10 C/m.y., penetration distance was estimated at approximately 0.5 mm using the coefficient of Cygan and Lasaga (1985), until measurable diffusion essentially ceased at 500°C after some 20 m.y.

Results based on this simplified model suggest that volume diffusion in high grade garnet may have been an active and successful process until garnet cooled to below approximately 500°C, where measurable diffusion ceased. Volume diffusion would have resumed in these garnets when temperatures rose above 500°C during Acadian reheating, allowing diffusion to continue to penetrate toward garnet cores. It has been shown that penetration of diffusion gradients up to 0.5 mm could have taken place during cooling from the peak of early high-grade metamorphism. Penetration of gradients up to about 1 mm could have formed over 40 m.y. at 580°C during Acadian reheating. Diffusion within garnet from sample W67B was apparently less active than in samples X43A and 160X, perhaps due to delayed initiation of the hydration reactions responsible for producing the Fe-rich gradients at garnet rims.

These models have not taken changing biotite composition into account, although such changes have clearly taken place in these rocks. Changes in modal amounts or interaction with other Fe-Mg phases also have not been included in this simplified model and must be considered before results may be interpreted quantitatively.

Hydration immediately following the peak of early metamorphism may have been a local phenomenon in these rocks and may have had some control on the amount of diffusion that took place as the rocks cooled to 500°C. Evidence for this early hydration event is found in only a few of the sheared schist samples. A correlation between textural evidence and penetration distance may show which rocks have undergone this early hydration.

Modal garnet decreased with the progress of various hydration reactions and individual garnets decreased in radius. The net effect of diffusion penetration concurrent with garnet consumption depends on the rates at which these processes took place. Higher temperature, longer time, and iron-enrichment of the garnet rim tend to increase diffusion penetration distances while consumption of garnet at the rim tends to reduce penetration distances.

Garnets from partially reconstituted pelitic rock (sample 160M) do not show strong zoning profiles, suggesting that the radius of remaining relict garnet is smaller than the diffusion penetration achieved in the grain. Although garnets from this sample are probably relics, the observed core composition is close to that in equilibrium with the Acadian matrix assemblage, due to effective diffusion.

HISTORY OF METAMORPHISM

Conditions of Early Metamorphism

Because varying amounts of hydration took place locally in these rocks, the geologist is able to see evidence concerning an early metamorphism which might otherwise have been destroyed. Based on textural and petrographic evidence, the early high-temperature mineral assemblage consisted of sillimanite, orthoclase, garnet, biotite, quartz, plagioclase, sulfide, and rutile. It appears that these rocks were relatively water-poor at the peak of early metamorphism due to prograde dehydration reactions.

Study of the Fe-Mg relations in analysed garnet-biotite pairs indicates that the temperature of peak metamorphism was greater than 635° C and was probably near 700°C. The composition of garnet cores, assuming a sillimanite-garnet-quartz assemblage at 700°C, yields a minimum pressure of 6.8 kbar (Tracy and others, 1976).

Little evidence has been found to constrain the cooling path of these high grade rocks. However, one may be fairly certain that the Precambrian rocks of the Pelham dome experienced shallow crustal conditions after the early high-grade metamorphism due to pre-Acadian erosion and uplift. They were probably at no more than 1-2 km depth during the Middle Ordovician orogeny, in that they appear to have been located east of any major Taconian deformation. Metamorphic conditions were again achieved during the Acadian orogeny over a time span of approximately 45 m.y. (405 to 361 m.y.; Robinson and others, 1986, p.208). Subsequent cooling resulted from post-Acadian uplift and erosion.

Aluminosilicate Stability

Inclusions of sillimanite within potassium feldspar porphyroblasts prove that sillimanite was stable in the early high-grade assemblage. The history of aluminosilicate stability between the peak of the early metamorphism and the Acadian regional metamorphism in the kyanite zone is not well constrained.

Sillimanite plus biotite rims on garnet porphyroblasts in sheared pelitic schist indicate that at least limited progress of the garnet-consuming reaction, GAR + KSP + H_2O = BIO + SILL + QTZ (1), must have occurred within the sillimanite zone. The simple interpretation of a pre-Middle Ordovician early metamorphism and cooling, and a mid-Devonian metamorphism to the kyanite zone necessitates the occurrence of some hydration following the peak of the early

metamorphism, before cooling below metamorphic temperatures. It is suggested that the sillimanite plus biotite rims must have formed on garnet late in the early metamorphism due to hydration before the rocks cooled below sillimanite stability conditions.

Several pelitic samples from locality M22 contain pods of kyanite and sillimanite up to a few centimeters in length. These are visible in hand sample where kyanite color gives the pods a pale blue color. In thin section, these pods are composed of both kyanite and sillimanite. Garnet-rim and adjacent aluminosilicate textures do not give conclusive evidence for resolving kyanite-sillimanite relationships.

A simple model would have sillimanite as a key part of the early peak metamorphic assemblage with additional sillimanite produced shortly after the early peak due to minor hydration via the reaction,

$$GAR + KSP + H_2O = BIO + SILL/KY + QTZ \quad (1)$$

The rock was then reheated in the Acadian to the kyanite zone. Hydration would have produced kyanite as a stable phase also via reaction (1). During this time, sillimanite may have dissolved and recrystallized as kyanite or may have been consumed once muscovite became stable in the rock. The sample containing 10% modal muscovite does not contain sillimanite as a matrix phase, further suggesting that sillimanite was unstable during the later stages of Acadian hydration.

Another possible P-T model is that during the suggested hydration just after the peak of early metamorphism, the rock cooled isobarically into the kyanite stability field, resulting in an early generation of kyanite unrelated to Acadian heating. Subsequent hydration and reheating remained within the kyanite stability region. This model is not likely from a tectonic perspective because it necessitates having cold rocks at depth.

Muscovite Stability

Textural evidence strongly supports the contention that muscovite was not stable during the peak of the early metamorphism. As the rocks cooled following early metamorphism, they appear to have been too water-poor for muscovite growth and stability. Any hydration occurring soon after the early metamorphism either 1) occurred within the K-feldspar stability field preventing muscovite growth or 2) was not sufficient to allow for muscovite growth.

Muscovite probably became stable during substantial localized hydration within relatively cooler Acadian conditions. The first muscovites to appear were probably potassium-rich. Such muscovites from sheared schists were probably only in local equilibrium with mineral assemblages. With continued hydration, muscovite was produced at the expense of potassium feldspar, plagioclase, and aluminosilicate, and became more sodic in composition.

Conditions of Acadian Metamorphism

Acadian heating of the Mt. Mineral Formation probably occurred concurrently with localized hydration. The effects of the Acadian

hydration appear to have been far more influential on these rocks than a mere low-grade reheating. With the amount of hydration varying locally, those localities receiving small influxes of water were able to preserve largely the early textures and minerals. Localities receiving greater amounts of water were increasingly reconstituted, forming typical Acadian kyanite-zone assemblages.

At least initially, and in some cases totally, the progress of hydration reactions was limited by the amounts of water available during metamorphic conditions. Therefore the changing conditions of pressure and temperature during prograde Acadian metamorphism had relatively little mineralogical effect on these rocks, and not until the rocks became fully hydrated, itself a spatially limited phenomenon, did they fully re-equilibrate to kyanite-zone conditions.

Figure 39 illustrates this Acadian prograde hydration on a Temperature vs. aH2O diagram. The Mt. Mineral Formation was reheated to kyanite zone temperatures (about 580°C, see Table 20) with variable water influx. Initially the reaction

GAR + KSP + H2O = BIO + SILL + QTZ (1)

would have been experienced by garnet- and K-feldspar-bearing assemblages which had any available water. Several rocks, in fact, were never able to proceed beyond this initial hydration reaction. Others would have acquired enough water for muscovite to become stable, allowing the reactions

KSP + Al-Sil. + H2O = MUSC + QTZ (2), and

GAR + KSP + H2O = BIO + MUSC + QTZ (3),

to take place. Finally, when sufficient water was provided to consume all potassium feldspar or garnet, the hydration reactions ceased to be important in the rock. At this point the rock was able to fully adjust to changing Acadian pressure and temperature conditions and a typical prograde assemblage was formed.

Sample Y33 contains euhedral garnets, apparently produced following complete (or near complete) hydration at this locality. Textural and chemical zoning evidence strongly suggest that new garnet nucleated and grew during kyanite zone metamorphism. It has been suggested, based on phase relationships and the model of Spear and Selverstone (1985), that these garnets grew with decreasing temperatures, probably following the thermal peak of Acadian metamorphism.

The mineral assemblage observed in sample Y33 of muscovite, biotite, garnet, kyanite, staurolite, plagioclase, ilmenite, and quartz is believed to represent this fully hydrated equilibrium. Prograde garnet probably grew at the expense of biotite, staurolite, and/or kyanite.

Pairs of garnet-rim and matrix-biotite from samples of reconstituted pelitic schist suggest a range of 540 to 580°C for peak Acadian temperatures. The corresponding pressure estimate in this kyanite-garnet-quartz assemblage is 5.5 kbar (Tracy and others, 1976).

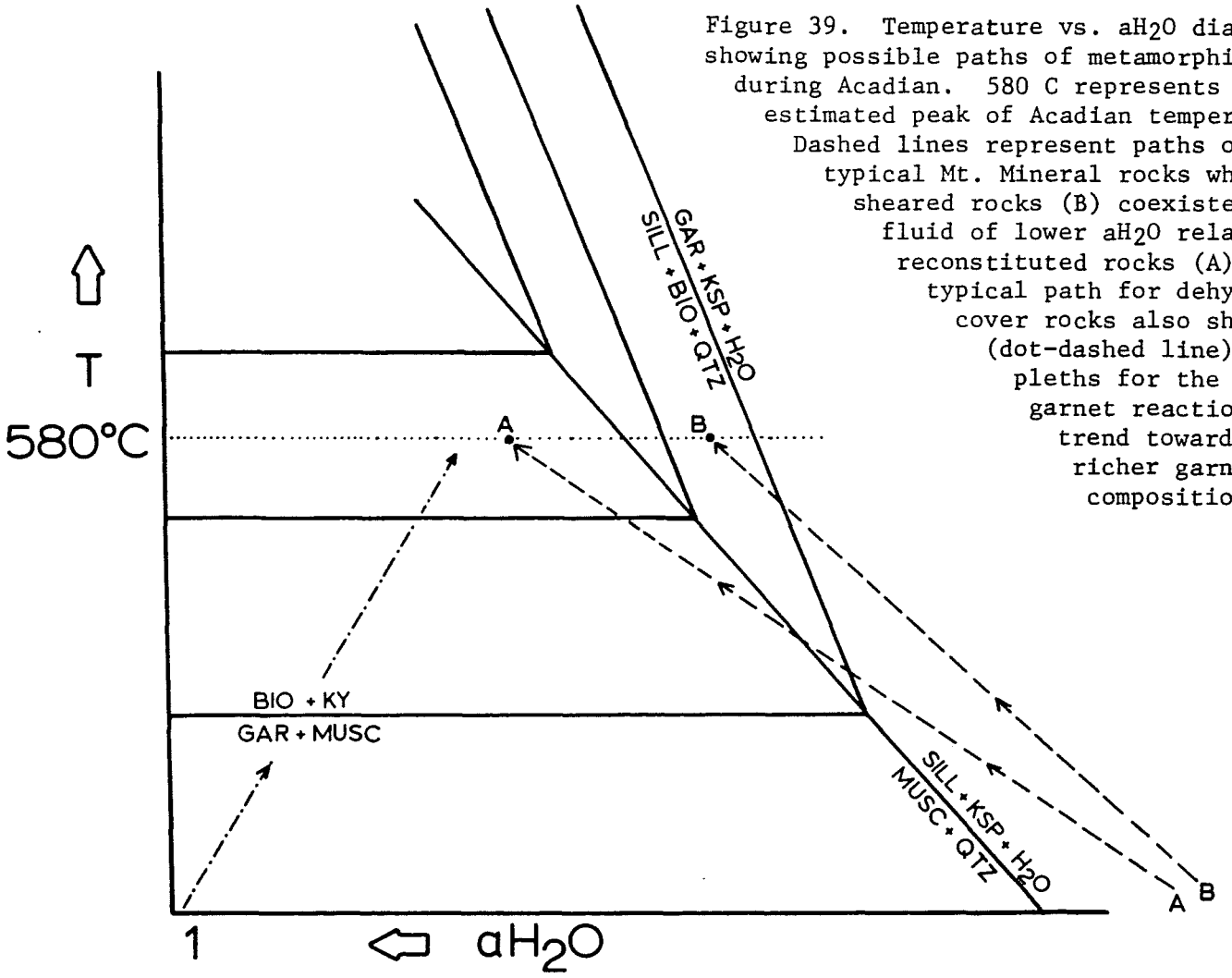

Figure 39. Temperature vs. aH_2O diagram showing possible paths of metamorphism during Acadian. 580 C represents estimated peak of Acadian temperature. Dashed lines represent paths of typical Mt. Mineral rocks where sheared rocks (B) coexisted with fluid of lower aH_2O relative to reconstituted rocks (A). A typical path for dehydrating cover rocks also shown (dot-dashed line). Isopleths for the two garnet reactions show trend toward iron-richer garnet compositions.

CONCLUSIONS

The Mt. Mineral Formation was metamorphosed to a sillimanite-orthoclase-biotite-garnet-rutile assemblage at approximately 700°C and 6.8 kbar, probably before Middle Ordovician time. Muscovite was not a stable phase during the peak of this high-grade metamorphism. Some hydration probably occurred as the rocks cooled from these peak metamorphic temperatures. During this suggested hydration, garnet and K-feldspar would have been consumed, producing biotite and sillimanite, but perhaps also producing biotite and kyanite with decreased temperature.

Chemical gradients were produced at the rims of garnet grains by diffusion as garnet rims re-equilibrated with co-existing matrix phases during hydration at (relatively) lower temperatures. Because initial Fe-enrichment of matrix phases was controlled by the progress of the reaction GAR + KSP + H_2O = BIO + SILL/KY + QTZ, penetration of the Fe-enriched gradient within garnet could not have begun prior to hydration. If, in fact, hydration began during cooling from early high-grade metamorphism, chemical gradients initiated at garnet rims may have penetrated up to 0.5 mm toward the cores. Once the rocks cooled below 500°C, measurable diffusion would have ceased.

Reheating during the Acadian metamorphism probably achieved conditions of 580°C and 5.5 kbar. Localized variations in hydration state were responsible for forming the wide range in textures and mineralogy in these rocks. Relics of the early high-grade assemblage occur where activity of water was very low. Where the activity of water was higher, garnet and K-feldspar were increasingly consumed, and biotite + kyanite or biotite + muscovite were produced.

Muscovite was probably not a stable phase until significant hydration took place in the reheated rocks. It was produced in certain rocks at the expense of K-feldspar and aluminosilicate. It was also produced in some rocks together with biotite at the expense of garnet and K-feldspar.

The hydration reactions active in these rocks included

GAR + KSP + H_2O = BIO + Al.-sil. + QTZ, (1)
KSP + Al-sil. + H_2O = MUSC + QTZ, (2) and
GAR + KSP + H_2O = BIO + MUSC + QTZ. (3)

In rocks where hydration reactions were not limited by low aH2O, typical Acadian kyanite-zone assemblages were able to form. Growth-zoning in garnet from one sample of the reconstituted rocks must have developed following almost complete recrystallization of the early high-temperature assemblage. Possible garnet-producing reactions have been suggested involving the phases garnet, biotite, kyanite, staurolite, quartz, and fluid. Pressure and temperature conditions during Acadian garnet growth have not been constrained.

Volume diffusion in garnets should have been active during the Acadian reheating to temperatures above 500°C. Chemical gradients,

possibly initiated during cooling from the early high-grade metamorphic peak, would have begun to or continued to penetrate toward garnet cores. Measurable diffusion would have ceased as rocks cooled below 500°C, leaving some relict garnets with penetration distances on the order of 1 mm, and in some cases, very steep chemical gradients of up to 15% pyrope over 0.5 mm.

REFERENCES CITED

Albee, A.L., and Ray, L., 1970, Correction factors for electron probe microanalysis of silicates, oxides, carbonates, phosphates, and sulfates: Analytical Chemistry v.42, p.1408-1414.

Anderson, D.E., and J.C. Olimpio, 1977, Progressive homogenization of metamorphic garnets, South Morar, Scotland: evidence for volume diffusion: Canadian Mineralogist v.15, p.206-216.

Ashenden, D.D., 1973, Stratigraphy and structure of the northern portion of the Pelham dome, north-central Massachusetts: Contribution No.16 (M.S. thesis), Department of Geology and Geography, University of Massachusetts, Amherst, 132 p.

Atherton, M.P., 1968, The variation in garnet, biotite, and chlorite composition in medium grade pelitic rocks from the Dalradian, Scotland, with particular reference to the zonation in garnet: Contributions to Mineralogy and Petrology v.18, p.347-371.

Balk, Robert, 1956, Bedrock geology of the Massachusetts portion of the Northfield quadrangle, Massachusetts, New Hampshire, and Vermont: U.S. Geological Survey Geologic Quadrangle Map GQ-92, scale 1:31,680.

Banno, S. and Kurata, H., 1972, Distribution of Ca in zoned garnet of low-grade pelitic schists: Journal of Geological Society of Japan v.78, p.507-512.

Bence, A.E., and Albee, A.L., 1968, Empirical correction factors for the electron microanalysis of silicates and oxides: Journal of Geology v.76, p.382-403.

Blackburn, W.H., 1969, Zoned and unzoned garnets from the Grenville gneisses around Gananoque, Ontario: Canadian Mineralogist v.9, p.691-698.

Bohlen, S.R., Wall, V.J., and Boettcher, A.L., 1983, Experimental investigations and geological applications of equilibria in the system $FeO-TiO_2-Al_2O_3-SiO_2-H_2O$: American Mineralogist v.68, p.1049-1058.

Chamberlain, C.P., and J.B. Lyons, 1983, Pressure, temperature, and metamorphic zonation studies of pelitic schists in the Merrimack Synclinorium, South-central New Hampshire: American Mineralogist v.68, p.530-540.

Chatterjee, N.D. and Flux, S., 1986, Thermodynamic mixing properties of muscovite-paragonite crystalline solutions at high temperatures and pressures and their geological applications: Journal of Petrology v.27, p.677-693.

Chinner, G.A., 1962, Almandine in thermal aureoles: Journal of Petrology v.3, p.316-340.

Crawford, M.L., 1977, Calcium zoning in almandine garnet, Wissahickon Formation, Philadelphia, Pennsylvania: Canadian Mineralogist v.15, p.243-249.

Crowley, Peter, 1987, Personal communication.

Cygan, R.T., and A.C. Lasaga, 1985, Self-diffusion of magnesium in garnet at 750-900 C : American Journal of Science v.285, p.328-350.

deBethune, P.D., D. Laduron, and J. Boquet, 1975, Diffusion processes in resorbed garnets: Contributions to Mineralogy and Petrology. v.50, p.197-204.

Dempster, T.J., 1985, Garnet zoning and metamorphism of the Barovian type area, Scotland: Contributions to Mineralogy and Petrology

v.89, p.30-38.
Elphick, S.C., J. Ganguly, and T.P. Loomis, 1985, Experimental determination of cation diffusivities in aluminosilicate garnets: I. Experimental methods and interdiffusion data: Contributions to Mineralogy and Petrology v.90, p.36-44.
Emerson, B.K., 1898, Geology of old Hampshire County, Massachusetts: U.S. Geological Survey Monograph 29, 790 p.
_____, 1917, Geology of Massachusetts and Rhode Island: U.S. Geological Survey Bulletin 597, 289 p.
Evans, B.W. and Guidotti, C.V., 1966, The sillimanite-potash feldspar isograd in western Maine, U.S.A.: Contributions to Mineralogy and Petrology v.12, p.25-62.
Ferry, J.M. and Spear, F.S., 1978, Experimental calibration of the partitioning of Fe and Mg between biotite and garnet: Contributions to Mineralogy and Petrology v.66, p.113-117.
Freer, R., 1979, An experimental measurement of cation diffusion in almandine garnet: Nature v.280, p.220-222.
Grant, J.A., and Weiblen, P.W., 1971, Retrograde zoning in garnet near the second sillimanite isograd: American Journal of Science v.270, p.281-296.
Harte, B., and K.J. Henley, 1966, Occurrence of compositionally zoned almanditic garnets in regionally metamorphosed rocks: Nature v.210, p.689-692.
Henry, D.J., and Guidotti, C.V., 1985, Tourmaline as a petrogenetic indicator mineral: an example from the staurolite-grade metapelites of NW Maine: American Mineralogist v.70, p.1-15.
Hess, P.C., 1971, Prograde and retrograde equilibria in garnet-cordierite gneisses in south-central Massachusetts: Contributions to Mineralogy and Petrology v.30, p.177-195.
Hodgkins, C.E., 1985, Geochemistry and petrology of the Dry Hill Gneiss and related gneisses, Pelham dome, central Massachusetts: Contribution No.48 (M.S. thesis), Department of Geology and Geography, University of Massachusetts, Amherst, 137 p.
Holdaway, M.J., 1971, Stability of andalusite and the aluminum-silicate phase diagram: American Journal of Science v.271, p.97-131.
Hollister, L., 1966, Garnet zoning: an interpretation based on the Rayleigh Fractionation model: Science v.154, p.1647-1651.
_____, 1977, The reaction forming cordierite from garnet, the Khtada Lake Metamorphic Complex, British Columbia: Canadian Mineralogist v.15, p.217-229.
Hollocher, K.T., 1981, Retrograde metamorphism of the Lower Devonian Littleton Formation in the New Salem area, west-central Massachusetts: Contribution No.37 (M.S. thesis), Department of Geology and Geography, University of Massachusetts, Amherst, 268 p.
Karabinos, P., 1984, Polymetamorphic garnet zoning from southeastern Vermont: American Journal of Science v.284, p.1008-1025.
Kerr, A., 1981, Zoning in garnet from the mainland Lewisian: Mineralogical Magazine v.44, p.191-194.
Kretz, R., 1973, Kinetics of the crystallization of garnet at two localities near Yellowknife: Canadian Mineralogist v.12, p.1-20.
Laird, H.S., 1974, Geology of the Pelham dome near Montague, west-central Massachusetts: Contribution No.14 (M.S. thesis), Department of Geology and Geography, University of Massachusetts, Amherst, 84 p.
Loomis, P.T. and Nimick, F.B., 1982, Equilibrium in Mn-Fe-Mg Al pelitic

compositions and equilibrium growth of garnet: Canadian Mineralogist v.20, p.393-410.

McAteer, C., 1976, Formation of garnets in a rock from Mallaig: Contributions to Mineralogy and Petrology v.55, p.293-301.

Michener, S.R., 1983, Bedrock geology of the Pelham-Shutesbury Syncline, Pelham dome, west-central Massachusetts: Contribution No.43 (M.S. thesis), Department of Geology and Geography, University of Massachusetts, Amherst, 101 p.

Miyashiro, Akiho, 1953, Calcium-poor garnet in relation to metamorphism: Geochimica et Cosmochemica Acta v.4, p.179-208.

Newton, R.C., 1966, Kyanite-andalusite equilibrium from 700 to 800 C : Science v.153, p.170-172.

Onasch, C.M., 1973, Analysis of the minor structural features in the north-central portion of the Pelham dome: Contribution No.12 (M.S. thesis), Department of Geology and Geography, University of Massachusetts, Amherst, 87 p.

Orville, P.M., 1967, Unit-cell parameters of the microcline-low albite and the sanidine-high albite solid solution series: American Mineralogist v.52, p.55-86.

Richardson, S.W., Gilbert, M.C., and Bell, P.M., 1969, Experimental determination of kyanite-andalusite and andalusite-sillimanite equilibria: the aluminosilicate triple point: American Journal of Science, v.267, p.259-272.

Robinson, Peter, 1979, Bronson Hill anticlinorium and Merrimack synclinorium in central Massachusetts. In Skehan, J.W., S.J., and Osberg, P.H., eds., The Caledonides in the U.S.A.: geological excursions in the northeast Appalachians. IGCP Project 27 , Caledonide Orogen, p.126-150. Weston Observatory, Weston, Massachusetts.

_____, and others, 1973, Progress bedrock geologic map, eastern part of the Shutesbury quadrangle, central Massachusetts: Department of Geology and Geography, University of Massachusetts, Amherst.

_____, Tracy, R.J., Ashwal, L.D., 1975, Relict sillimanite-orthoclase assemblage in kyanite-muscovite schist, Pelham dome, west-central Massachusetts, abstract: Transactions of the American Geophysical Union v.56, p.466.

_____, Tracy, R.J., Hollocher, K.T. and Dietsch, C.W., 1982, High grade Acadian regional metamorphism in south-central Massachusetts: In Joesten, R., and Quarrier, S.D., eds., 1982 New England Intercollegiate Geological Conference, 74th Annual M e eting Guidebook, Field Trip P3, 1-51.

_____, Tracy, R.J., Hollocher, K.T., Schumacher, J.C., and Berry, H.N. IV, 1986, The central Massachusetts metamorphic high. In Robinson, Peter and Elbert, D.C., eds., Field trip guidebook: Regional Metamorphism and Metamorphic Phase Relations in Northwestern and Central New England: Contribution No. 59 (IMA Trip B-5), Department of Geology and Geography, University of Massachusetts, Amherst, p.195-266.

Sanford, R.F., 1982, Three Fortran programs for finite-difference solutions to binary diffusion in one and two phases with composition-and time-dependent diffusion coefficients: Computers and Geosciences v.8, p.235-263.

Spear, F.S., and Selverstone, J., 1984, Quantitative P-T paths from zoned minerals: Theory and tectonic applications: Contributions to

Mineralogy and Petrology v.83, p.348-357.
Stanley, R.S., and Ratcliffe, N.M., 1985, Tectonic synthesis of the Taconian Orogeny in western New England: Geological Society of America Bulletin v.96, p.1227-1250.
Thompson, A.B., 1976, Mineral reactions in pelitic rocks. II. Calculation of some P-T-X, Fe-Mg, phase relations: American Journal of Science v.276, p.425-454.
Thompson, J.B., Jr., 1957, The graphical analysis of mineral assemblages in pelitic schists: American Mineralogist v.42, p.842-858.
_____, Robinson, Peter, Clifford, T.N., and Trask, J.J., 1968, Nappes and gneiss domes in west-central New England: _in_ Zen, E-an and others, eds., Studies of Appalachian geology, Northern and Maritime: New York, John Wiley and Sons, p.203-218.
Thompson, Peter J., 1985, Stratigraphy, structure, and metamorphism in the Monadnock Quadrangle, New Hampshire: Contribution No.58 (Ph.D. thesis), Department of Geology and Geography, University of Massachusetts, Amherst, 191 p.
Tracy, R.J., 1975, High grade metamorphic reactions and partial melting in pelitic schist, Quabbin Reservoir area, Massachusetts: Contribution No.20 (M.S. thesis), Department of Geology and Geography, University of Massachusetts, Amherst, 127 p.
_____, 1978, High grade metamorphic reactions and partial melting in pelitic schist, west-central Massachusetts: American Journal of Science v.278, p.150-178.
_____, and Dietsch, C.W., 1982, High temperature retrograde reactions in pelitic gneiss, central Massachusetts: Canadian Mineralogist v.20, p.425-437.
_____, Robinson, Peter, and Thompson, A.B., 1976, Garnet composition and zoning in the determination of temperature and pressure of metamorphism, central Massachusetts: American Mineralogist v.61, p.762-775.
_____, Robinson, Peter, and Wolff, R.A., 1984, Metamorphosed ultramafic rocks in the Bronson Hill anticlinorium, central Massachusetts: American Journal of Science v.284, p.530-558.
Woodsworth, G.J., 1977, Homogenization of zoned garnets from pelitic schists: Canadian Mineralogist v.15, p.230-242.
Wright, T.L., 1968, X-ray and optical study of alkali feldspar: II. An X-ray method for determining the composition and structural state from measurement of 2-theta values for three reflections: American Mineralogist v.53, p.88-104.
_____, and Stewart, D.B., 1968, X-ray and optical study of alkali feldspar: I. Determination of composition and structural state from refined unit-cell parameters and 2V: American Mineralogist v.53, p.38-87.
Yardley, B.W.D., 1977, An empirical study of diffusion in garnet: American Mineralogist v.62, p.793-800.
Zartman, R.E., and Leo, G.W., 1985, New Radiometric ages on gneisses of the Oliverian domes in New Hampshire and Massachusetts: American Journal of Science, v.285, no.3, p.267-280.
Zen, E-an, ed., Goldsmith, Richard, Ratcliffe, N.M., Robinson, Peter, and Stanley, R.S., compilers, 1983, Bedrock geologic map of Massachusetts: U.S. Geological Survey special map, scale 1:250,000.

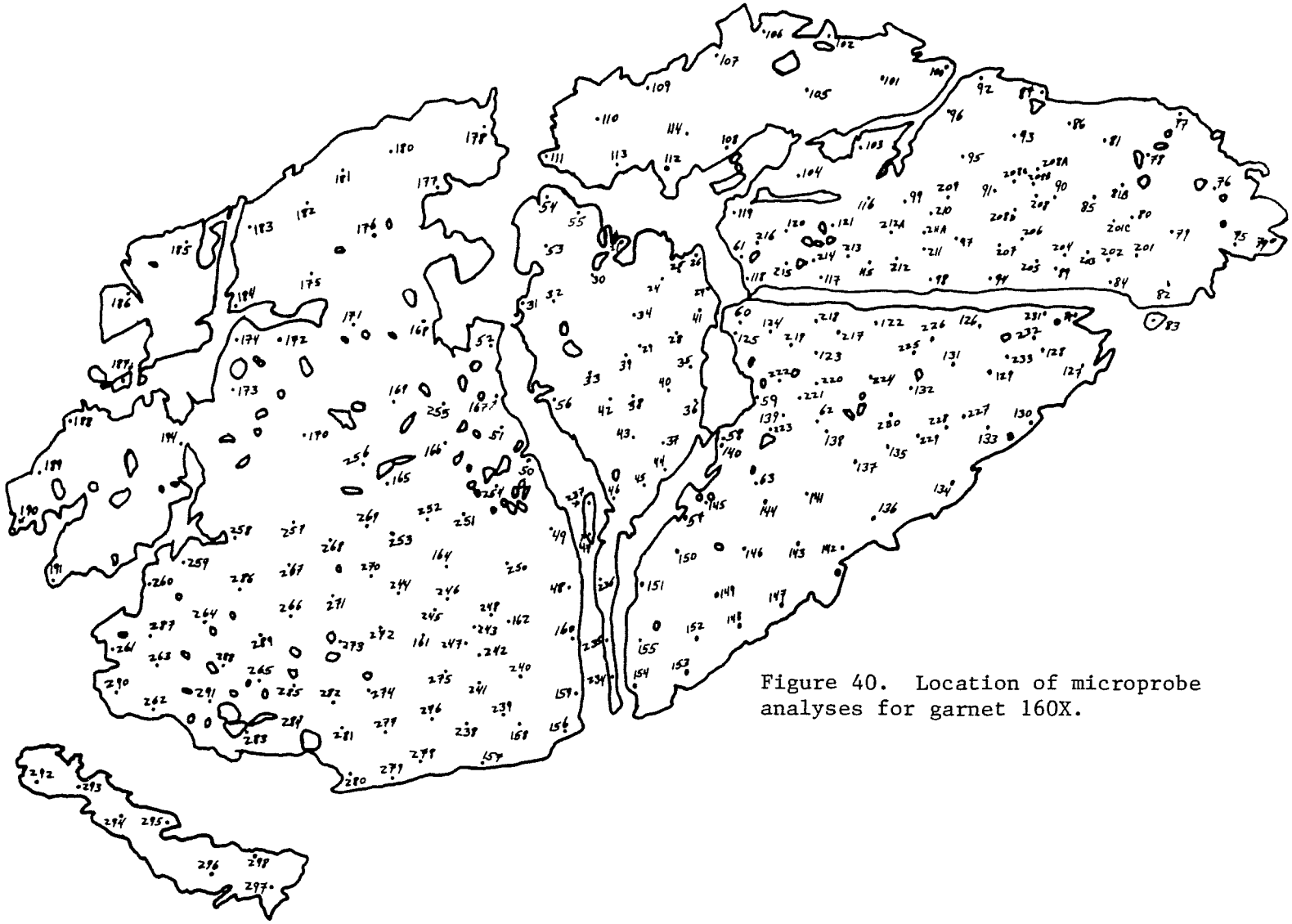

Figure 40. Location of microprobe analyses for garnet 160X.

Table 21. 160X Garnet Microprobe Analyses.

Alys#	21	23	24	25	26	27	28	29	30	31
SiO_2	37.82	38.45	37.49	38.58	38.08	37.20	38.60	37.94	38.32	37.12
TiO_2	0.12	0.13	0.12	0.13	0.12	0.11	0.10	0.0	0.01	0.0
Al_2O_3	21.02	21.93	22.36	21.69	21.11	19.74	20.97	21.95	21.58	21.67
Cr_2O_3	0.09	0.11	0.09	0.09	0.12	0.09	0.09	0.0	0.0	0.0
FeO	35.18	34.99	32.23	34.31	36.40	37.14	30.28	29.68	31.87	35.11
MnO	1.01	0.89	0.61	0.80	1.06	1.18	0.57	0.55	0.62	1.16
MgO	3.52	3.76	4.71	3.55	2.55	1.96	9.82	8.18	5.47	3.58
CaO	1.43	1.31	1.30	1.20	1.23	1.20	1.14	1.20	1.41	1.40
Total	100.19	101.57	98.91	100.35	100.67	98.62	101.57	99.50	99.28	100.04
Formulae based on 12 oxygens										
Si	3.022	3.015	2.985	3.049	3.040	3.060	2.965	2.966	3.032	2.974
Al	1.981	2.027	2.100	2.022	1.987	1.915	1.899	2.023	2.013	2.047
Cr	0.006	0.007	0.006	0.006	0.007	0.006	0.005			
Total	1.987	2.034	2.106	2.028	1.994	1.921	1.904			
Ti	0.006	0.007	0.007	0.007	0.007	0.007	0.006			
Fe	2.352	2.295	2.147	2.270	2.432	2.556	1.946	1.942	2.110	2.354
Mg	0.420	0.440	0.559	0.419	0.303	0.240	1.125	0.954	0.646	0.428
Mn	0.068	0.059	0.041	0.054	0.072	0.082	0.037	0.037	0.041	0.078
Ca	0.122	0.110	0.111	0.102	0.106	0.106	0.094	0.101	0.119	0.120
Total	2.969	2.911	2.865	2.852	2.920	2.991	3.208	3.034	2.916	2.980
Alm	79.22	79.03	74.94	79.59	83.29	85.46	60.77	64.01	72.36	78.99
Pyr	14.15	15.15	19.51	14.69	10.38	8.02	35.13	31.44	22.15	14.36
Spes	2.29	2.03	1.43	1.89	2.47	2.74	1.16	1.22	1.41	2.62
Gros	4.11	3.79	3.87	3.58	3.63	3.54	2.94	3.33	4.08	4.03
$\frac{Fe}{(Fe+Mg)}$	.848	.839	.793	.844	.889	.914	.664	.671	.766	.846

Table 21, continued. 160X Garnet Microprobe Analyses.

Alys#	32	33	34	35	36	37	38	39	40	41
SiO_2	38.12	38.24	39.13	38.49	38.23	38.51	38.38	39.09	38.93	39.20
TiO_2	0.0	0.0	0.0	0.0	0.0	0.0	0.0	0.0	0.0	0.0
Al_2O_3	21.46	22.15	22.11	22.37	21.31	21.68	22.24	20.95	22.21	21.83
Cr_2O_3	0.05	0.01	0.0	0.01	0.02	0.02	0.03	0.04	0.04	0.0
FeO	32.47	29.76	29.32	29.32	33.60	30.52	29.45	29.51	29.47	30.35
MnO	0.58	0.55	0.48	0.53	0.81	0.58	0.58	0.56	0.57	0.56
MgO	6.19	7.46	7.38	7.37	5.14	7.39	7.72	8.31	7.47	7.20
CaO	1.38	1.38	1.40	1.36	1.40	1.31	1.29	1.24	1.40	1.36
Total	100.25	99.55	99.82	99.45	100.51	100.01	99.69	99.70	100.09	100.50
Formulae based on 12 oxygens										
Si	2.997	2.987	3.033	2.999	3.015	3.004	2.988	3.043	3.014	3.033
Al	1.989	2.041	2.022	2.056	1.982	1.994	2.042	1.923	2.028	1.992
Cr	0.003	0.001		0.001	0.001	0.001	0.002	0.002	0.002	
Total	1.992	2.042		2.057	1.983	1.995	2.044	1.925	2.030	
Ti										
Fe	2.136	1.945	1.901	1.912	2.218	1.992	1.918	1.922	1.909	1.965
Mg	0.726	0.869	0.853	0.856	0.605	0.859	0.896	0.964	0.863	0.830
Mn	0.039	0.036	0.032	0.035	0.054	0.038	0.038	0.037	0.037	0.037
Ca	0.117	0.115	0.116	0.114	0.118	0.110	0.107	0.103	0.116	0.113
Total	3.018	2.965	2.902	2.917	2.995	2.999	2.959	3.026	2.925	2.945
Alm	70.78	65.60	65.51	65.55	74.06	66.42	64.82	63.52	65.26	66.72
Pyr	24.06	29.31	29.39	29.35	20.20	28.64	30.28	31.86	29.50	28.18
Spes	1.29	1.21	1.10	1.20	1.80	1.27	1.28	1.22	1.26	1.26
Gros	3.88	3.88	4.00	3.91	3.94	3.67	3.62	3.40	3.97	3.84
$\frac{Fe}{(Fe+Mg)}$	.756	.691	.690	.691	.786	.699	.682	.666	.689	.703

Table 21, continued. 160X Garnet Microprobe Analyses.

Alys#	42	43	44	45	46	47	48	49	50	51
SiO_2	39.05	38.62	38.40	39.09	38.47	38.17	39.27	39.47	38.45	38.47
TiO_2	0.0	0.0	0.0	0.0	0.0	0.0	0.0	0.0	0.0	0.0
Al_2O_3	21.79	22.16	21.65	21.56	21.67	21.50	22.04	21.74	21.43	21.58
Cr_2O_3	0.03	0.02	0.06	0.04	0.03	0.04	0.01	0.0	0.05	0.02
FeO	29.26	29.35	34.02	31.47	35.41	35.95	32.11	30.98	32.26	35.05
MnO	0.55	0.58	0.81	0.67	1.31	1.30	0.51	0.56	0.58	0.73
MgO	7.60	7.39	4.77	6.47	3.30	3.22	5.92	6.94	5.92	4.22
CaO	1.30	1.40	1.31	1.33	1.43	1.37	1.35	1.33	1.27	1.28
Total	99.58	99.52	101.02	100.63	101.62	101.55	101.21	101.02	99.96	101.35
Formulae based on 12 oxygens										
Si	3.036	3.008	3.015	3.039	3.027	3.016	3.038	3.044	3.025	3.022
Al	1.998	2.036	2.004	1.977	2.011	2.003	2.011	1.978	1.988	1.999
Cr	0.002	0.001	0.003	0.002	0.002	0.002	0.001		0.003	0.001
Total	2.000	2.037	2.007	1.979	2.013	2.005	2.012		1.991	2.000
Ti										
Fe	1.903	1.913	2.235	2.047	2.332	2.377	2.079	2.000	2.124	2.304
Mg	0.881	0.859	0.559	0.750	0.387	0.379	0.683	0.798	0.695	0.495
Mn	0.036	0.039	0.054	0.044	0.087	0.087	0.033	0.036	0.039	0.049
Ca	0.108	0.117	0.110	0.111	0.120	0.116	0.112	0.110	0.107	0.108
Total	2.928	2.928	2.958	2.952	2.926	2.959	2.907	2.944	2.965	2.956
Alm	65.00	65.33	75.56	69.34	79.70	80.33	71.52	67.93	71.64	77.94
Pyr	30.09	29.34	18.90	25.41	13.23	12.81	23.50	27.11	23.44	16.75
Spes	1.23	1.33	1.83	1.49	2.97	2.94	1.14	1.22	1.32	1.66
Gros	3.69	4.00	3.72	3.76	4.10	3.92	3.85	3.74	3.61	3.65
$\frac{Fe}{(Fe+Mg)}$	.684	.690	.800	.732	.858	.862	.753	.715	.753	.823

Table 21, continued. 160X Garnet Microprobe Analyses.

Alys#	52	53	54	55	56	57	58	59	60	61
SiO_2	38.77	39.45	38.45	38.95	38.81	39.17	38.89	38.55	39.85	38.78
TiO_2	0.0	0.0	0.0	0.0	0.0	0.0	0.0	0.0	0.0	0.0
Al_2O_3	21.69	21.75	21.56	21.19	20.68	21.93	21.48	21.76	21.40	21.34
Cr_2O_3	0.03	0.02	0.04	0.05	0.06	0.12	0.01	0.02	0.06	0.04
FeO	34.26	31.43	34.53	35.82	34.87	31.38	34.54	35.40	29.91	34.92
MnO	0.61	0.63	0.86	1.01	1.15	0.61	0.80	0.96	0.52	0.83
MgO	4.87	6.32	4.33	3.86	4.05	6.40	4.22	4.11	7.84	4.42
CaO	1.31	1.41	1.40	1.42	1.34	1.38	1.33	1.37	1.32	1.35
Total	101.54	101.01	101.17	102.30	100.96	100.99	101.27	102.17	100.90	101.68
Formulae based on 12 oxygens										
Si	3.024	3.051	3.022	3.044	3.066	3.031	3.048	3.011	3.061	3.035
Al	1.996	1.983	1.999	1.953	1.926	2.001	1.985	2.005	1.939	1.970
Cr	0.002	0.001	0.002	0.003	0.004	0.008	0.001	0.001	0.004	0.002
Total	1.998	1.984	2.001	1.956	1.930	2.009	1.986	2.006	1.943	1.972
Ti										
Fe	2.237	2.034	2.271	2.343	2.305	2.032	2.266	2.314	1.923	2.287
Mg	0.567	0.729	0.508	0.450	0.477	0.738	0.494	0.478	0.899	0.516
Mn	0.041	0.041	0.057	0.067	0.077	0.040	0.053	0.063	0.034	0.055
Ca	0.110	0.117	0.118	0.119	0.113	0.114	0.112	0.114	0.108	0.113
Total	2.955	2.921	2.954	2.979	2.972	2.924	2.925	2.969	2.964	2.971
Alm	75.70	69.63	76.88	78.65	77.56	69.49	77.47	77.94	64.88	76.98
Pyr	19.19	24.96	17.20	15.11	16.05	25.24	16.89	16.10	30.33	17.37
Spes	1.39	1.40	1.93	2.25	2.59	1.37	1.81	2.12	1.15	1.85
Gros	3.72	4.01	3.99	3.99	3.80	3.90	3.83	3.84	3.64	3.80
$\frac{Fe}{(Fe+Mg)}$	.798	.736	.817	.839	.829	.734	.821	.829	.681	.816

Table 21, continued. 160X Garnet Microprobe Analyses.

Alys#	62	63	71	72	73	74	75	76	77	78
SiO_2	39.04	39.55	38.70	37.60	37.26	37.99	38.31	37.44	38.51	38.23
TiO_2	0.0	0.0	0.0	0.01	0.0	0.0	0.0	0.0	0.0	0.0
Al_2O_3	22.68	22.25	21.28	20.62	20.55	20.43	21.95	21.59	20.68	21.81
Cr_2O_3	0.01	0.03	0.0	0.05	0.02	0.01	0.0	0.03	0.0	0.02
FeO	29.43	30.03	30.44	35.13	35.63	36.17	33.44	34.13	34.11	32.87
MnO	0.59	0.51	0.53	1.35	1.41	1.64	0.81	0.79	0.66	0.80
MgO	7.24	7.77	7.12	3.58	3.26	2.93	5.64	4.95	4.55	5.47
CaO	1.34	1.21	1.36	1.34	1.57	1.44	1.41	1.47	1.30	1.41
Total	100.33	101.35	99.43	99.68	99.70	100.61	101.56	100.40	99.81	100.61
Formulae based on 12 oxygens										
Si	3.011	3.024	3.034	3.027	3.012	3.067	2.984	2.969	3.063	3.000
Al	2.063	2.007	1.968	1.958	1.959	1.895	2.017	2.019	1.939	2.018
Cr	0.001	0.002		0.003	0.001			0.002		0.001
Total	2.064	2.009		1.961	1.960			2.021		2.019
Ti										
Fe	1.900	1.922	1.997	2.366	2.410	2.446	2.180	2.265	2.270	2.159
Mg	0.833	0.887	0.833	0.430	0.392	0.341	0.655	0.585	0.540	0.640
Mn	0.039	0.033	0.035	0.092	0.097	0.113	0.054	0.053	0.045	0.053
Ca	0.111	0.099	0.114	0.115	0.136	0.125	0.117	0.125	0.111	0.119
Total	2.883	2.941	2.979	3.003	3.035	3.025	3.006	3.028	2.966	2.971
Alm	65.90	65.35	67.04	78.80	79.41	80.86	72.52	74.80	76.53	72.67
Pyr	28.89	30.16	27.96	14.30	12.92	11.27	21.79	19.32	18.21	21.54
Spes	1.35	1.12	1.17	3.10	3.20	3.74	1.80	1.75	1.52	1.78
Gros	3.85	3.37	3.83	3.80	4.48	4.13	3.89	4.13	3.74	4.01
$\frac{Fe}{(Fe+Mg)}$	.695	.684	.706	.846	.860	.878	.769	.795	.801	.771

Table 21, continued. 160X Garnet Microprobe Analyses.

Alys#	79	80	81	82	83	84	85	86	87	88
SiO_2	38.83	38.96	38.63	38.10	38.05	38.85	38.83	39.18	37.99	37.75
TiO_2	0.0	0.0	0.0	0.0	0.0	0.0	0.0	0.0	0.0	0.0
Al_2O_3	22.19	22.45	22.22	20.73	21.14	21.81	22.38	21.76	20.96	21.23
Cr_2O_3	0.02	0.01	0.01	0.03	0.02	0.05	0.04	0.04	0.0	0.04
Fe_2O_3										
FeO	31.01	30.74	30.50	32.59	36.07	31.99	30.49	30.40	34.66	35.61
MnO	0.62	0.58	0.53	0.60	1.26	0.69	0.54	0.60	1.00	1.09
MgO	6.75	7.33	7.34	5.51	3.02	5.90	7.14	6.85	3.80	3.33
CaO	1.33	1.37	1.42	1.28	1.35	1.32	1.31	1.34	1.27	1.23
Total	100.75	101.44	100.65	98.84	100.91	100.61	100.73	100.17	99.68	100.33
Formulae based on 12 oxygens										
Si	3.016	2.995	2.992	3.049	3.038	3.042	3.008	3.059	3.052	3.024
Al	2.033	2.036	2.030	1.957	1.990	2.014	2.044	2.004	1.986	2.006
Cr	0.001	0.001	0.001	0.002	0.001	0.003	0.002	0.002		0.003
Total	2.034	2.037	2.031	1.959	1.991	2.017	2.046	2.006		2.009
Ti										
Fe	2.016	1.978	1.977	2.183	2.410	2.096	1.976	1.986	2.330	2.387
Mg	0.782	0.840	0.848	0.658	0.360	0.689	0.825	0.797	0.456	0.398
Mn	0.041	0.038	0.035	0.041	0.085	0.046	0.036	0.040	0.068	0.074
Ca	0.111	0.113	0.118	0.110	0.116	0.111	0.108	0.112	0.109	0.110
Total	2.950	2.969	2.978	2.992	2.971	2.942	2.945	2.935	2.963	2.969
Alm	68.30	66.60	66.39	72.96	81.12	71.24	67.10	67.67	78.64	80.40
Pyr	26.50	28.30	28.48	21.99	12.12	23.42	28.01	27.16	15.39	13.41
Spes	1.40	1.30	1.18	1.37	2.86	1.56	1.22	1.36	2.29	2.49
Gros	3.80	3.80	3.96	3.68	3.90	3.77	3.67	3.82	3.68	3.70
$\frac{Fe}{(Fe+Mg)}$	.721	.702	.700	.768	.870	.753	.705	.714	.836	.857

Table 21, continued. 160X Garnet Microprobe Analyses.

Alys#	89	90	91	92	93	94	95	96	97	98
SiO_2	35.50	39.31	39.22	38.65	39.49	38.47	38.98	38.21	38.81	38.66
TiO_2	0.0	0.0	0.0	0.0	0.0	0.0	0.0	0.0	0.0	0.0
Al_2O_3	22.04	22.63	22.02	22.00	22.97	21.27	22.36	22.06	21.97	22.79
Cr_2O_3	0.02	0.0	0.02	0.02	0.0	0.0	0.03	0.02	0.0	0.01
Fe_2O_3	6.17									
FeO	26.49	29.91	29.72	33.92	30.32	31.43	30.18	34.38	29.90	30.60
MnO	0.60	0.56	0.48	0.66	0.58	0.62	0.56	0.90	0.53	0.61
MgO	7.63	7.53	7.44	5.13	7.41	5.98	7.10	4.55	7.17	6.86
CaO	1.36	1.34	1.36	1.34	1.39	1.31	1.35	1.28	1.34	1.29
Total	99.81	101.28	100.26	101.72	102.16	99.08	100.56	101.40	99.72	100.82
Formulae based on 12 oxygens										
Si	2.794	3.019	3.045	3.012	3.009	3.056	3.024	2.999	3.035	2.994
Al	2.046	2.049	2.017	2.023	2.064	1.993	2.045	2.042	2.025	2.082
Cr	0.001		0.001	0.001			0.002	0.001		0.001
Total	2.047		2.018	2.024			2.047	2.043		2.083
Ti										
Fe	2.110	1.922	1.931	2.212	1.933	2.090	1.959	2.258	1.956	1.983
Mg	0.895	0.863	0.861	0.596	0.842	0.708	0.822	0.533	0.836	0.792
Mn	0.040	0.037	0.032	0.044	0.037	0.041	0.037	0.060	0.035	0.040
Ca	0.114	0.110	0.113	0.112	0.114	0.111	0.112	0.108	0.112	0.107
Total	3.159	2.932	2.937	2.964	2.926	2.950	2.930	2.959	2.939	2.922
Alm	66.79	65.55	65.75	74.63	66.06	70.85	66.86	76.31	66.55	67.86
Pyr	28.33	29.43	29.32	20.11	28.78	24.00	28.05	18.01	28.45	27.10
Spes	1.27	1.26	1.09	1.48	1.26	1.39	1.26	2.03	1.19	1.37
Gros	3.61	3.75	3.85	3.78	3.90	3.76	3.82	3.65	3.81	3.66
$\frac{Fe}{(Fe+Mg)}$	.702	.690	.692	.788	.697	.747	.704	.809	.701	.715

Table 21, continued. 160X Garnet Microprobe Analyses.

Alys#	99	100	101	102	103	104	105	106	107	108
SiO_2	39.13	37.57	38.64	36.12	38.23	38.64	38.82	37.60	37.88	38.73
TiO_2	0.0	0.0	0.0	0.0	0.0	0.0	0.0	0.0	0.0	0.0
Al_2O_3	21.50	22.21	22.87	22.01	21.34	21.55	20.90	20.88	22.03	21.07
Cr_2O_3	0.03	0.06	0.0	0.03	0.04	0.0	0.02	0.0	0.02	0.0
Fe_2O_3		0.46		3.96						
FeO	29.98	35.59	30.64	32.59	34.99	31.51	30.09	33.34	33.99	29.77
MnO	0.49	1.06	0.56	1.44	0.83	0.54	0.58	0.75	0.81	0.57
MgO	6.81	3.74	7.21	3.71	3.76	5.94	6.44	4.55	4.44	6.88
CaO	1.23	1.22	1.37	1.96	1.35	1.34	1.23	1.24	1.46	1.24
Total	99.17	101.91	101.29	101.82	100.54	99.52	98.08	98.36	100.63	98.26
Formulae based on 12 oxygens										
Si	3.085	2.955	2.974	2.855	3.044	3.056	3.104	3.042	2.995	3.081
Al	1.999	2.060	2.076	2.052	2.004	2.009	1.970	1.992	2.054	1.977
Cr	0.002	0.003		0.002	0.002		0.001		0.001	
Total	2.001	2.063		2.054	2.006		1.971		2.055	
Ti										
Fe	1.978	2.369	1.973	2.391	2.332	2.085	2.013	2.257	2.249	1.982
Mg	0.800	0.439	0.827	0.437	0.447	0.700	0.768	0.549	0.524	0.816
Mn	0.033	0.070	0.036	0.097	0.056	0.036	0.039	0.052	0.054	0.039
Ca	0.104	0.103	0.113	0.166	0.115	0.113	0.105	0.108	0.123	0.106
Total	2.915	2.981	2.949	3.091	2.950	2.934	2.925	2.966	2.950	2.943
Alm	67.86	79.47	66.90	77.35	79.05	71.06	68.82	76.10	76.24	67.35
Pyr	27.44	14.73	28.04	14.14	15.15	23.86	26.26	18.51	17.76	27.73
Spes	1.13	2.35	1.22	3.14	1.90	1.23	1.33	1.75	1.83	1.33
Gros	3.57	3.46	3.83	5.37	3.90	3.85	3.59	3.64	4.17	3.60
$\frac{Fe}{(Fe+Mg)}$	.712	.844	.705	.845	.839	.749	.724	.804	.811	.708

Table 21, continued. 160X Garnet Microprobe Analyses.

Alys#	109	110	111	112	113	114	115	116	117	118
SiO_2	38.39	38.93	37.63	38.58	38.69	38.60	38.09	37.69	39.00	37.91
TiO_2	0.0	0.0	0.01	0.0	0.0	0.0	0.0	0.0	0.0	0.0
Al_2O_3	21.97	21.82	21.53	22.45	22.11	22.07	21.52	21.21	20.76	20.90
Cr_2O_3	0.05	0.03	0.02	0.02	0.0	0.01	0.01	0.0	0.02	0.0
Fe_2O_3			0.08							
FeO	32.17	29.98	36.10	29.53	30.88	30.14	30.27	34.69	30.76	34.93
MnO	0.75	0.49	1.34	0.51	0.65	0.53	0.56	0.70	0.50	0.82
MgO	6.05	6.75	3.23	7.01	6.56	7.49	7.09	4.51	6.46	3.85
CaO	1.34	1.22	1.36	1.39	1.29	1.33	1.18	1.24	1.23	1.35
Total	100.72	99.22	101.30	99.49	100.18	100.17	98.72	100.04	98.73	99.76
Formulae based on 12 oxygens										
Si	3.000	3.066	2.988	3.021	3.025	3.000	3.013	3.004	3.101	3.043
Al	2.025	2.027	2.016	2.073	2.039	2.024	2.008	1.994	1.947	1.978
Cr	0.003	0.002	0.001	0.002		0.001	0.001		0.001	
Total	2.028	2.029	2.017	2.075		2.025	2.009		1.948	
Ti										
Fe	2.104	1.976	2.404	1.935	2.020	1.964	2.004	2.314	2.047	2.346
Mg	0.706	0.793	0.383	0.818	0.765	0.869	0.837	0.536	0.766	0.461
Mn	0.050	0.033	0.090	0.034	0.043	0.035	0.038	0.047	0.034	0.056
Ca	0.112	0.103	0.116	0.117	0.108	0.111	0.100	0.106	0.105	0.116
Total	2.974	2.905	2.993	2.904	2.936	2.979	2.979	3.003	2.952	2.979
Alm	70.79	68.02	80.32	66.63	68.80	65.93	67.27	77.06	69.34	78.75
Pyr	23.76	27.30	12.80	28.17	26.06	29.17	28.10	17.85	25.95	15.47
Spes	1.68	1.14	3.01	1.17	1.46	1.17	1.28	1.57	1.15	1.88
Gros	3.77	3.55	3.88	4.03	3.68	3.73	3.36	3.53	3.56	3.89
$\frac{Fe}{(Fe+Mg)}$	.749	.714	.863	.703	.725	.693	.705	.812	.728	.836

Table 21, continued. 160X Garnet Microprobe Analyses.

Alys#	119	120	121	122	123	124	125	126	127	128
SiO_2	38.02	37.98	38.65	38.80	39.48	39.29	37.36	38.79	38.02	38.92
TiO_2	0.0	0.0	0.0	0.0	0.0	0.0	0.0	0.0	0.0	0.0
Al_2O_3	21.17	21.63	20.50	21.70	21.96	22.04	21.04	21.56	21.29	21.71
Cr_2O_3	0.06	0.01	0.01	0.0	0.0	0.0	0.02	0.0	0.02	0.0
Fe_2O_3							0.27			
FeO	34.05	30.60	31.47	31.99	30.15	30.86	34.96	31.62	35.95	31.02
MnO	0.73	0.57	0.61	0.61	0.50	0.54	0.98	0.56	1.43	0.57
MgO	4.65	6.51	5.69	5.88	7.51	6.97	3.87	6.07	3.17	7.04
CaO	1.30	1.38	1.20	1.13	1.30	1.28	1.41	1.33	1.31	1.36
Total	99.98	98.68	98.13	100.11	100.90	100.98	99.91	99.93	101.19	100.62
Formulae based on 12 oxygens										
Si	3.028	3.015	3.108	3.053	3.048	3.042	2.996	3.053	3.024	3.025
Al	1.988	2.025	1.945	2.014	1.999	2.012	1.990	2.002	1.997	1.990
Cr	0.004	0.001	0.001				0.001		0.001	
Total	1.992	2.026	1.946				1.991		1.998	
Ti										
Fe	2.268	2.033	2.118	2.107	1.948	1.999	2.363	2.083	2.393	2.018
Mg	0.552	0.771	0.683	0.690	0.864	0.805	0.462	0.712	0.376	0.817
Mn	0.049	0.038	0.042	0.041	0.033	0.036	0.066	0.037	0.097	0.038
Ca	0.111	0.118	0.104	0.096	0.108	0.107	0.122	0.112	0.112	0.113
Total	2.980	2.960	2.947	2.934	2.953	2.947	3.013	2.944	2.978	2.986
Alm	76.11	68.68	71.87	71.81	65.97	67.83	78.43	70.75	80.36	67.58
Pyr	18.52	26.05	23.18	23.52	29.26	27.32	15.33	24.18	12.63	27.36
Spes	1.64	1.28	1.43	1.40	1.12	1.22	2.19	1.26	3.26	1.27
Gros	3.72	3.99	3.53	3.27	3.66	3.63	4.05	3.80	3.76	3.78
$\frac{Fe}{(Fe+Mg)}$	.804	.725	.756	.753	.693	.713	.836	.745	.864	.712

Table 21, continued. 160X Garnet Microprobe Analyses.

Alys#	129	130	131	132	133	134	135	136	137	138
SiO_2	39.42	38.19	39.44	39.63	39.39	39.19	39.42	38.91	39.52	39.27
TiO_2	0.0	0.0	0.0	0.0	0.0	0.0	0.0	0.0	0.0	0.0
Al_2O_3	21.85	21.32	21.85	21.73	21.49	21.69	21.84	21.56	22.02	21.31
Cr_2O_3	0.0	0.0	0.0	0.0	0.0	0.0	0.01	0.0	0.0	0.0
Fe_2O_3										
FeO	29.79	35.36	29.63	29.60	31.13	31.10	30.27	32.94	30.18	29.56
MnO	0.55	1.08	0.56	0.59	0.55	0.53	0.60	0.81	0.59	0.58
MgO	7.16	3.83	7.37	7.02	6.96	6.37	7.08	5.41	7.22	6.82
CaO	1.27	1.28	1.32	1.25	1.26	1.34	1.24	1.58	1.28	1.22
Total	100.04	101.06	100.17	99.82	100.78	100.22	100.46	101.21	100.81	98.76
Formulae based on 12 oxygens										
Si	3.073	3.027	3.066	3.097	3.060	3.068	3.064	3.042	3.058	3.107
Al	2.009	1.993	2.004	2.003	1.969	2.003	2.002	1.987	2.010	1.988
Cr							0.001			
Total							2.003			
Ti										
Fe	1.944	2.345	1.928	1.936	2.024	2.037	1.969	2.154	1.954	1.957
Mg	0.832	0.453	0.855	0.821	0.806	0.744	0.821	0.631	0.833	0.805
Mn	0.036	0.073	0.037	0.039	0.036	0.035	0.039	0.054	0.038	0.039
Ca	0.106	0.109	0.110	0.105	0.105	0.113	0.104	0.133	0.106	0.104
Total	2.918	2.980	2.930	2.901	2.971	2.929	2.933	2.972	2.931	2.905
Alm	66.62	78.69	65.80	66.74	68.13	69.55	67.13	72.48	66.67	67.37
Pyr	28.51	15.20	29.18	28.30	27.13	25.40	27.99	21.23	28.42	27.71
Spes	1.23	2.45	1.26	1.34	1.21	1.19	1.33	1.82	1.30	1.34
Gros	3.63	3.66	3.75	3.62	3.53	3.86	3.55	4.48	3.62	3.58
$\frac{Fe}{(Fe+Mg)}$	.700	.838	.693	.702	.715	.732	.706	.773	.701	.709

Table 21, continued. 160X Garnet Microprobe Analyses.

Alys#	139	140	141	142	143	144	145	146	147	148
SiO_2	38.39	37.41	39.91	38.05	39.62	39.44	38.30	39.39	38.30	39.17
TiO_2	0.0	0.0	0.0	0.0	0.0	0.0	0.0	0.0	0.0	0.0
Al_2O_3	21.35	21.44	21.95	21.49	21.81	21.81	21.85	22.02	21.47	21.98
Cr_2O_3	0.0	0.0	0.0	0.0	0.0	0.0	0.0	0.0	0.0	0.0
Fe_2O_3		1.57		0.59			0.60			
FeO	34.05	34.30	29.91	33.02	30.15	29.91	30.60	29.86	32.50	31.50
MnO	0.78	0.93	0.62	0.84	0.58	0.61	0.65	0.57	0.70	0.56
MgO	4.70	4.34	7.54	5.51	6.97	7.69	7.13	7.07	5.99	6.73
CaO	1.34	1.35	1.33	1.38	1.36	1.30	1.41	1.31	1.33	1.37
Total	100.61	101.34	101.26	100.88	100.49	100.76	100.54	100.22	100.29	101.31
Formulae based on 12 oxygens										
Si	3.036	2.955	3.070	2.987	3.080	3.046	2.980	3.066	3.011	3.029
Al	1.991	1.997	1.991	1.990	2.000	1.987	2.005	2.022	1.990	2.005
Cr										
Ti										
Fe	2.253	2.360	1.925	2.204	1.961	1.933	2.028	1.945	2.138	2.039
Mg	0.555	0.512	0.865	0.645	0.808	0.886	0.827	0.821	0.702	0.777
Mn	0.052	0.063	0.041	0.056	0.038	0.040	0.043	0.038	0.047	0.037
Ca	0.114	0.114	0.109	0.117	0.113	0.108	0.117	0.110	0.112	0.114
Total	2.974	3.049	2.940	3.022	2.920	2.967	3.015	2.914	2.999	2.967
Alm	75.76	77.40	65.48	72.93	67.16	65.15	67.26	66.75	71.29	68.72
Pyr	18.66	16.79	29.42	21.34	27.67	29.86	27.43	28.17	23.41	26.19
Spes	1.75	2.07	1.39	1.85	1.30	1.35	1.43	1.30	1.57	1.25
Gros	3.83	3.74	3.71	3.87	3.87	3.64	3.88	3.77	3.73	3.84
$\frac{Fe}{(Fe+Mg)}$	.802	.822	.690	.774	.708	.686	.710	.703	.753	.724

Table 21, continued. 160X Garnet Microprobe Analyses.

Alys#	149	150	151	152	153	154	155	156	157	158
SiO_2	38.68	38.68	36.50	40.05	38.85	38.02	39.24	39.17	39.22	39.55
TiO_2	0.0	0.0	0.0	0.0	0.0	0.0	0.0	0.0	0.0	0.0
Al_2O_3	22.13	21.80	21.30	21.97	21.50	21.64	21.64	21.41	21.05	21.91
Cr_2O_3	0.0	0.0	0.0	0.0	0.01	0.02	0.0	0.0	0.0	0.0
Fe_2O_3	0.41	0.20	2.64			0.54				
FeO	30.18	31.68	31.23	30.65	33.68	34.03	31.28	33.83	31.50	30.36
MnO	0.61	0.62	0.77	0.51	0.78	0.73	0.62	0.73	0.60	0.49
MgO	7.72	6.83	5.58	6.89	5.38	5.04	6.61	5.14	5.76	7.30
CaO	1.30	1.36	1.29	1.34	1.35	1.31	1.36	1.35	1.42	1.29
Total	101.03	101.17	99.31	101.41	101.55	101.33	100.75	101.63	99.55	100.90
Formulae based on 12 oxygens										
Si	2.982	2.998	2.917	3.088	3.031	2.982	3.055	3.058	3.106	3.058
Al	2.012	1.993	2.008	1.998	1.979	2.002	1.986	1.972	1.966	1.998
Cr					0.001	0.001				
Total					1.980	2.003				
Ti										
Fe	1.971	2.067	2.248	1.978	2.199	2.266	2.037	2.210	2.088	1.964
Mg	0.888	0.789	0.665	0.793	0.626	0.589	0.767	0.598	0.680	0.841
Mn	0.040	0.041	0.052	0.033	0.051	0.048	0.041	0.048	0.040	0.032
Ca	0.108	0.113	0.111	0.111	0.113	0.110	0.113	0.113	0.120	0.107
Total	3.007	3.010	3.076	2.915	2.989	3.013	2.958	2.969	2.928	2.944
Alm	65.55	68.67	73.08	67.86	73.57	75.21	68.86	74.44	71.31	66.71
Pyr	29.53	26.21	21.62	27.20	20.94	19.55	25.93	20.14	23.22	28.57
Spes	1.33	1.36	1.69	1.13	1.71	1.59	1.39	1.62	1.37	1.09
Gros	3.59	3.75	3.61	3.81	3.78	3.65	3.82	3.81	4.10	3.63
$\frac{Fe}{(Fe+Mg)}$	.689	.724	.772	.714	.778	.794	.726	.787	.754	.700

Table 21, continued. 160X Garnet Microprobe Analyses.

Alys#	159	160	161	162	163	164	165	166	167	168
SiO_2	38.92	38.47	38.70	38.69	38.34	37.03	38.56	38.44	37.90	37.76
TiO_2	0.0	0.0	0.0	0.0	0.0	0.0	0.0	0.0	0.0	0.0
Al_2O_3	21.16	21.64	22.06	22.28	21.74	21.85	21.78	22.15	21.60	21.65
Cr_2O_3	0.0	0.0	0.0	0.0	0.0	0.0	0.0	0.0	0.0	0.0
Fe_2O_3						3.03			0.24	0.25
FeO	33.78	34.14	29.67	29.49	31.49	27.03	29.84	31.74	35.21	35.20
MnO	0.78	0.78	0.51	0.57	0.55	0.51	0.58	0.56	0.78	0.90
MgO	4.68	4.90	7.19	7.49	6.44	8.43	7.33	6.45	4.24	4.06
CaO	1.33	1.19	1.23	1.29	1.32	1.31	1.32	1.33	1.35	1.38
Total	100.65	101.12	99.36	99.81	99.89	99.19	99.41	100.67	101.32	101.20
Formulae based on 12 oxygens										
Si	3.077	3.023	3.035	3.014	3.012	2.901	3.022	2.996	2.989	2.984
Al	1.972	2.005	2.040	2.047	2.015	2.019	2.014	2.036	2.009	2.017
Cr										
Ti										
Fe	2.234	2.245	1.947	1.922	2.071	1.951	1.958	2.070	2.337	2.343
Mg	0.552	0.574	0.841	0.871	0.754	0.985	0.857	0.750	0.499	0.479
Mn	0.052	0.052	0.034	0.038	0.037	0.034	0.038	0.037	0.052	0.060
Ca	0.113	0.101	0.104	0.107	0.111	0.110	0.111	0.111	0.114	0.117
Total	2.951	2.972	2.926	2.938	2.973	3.080	2.964	2.968	3.002	2.999
Alm	75.70	75.54	66.54	65.42	69.66	63.34	66.06	69.74	77.85	78.13
Pyr	18.71	19.31	28.74	29.65	25.36	31.98	28.91	25.27	16.62	15.97
Spes	1.76	1.75	1.16	1.29	1.24	1.10	1.28	1.25	1.73	2.00
Gros	3.83	3.40	3.55	3.64	3.73	3.57	3.74	3.74	3.80	3.90
$\frac{Fe}{(Fe+Mg)}$	.802	.796	.698	.688	.733	.665	.696	.734	.824	.830

Table 21, continued. 160X Garnet Microprobe Analyses.

Alys#	169	170	171	172	173	174	175	176	177	178
SiO_2	37.92	38.28	38.18	38.33	38.06	37.94	38.89	38.38	38.27	37.84
TiO_2	0.0	0.0	0.0	0.0	0.0	0.0	0.0	0.0	0.0	0.0
Al_2O_3	21.46	21.63	22.00	21.91	21.65	21.86	22.12	21.87	22.09	21.56
Cr_2O_3	0.0	0.0	0.0	0.0	0.01	0.0	0.0	0.0	0.0	0.0
Fe_2O_3						0.76				
FeO	30.08	29.66	29.91	30.73	34.87	33.97	29.58	32.64	32.59	34.03
MnO	0.56	0.65	0.56	0.56	0.84	0.67	0.58	0.65	0.62	0.93
MgO	7.07	6.98	7.23	7.03	4.42	5.06	7.51	5.41	5.87	4.57
CaO	1.19	1.29	1.34	1.33	1.27	1.30	1.31	1.36	1.39	1.27
Total	98.28	98.49	99.22	99.89	101.12	101.56	99.99	100.31	100.83	100.20
Formulae based on 12 oxygens										
Si	3.014	3.033	2.999	2.999	3.001	2.969	3.026	3.023	2.991	3.007
Al	2.008	2.021	2.038	2.021	2.014	2.017	2.030	2.031	2.036	2.020
Cr					0.001					
Total					2.015					
Ti										
Fe	2.001	1.967	1.966	2.011	2.301	2.270	1.926	2.152	2.132	2.262
Mg	0.838	0.825	0.847	0.821	0.519	0.590	0.871	0.636	0.684	0.541
Mn	0.038	0.044	0.037	0.037	0.056	0.045	0.039	0.043	0.041	0.062
Ca	0.101	0.110	0.113	0.111	0.107	0.109	0.109	0.115	0.116	0.108
Total	2.978	2.946	2.963	2.980	2.983	3.014	2.945	2.946	2.973	2.973
Alm	67.19	66.77	66.35	67.48	77.14	75.32	65.40	73.05	71.71	76.08
Pyr	28.14	28.00	28.59	27.55	17.40	19.58	29.58	21.59	23.01	18.20
Spes	1.28	1.49	1.25	1.24	1.88	1.49	1.32	1.46	1.38	2.09
Gros	3.39	3.73	3.81	3.72	3.59	3.62	3.70	3.90	3.90	3.63
$\frac{Fe}{(Fe+Mg)}$	.705	.705	.699	.710	.816	.794	.689	.772	.757	.807

Table 21, continued. 160X Garnet Microprobe Analyses.

Alys#	179	180	181	182	183	184	185	186	187	188
SiO_2	38.23	38.51	38.63	38.81	38.54	38.65	36.93	38.98	37.43	37.78
TiO_2	0.0	0.0	0.0	0.0	0.0	0.0	0.0	0.0	0.04	0.0
Al_2O_3	21.55	22.16	22.60	22.34	22.32	22.42	22.03	22.60	21.92	22.17
Cr_2O_3	0.0	0.0	0.0	0.0	0.0	0.0	0.0	0.0	0.0	0.0
Fe_2O_3							2.39		0.96	1.36
FeO	32.91	30.41	31.08	30.26	30.76	33.16	32.86	30.70	34.17	34.34
MnO	0.65	0.55	0.53	0.67	0.57	0.63	1.12	0.57	0.90	1.01
MgO	5.51	6.98	6.81	7.30	6.80	5.78	4.73	7.21	4.41	4.53
CaO	1.29	1.22	1.33	1.38	1.38	1.31	1.33	1.65	1.42	1.34
Total	100.14	99.83	100.98	100.76	100.37	101.95	101.39	101.71	101.25	102.53
Formulae based on 12 oxygens										
Si	3.018	3.012	2.991	3.002	3.002	2.990	2.907	2.989	2.951	2.942
Al	2.006	2.044	2.063	2.038	2.051	2.046	2.045	2.044	2.038	2.036
Cr										
Ti										
Fe	2.174	1.990	2.014	1.959	2.005	2.147	2.306	1.970	2.311	2.318
Mg	0.649	0.815	0.787	0.842	0.790	0.666	0.555	0.825	0.519	0.526
Mn	0.044	0.036	0.035	0.044	0.038	0.041	0.075	0.037	0.060	0.066
Ca	0.110	0.102	0.110	0.115	0.115	0.109	0.113	0.136	0.120	0.112
Total	2.977	2.943	2.946	2.960	2.948	2.963	3.049	2.968	3.010	3.022
Alm	73.03	67.62	68.36	66.18	68.01	72.46	75.63	66.37	76.78	75.70
Pyr	21.80	27.69	26.71	28.45	26.80	22.48	18.20	27.80	17.24	17.41
Spes	1.48	1.22	1.19	1.49	1.29	1.38	2.46	1.25	1.99	2.18
Gros	3.69	3.47	3.73	3.89	3.90	3.68	3.71	4.58	3.99	3.71
$\frac{Fe}{(Fe+Mg)}$	.770	.709	.719	.699	.717	.763	.806	.705	.817	.815

Table 21, continued. 160X Garnet Microprobe Analyses.

Alys#	189	190	191	192	201A	202	203	204	205	206
SiO_2	37.99	37.70	38.11	38.30	38.82	38.53	38.52	38.54	39.23	38.57
TiO_2	0.0	0.0	0.0	0.0	0.03	0.02	0.0	0.0	0.04	0.03
Al_2O_3	21.85	21.57	22.12	22.32	22.30	22.22	22.13	22.34	22.13	21.87
Cr_2O_3	0.0	0.0	0.0	0.0	0.0					
Fe_2O_3	0.39		0.27	0.08						
FeO	34.66	34.75	36.21	34.98	30.81	30.36	29.93	30.08	30.40	29.96
MnO	0.82	1.18	1.09	0.93	0.56	0.57	0.50	0.54	0.56	0.56
MgO	4.60	3.58	3.58	4.53	7.07	7.81	7.32	7.24	7.14	7.13
CaO	1.33	1.88	1.44	1.38	1.34	1.37	1.39	1.38	1.35	1.31
Total	101.64	100.66	102.82	102.52	100.93	100.88	99.79	100.12	100.85	99.43
Formulae based on 12 oxygens										
Si	2.978	2.999	2.974	2.975	2.998	2.975	3.000	2.994	3.024	3.016
Al	2.020	2.023	2.036	2.045	2.031	2.024	2.033	2.046	2.012	2.017
Cr										
Ti					0.002	0.001			0.002	0.002
Fe	2.297	2.313	2.380	2.279	1.991	1.962	1.951	1.955	1.961	1.960
Mg	0.538	0.425	0.416	0.525	0.815	0.899	0.851	0.838	0.821	0.832
Mn	0.054	0.080	0.072	0.061	0.036	0.037	0.033	0.036	0.037	0.037
Ca	0.112	0.161	0.121	0.115	0.111	0.114	0.116	0.115	0.111	0.110
Total	3.001	2.979	2.989	2.980	2.953	3.012	2.951	2.944	2.930	2.939
Alm	76.54	77.64	79.63	76.48	67.42	65.14	66.11	66.41	66.93	66.68
Pyr	17.93	14.27	13.92	17.62	27.60	29.85	28.84	28.46	28.02	28.31
Spes	1.80	2.69	2.41	2.05	1.22	1.23	1.12	1.22	1.26	1.26
Gros	3.73	5.40	4.05	3.86	3.76	3.78	3.93	3.91	3.79	3.74
$\frac{Fe}{(Fe+Mg)}$	.810	.845	.851	.813	.710	.686	.696	.700	.705	.702

Table 21, continued. 160X Garnet Microprobe Analyses.

Alys#	207	208	208A	208C	209	210	211	212	213	214
SiO_2	38.59	38.80	39.05	38.56	38.35	38.63	38.11	37.40	37.40	36.69
TiO_2	0.01	0.01	0.01	0.03	0.03	0.0	0.03	0.0	0.0	0.01
Al_2O_3	22.27	22.39	22.37	22.27	22.49	22.38	22.34	22.53	22.30	22.80
FeO	29.62	29.98	30.33	29.68	29.74	29.59	29.56	29.92	30.05	30.01
MnO	0.50	0.54	0.52	0.50	0.56	0.50	0.59	0.54	0.49	0.51
MgO	7.48	7.84	6.89	7.66	7.69	8.10	8.17	8.31	7.94	7.80
CaO	1.41	1.39	1.42	1.46	1.41	1.29	1.36	1.33	1.27	1.32
Total	99.88	100.95	100.59	100.16	100.27	100.49	100.16	100.03	99.45	99.14
Formulae based on 12 oxygens										
Si	2.998	2.985	3.017	2.989	2.972	2.981	2.957	2.915	2.933	2.890
Al	2.040	2.032	2.038	2.036	2.055	2.037	2.044	2.071	2.062	2.118
Ti	0.001	0.001	0.001	0.002	0.002		0.002			
Fe	1.926	1.930	1.961	1.926	1.928	1.911	1.919	1.952	1.972	1.979
Mg	0.866	0.900	0.794	0.885	0.889	0.933	0.945	0.965	0.929	0.917
Mn	0.033	0.035	0.034	0.033	0.037	0.033	0.039	0.035	0.033	0.034
Ca	0.118	0.115	0.118	0.122	0.118	0.107	0.113	0.111	0.107	0.112
Total	2.943	2.980	2.907	2.966	2.972	2.984	3.016	3.063	3.041	3.042
Alm	64.98	64.77	67.46	64.94	64.87	64.04	63.63	63.73	64.85	65.06
Pyr	29.22	30.20	27.31	29.84	29.91	31.27	31.33	31.51	30.55	30.14
Spes	1.11	1.17	1.17	1.11	1.24	1.11	1.29	1.14	1.09	1.12
Gros	3.98	3.86	4.06	4.11	3.97	3.59	3.75	3.62	3.52	3.68
$\frac{Fe}{(Fe+Mg)}$	.690	.682	.712	.685	.684	.672	.670	.669	.680	.683

Table 21, continued. 160X Garnet Microprobe Analyses.

Alys#	215	216	217	218	219	220	221	222	223	224
SiO_2	38.02	36.84	38.16	38.27	38.58	38.96	38.58	37.42	38.62	39.05
TiO_2	0.01	0.0	0.0	0.02	0.0	0.04	0.0	0.04	0.03	0.02
Al_2O_3	22.43	22.08	22.19	22.13	22.45	22.42	22.54	21.92	22.16	22.46
FeO	30.29	32.24	30.81	31.23	30.04	29.69	29.99	34.33	32.16	29.71
MnO	0.52	0.53	0.62	0.55	0.45	0.53	0.51	0.82	0.65	0.49
MgO	7.24	6.32	7.90	7.22	7.94	7.57	7.99	5.33	6.34	7.83
CaO	1.44	1.49	1.23	1.30	1.34	1.34	1.42	1.39	1.43	1.19
Total	99.95	99.50	100.91	100.72	100.80	100.55	101.03	101.25	101.39	100.75
Formulae based on 12 oxygens										
Si	2.965	2.924	2.955	2.973	2.974	3.003	2.967	2.944	2.991	3.002
Al	2.063	2.067	2.026	2.028	2.041	2.038	2.044	2.034	2.024	2.036
Ti	0.001			0.001		0.002		0.002	0.002	0.001
Fe	1.977	2.141	1.997	2.030	1.938	1.916	1.930	2.260	2.084	1.911
Mg	0.842	0.749	0.912	0.837	0.913	0.871	0.916	0.625	0.732	0.898
Mn	0.035	0.036	0.041	0.036	0.030	0.035	0.033	0.054	0.043	0.032
Ca	0.121	0.127	0.102	0.108	0.111	0.111	0.120	0.117	0.119	0.098
Total	2.975	3.053	3.052	3.011	2.992	2.933	2.999	3.056	2.978	2.939
Alm	66.45	70.13	65.43	67.42	64.77	65.33	64.35	73.95	69.98	65.02
Pyr	28.30	24.53	29.88	27.80	30.51	29.70	30.54	20.45	24.58	30.55
Spes	1.18	1.18	1.34	1.20	1.00	1.19	1.10	1.77	1.44	1.09
Gros	4.07	4.16	3.34	3.59	3.71	3.78	4.00	3.83	4.00	3.33
$\frac{Fe}{.680(Fe+Mg)}$	.701	.741	.686	.708	.680	.687	.678	.783	.740	

Table 21, continued. 160X Garnet Microprobe Analyses.

Alys#	225	226	227	228	229	230	231	232	233	234
SiO_2	39.20	38.00	39.02	38.89	38.76	38.96	38.09	38.75	38.18	37.45
TiO_2	0.03	0.01	0.02	0.02	0.01	0.0	0.05	0.04	0.02	0.02
Al_2O_3	22.69	22.42	22.23	22.57	22.30	22.41	21.92	22.35	22.20	21.72
FeO	30.15	30.95	30.36	30.32	29.99	29.97	34.02	31.40	30.30	36.14
MnO	0.49	0.49	0.57	0.51	0.57	0.56	0.74	0.55	0.57	1.45
MgO	7.82	7.74	6.95	7.76	7.47	7.90	5.16	7.21	7.91	3.09
CaO	1.35	1.34	1.38	1.39	1.41	1.36	1.43	1.39	1.38	1.44
Total	101.73	100.95	100.53	101.46	100.51	101.16	101.41	101.69	100.56	101.31
Formulae based on 12 oxygens										
Si	2.990	2.942	3.018	2.980	2.997	2.990	2.980	2.979	2.960	2.977
Al	2.041	2.047	2.028	2.040	2.033	2.028	2.023	2.026	2.030	2.036
Ti	0.002	0.001	0.001	0.001	0.001		0.003	0.002	0.001	0.001
Fe	1.924	2.006	1.965	1.944	1.940	1.925	2.228	2.020	1.966	2.403
Mg	0.890	0.894	0.801	0.887	0.861	0.904	0.602	0.827	0.915	0.366
Mn	0.032	0.032	0.037	0.033	0.037	0.036	0.049	0.036	0.037	0.098
Ca	0.110	0.111	0.115	0.114	0.117	0.112	0.120	0.114	0.115	0.122
Total	2.958	3.044	2.919	2.979	2.956	2.977	3.002	2.999	3.034	2.990
Alm	65.09	65.92	67.34	65.28	65.65	64.66	74.22	67.40	64.82	80.39
Pyr	30.11	29.38	27.45	29.79	29.14	30.37	20.05	27.59	30.17	12.24
Spes	1.08	1.05	1.27	1.11	1.25	1.21	1.63	1.20	1.22	3.28
Gros	3.72	3.65	3.94	3.83	3.96	3.76	4.00	3.80	3.79	4.08
$\frac{Fe}{(Fe+Mg)}$	.684	.692	.710	.687	.693	.680	.787	.710	.682	.868

Table 21, continued. 160X Garnet Microprobe Analyses.

Alys#	235	236	237	238	239	240	241	242	243	244
SiO_2	37.67	37.69	37.68	38.81	38.74	38.56	39.21	39.02	39.27	39.02
TiO_2	0.04	0.01	0.0	0.0	0.02	0.05	0.01	0.0	0.0	0.01
Al_2O_3	21.75	21.99	21.51	22.24	22.01	22.23	21.96	22.55	22.45	22.24
FeO	36.52	35.73	36.14	30.55	29.81	29.99	29.97	29.86	30.30	29.96
MnO	1.39	0.74	1.20	0.61	0.60	0.54	0.52	0.53	0.51	0.54
MgO	3.30	4.40	3.29	6.96	6.95	7.58	7.34	7.70	7.88	7.58
CaO	1.29	1.39	1.56	1.38	1.41	1.42	1.38	1.37	1.29	1.34
Total	101.96	101.95	101.38	100.55	99.54	100.37	100.39	101.03	101.70	100.69
Formulae based on 12 oxygens										
Si	2.976	2.958	2.989	3.006	3.023	2.987	3.031	2.995	2.998	3.008
Al	2.026	2.036	2.013	2.032	2.026	2.031	2.002	2.041	2.021	2.022
Ti	0.002	0.001			0.001	0.003	0.001			
Fe	2.414	2.347	2.400	1.980	1.947	1.944	1.939	1.918	1.936	1.933
Mg	0.389	0.515	0.389	0.805	0.809	0.875	0.846	0.882	0.898	0.871
Mn	0.093	0.049	0.081	0.040	0.040	0.036	0.034	0.035	0.033	0.035
Ca	0.109	0.117	0.133	0.114	0.118	0.118	0.115	0.113	0.105	0.111
Total	3.007	3.029	3.003	2.939	2.915	2.976	2.935	2.948	2.972	2.950
Alm	80.33	77.51	79.92	67.37	66.82	65.32	66.09	65.06	65.14	65.53
Pyr	12.95	17.01	12.95	27.39	27.76	29.40	28.83	29.92	30.22	29.53
Spes	3.09	1.62	2.70	1.36	1.37	1.21	1.16	1.19	1.11	1.19
Gros	3.63	3.86	4.43	3.88	4.05	3.97	3.92	3.83	3.53	3.76
$\frac{Fe}{(Fe+Mg)}$	.861	.820	.861	.711	.706	.690	.696	.685	.683	.689

Table 21, continued. 160X Garnet Microprobe Analyses.

Alys#	245	246	247	248	249	250	251	252	253	254
SiO_2	38.98	38.87	39.39	39.12	39.10	39.12	39.23	39.00	38.67	38.87
TiO_2	0.0	0.01	0.0	0.01	0.0	0.02	0.0	0.0	0.0	0.04
Al_2O_3	22.28	22.13	22.28	22.51	22.49	22.46	22.40	22.27	22.06	22.26
FeO	29.59	29.61	29.84	30.40	30.05	29.68	30.05	29.67	29.67	32.49
MnO	0.56	0.59	0.47	0.54	0.51	0.53	0.53	0.52	0.50	0.55
MgO	7.35	7.53	7.52	7.66	7.44	7.84	7.59	7.68	7.33	5.75
CaO	1.24	1.20	1.29	1.39	1.30	1.34	1.37	1.35	1.28	1.40
Total	100.00	99.94	100.79	101.63	100.89	100.99	101.17	100.49	99.51	101.36
Formulae based on 12 oxygens										
Si	3.020	3.015	3.027	2.993	3.007	3.001	3.009	3.008	3.015	3.011
Al	2.035	2.024	2.019	2.030	2.040	2.033	2.026	2.026	2.028	2.03-
Ti		0.001				0.001				0.002
Fe	1.918	1.922	1.919	1.946	1.934	1.905	1.928	1.915	1.935	2.106
Mg	0.849	0.871	0.862	0.873	0.853	0.897	0.868	0.884	0.853	0.66-
Mn	0.037	0.039	0.031	0.035	0.033	0.035	0.034	0.034	0.033	0.036
Ca	0.103	0.100	0.107	0.114	0.107	0.110	0.113	0.112	0.107	0.116
Total	2.907	2.933	2.919	2.968	2.927	2.948	2.943	2.945	2.928	2.924
Alm	65.98	65.55	65.74	65.57	66.07	64.64	65.51	65.03	66.09	72.07
Pyr	29.21	29.71	29.53	29.41	29.14	30.44	29.49	30.02	29.13	22.72
Spes	1.27	1.33	1.06	1.18	1.13	1.19	1.16	1.15	1.13	1.23
Gros	3.54	3.41	3.67	3.84	3.66	3.73	3.84	3.80	3.65	3.97
$\frac{Fe}{(Fe+Mg)}$	.693	.688	.690	.690	.694	.680	.690	.684	.694	.760

Table 21, continued. 160X Garnet Microprobe Analyses.

Alys#	255	256	257	258	259	260	261	262	263	264
SiO_2	38.54	39.10	38.90	38.90	38.66	38.53	38.57	38.38	38.56	38.76
TiO_2	0.0	0.02	0.0	0.02	0.02	0.02	0.02	0.0	0.0	0.0
Al_2O_3	21.83	22.27	22.39	22.39	22.32	22.33	21.98	22.19	22.27	22.12
FeO	30.98	30.06	30.05	29.87	29.79	32.37	34.08	32.20	30.20	29.83
MnO	0.55	0.58	0.58	0.55	0.67	0.59	0.66	0.58	0.62	0.62
MgO	6.77	7.47	7.92	7.45	7.17	6.46	5.15	6.03	7.38	7.28
CaO	1.31	1.30	1.41	1.53	1.37	1.39	1.42	1.46	1.41	1.40
Total	99.98	100.80	101.25	100.71	100.00	101.69	101.88	100.84	100.54	100.01
Formulae based on 12 oxygens										
Si	3.011	3.011	2.985	2.999	3.003	2.977	2.999	2.991	2.987	3.010
Al	2.011	2.023	2.026	2.035	2.045	2.034	2.015	2.039	2.035	2.026
Ti		0.001		0.001	0.001	0.001	0.001			
Fe	2.025	1.937	1.930	1.927	1.936	2.093	2.217	2.100	1.964	1.939
Mg	0.789	0.858	0.907	0.857	0.831	0.745	0.597	0.701	0.852	0.843
Mn	0.037	0.038	0.038	0.036	0.044	0.039	0.044	0.038	0.041	0.041
Ca	0.110	0.107	0.116	0.127	0.114	0.115	0.118	0.122	0.117	0.116
Total	2.961	2.941	2.991	2.948	2.926	2.993	2.977	2.961	2.974	2.939
Alm	68.39	65.88	64.53	65.39	66.19	69.95	74.50	70.92	66.04	65.97
Pyr	26.65	29.18	30.32	29.08	28.41	24.90	20.06	23.67	28.65	28.63
Spes	1.25	1.29	1.27	1.22	1.50	1.30	1.48	1.28	1.38	1.40
Gros	3.71	3.64	3.88	4.31	3.90	3.84	3.97	4.12	3.93	3.95
$\frac{Fe}{(Fe+Mg)}$	.720	.693	.680	.692	.700	.737	.788	.750	.697	.697

Table 21, continued. 160X Garnet Microprobe Analyses.

Alys#	265	266	267	268	269	270	271	272	273	274
SiO_2	38.85	39.21	38.08	38.63	38.95	39.05	39.23	38.75	39.37	38.85
TiO_2	0.17	0.02	0.01	0.0	0.0	0.03	0.02	0.0	0.04	0.0
Al_2O_3	21.88	22.50	22.06	22.64	22.26	22.47	22.47	22.61	22.24	22.26
FeO	30.21	29.74	30.12	29.89	29.69	30.02	29.94	29.67	29.78	30.31
MnO	0.64	0.52	0.51	0.47	0.53	0.62	0.52	0.48	0.57	0.55
MgO	7.15	7.28	7.04	7.93	7.59	7.45	7.40	7.97	7.53	7.63
CaO	1.38	1.33	1.28	1.30	1.20	1.23	1.29	1.31	1.28	1.36
Total	100.28	100.60	99.10	100.86	100.22	100.87	100.87	100.79	100.81	100.99
Formulae based on 12 oxygens										
Si	3.015	3.019	2.992	2.973	3.012	3.005	3.015	2.980	3.026	2.993
Al	2.003	2.043	2.045	2.054	2.030	2.039	2.036	2.050	2.015	2.022
Ti	0.010	0.001	0.001			0.002	0.001		0.002	
Fe	1.962	1.916	1.981	1.924	1.921	1.933	1.925	1.909	1.915	1.954
Mg	0.827	0.836	0.825	0.910	0.875	0.855	0.848	0.915	0.863	0.877
Mn	0.042	0.034	0.034	0.031	0.035	0.040	0.034	0.031	0.037	0.038
Ca	0.115	0.110	0.108	0.107	0.100	0.101	0.107	0.108	0.105	0.112
Total	2.956	2.897	2.949	2.972	2.931	2.931	2.915	2.963	2.922	2.981
Alm	66.60	66.16	67.20	64.74	65.54	66.00	66.06	64.43	65.58	65.55
Pyr	28.07	28.87	27.99	30.62	29.85	29.19	29.10	30.88	29.55	29.42
Spes	1.43	1.17	1.15	1.04	1.19	1.37	1.17	1.05	1.27	1.27
Gros	3.90	3.80	3.66	3.60	3.41	3.45	3.67	3.64	3.60	3.76
$\frac{Fe}{(Fe+Mg)}$	.703	.696	.706	.679	.687	.693	.694	.676	.689	.690

Table 21, continued. 160X Garnet Microprobe Analyses.

Alys#	275	276	277	278	279	280	281	282	283	284
SiO_2	38.80	38.43	38.55	38.49	37.92	37.69	38.89	38.75	37.59	39.03
TiO_2	0.01	0.02	0.01	0.01	0.03	0.01	0.0	0.0	0.03	0.0
Al_2O_3	22.37	22.29	21.64	22.00	21.74	21.66	22.25	22.16	21.70	22.06
FeO	30.33	30.09	30.44	32.67	35.06	35.14	30.28	29.92	34.81	30.27
MnO	0.55	0.56	0.52	0.58	1.23	1.25	0.57	0.47	1.04	0.52
MgO	7.90	7.91	6.86	6.09	3.95	3.49	7.15	7.27	4.17	7.38
CaO	1.37	1.44	1.33	1.35	1.32	1.59	1.35	1.36	1.35	1.41
Total	101.33	100.74	99.35	101.19	101.25	100.83	100.49	99.93	100.69	100.67
Formulae based on 12 oxygens										
Si	2.979	2.969	3.024	2.994	2.993	2.994	3.009	3.011	2.981	3.014
Al	2.026	2.031	2.002	2.018	2.023	2.029	2.030	2.031	2.030	2.009
Ti		0.001	0.001	0.001	0.002				0.002	
Fe	1.949	1.946	1.998	2.126	2.316	2.335	1.961	1.946	2.310	1.956
Mg	0.905	0.912	0.803	0.706	0.465	0.414	0.826	0.842	0.493	0.850
Mn	0.036	0.037	0.034	0.038	0.082	0.084	0.038	0.031	0.070	0.034
Ca	0.113	0.120	0.112	0.113	0.112	0.135	0.112	0.113	0.115	0.117
Total	3.003	3.016	2.948	2.984	2.977	2.968	2.937	2.932	2.990	2.957
Alm	64.90	64.54	67.80	71.27	77.85	78.67	66.77	66.37	77.31	66.15
Pyr	30.14	30.25	27.25	23.67	15.63	13.95	28.12	28.72	16.50	28.75
Spes	1.20	1.23	1.15	1.27	2.76	2.83	1.29	1.06	2.34	1.15
Gros	3.76	3.98	3.80	3.79	3.76	4.55	3.81	3.85	3.85	3.96
$\frac{Fe}{(Fe+Mg)}$	.683	.681	.713	.751	.833	.849	.704	.698	.824	.697

Table 21, continued. 160X Garnet Microprobe Analyses.

Alys#	285	286	287	288	289	290	291	292	293	294
SiO_2	39.04	38.93	38.79	39.13	38.64	38.47	36.70	37.73	38.00	38.29
TiO_2	0.03	0.02	0.03	0.01	0.0	0.03	0.02	0.02	0.03	0.02
Al_2O_3	22.23	22.66	22.26	22.25	22.63	21.94	21.91	21.57	21.73	21.81
FeO	30.28	29.95	30.65	30.24	29.80	34.09	31.52	34.77	35.37	34.64
MnO	0.53	0.52	0.50	0.59	0.54	0.70	0.58	0.71	0.96	0.77
MgO	7.28	7.62	7.41	7.12	7.69	5.01	6.37	4.33	4.05	4.58
CaO	1.32	1.46	1.43	1.35	1.40	1.35	1.33	1.45	1.51	1.37
Total	100.71	101.16	101.07	100.69	100.70	101.59	98.43	100.58	101.65	101.[illegible]8
Formulae based on 12 oxygens										
Si	3.013	2.986	2.990	2.025	2.978	3.001	2.936	2.992	2.989	3.001
Al	2.023	2.050	2.023	3.020	2.058	2.018	2.067	2.017	2.016	2.015
Ti	0.002	0.001	0.002	0.001		0.002	0.001	0.001	0.002	0.001
Fe	1.955	1.923	1.977	1.953	1.922	2.225	2.110	2.307	2.328	2.271
Mg	0.837	0.872	0.852	0.817	0.884	0.583	0.761	0.511	0.476	0.535
Mn	0.035	0.034	0.033	0.038	0.036	0.046	0.039	0.047	0.064	0.051
Ca	0.109	0.120	0.118	0.112	0.115	0.113	0.114	0.123	0.127	0.115
Total	2.938	2.950	2.982	2.921	2.957	2.969	3.025	2.989	2.997	2.973
Alm	66.59	65.21	66.34	66.88	65.00	74.99	69.78	77.21	77.73	76.41
Pyr	28.51	29.57	28.59	27.98	29.90	19.65	25.17	17.10	15.89	18.00
Spes	1.19	1.15	1.11	1.30	1.22	1.55	1.29	1.57	2.14	1.72
Gros	3.71	4.07	3.96	3.84	3.89	3.81	3.77	4.12	4.24	3.87
$\frac{Fe}{(Fe+Mg)}$	.700	.688	.699	.705	.685	.792	.735	.819	.830	.809

Table 21, continued. 160X Garnet Microprobe Analyses.

Alys#	295	296	297	298	299	300	301	302	303	304
SiO_2	37.77	38.45	38.33	36.82	39.10	39.24	39.08	37.15	38.92	39.19
TiO_2	0.0	0.0	0.02	0.01	0.0	0.0	0.0	0.0	0.0	0.0
Al_2O_3	21.52	21.91	21.72	21.73	22.42	22.22	22.22	21.63	22.40	21.90
FeO	35.10	33.07	32.92	34.37	30.11	29.92	29.43	29.77	30.11	29.77
MnO	1.39	0.67	0.65	0.74	0.57	0.57	0.52	0.50	0.54	0.54
MgO	3.23	5.46	5.12	4.62	7.43	7.70	7.64	6.79	7.71	7.71
CaO	1.93	1.60	1.47	1.27	1.38	1.34	1.26	1.20	1.27	1.33
Total	100.94	101.16	100.23	99.56	101.05	101.05	100.20	97.15	101.02	100.-8
Formulae based on 12 oxygens										
Si	3.001	3.001	3.018	2.951	3.012	3.018	3.030	2.983	2.994	3.033
Al	2.016	2.017	2.017	2.054	2.037	2.016	2.031	2.048	2.033	1.998
Ti			0.001							
Fe	2.334	2.160	2.169	2.305	1.941	1.926	1.909	2.001	1.939	1.928
Mg	0.382	0.635	0.601	0.552	0.853	0.884	0.884	0.813	0.884	0.890
Mn	0.093	0.044	0.043	0.050	0.037	0.037	0.034	0.034	0.035	0.035
Ca	0.164	0.134	0.124	0.109	0.114	0.111	0.104	0.104	0.105	0.111
Total	2.973	2.973	2.938	3.016	2.945	2.958	2.931	2.952	2.963	2.964
Alm	78.51	72.65	73.85	76.43	65.91	65.11	65.13	67.78	65.44	65.05
Pyr	12.85	21.36	20.46	18.30	28.96	29.89	30.16	27.54	29.83	30.03
Spes	3.13	1.48	1.46	1.66	1.26	1.25	1.16	1.15	1.18	1.18
Gros	5.52	4.51	4.22	3.61	3.87	3.75	3.55	3.52	3.54	3.74
$\frac{Fe}{(Fe+Mg)}$	.859	.773	.783	.807	.695	.685	.683	.711	.687	.684

Table 22. 160X Biotite Microprobe Analyses.

Color	Brn	Grn	Grn	Grn	Grn	Grn	Grn	Grn	Grn	Grn	Grn	Grn
Alys#	1	2	3	4	5	6	7	8	9	10	11	12
SiO_2	37.39	36.47	36.61	36.79	37.00	37.45	37.04	37.13	37.07	35.97	37.99	37.73
TiO_2	1.78	0.79	0.63	0.44	0.22	0.16	0.15	0.14	0.45	0.43	0.23	0.26
Al_2O_3	19.08	20.76	19.35	20.46	20.26	21.53	20.87	20.50	21.73	22.11	20.96	21.66
Cr_2O_3									0.0	0.01	0.04	0.0
FeO	17.03	16.48	16.98	16.33	16.25	14.87	15.87	15.50	16.29	16.69	16.44	16.29
MnO	0.05	0.03	0.03	0.02	0.03	0.03	0.04	0.02	0.03	0.02	0.01	0.01
MgO	11.07	11.17	12.17	11.85	11.76	11.48	12.32	12.04	12.41	12.66	12.13	12.56
CaO	0.0	0.0	0.0	0.0	0.0	0.0	0.0	0.0	0.0	0.0	0.0	0.0
Na_2O	0.25	0.30	0.27	0.25	0.26	0.29	0.28	0.22	0.12	0.12	0.08	0.16
K_2O	9.58	9.43	9.41	9.38	9.42	8.80	9.19	9.16	9.18	9.03	9.15	9.14
Total	96.23	95.43	95.45	95.52	95.20	94.61	95.76	94.71	97.28	97.04	97.03	97.81

Formulae based on 11 oxygens

Si	2.773	2.718	2.740	2.735	2.759	2.771	2.735	2.766	2.693	2.630	2.763	2.721
Al	1.227	1.282	1.260	1.265	1.241	1.229	1.265	1.234	1.307	1.370	1.237	1.279
Total	4.000	4.000	4.000	4.000	4.000	4.000	4.000	4.000	4.000	4.000	4.000	4.000
Al	0.441	0.542	0.446	0.528	0.539	0.649	0.550	0.565	0.555	0.536	0.561	0.563
Ti	0.099	0.044	0.035	0.025	0.012	0.009	0.008	0.008	0.025	0.024	0.013	0.014
Cr										0.001	0.002	
Fe	1.056	1.027	1.062	1.015	1.013	0.920	0.980	0.965	0.991	1.021	1.001	0.983
Mn	0.003	0.002	0.002	0.001	0.002	0.002	0.003	0.001	0.002	0.001		0.001
Mg	1.224	1.241	1.357	1.313	1.307	1.266	1.355	1.336	1.345	1.380	1.316	1.351
Total	2.823	2.856	2.902	2.882	2.873	2.846	2.896	2.875	2.918	2.963	2.893	2.912
Ca												
Na	0.037	0.043	0.039	0.036	0.038	0.042	0.040	0.032	0.017	0.017	0.011	0.022
K	0.906	0.896	0.898	0.889	0.896	0.830	0.865	0.870	0.851	0.843	0.849	0.841
Total	0.943	0.939	0.937	0.925	0.934	0.872	0.905	0.902	0.868	0.860	0.860	0.863
$\frac{Fe}{(Fe+Mg)}$	.463	.453	.439	.436	.437	.421	.420	.419	.424	.425	.432	.421
$\frac{K}{(K+Na)}$	.961	.954	.958	.961	.959	.952	.956	.965	.980	.980	.987	.975

Table 22, continued. 160X Biotite Microprobe Analyses.

Color	Grn	Grn	Grn	Grn	Grn	Grn	Grn	Grn	Grn	Brn	Brn	Brn
Alys#	13	14	15	16	17	18	19	20	21	22	23	24
SiO_2	36.89	38.64	37.69	38.93	38.49	37.62	38.27	38.14	37.80	37.77	37.77	36.03
TiO_2	0.26	0.13	0.14	0.16	0.12	0.09	0.17	0.24	0.17	2.36	2.40	2.18
Al_2O_3	21.66	21.01	21.22	21.14	21.76	21.06	21.49	21.23	21.03	20.24	20.51	20.82
Cr_2O_3	0.0	0.0	0.0	0.0	0.0	0.02	0.0	0.02	0.03	0.0	0.0	0.01
FeO	16.03	15.31	16.07	15.52	15.31	15.32	14.92	15.12	14.89	15.82	15.66	16.20
MnO	0.0	0.01	0.02	0.03	0.0	0.02	0.0	0.0	0.03	0.03	0.03	0.02
MgO	12.68	12.16	12.18	12.40	12.43	12.74	12.49	12.47	13.06	12.18	11.87	12.51
CaO												
Na_2O	0.07	0.14	0.08	0.14	0.03	0.08	0.06	0.05	0.07	0.10	0.08	0.15
K_2O	9.14	9.01	9.15	8.99	9.09	9.16	9.08	9.04	8.76	9.20	9.32	9.28
Total	96.73	96.41	96.55	97.31	97.23	96.11	96.48	96.31	95.84	97.70	97.64	97.20

Formulae based on 11 oxygens

Si	2.693	2.806	2.751	2.801	2.770	2.751	2.773	2.773	2.759	2.728	2.728	2.634
Al	1.307	1.194	1.249	1.199	1.230	1.249	1.227	1.227	1.241	1.272	1.272	1.366
Total	4.000	4.000	4.000	4.000	4.000	4.000	4.000	4.000	4.000	4.000	4.000	4.000
Al	0.557	0.605	0.578	0.595	0.617	0.568	0.609	0.593	0.569	0.452	0.476	0.429
Ti	0.014	0.007	0.008	0.009	0.007	0.005	0.010	0.013	0.009	0.128	0.130	0.120
Cr						0.001		0.001	0.002			0.001
Fe	0.979	0.930	0.982	0.935	0.922	0.938	0.905	0.920	0.909	0.956	0.947	0.991
Mn		0.001	0.001	0.002		0.002			0.002	0.002	0.002	0.001
Mg	1.381	1.317	1.326	1.330	1.335	1.390	1.350	1.353	1.422	1.312	1.278	1.364
Total	2.931	2.860	2.895	2.871	2.881	2.904	2.874	2.880	2.913	2.850	2.833	2.906
Ca												
Na	0.010	0.020	0.011	0.020	0.005	0.011	0.009	0.008	0.010	0.014	0.011	0.021
K	0.851	0.835	0.852	0.826	0.835	0.855	0.840	0.839	0.816	0.848	0.860	0.866
	0.861	0.855	0.863	0.846	0.840	0.866	0.849	0.847	0.826	0.862	0.871	0.887
$\frac{Fe}{(Fe+Mg)}$	.415	.414	.425	.413	.409	.402	.401	.405	.390	.402	.426	.420
$\frac{K}{(K+Na)}$	.988	.977	.987	.976	.994	.987	.989	.991	.988	.984	.987	.976

Table 22, continued. 160X Biotite Microprobe Analyses.

Color	Brn	Brn	Brn
Alys#	25	26	27
SiO_2	36.52	37.01	35.64
TiO_2	2.52	1.85	2.87
Al_2O_3	20.42	20.36	20.33
Cr_2O_3	0.0	0.05	0.03
FeO	16.24	16.75	17.71
MnO	0.01	0.05	0.06
MgO	12.26	10.99	10.67
CaO	0.00	0.00	0.00
Na_2O	0.17	0.18	0.04
K_2O	9.31	9.13	9.47
Total	97.45	96.37	96.82

Formulae based on 11 oxygens

Si	2.661	2.727	2.640
Al	1.339	1.273	1.360
Total	4.000	4.000	4.000
Al	0.416	0.496	0.416
Ti	0.138	0.102	0.160
Cr		0.003	0.002
Fe	0.990	1.032	1.098
Mn	0.001	0.003	0.004
Mg	1.333	1.207	1.179
Total	2.878	2.843	2.859
Ca			
Na	0.024	0.025	0.006
K	0.866	0.859	0.896
Total	0.890	0.884	0.902
$\frac{Fe}{(Fe+Mg)}$	.426	.461	.482
$\frac{K}{(K+Na)}$	.973	.972	.993

Figure 41. Location of microprobe analyses for garnet W67B.

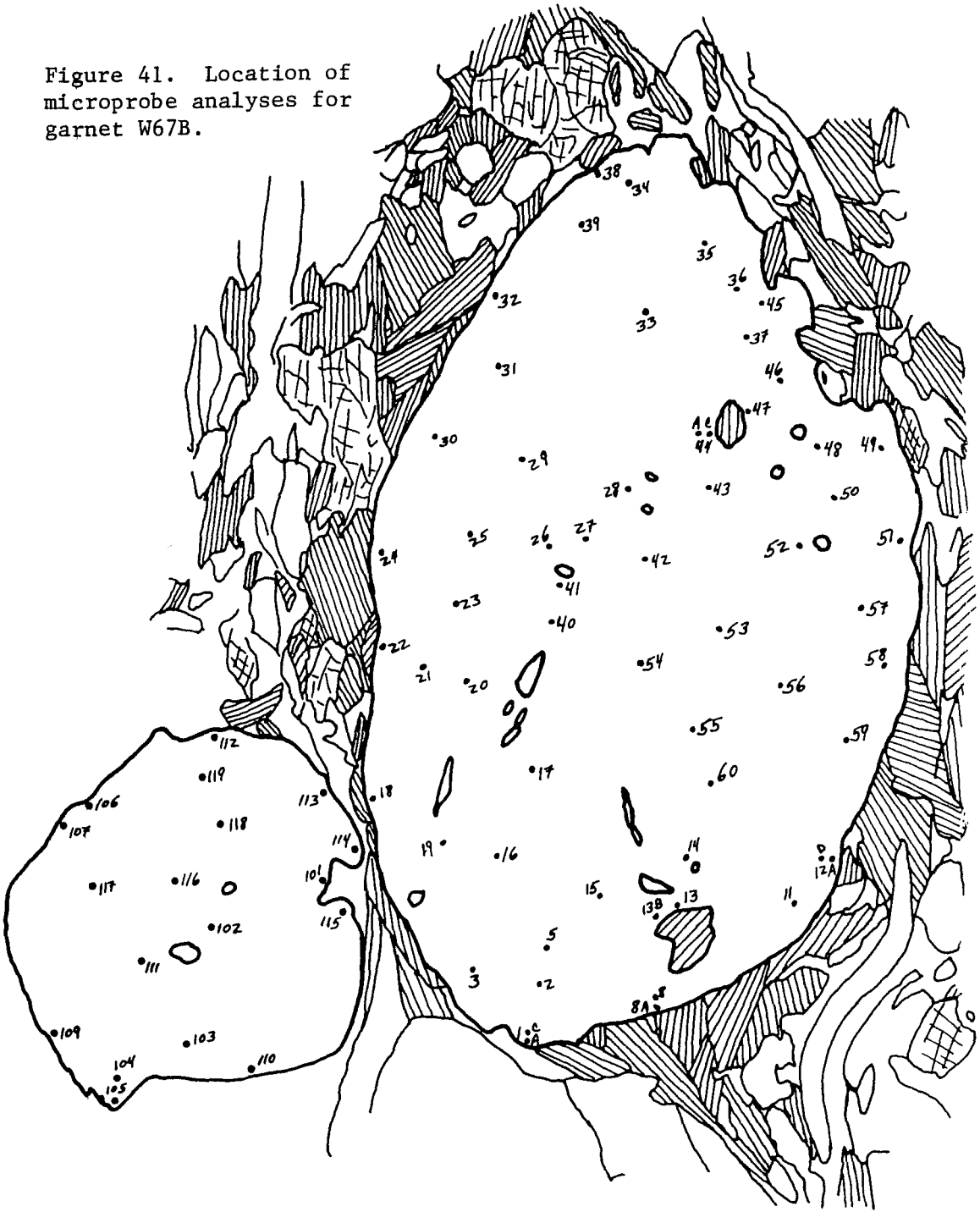

Table 23. W67B Garnet Microprobe Analyses.

Alys#	1A	1B	1C	2	3A	3B	5	8	11	12A
SiO_2	38.09	37.92	37.86	38.43	37.98	38.16	38.16	37.75	38.10	37.95
TiO_2	0.0	0.01	0.0	0.0	0.0	0.0	0.0	0.0	0.03	0.02
Al_2O_3	21.60	21.78	21.71	21.73	21.74	21.80	21.79	21.69	21.74	21.64
Cr_2O_3	0.02	0.01	0.04	0.05	0.0	0.02	0.03	0.05	0.0	0.0
FeO	32.93	33.18	32.90	32.04	31.76	31.97	31.53	32.74	33.25	33.88
MnO	2.21	2.26	1.86	1.40	1.32	1.41	1.36	1.77	1.55	2.93
MgO	3.83	4.02	4.63	5.83	5.55	5.43	5.98	4.54	4.45	3.15
CaO	1.39	1.44	1.46	1.11	1.19	1.26	1.19	1.30	1.14	1.24
Total	100.07	100.62	100.46	100.59	99.54	100.05	100.04	99.84	100.26	100.81
Formulae based on 12 oxygens										
Si	3.026	3.001	2.994	3.009	3.005	3.007	3.000	3.000	3.014	3.014
Al	2.023	2.033	2.024	2.006	2.028	2.025	2.020	2.033	2.028	2.027
Cr	0.001	0.001		0.003		0.001	0.002	0.003		
Total	2.024	2.034		2.009		2.026	2.022	2.036		
Ti		0.001							0.002	0.002
Fe	2.189	2.197	2.177	2.100	2.103	2.108	2.075	2.177	2.201	2.252
Mg	0.454	0.474	0.546	0.681	0.654	0.638	0.701	0.538	0.525	0.373
Mn	0.149	0.152	0.125	0.093	0.089	0.094	0.091	0.119	0.104	0.198
Ca	0.118	0.122	0.124	0.093	0.101	0.106	0.100	0.111	0.096	0.106
Total	2.910	2.946	2.972	2.967	2.947	2.946	2.967	2.945	2.928	2.931
Alm	75.22	74.60	73.25	70.78	71.36	71.55	69.94	73.92	75.22	76.69
Pyr	15.60	16.10	18.37	22.95	22.19	21.66	23.63	18.27	17.94	12.73
Spes	5.12	5.16	4.21	3.13	3.02	3.19	3.07	4.04	3.55	6.76
Gros	4.05	4.14	4.17	3.13	3.42	3.60	3.37	3.77	3.28	3.62
$\frac{Fe}{(Fe+Mg)}$	.828	.823	.799	.755	.763	.768	.747	.802	.807	.858

Table 23, continued. W67B Garnet Microprobe Analyses.

Alys#	12D	13	13B	14	15A	16	17	18	19	20
SiO_2	38.26	38.24	38.13	38.46	38.30	38.27	38.17	37.71	38.45	38.01
TiO_2	0.03	0.0	0.0	0.0	0.0	0.01	0.0	0.02	0.0	0.03
Al_2O_3	21.73	21.68	21.80	21.96	21.86	21.90	21.57	21.62	21.95	21.91
Cr_2O_3	0.0	0.01	0.01	0.03	0.03	0.0	0.0	0.0	0.0	0.0
FeO	33.25	32.24	32.33	31.56	31.82	33.03	32.12	34.09	31.93	32.47
MnO	1.56	1.52	1.50	1.54	1.44	1.62	1.56	2.52	1.38	1.45
MgO	4.38	5.77	5.45	5.91	6.00	5.16	5.05	3.15	5.53	4.94
CaO	1.14	1.27	1.28	1.29	1.08	1.13	1.15	1.71	1.34	1.12
Total	100.35	100.73	100.50	100.75	100.53	101.12	99.62	100.82	100.58	99.93
Formulae based on 12 oxygens										
Si	3.022	2.998	2.997	3.003	2.999	2.998	3.024	2.999	3.009	3.005
Al	2.025	2.004	2.021	2.022	2.019	2.023	2.015	2.028	2.027	2.043
Cr		0.001		0.002	0.002					
Total		2.005		2.024	2.021					
Ti	0.002							0.001		0.002
Fe	2.198	2.115	2.127	2.062	2.085	2.165	2.129	2.269	2.091	2.148
Mg	0.516	0.675	0.639	0.688	0.701	0.603	0.597	0.374	0.645	0.582
Mn	0.105	0.101	0.100	0.102	0.095	0.108	0.105	0.170	0.092	0.097
Ca	0.096	0.107	0.108	0.108	0.091	0.095	0.097	0.146	0.113	0.095
Total	2.917	2.998	2.974	2.960	2.972	2.971	2.928	2.960	2.941	2.924
Alm	75.40	70.55	71.52	69.66	70.15	72.87	72.71	76.68	71.10	73.51
Pyr	17.70	22.52	21.49	23.24	23.59	20.30	20.39	12.64	21.93	19.92
Spes	3.60	3.37	3.36	3.45	3.20	3.64	3.59	5.75	3.13	3.32
Gros	3.29	3.57	3.63	3.65	3.06	3.20	3.31	4.93	3.84	3.25
$\frac{Fe}{(Fe+Mg)}$	.810	.758	.769	.750	.748	.782	.781	.858	.764	.787

Table 23, continued. W67B Garnet Microprobe Analyses.

Alys#	21	22	23	24	25	26	27	28	29	30
SiO_2	38.23	37.30	37.84	37.85	38.38	38.59	38.61	38.63	37.65	38.22
TiO_2	0.01	0.01	0.02	0.04	0.0	0.02	0.0	0.0	0.02	0.05
Al_2O_3	21.73	21.07	21.93	21.87	21.93	21.99	21.80	21.75	21.91	21.50
Cr_2O_3	0.02	0.01	0.0	0.0	0.04	0.03	0.0	0.04	0.0	0.0
FeO	32.33	33.29	33.69	33.85	31.47	31.37	31.56	31.05	32.39	32.80
MnO	1.49	2.61	1.52	1.80	1.49	1.70	1.69	1.65	1.58	1.56
MgO	5.56	3.69	5.08	3.83	5.78	5.91	5.85	5.87	5.19	4.74
CaO	1.11	1.69	1.13	1.56	1.14	1.17	1.15	1.17	1.11	1.30
Total	100.48	99.67	100.21	100.80	100.23	100.78	100.66	100.16	99.85	100.17
Formulae based on 12 oxygens										
Si	3.004	2.998	2.989	2.994	3.009	3.009	3.017	3.026	2.983	3.022
Al	2.013	1.998	2.043	2.041	2.028	2.022	2.008	2.009	2.047	2.005
Cr	0.001	0.001			0.002	0.002		0.002		
Total	2.014	1.999			2.030	2.024		2.011		
Ti	0.001	0.001	0.001	0.002		0.001			0.001	0.003
Fe	2.125	2.239	2.161	2.241	2.055	2.047	2.064	2.036	2.147	2.170
Mg	0.651	0.442	0.598	0.452	0.676	0.687	0.682	0.686	0.613	0.559
Mn	0.099	0.178	0.102	0.121	0.097	0.112	0.112	0.110	0.106	0.105
Ca	0.094	0.146	0.095	0.133	0.098	0.098	0.096	0.098	0.095	0.110
Total	2.970	3.006	2.957	2.949	2.926	2.945	2.954	2.930	2.962	2.947
Alm	71.57	74.51	73.11	76.04	70.23	69.53	69.87	69.49	72.51	73.71
Pyr	21.93	14.71	20.23	15.34	23.10	23.34	23.09	23.41	20.70	18.99
Spes	3.33	5.92	3.45	4.11	3.32	3.80	3.79	3.75	3.58	3.57
Gros	3.17	4.86	3.21	4.51	3.35	3.33	3.25	3.34	3.21	3.74
$\frac{Fe}{(Fe+Mg)}$	.765	.835	.783	.832	.752	.749	.752	.748	.778	.795

Table 23, continued. W67B Garnet Microprobe Analyses.

Alys#	31	32	33	34	35	36	37	38	39	40
SiO_2	38.57	37.83	38.40	38.09	38.40	37.80	38.70	37.72	38.16	38.55
TiO_2	0.0	0.0	0.0	0.0	0.02	0.0	0.0	0.0	0.0	0.03
Al_2O_3	21.67	21.53	21.35	21.62	21.60	21.81	21.73	21.21	21.90	21.96
Cr_2O_3	0.04	0.01	0.0	0.0	0.0	0.0	0.0	0.0	0.02	0.02
FeO	31.79	33.83	31.68	31.72	31.44	31.99	32.23	33.35	32.35	31.85
MnO	1.47	2.28	1.55	1.37	1.34	1.46	1.47	2.57	1.34	1.65
MgO	5.72	3.95	5.99	5.44	5.75	5.27	5.57	3.53	5.57	5.80
CaO	1.25	1.21	1.27	1.20	1.31	1.50	1.39	1.36	1.20	1.20
Total	100.51	100.64	100.24	99.44	99.86	99.83	101.09	99.74	100.54	101.06
Formulae base on 12 oxygens										
Si	3.020	3.003	3.018	3.017	3.022	2.991	3.018	3.022	2.996	3.004
Al	2.001	2.015	1.979	2.019	2.005	2.035	1.999	2.003	2.027	2.018
Cr	0.002	0.001							0.001	0.001
Total	2.003	2.016							2.028	2.019
Ti					0.001					0.002
Fe	2.083	2.247	2.083	2.102	2.071	2.118	2.103	2.236	2.125	2.077
Mg	0.668	0.468	0.702	0.642	0.675	0.622	0.648	0.421	0.652	0.674
Mn	0.098	0.153	0.103	0.092	0.090	0.098	0.097	0.175	0.089	0.109
Ca	0.105	0.103	0.107	0.102	0.110	0.127	0.116	0.117	0.101	0.100
Total	2.954	2.971	2.995	2.938	2.947	2.965	2.964	2.949	2.967	2.962
Alm	70.51	75.63	69.55	71.55	70.30	71.43	70.95	75.82	71.62	70.17
Pyr	22.61	15.75	23.44	21.85	22.91	20.98	21.86	14.28	21.98	22.77
Spes	3.32	5.15	3.44	3.13	3.05	3.31	3.27	5.93	3.00	3.68
Gros	3.55	3.47	3.57	3.47	3.73	4.28	3.91	3.97	3.40	3.38
$\frac{Fe}{(Fe+Mg)}$	.757	.828	.748	.766	.754	.773	.764	.842	.765	.755

Table 23, continued. W67B Garnet Microprobe Analyses.

Alys#	41	42	43	44A	44B	44C	45	46	47	48
SiO_2	38.27	38.42	38.09	38.55	38.84	38.67	38.02	38.53	38.35	38.65
TiO_2	0.02	0.0	0.0	0.0	0.0	0.01	0.01	0.02	0.0	0.03
Al_2O_3	21.59	21.74	21.81	21.81	21.71	21.79	21.16	21.54	21.91	21.71
Cr_2O_3	0.0	0.0	0.0	0.04	0.0	0.0	0.05	0.03	0.05	0.01
FeO	31.47	31.83	31.76	32.17	32.18	32.46	32.97	31.67	31.96	32.75
MnO	1.68	1.68	1.60	1.54	1.57	1.57	1.85	1.46	1.43	1.38
MgO	5.52	5.35	5.85	5.87	5.95	5.77	4.65	5.38	5.37	5.51
CaO	1.16	1.18	1.39	1.35	1.31	1.38	1.62	1.59	1.32	1.43
Total	99.71	100.20	100.50	101.33	101.56	101.65	100.33	100.22	100.39	101.47
Formulae based on 12 oxygens										
Si	3.021	3.021	2.989	3.000	3.014	3.004	3.014	3.028	3.010	3.010
Al	2.010	2.016	2.019	2.002	1.987	1.996	1.978	1.996	2.028	1.994
Cr				0.003			0.003	0.002	0.003	0.001
Total				2.005			1.981	1.998	2.031	1.995
Ti	0.001						0.001	0.001		0.002
Fe	2.079	2.094	2.086	2.095	2.090	2.110	2.187	2.083	2.099	2.134
Mg	0.650	0.628	0.685	0.682	0.689	0.669	0.549	0.631	0.628	0.640
Mn	0.113	0.112	0.106	0.102	0.104	0.103	0.124	0.097	0.095	0.091
Ca	0.098	0.100	0.117	0.113	0.109	0.115	0.138	0.134	0.111	0.120
Total	2.941	2.934	2.994	2.982	2.992	2.997	2.999	2.946	2.933	2.987
Alm	70.71	71.37	69.67	70.02	69.85	70.40	72.95	70.73	71.56	71.49
Pyr	22.11	21.40	22.88	22.79	23.03	22.32	18.31	21.43	21.41	21.44
Spes	3.84	3.82	3.54	3.41	3.48	3.44	4.14	3.29	3.24	3.05
Gros	3.33	3.41	3.91	3.78	3.64	3.84	4.60	4.55	3.78	4.02
$\frac{Fe}{(Fe+Mg)}$	.762	.769	.753	.754	.752	.759	.799	.768	.770	.769

Table 23, continued. W67B Garnet Microprobe Analyses.

Alys#	49	50	51	52	53	54	55	56	57	58
SiO_2	38.36	38.51	37.61	38.60	38.56	38.46	38.72	38.25	38.21	38.56
TiO_2	0.0	0.02	0.02	0.0	0.0	0.0	0.0	0.0	0.01	0.03
Al_2O_3	21.63	21.97	21.54	21.94	21.71	21.70	21.77	21.58	21.57	21.84
Cr_2O_3	0.03	0.04	0.04	0.04	0.01	0.0	0.0	0.03	0.01	0.02
FeO	32.58	32.11	34.02	31.74	31.49	31.88	32.25	31.54	32.21	32.77
MnO	1.60	1.38	2.67	1.50	1.50	1.57	1.63	1.50	1.33	1.43
MgO	4.82	5.54	3.79	5.88	5.90	6.13	5.87	5.98	5.86	5.35
CaO	1.47	1.19	1.27	1.13	1.17	1.21	1.19	1.18	1.23	1.23
Total	100.49	100.76	100.96	100.83	100.34	100.95	101.43	100.06	100.43	101.23
Formulae based on 12 oxygens										
Si	3.020	3.010	2.985	3.010	3.020	3.002	3.010	3.009	3.002	3.009
Al	2.008	2.025	2.017	2.018	2.005	1.998	1.996	2.002	1.999	2.010
Cr	0.002	0.002	0.003	0.002	0.001			0.002		0.001
Total	2.010	2.027	2.020	2.020	2.006			2.004		2.011
Ti		0.001	0.001							0.002
Fe	2.147	2.100	2.260	2.071	2.064	2.082	2.098	2.076	2.118	2.140
Mg	0.566	0.646	0.449	0.684	0.689	0.714	0.681	0.701	0.687	0.623
Mn	0.107	0.091	0.180	0.099	0.100	0.104	0.107	0.100	0.089	0.095
Ca	0.124	0.100	0.108	0.094	0.099	0.101	0.099	0.099	0.104	0.103
Total	2.944	2.938	2.998	2.948	2.952	3.001	2.985	2.976	2.998	2.963
Alm	72.93	71.50	75.41	70.25	69.92	69.38	70.28	69.76	70.65	72.27
Pyr	19.23	22.00	14.98	23.20	23.34	23.79	22.81	23.56	22.92	21.04
Spes	3.63	3.10	6.01	3.36	3.39	3.47	3.58	3.36	2.97	3.21
Gros	4.21	3.40	3.60	3.19	3.35	3.37	3.32	3.33	3.47	3.48
$\frac{Fe}{(Fe+Mg)}$	.791	.765	.834	.752	.750	.745	.755	.748	.755	.775

Table 23, continued. W67B Garnet Microprobe Analyses.

Alys#	59	60	101	102	103	104	105	106	107
SiO_2	37.47	38.58	37.05	38.24	38.39	38.19	38.06	37.84	37.86
TiO_2	0.01	0.0	0.01	0.0	0.0	0.0	0.0	0.0	0.0
Al_2O_3	21.40	21.53	21.64	21.67	21.86	21.72	21.64	21.15	21.66
Cr_2O_3	0.04	0.0	0.0	0.07	0.04	0.01	0.0	0.0	0.0
FeO	32.05	31.82	33.94	31.99	31.41	32.44	32.02	33.51	32.89
MnO	1.44	1.59	2.81	1.41	1.32	1.51	1.61	2.55	2.64
MgO	5.75	5.93	2.97	5.84	5.88	5.10	5.03	3.75	3.53
CaO	1.14	1.23	1.50	1.18	1.18	1.38	1.63	1.58	1.71
Total	99.30	100.68	99.92	100.40	100.08	100.35	99.99	100.38	100.29
Formulae based on 12 oxygens									
Si	2.984	3.018	2.980	3.002	3.012	3.008	3.008	3.015	3.011
Al	2.010	1.987	2.052	2.007	2.023	2.018	2.018	1.988	2.031
Cr	0.003			0.004	0.002	0.001			
Total	2.013			2.011	2.025	2.019			
Ti	0.001								
Fe	2.135	2.083	2.284	2.102	2.062	2.138	2.118	2.235	2.189
Mg	0.683	0.692	0.356	0.684	0.688	0.599	0.593	0.445	0.419
Mn	0.097	0.105	0.192	0.094	0.088	0.101	0.108	0.172	0.178
Ca	0.098	0.103	0.129	0.099	0.099	0.117	0.138	0.135	0.145
Total	3.014	2.983	2.961	2.979	2.937	2.955	2.957	2.987	2.931
Alm	70.86	69.83	77.14	70.56	70.21	72.35	71.63	74.82	74.68
Pyr	22.67	23.20	12.02	22.96	23.43	20.27	20.05	14.90	14.30
Spes	3.22	3.52	6.48	3.16	3.00	3.42	3.65	5.75	6.07
Gros	3.25	3.45	4.36	3.32	3.37	3.96	4.67	4.52	4.95
$\frac{Fe}{(Fe+Mg)}$	.758	.751	.865	.754	.750	.781	.781	.834	.839

Table 23, continued. W67B Garnet Microprobe Analyses.

Alys#	109	110	111	112	113	114	115	116	117	118A
SiO_2	37.94	38.43	38.58	38.05	36.99	37.58	37.29	38.12	38.29	37.37
TiO_2	0.0	0.0	0.0	0.0	0.0	0.0	0.0	0.0	0.0	0.01
Al_2O_3	21.43	21.98	22.00	21.66	21.00	21.70	21.31	21.52	21.73	22.47
Cr_2O_3	0.02	0.0	0.04	0.01	0.0	0.02	0.02	0.02	0.0	0.01
FeO	33.32	31.45	31.30	33.22	33.61	33.82	33.10	31.46	32.17	31.98
MnO	2.94	1.30	1.26	2.23	2.93	2.44	3.04	1.42	1.26	1.38
MgO	3.26	5.56	5.87	3.95	3.19	3.41	2.62	6.08	5.72	5.65
CaO	1.76	1.60	1.17	1.64	1.43	1.75	2.01	1.21	1.14	1.10
Total	100.67	100.32	100.22	100.76	99.15	100.72	99.39	99.83	100.31	99.97
Formulae based on 12 oxygens										
Si	3.016	3.011	3.018	3.008	2.999	2.988	3.011	3.005	3.008	2.950
Al	2.009	2.031	2.029	2.020	2.007	2.035	2.029	2.001	2.013	2.091
Cr	0.001		0.002	0.001		0.001	0.C01			0.001
Total	2.010		2.031	2.021		2.036	2.030			2.092
Ti										
Fe	2.217	2.062	2.049	2.198	2.280	2.250	2.236	2.075	2.114	2.112
Mg	0.386	0.650	0.685	0.466	0.386	0.404	0.315	0.715	0.670	0.664
Mn	0.198	0.086	0.084	0.149	0.201	0.164	0.208	0.095	0.084	0.093
Ca	0.150	0.135	0.098	0.139	0.124	0.149	0.174	0.102	0.096	0.093
Total	2.951	2.933	2.916	2.952	2.991	2.967	2.933	2.987	2.964	2.962
Alm	75.13	70.30	70.27	74.46	76.23	75.83	76.24	69.47	71.32	71.30
Pyr	13.08	22.16	23.49	15.79	12.91	13.62	10.74	23.94	22.60	22.42
Spes	6.71	2.93	2.88	5.05	6.72	5.53	7.09	3.18	2.83	3.14
Gros	5.08	4.60	3.36	4.71	4.15	5.02	5.93	3.41	3.24	3.14
$\frac{Fe}{(Fe+Mg)}$	.852	.760	.749	.825	.855	.848	.877	.744	.759	.761

Table 23, continued. W67B Garnet Microprobe Analyses.

Alys#	118B	119A	119B
SiO_2	36.87	38.81	37.93
TiO_2	0.0	0.02	0.02
Al_2O_3	22.44	22.41	22.21
Cr_2O_3	0.05	0.01	0.0
FeO	32.50	32.66	32.77
MnO	1.30	1.38	1.40
MgO	5.84	5.50	6.02
CaO	1.15	1.14	1.31
Total	100.15	101.93	101.66

Formulae based on 12 oxygens

Si	2.916	3.000	2.952
Al	2.093	2.043	2.039
Cr	0.003		
Total	2.096		
Ti		0.001	0.001
Fe	2.151	2.113	2.134
Mg	0.689	0.630	0.698
Mn	0.087	0.090	0.093
Ca	0.097	0.094	0.109
Total	3.024	2.928	3.035
Alm	71.13	72.19	70.34
Pyr	22.78	21.52	23.01
Spes	2.88	3.07	3.07
Gros	3.21	3.21	3.59
$\frac{Fe}{(Fe+Mg)}$	.757	.770	.754

Table 24. W67B Biotite Microprobe Analyses.

Positn	Matr	Rim	Rim	Rim	Matr	Rim	Rim	Rim	Rim	Rim	Rim	Rim
Alys#	1	2	3	4	5	6	7	8	9	10	11	12
SiO_2	34.20	33.12	34.73	34.29	33.84	35.16	35.24	34.45	34.83	35.01	35.27	35.39
TiO_2	4.08	4.07	3.53	3.92	4.06	3.52	3.38	3.25	3.54	3.94	3.44	3.52
Al_2O_3	18.50	18.93	18.69	18.83	19.29	19.07	20.22	19.02	18.57	19.01	19.29	19.37
Cr_2O_3	0.0	0.02	0.04	0.0	0.0	0.03	0.07	0.08	0.03	0.04	0.03	0.05
FeO	18.02	18.05	17.76	17.37	17.79	18.20	18.20	19.26	18.58	18.70	17.98	17.92
MnO	0.01	0.04	0.05	0.02	0.09	0.04	0.09	0.09	0.09	0.10	0.13	0.08
MgO	8.91	9.72	9.35	9.00	8.95	9.85	9.42	9.66	9.52	10.04	9.66	9.87
CaO	0.0	0.0	0.0	0.0	0.0	0.0	0.0	0.0	0.0	0.0	0.0	0.0
Na_2O	0.02	0.03	0.06	0.03	0.10	0.01	0.06	0.10	0.09	0.04	0.02	0.0
K_2O	9.87	9.90	9.73	9.75	9.54	9.61	8.80	9.23	9.73	9.69	9.75	9.74
Total	93.61	93.88	93.94	93.21	93.66	95.49	95.48	95.14	94.98	96.57	95.57	95.94
Formulae based on 11 oxygens												
Si	2.650	2.568	2.672	2.656	2.614	2.658	2.647	2.629	2.661	2.628	2.663	2.659
Al	1.350	1.432	1.328	1.344	1.386	1.342	1.353	1.371	1.339	1.372	1.337	1.341
Total	4.000	4.000	4.000	4.000	4.000	4.000	4.000	4.000	4.000	4.000	4.000	4.000
Al	0.340	0.300	0.368	0.376	0.371	0.358	0.438	0.341	0.334	0.311	0.381	0.376
Ti	0.238	0.237	0.204	0.228	0.236	0.200	0.191	0.187	0.204	0.222	0.195	0.199
Cr		0.001	0.003			0.002	0.004	0.005	0.002	0.002	0.002	0.003
Fe	1.168	1.171	1.143	1.126	1.150	1.152	1.144	1.230	1.187	1.175	1.136	1.126
Mn	0.001	0.003	0.003	0.001	0.006	0.003	0.006	0.006	0.006	0.006	0.008	0.005
Mg	1.030	1.124	1.073	1.040	1.031	1.110	1.055	1.100	1.085	1.124	1.088	1.107
Total	2.776	2.836	2.794	2.771	2.794	2.825	2.838	2.869	2.818	2.840	2.810	2.816
Ca												
Na	0.003	0.004	0.009	0.005	0.015	0.001	0.009	0.014	0.014	0.006	0.003	
K	0.976	0.980	0.956	0.964	0.941	0.927	0.844	0.899	0.949	0.928	0.940	0.934
Total	0.979	0.984	0.965	0.969	0.956	0.928	0.853	0.913	0.963	0.934	0.943	0.934
$\frac{Fe}{(Fe+Mg)}$	.531	.510	.516	.520	.527	.509	.520	.528	.522	.511	.511	.504
$\frac{K}{(K+Na)}$	.997	.996	.991	.995	.984	.999	.989	.985	.985	.994	.997	1.000

Table 24, continued. W67B Biotite Microprobe Analyses.

Positn	Rim	Rim	Incl	Incl	Incl	Incl	Incl	Rim	Rim	Rim	Rim	Rim
Alys#	13	14	15	16	17	18	19	20	21	22	23	24
SiO_2	35.52	36.26	35.53	36.08	36.15	36.25	36.03	36.04	36.35	34.95	35.29	34.68
TiO_2	3.65	3.92	3.31	3.32	3.23	3.83	2.69	4.52	4.39	3.34	3.46	2.26
Al_2O_3	19.25	20.12	19.38	19.57	19.77	19.68	18.70	18.76	18.73	18.06	18.14	18.42
Cr_2O_3	0.01	0.02	0.02	0.03	0.05	0.09	0.0	0.04	0.06	0.05	0.07	0.05
FeO	16.89	15.66	14.14	14.09	14.36	14.10	12.35	17.64	17.53	18.94	19.76	19.40
MnO	0.08	0.04	0.02	0.01	0.04	0.02	0.01	0.13	0.10	0.07	0.17	0.12
MgO	10.58	11.30	12.52	12.79	12.83	12.43	14.53	9.76	9.52	9.54	9.77	10.09
CaO	0.0	0.0	0.0	0.0	0.0	0.0	0.0	0.0	0.0	0.0	0.0	0.0
Na_2O	0.01	0.01	0.14	0.10	0.15	0.16	0.41	0.10	0.03	0.0	0.13	0.04
K_2O	9.61	9.59	9.59	9.78	9.49	9.54	8.83	9.72	9.81	9.63	9.68	9.65
Total	95.60	96.99	94.65	95.77	96.07	96.10	93.55	96.71	96.52	94.58	96.47	94.71
Formulae based on 11 oxygens												
Si	2.663	2.655	2.656	2.663	2.658	2.662	2.692	2.682	2.706	2.684	2.668	2.668
Al	1.337	1.345	1.344	1.337	1.342	1.338	1.308	1.318	1.294	1.316	1.332	1.332
Total	4.000	4.000	4.000	4.000	4.000	4.000	4.000	4.000	4.000	4.000	4.000	4.000
Al	0.365	0.393	0.365	0.367	0.373	0.366	0.340	0.328	0.351	0.320	0.285	0.285
Ti	0.206	0.216	0.186	0.184	0.179	0.212	0.151	0.253	0.246	0.193	0.196	0.131
Cr		0.001	0.001	0.002	0.003	0.005		0.002	0.004	0.003	0.004	0.003
Fe	1.060	0.960	0.885	0.870	0.884	0.867	0.772	1.098	1.092	1.217	1.250	1.249
Mn	0.005	0.002	0.001	0.001	0.002	0.001	0.001	0.008	0.007	0.005	0.011	0.008
Mg	1.183	1.234	1.396	1.409	1.407	1.362	1.619	1.083	1.057	1.093	1.102	1.158
Total	2.819	2.806	2.834	2.833	2.848	2.813	2.883	2.722	2.757	2.831	2.848	2.834
Ca												
Na	0.001	0.012	0.020	0.015	0.021	0.023	0.060	0.015	0.004	0.0	0.019	0.007
K	0.920	0.896	0.915	0.921	0.891	0.894	0.842	0.923	0.933	0.944	0.935	0.947
Total	0.921	0.908	0.917	0.936	0.912	0.917	0.902	0.938	0.937	0.944	0.954	0.954
$\frac{Fe}{(Fe+Mg)}$	.473	.438	.388	.382	.386	.389	.323	.503	.508	.527	.531	.519
$\frac{K}{(K+Na)}$	.999	.987	.998	.984	.977	.975	.933	.984	.996	1.000	.980	.993

Table 24, continued. W67B Biotite Microprobe Analyses.

Sample W67B (Sheared pelitic schist)

Positn	Rim	Rim	Matr	Matr	Rim	Rim
Alys#	25	26	27	28	29	30
SiO_2	37.15	36.88	35.90	35.66	37.38	37.54
TiO_2	2.15	3.39	3.76	3.92	4.04	4.17
Al_2O_3	19.45	19.41	19.43	18.79	19.03	18.82
Cr_2O_3	0.05	0.07	0.08	0.05	0.03	0.06
FeO	18.40	17.72	17.77	18.25	19.03	18.82
MnO	0.15	0.06	0.08	0.11	0.15	0.11
MgO	9.80	9.94	10.39	10.04	10.31	9.98
CaO	0.0	0.0	0.0	0.0	0.0	0.0
Na_2O	0.07	0.13	0.09	0.05	0.12	0.02
K_2O	9.61	9.47	9.57	9.61	9.59	9.85
Total	96.83	97.07	97.07	96.48	98.89	98.67

Formulae based on 11 oxygens

Si	2.755	2.720	2.658	2.668	2.713	2.732
Al	1.245	1.280	1.342	1.332	1.287	1.268
Total	4.000	4.000	4.000	4.000	4.000	4.000
Al	0.456	0.408	0.355	0.326	0.342	0.347
Ti	0.120	0.188	0.210	0.220	0.221	0.228
Cr	0.003	0.004	0.004	0.003	0.002	0.004
Fe	1.142	1.094	1.101	1.143	1.108	1.103
Mn	0.009	0.004	0.005	0.007	0.009	0.007
Mg	1.084	1.094	1.148	1.121	1.117	1.083
Total	2.814	2.792	2.823	2.820	2.799	2.772
Ca						
Na	0.011	0.019	0.013	0.007	0.018	0.003
K	0.909	0.891	0.905	0.918	0.888	0.915
Total	0.920	0.910	0.918	0.925	0.906	0.918
$\frac{Fe}{(Fe+Mg)}$	.513	.500	.490	.505	.498	.505
$\frac{K}{(K+Na)}$	.988	.979	.986	.992	.980	.997

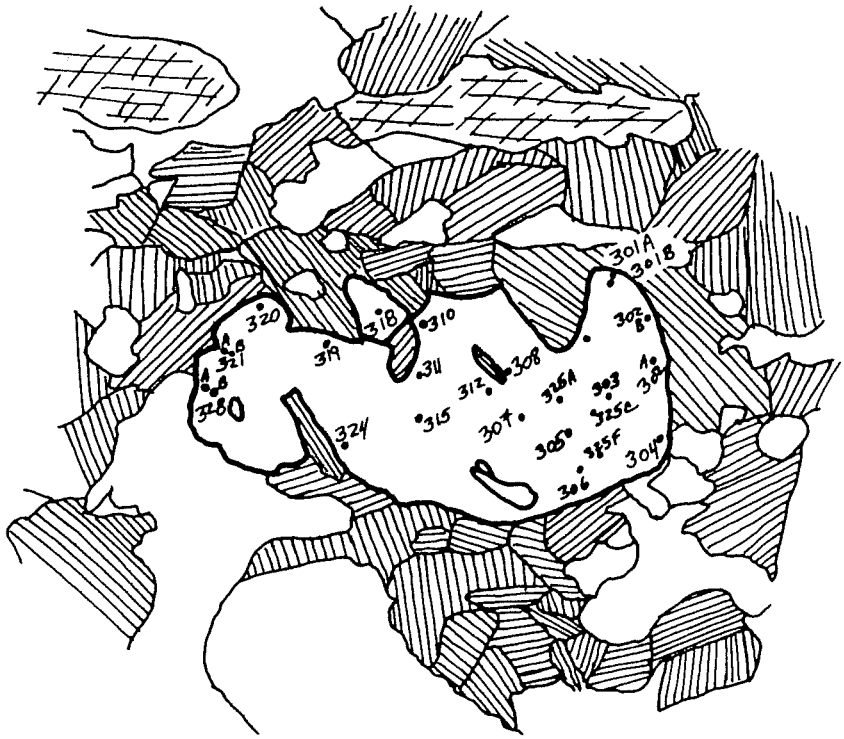

Figure 42. Location of microprobe analyses for garnet X43A.

Table 25. X43A Garnet Microprobe Analyses.

Alys#	301A	301B	301C	302A	302B	303	304	305	306	307
SiO_2	35.59	36.89	37.11	36.90	36.67	37.83	37.37	37.46	37.09	37.74
Al_2O_3	20.38	21.07	20.11	20.66	21.03	21.57	20.61	20.88	20.40	21.25
FeO	36.80	37.27	36.70	36.38	35.99	32.02	35.22	31.35	34.81	30.51
MnO	2.10	1.66	1.58	0.90	1.42	0.74	0.99	0.25	1.43	0.68
MgO	3.89	4.73	4.21	6.20	4.85	9.05	6.22	8.57	5.88	9.07
CaO	0.85	0.83	0.74	0.25	0.37	0.0	0.31	0.30	0.73	0.16
Total	99.61	102.45	100.45	101.29	100.33	101.21	100.72	98.81	100.34	99.41
Formulae based on 12 oxygens										
Si	2.916	2.921	2.991	2.932	2.944	2.934	2.964	2.970	2.965	2.963
Al	1.968	1.966	1.911	1.935	1.990	1.972	1.927	1.951	1.922	1.967
Fe	2.521	2.468	2.474	2.418	2.417	2.077	2.336	2.078	2.327	2.003
Mg	0.475	0.558	0.506	0.734	0.581	1.047	0.735	1.013	0.701	1.061
Mn	0.146	0.111	0.108	0.060	0.097	0.049	0.066	0.017	0.097	0.045
Ca	0.074	0.071	0.064	0.021	0.032		0.026	0.026	0.062	0.013
Total	3.216	3.208	3.152	3.233	3.127	3.173	3.163	3.134	3.187	3.122
Alm	78.39	76.93	78.49	74.79	77.29	65.46	73.85	66.31	73.02	64.16
Pyr	14.77	17.39	16.05	22.70	18.58	33.00	23.24	32.32	22.00	33.98
Spes	4.54	3.46	3.43	1.86	3.10	1.54	2.09	0.54	3.04	1.44
Gros	2.30	2.21	2.03	0.65	1.02		0.82	0.83	1.95	0.42
$\frac{Fe}{(Fe+Mg)}$	.841	.816	.830	.767	.806	.655	.761	.672	.768	.654

Table 25, continued. X43A Garnet Microprobe Analyses.

Alys#	308	310	311	312	315	318	319	320	321A	321B
SiO_2	37.33	36.61	36.89	37.50	36.62	36.30	37.14	36.60	36.82	36.56
Al_2O_3	21.18	20.34	20.74	20.82	20.69	21.06	20.42	20.80	20.45	21.18
FeO	33.93	36.08	35.12	33.70	35.47	36.78	35.50	35.78	36.51	35.82
MnO	1.21	1.60	1.36	0.57	1.42	1.19	1.11	1.53	1.98	1.64
MgO	7.43	5.04	5.91	7.16	5.13	4.94	4.94	3.93	3.83	4.30
CaO	0.48	0.41	0.69	0.41	0.24	0.67	0.91	1.63	1.19	1.23
Total	101.56	100.08	100.71	100.16	99.57	100.94	100.02	100.27	100.78	100.73
Formulae based on 12 oxygens										
Si	2.926	2.955	2.941	2.968	2.957	2.905	2.979	2.946	2.965	2.932
Al	1.956	1.935	1.949	1.942	1.970	1.986	1.931	1.973	1.941	2.002
Fe	2.224	2.435	2.341	2.231	2.396	2.461	2.381	2.408	2.459	2.402
Mg	0.869	0.607	0.702	0.845	0.618	0.590	0.590	0.471	0.460	0.514
Mn	0.080	0.109	0.092	0.038	0.097	0.080	0.076	0.106	0.135	0.112
Ca	0.040	0.035	0.059	0.035	0.020	0.057	0.078	0.140	0.103	0.106
Total	3.213	3.186	3.194	3.149	3.131	3.188	3.125	3.125	3.157	3.134
Alm	69.22	76.43	73.29	70.85	76.53	77.20	76.19	77.06	77.89	76.64
Pyr	27.05	19.05	21.98	26.83	19.74	18.51	18.88	15.07	14.57	16.40
Spes	2.49	3.42	2.88	1.21	3.10	2.51	2.43	3.39	4.28	3.57
Gros	1.24	1.10	1.85	1.11	0.64	1.79	2.50	4.48	3.26	3.38
$\frac{Fe}{(Fe+Mg)}$	.719	.800	.769	.725	.795	.807	.801	.836	.842	.824

Table 25, continued. X43A Garnet Microprobe Analyses.

Alys#	324	325A	325C	325F	326	328A	328B	CR120*	RM105
SiO_2	37.90	38.24	37.81	37.95	36.82	36.62	36.84	36.87	37.35
Al_2O_3	20.98	21.67	21.39	21.79	20.13	21.35	21.37	21.29	21.33
FeO	34.77	30.51	30.16	31.73	35.73	34.28	34.32	33.55	33.51
MnO	1.50	0.56	0.66	0.36	1.51	1.73	1.29	0.90	1.50
MgO	3.54	8.86	9.26	8.72	4.74	4.87	5.13	5.96	5.28
CaO	1.76	0.21	0.20	0.16	0.28	1.46	1.15	0.95	1.84
Total	100.45	100.05	99.48	100.71	99.21	100.31	100.10	99.51	100.81
Formulae based on 12 oxygens									
Si	3.024	2.976	2.961	2.949	2.990	2.931	2.945	2.948	2.958
Al	1.972	1.987	1.974	1.995	1.927	2.014	2.013	2.006	1.990
Fe	2.320	1.985	1.975	2.062	2.427	2.294	2.294	2.243	2.219
Mg	0.421	1.028	1.081	1.010	0.574	0.581	0.611	0.710	0.623
Mn	0.102	0.037	0.044	0.024	0.104	0.117	0.087	0.061	0.101
Ca	0.151	0.017	0.017	0.014	0.024	0.125	0.098	0.082	0.156
Total	2.994	3.067	3.117	3.110	3.129	3.117	3.090	3.096	3.099
Alm	77.49	64.72	63.36	66.30	77.56	73.60	74.24	72.30	71.60
Pyr	14.06	33.52	34.68	32.48	18.34	18.64	19.77	22.89	20.10
Spes	3.41	1.21	1.41	0.77	3.32	3.75	2.82	1.97	3.26
Gros	5.04	0.55	0.55	0.45	0.77	4.01	3.17	2.64	5.03
$\frac{Fe}{(Fe+Mg)}$	.846	.659	.646	.671	.809	.798	.790	.760	.781

* Core and rim analyses from another garnet grain in thin section X43A.

Table 26. X43A Biotite Microprobe Analyses.

Positn	Incl	Incl	Incl	Incl	Incl	Incl	Rim	Rim	Rim	Rim	Rim	Rim
Alys#	1	2	3	4	5	6	7	8	9	10	11	12
SiO_2	38.08	38.20	37.54	37.44	36.58	37.52	35.67	36.08	35.86	36.16	35.39	35.96
TiO_2	2.38	2.37	2.33	2.36	2.36	2.21	3.03	2.53	3.04	3.13	3.14	3.26
Al_2O_3	17.43	17.33	16.83	17.58	18.10	18.05	17.82	17.73	18.01	17.73	17.47	17.35
Cr_2O_3	0.0	0.06	0.04	0.08	0.04	0.08	0.10	0.05	0.04	0.09	0.10	0.09
FeO	13.10	12.76	12.94	12.73	12.69	12.66	20.30	17.48	18.46	19.13	18.30	18.41
MnO	0.03	0.06	0.02	0.01	0.07	0.06	0.08	0.08	0.07	0.08	0.07	0.10
MgO	15.45	15.30	15.01	14.91	14.76	15.23	9.31	11.32	10.54	10.31	10.33	10.24
CaO	0.0	0.0	0.0	0.0	0.0	0.0	0.0	0.0	0.0	0.0	0.0	0.0
Na_2O	0.31	0.41	0.31	0.41	0.38	0.46	0.25	0.23	0.22	0.19	0.21	0.23
K_2O	7.96	8.32	8.19	8.33	8.51	8.34	8.67	8.74	8.80	8.98	8.81	8.73
Total	94.74	94.81	93.21	93.85	93.49	94.61	95.23	94.24	95.04	95.80	93.82	94.37
Formulae based on 11 oxygens												
Si	2.792	2.803	2.806	2.778	2.733	2.761	2.720	2.742	2.716	2.727	2.720	2.743
Al	1.208	1.197	1.194	1.222	1.267	1.239	1.280	1.258	1.284	1.273	1.280	1.257
Al	0.300	0.302	0.290	0.317	0.327	0.327	0.323	0.331	0.324	0.304	0.304	0.304
Ti	0.131	0.131	0.131	0.132	0.132	0.122	0.174	0.144	0.173	0.177	0.181	0.187
Cr									0.002	0.005	0.006	0.006
Fe	0.804	0.784	0.810	0.791	0.793	0.779	1.296	1.112	1.169	1.207	1.177	1.175
Mn	0.002	0.004	0.001	0.001	0.004	0.004	0.005	0.005	0.005	0.005	0.004	0.007
Mg	1.690	1.674	1.673	1.650	1.645	1.671	1.059	1.282	1.191	1.159	1.184	1.165
Total	2.927	2.895	2.905	2.891	2.901	2.903	2.857	2.874	2.864	2.857	2.856	2.844
Ca												
Na	0.044	0.058	0.045	0.059	0.054	0.066	0.037	0.033	0.032	0.028	0.032	0.035
K	0.746	0.779	0.782	0.789	0.811	0.783	0.844	0.848	0.851	0.864	0.864	0.850
Total	0.790	0.837	0.827	0.848	0.865	0.849	0.881	0.881	0.883	0.892	0.896	0.885
$\frac{Fe}{(Fe+Mg)}$	.322	.319	.326	.324	.325	.318	.550	.464	.495	.510	.499	.502
$\frac{K}{(K+Na)}$	.944	.931	.946	.930	.938	.922	.958	.963	.964	.969	.964	.960

Table 26, continued. X43A Biotite Microprobe Analyses.

Positn	Rim	Rim	Rim	Rim	Incl	Rim	Rim	Incl	Incl	Rim	Rim	Rim
Alys#	13	14	15	16	17	18	19	20	21	22	23	24
SiO_2	35.60	36.28	35.50	35.84	38.58	36.02	36.63	36.20	36.41	35.24	35.96	35.90
TiO_2	2.97	2.81	2.75	2.75	1.57	2.67	3.07	2.24	2.50	2.98	2.64	2.43
Al_2O_3	17.47	17.66	18.31	17.93	17.73	17.19	17.31	18.72	18.39	18.39	18.43	18.76
Cr_2O_3	0.09	0.05	0.08	0.07	0.05	0.08	0.09					
FeO	18.27	18.10	17.58	17.46	12.38	18.60	17.79	13.53	13.04	19.46	18.96	19.08
MnO	0.04	0.0	0.03	0.05	0.05	0.08	0.09	0.0	0.18	0.15	0.0	0.0
MgO	10.32	11.12	10.98	11.19	16.66	10.91	11.17	15.13	15.28	11.20	11.40	11.51
CaO	0.0	0.0	0.0	0.0	0.0	0.0	0.0	0.0	0.0	0.0	0.0	0.0
Na_2O	0.22	0.19	0.28	0.17	0.96	0.26	0.26	0.67	0.92	0.0	0.0	0.89
K_2O	8.57	8.43	8.87	8.55	7.01	8.36	8.54	8.19	8.05	8.65	8.75	8.98
Total	93.55	94.64	94.38	94.01	94.97	94.14	94.94	94.69	94.77	96.07	96.14	97.56
Formulae based on 11 oxygens												
Si	2.737	2.745	2.699	2.726	2.800	2.751	2.761	2.680	2.689	2.654	2.693	2.662
Al	1.263	1.255	1.301	1.274	1.200	1.249	1.239	1.320	1.311	1.346	1.307	1.338
Al	0.321	0.321	0.341	0.335	0.318	0.299	0.300	0.313	0.389	0.286	0.319	0.302
Ti	0.172	0.160	0.157	0.158	0.086	0.153	0.174	0.125	0.139	0.169	0.149	0.136
Cr	0.005	0.003	0.003	0.004	0.003	0.005	0.005					
Fe	1.175	1.146	1.118	1.112	0.752	1.189	1.122	0.838	0.805	1.225	1.187	1.183
Mn	0.002		0.002	0.003	0.002	0.003	0.005		0.011	0.010		
Mg	1.183	1.254	1.246	1.269	1.803	1.243	1.255	1.669	1.683	1.257	1.272	1.273
Total	2.858	2.884	2.867	2.881	2.964	2.892	2.861	2.945	3.027	2.947	2.927	2.894
Ca												
Na	0.033	0.028	0.041	0.025	0.135	0.039	0.038	0.097	0.132			0.127
K	0.841	0.814	0.860	0.830	0.649	0.815	0.821	0.773	0.759	0.831	0.836	0.850
Total	0.874	0.842	0.901	0.855	0.784	0.854	0.859	0.870	0.891	0.831	0.836	0.977
$\frac{Fe}{(Fe+Mg)}$	.498	.478	.473	.467	.294	.489	.472	.334	.324	.494	.483	.482
$\frac{K}{(K+Na)}$	.962	.967	.954	.971	.828	.954	.956	.889	.852	1.000	1.000	.870

Table 26, continued. X43A Biotite Microprobe Analyses.

Positn	Rim	Rim	Matr	Rim	Rim	Rim
Alys#	25	26	27	28	29	30
SiO_2	35.87	35.40	36.47	38.40	37.86	36.04
TiO_2	2.90	2.70	2.98	1.63	1.68	2.89
Al_2O_3	18.85	18.20	19.13	18.50	17.83	18.64
Cr_2O_3						
FeO	18.87	19.24	18.39	12.99	12.96	17.24
MnO	0.0	0.0	0.0	0.0	0.0	0.0
MgO	10.89	11.17	11.56	17.28	17.11	11.58
CaO	0.0	0.0	0.0	0.0	0.0	0.0
Na_2O	0.0	0.0	0.0	1.74	1.82	0.0
K_2O	8.65	8.54	8.65	7.01	7.38	8.77
Total	96.14	95.25	97.18	97.55	96.64	95.16

Formulae based on 11 oxygens

Si	2.683	2.681	2.686	2.730	2.729	2.704
Al	1.317	1.319	1.314	1.270	1.271	1.296
Total	4.000	4.000	4.000	4.000	4.000	4.000
Al	0.345	0.306	0.356	0.280	0.344	0.352
Ti	0.163	0.154	0.165	0.087	0.091	0.163
Cr						
Fe	1.187	1.219	1.132	0.772	0.781	1.081
Mn						
Mg	1.215	1.262	1.269	1.831	1.839	1.295
Total	2.910	2.941	2.922	2.970	3.055	2.891
Ca						
Na				0.239	0.254	
K	0.826	0.825	0.813	0.636	0.679	0.839
Total	0.826	0.825	0.813	0.875	0.933	0.839
$\frac{Fe}{(Fe+Mg)}$	.494	.491	.471	.297	.298	.455
$\frac{K}{(K+Na)}$	1.000	1.000	1.000	.727	.728	1.000

Figure 43. Location of microprobe analyses for garnet 160M.

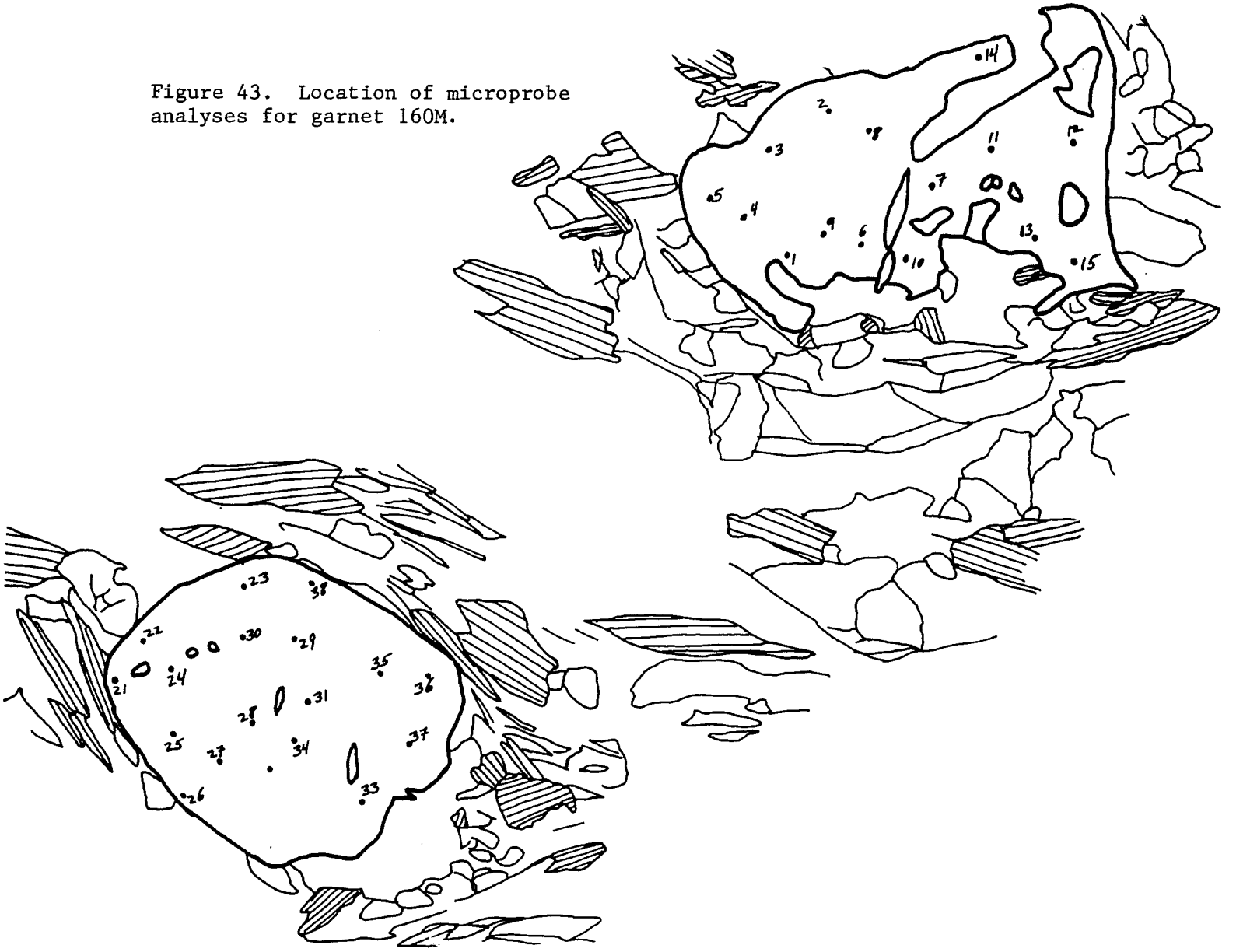

Table 27. M160 Garnet Microprobe Analyses.

Alys#	1	2	3	4	5	6	7	8	9	10
SiO_2	37.78	37.68	37.26	38.18	36.54	37.71	38.08	37.91	37.93	37.56
Al_2O_3	19.66	20.34	20.52	20.25	20.50	20.67	20.33	20.38	20.31	20.09
Fe_2O_3	0.22	0.69	0.71		1.56	0.92				0.03
FeO	37.06	37.05	36.67	37.59	36.15	36.58	37.03	37.06	36.99	37.06
MnO	0.99	0.72	0.63	0.62	0.46	1.40	1.06	0.81	1.23	1.19
MgO	3.15	3.29	3.30	3.30	3.22	3.15	3.15	3.28	3.00	2.88
CaO	1.15	1.07	1.05	1.08	1.02	1.15	1.14	1.16	1.15	1.16
Total	100.01	100.84	100.14	101.02	99.45	101.58	100.79	100.60	100.61	99.97
Formulae based on 12 oxygens										
Si	3.055	3.018	3.003	3.050	2.970	3.001	3.050	3.039	3.047	3.040
Al	1.876	1.922	1.951	1.908	1.965	1.940	1.920	1.927	1.924	1.918
Fe	2.522	2.526	2.516	2.513	2.554	2.492	2.482	2.487	2.486	2.513
Mg	0.380	0.393	0.396	0.393	0.390	0.374	0.377	0.392	0.360	0.348
Mn	0.068	0.049	0.043	0.042	0.032	0.094	0.072	0.055	0.084	0.081
Ca	0.100	0.092	0.090	0.093	0.089	0.098	0.098	0.099	0.099	0.100
Total	3.070	3.060	3.045	3.041	3.065	3.058	3.029	3.033	3.029	3.042
Alm	82.15	82.55	82.63	82.64	83.33	81.49	81.94	82.00	82.07	82.61
Pyr	12.38	12.84	13.00	12.92	12.72	12.23	12.45	12.92	11.89	11.44
Spes	2.21	1.60	1.41	1.38	1.04	3.07	2.38	1.81	2.77	2.66
Gros	3.26	3.01	2.96	3.06	2.90	3.20	3.24	3.26	3.27	3.29
$\frac{Fe}{(Fe+Mg)}$	.869	.865	.864	.865	.868	.870	.868	.864	.874	.878

Table 27, continued. M160 Garnet Microprobe Analyses.

Alys#	11	12	13	14	15	21	22
SiO_2	37.02	38.12	37.19	37.97	37.91	36.68	37.72
Al_2O_3	20.38	20.60	19.88	20.56	20.60	21.02	21.30
Fe_2O_3	0.68		0.33				
FeO	35.88	37.23	37.03	37.53	37.75	38.29	37.59
MgO	3.10	3.20	2.80	3.16	2.95	3.69	3.66
MnO	1.29	0.73	0.94	0.60	0.78	0.32	0.36
CaO	1.19	1.15	1.16	1.05	1.15	0.56	0.52
Total	99.54	101.03	99.33	100.87	101.14	100.56	101.15
Formulae based on 12 oxygens							
Si	3.004	3.044	3.033	3.038	3.030	2.938	3.000
Al	1.950	1.940	1.912	1.940	1.942	1.985	1.997
Fe	2.478	2.488	2.548	2.513	2.525	2.566	2.501
Mg	0.375	0.381	0.340	0.377	0.351	0.441	0.434
Mn	0.089	0.050	0.065	0.041	0.053	0.022	0.024
Ca	0.103	0.098	0.102	0.090	0.099	0.048	0.044
Total	3.045	3.017	3.055	3.021	3.028	3.077	3.003
Alm	81.38	82.47	83.40	83.18	83.39	83.39	83.28
Pyr	12.32	12.63	11.13	12.48	11.59	14.33	14.45
Spes	2.92	1.66	2.13	1.36	1.75	0.71	0.80
Gros	3.38	3.25	3.34	2.98	3.27	1.56	1.47
$\frac{Fe}{(Fe+Mg)}$	.869	.867	.882	.870	.878	.853	.852

Table 27, continued. M160 Garnet Microprobe Analyses.

Alys#	23	24	25	26	27	28	29	30	31	33
SiO_2	37.35	38.09	37.85	37.61	37.58	36.76	38.26	36.47	36.88	36.88
Al_2O_3	20.89	21.38	21.06	21.55	21.43	20.25	21.29	21.09	20.75	20.97
Fe_2O_3						1.6		2.42	2.50	1.09
FeO	37.89	37.50	37.23	37.46	37.53	36.24	37.42	35.38	36.53	37.23
MgO	3.56	3.92	3.77	3.32	3.72	3.64	3.84	4.04	3.67	3.17
MnO	0.23	0.32	0.32	0.43	0.37	0.43	0.24	0.32	0.34	0.42
CaO	0.55	0.57	0.56	0.50	0.61	0.59	0.58	0.52	0.51	0.48
Total	100.47	101.78	100.79	100.87	101.24	99.51	101.63	100.24	101.18	100.12
Formulae based on 12 oxygens										
Si	2.994	3.005	3.018	3.002	2.983	2.982	3.024	2.928	2.947	2.968
Al	1.975	1.989	1.980	2.028	2.006	1.937	1.984	1.998	1.956	1.997
Fe	2.542	2.476	2.484	2.502	2.493	2.558	2.475	2.524	2.593	2.582
Mg	0.426	0.461	0.448	0.395	0.441	0.441	0.453	0.484	0.438	0.382
Mn	0.016	0.022	0.021	0.029	0.025	0.030	0.016	0.022	0.023	0.028
Ca	0.047	0.048	0.048	0.043	0.052	0.051	0.049	0.045	0.044	0.042
Total	3.031	3.007	3.001	2.969	3.011	3.080	2.993	3.075	3.098	3.034
Alm	83.87	82.23	82.77	84.27	82.80	83.05	82.69	82.08	83.70	85.10
Pyr	14.05	15.33	14.93	13.30	14.65	14.32	15.14	15.74	14.14	12.59
Spes	0.53	0.73	0.70	0.98	0.83	0.97	0.53	0.72	0.74	0.92
Gros	1.55	1.60	1.60	1.45	1.73	1.66	1.64	1.46	1.42	1.38
$\frac{Fe}{(Fe+Mg)}$	.856	.843	.847	.864	.850	.853	.845	.839	.855	.871

Table 27, continued. M160 Garnet Microprobe Analyses.

Alys#	34	35	36	37	38
SiO_2	37.57	37.88	37.78	37.13	37.23
Al_2O_3	21.01	21.16	21.61	20.94	21.21
Fe_2O_3	0.67	0.43	0.43	0.84	0.77
FeO	37.50	37.67	37.71	37.26	37.50
MgO	3.48	3.67	3.61	3.43	3.33
MnO	0.42	0.32	0.34	0.39	0.37
CaO	0.60	0.57	0.52	0.48	0.53
Total	101.25	101.70	102.00	100.47	100.94

Formulae based on 12 oxygens

Si	2.993	2.999	2.982	2.983	2.977
Al	1.974	1.976	2.011	1.984	2.000
Fe	2.540	2.522	2.516	2.555	2.555
Mg	0.413	0.433	0.425	0.410	0.397
Mn	0.029	0.022	0.023	0.027	0.025
Ca	0.052	0.048	0.044	0.041	0.046
Total	3.034	3.025	3.008	3.033	3.023
Alm	83.72	83.37	83.64	84.24	84.52
Pyr	13.61	14.31	14.13	13.52	13.13
Spes	0.96	0.73	0.76	0.89	0.83
Gros	1.71	1.59	1.46	1.35	1.52
$\frac{Fe}{(Fe+Mg)}$	.860	.853	.855	.862	.866

Table 28. M160 Muscovite Microprobe Analyses.

Alys#	1	2	3	4	5	6	7	8	9	10	11	12
SiO_2	45.74	47.74	48.87	46.79	46.36	46.68	46.32	46.47	47.04	45.83	46.53	46.23
TiO_2	1.02	1.20	1.05	0.82	1.14	1.18	0.99	0.96	0.94	0.67	0.53	1.01
Al_2O_3	35.53	35.51	33.54	34.15	33.35	33.02	33.90	33.46	34.25	33.17	34.97	33.85
Cr_2O_3				0.0	0.02	0.0	0.01	0.0	0.02	0.01	0.0	0.0
FeO	1.26	1.12	1.27	1.18	1.14	1.17	1.12	1.19	1.45	1.29	1.11	1.18
MnO	0.0	0.05	0.03	0.0	0.0	0.02	0.0	0.01	0.0	0.0	0.0	0.0
MgO	0.70	0.65	0.73	0.57	0.63	0.66	0.84	0.78	0.71	0.62	0.48	0.62
CaO	0.03	0.0	0.0	0.0	0.0	0.0	0.0	0.0	0.0	0.0	0.0	0.0
Na_2O	0.91	0.96	0.97	1.32	1.42	1.24	1.37	1.30	1.34	1.33	1.37	1.30
K_2O	7.94	7.85	7.91	9.06	9.42	9.38	9.42	9.48	9.25	9.29	9.07	9.46
Total	93.13	95.08	94.40	93.89	93.51	93.35	93.97	93.65	95.00	92.21	94.06	93.65
Formulae based on 11 oxygens												
Si	3.070	3.127	3.224	3.136	3.133	3.156	3.113	3.135	3.125	3.140	3.112	3.118
Al	0.930	0.873	0.776	0.864	0.867	0.844	0.887	0.865	0.875	0.860	0.888	0.882
Total	4.000	4.000	4.000	4.000	4.000	4.000	4.000	4.000	4.000	4.000	4.000	4.000
Al	1.880	1.868	1.831	1.835	1.791	1.788	1.801	1.797	1.808	1.820	1.870	1.811
Ti	0.051	0.059	0.052	0.041	0.058	0.060	0.050	0.049	0.047	0.035	0.027	0.051
Cr				0.001				0.001	0.001			
Fe	0.071	0.061	0.070	0.066	0.065	0.066	0.063	0.067	0.080	0.074	0.062	0.066
Mn		0.003	0.002			0.001		0.001				
Mg	0.070	0.063	0.072	0.057	0.063	0.066	0.085	0.079	0.070	0.063	0.048	0.063
Total	2.072	2.054	2.027	1.999	1.978	1.981	1.999	1.993	2.006	1.993	2.007	1.991
Ca												
Na	0.118	0.122	0.124	0.171	0.190	0.163	0.179	0.171	0.173	0.177	0.178	0.170
K	0.680	0.656	0.665	0.775	0.813	0.810	0.808	0.816	0.784	0.812	0.774	0.814
Total	0.798	0.778	0.789	0.946	1.003	0.973	0.987	0.963	0.957	0.989	0.952	0.984
$\frac{Fe}{(Fe+Mg)}$	0.504	0.492	0.493	0.537	0.508	0.500	0.426	0.459	0.533	0.540	0.564	0.512
$\frac{K}{(K+Na)}$	0.852	0.843	0.842	0.819	0.811	0.832	0.819	0.847	0.819	0.821	0.813	0.827

Table 28, continued. M160 Muscovite Microprobe Analyses.

Alys#	13	14	15	16	17	18	19	20	21	22	23	24
SiO_2	45.92	47.46	47.72	47.82	45.13	46.66	46.32	46.90	46.44	46.08	46.02	46.41
TiO_2	0.76	0.74	0.61	0.59	0.53	0.59	0.49	0.48	0.67	0.99	1.09	1.02
Al_2O_3	33.67	34.58	33.46	33.67	33.67	34.70	34.17	34.67	33.99	32.88	33.46	33.63
Cr_2O_3	0.01	0.0	0.0	0.0	0.0	0.0	0.0	0.0	0.0	0.0	0.0	0.01
FeO	1.08	1.03	1.23	1.11	2.36	1.07	1.00	0.97	1.18	1.11	1.25	1.25
MnO	0.0	0.0	0.0	0.0	0.0	0.0	0.02	0.0	0.0	0.02	0.0	0.0
MgO	0.64	0.66	0.88	0.84	0.54	0.58	0.51	0.51	0.62	0.73	0.72	0.68
CaO	0.0	0.0	0.0	0.0	0.0	0.0	0.0	0.0	0.0	0.0	0.0	0.0
Na_2O	1.34	0.91	1.31	1.20	1.45	1.30	1.25	1.49	1.51	1.37	1.32	1.40
K_2O	9.35	8.47	9.44	9.35	8.89	8.86	8.86	9.13	9.17	9.30	9.09	9.45
Total	92.77	93.85	94.65	94.58	92.55	93.76	92.62	94.15	93.58	92.48	92.95	93.85

Formulae based on 11 oxygens

Si	3.124	3.158	3.178	3.180	3.094	3.124	3.139	3.132	3.129	3.146	3.123	3.126
Al	0.876	0.842	0.822	0.820	0.906	0.876	0.861	0.868	0.871	0.854	0.877	0.874
Total	4.000	4.000	4.000	4.000	4.000	4.000	4.000	4.000	4.000	4.000	4.000	4.000
Al	1.826	1.872	1.806	1.821	1.816	1.864	1.870	1.863	1.830	1.794	1.801	1.798
Ti	0.039	0.037	0.031	0.030	0.027	0.030	0.025	0.024	0.034	0.051	0.056	0.052
Cr	0.001											0.001
Fe	0.062	0.057	0.068	0.062	0.135	0.060	0.057	0.054	0.067	0.064	0.071	0.071
Mn							0.001			0.001		
Mg	0.065	0.065	0.087	0.083	0.055	0.058	0.051	0.051	0.062	0.074	0.073	0.068
Total	1.993	2.031	1.992	1.996	2.033	2.012	2.004	1.992	1.993	1.984	2.001	1.989
Ca												
Na	0.177	0.117	0.169	0.155	0.193	0.169	0.165	0.193	0.198	0.181	0.174	
K	0.812	0.719	0.802	0.793	0.776	0.757	0.766	0.778	0.789	0.810	0.788	0.812
Total	0.989	0.836	0.971	0.948	0.969	0.926	0.931	0.971	0.987	0.991	0.962	0.995
Fe/(Fe+Mg)	0.488	0.467	0.439	0.428	0.711	0.508	0.528	0.514	0.519	0.464	0.493	0.511
K/(K+Na)	0.827	0.821	0.860	0.826	0.836	0.801	0.817	0.823	0.801	0.799	0.817	0.819

Table 28, continued. M160 Muscovite Microprobe Analyses.

Alys#	25	26	27	28	29
SiO_2	47.13	47.18	47.82	48.20	48.51
TiO_2	0.68	0.84	0.82	1.06	1.10
Al_2O_3	33.77	34.12	34.29	33.18	33.60
Cr_2O_3	0.0	0.0	0.0	0.01	0.0
FeO	1.28	1.17	1.13	1.05	1.07
MnO	0.03	0.0	0.0	0.02	0.02
MgO	0.74	0.65	0.69	0.73	0.74
CaO	0.0	0.0	0.0	0.0	0.0
Na_2O	1.13	1.21	1.54	1.21	1.36
K_2O	9.49	9.39	9.20	9.13	9.33
Total	94.25	94.56	95.49	94.59	95.73

Formulae based on 11 oxygens

Si	3.154	3.143	3.153	3.200	3.188
Al	0.846	0.857	0.847	0.800	0.812
Total	4.000	4.000	4.000	4.000	4.000
Al	1.819	1.824	1.819	1.798	1.792
Ti	0.034	0.042	0.040	0.053	0.054
Cr					
Fe	0.072	0.065	0.062	0.058	0.059
Mn	0.002			0.001	0.001
Mg	0.074	0.065	0.067	0.073	0.072
Total	2.001	1.996	1.988	1.983	1.978
Ca					
Na	0.147	0.157	0.197	0.156	0.174
K	0.811	0.799	0.775	0.774	0.783
Total	0.958	0.956	0.972	0.930	0.957
$\frac{Fe}{(Fe+Mg)}$	0.493	0.500	0.481	0.443	0.450
$\frac{K}{(K+Na)}$	0.847	0.836	0.797	0.832	0.818

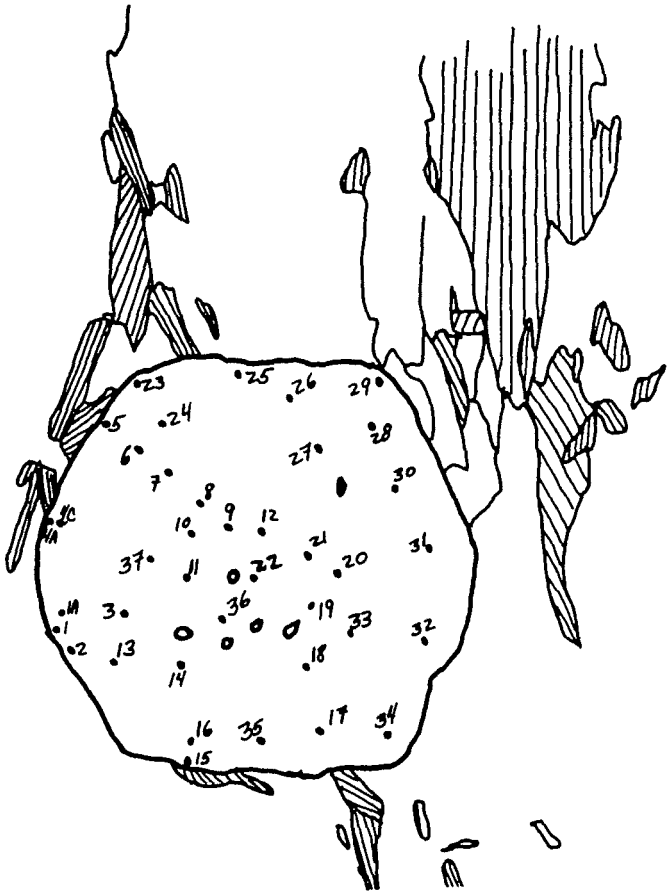

Figure 44. Location of microprobe analyses for garnet Y33.

Table 29. Y33 Garnet Microprobe Analyses.

Alys#	1	1A	2	3	4A	4B	4C	5	6	7
SiO_2	35.79	36.28	36.56	36.41	36.82	36.69	36.69	35.64	35.98	36.76
Al_2O_3	20.39	20.23	20.48	20.92	20.65	20.43	20.40	20.45	20.32	21.36
FeO	38.43	37.83	38.12	36.85	39.49	39.34	39.28	38.73	37.47	37.86
MnO	0.98	0.60	0.60	1.04	0.58	0.75	0.51	0.83	0.74	0.94
MgO	3.08	3.29	3.19	3.89	3.24	3.42	3.59	2.52	3.74	3.78
CaO	0.64	0.53	0.52	0.71	0.50	0.62	0.67	0.70	1.02	0.70
Total	99.31	98.76	99.47	99.82	101.28	101.25	101.14	98.87	99.27	101.64
Formulae based on 12 oxygens										
Si	2.944	2.983	2.984	2.951	2.965	2.959	2.959	2.948	2.947	2.933
Al	1.977	1.961	1.970	1.998	1.960	1.942	1.939	1.994	1.961	2.008
Fe	2.644	2.601	2.602	2.497	2.659	2.653	2.649	2.680	2.566	2.526
Mg	0.378	0.404	0.388	0.470	0.389	0.411	0.432	0.311	0.457	0.450
Mn	0.068	0.042	0.041	0.071	0.040	0.051	0.035	0.058	0.051	0.063
Ca	0.056	0.047	0.046	0.062	0.043	0.053	0.058	0.062	0.089	0.060
Total	3.146	3.094	3.077	3.100	3.131	3.168	3.174	3.111	3.163	3.099
Alm	84.04	84.07	84.56	80.55	84.92	83.74	83.46	86.15	81.13	81.51
Pyr	12.02	13.06	12.61	15.16	12.42	12.97	13.61	10.00	14.44	14.52
Spes	2.16	1.36	1.33	2.29	1.28	1.61	1.10	1.86	1.61	2.03
Gros	1.78	1.52	1.49	2.00	1.37	1.67	1.83	1.99	2.81	1.94
$\frac{Fe}{(Fe+Mg)}$	.875	.866	.870	.842	.872	.866	.860	.896	.849	.849

Table 29, continued. Y33 Garnet Microprobe Analyses.

Alys#	8	9	10	11	12	13	14	15	16	17
SiO_2	36.78	36.58	35.65	36.42	35.80	36.66	36.39	35.75	36.83	36.27
Al_2O_3	20.28	20.39	20.36	21.01	20.43	20.82	21.14	20.54	20.65	20.00
FeO	37.17	36.86	37.40	37.17	35.95	38.02	36.77	39.12	39.29	38.56
MnO	1.33	1.16	0.81	1.13	1.26	0.68	0.84	0.68	0.75	0.77
MgO	3.77	3.61	3.47	3.81	3.65	4.07	3.57	3.18	3.22	3.35
CaO	0.70	0.89	0.81	0.79	1.40	0.82	0.94	0.52	0.57	0.77
Total	100.03	99.49	98.50	100.33	98.49	101.07	99.65	99.79	101.31	99.72
Formulae based on 12 oxygens										
Si	2.982	2.979	2.937	2.942	2.947	2.944	2.952	2.931	2.965	2.968
Al	1.938	1.957	1.977	2.000	1.982	1.971	2.021	1.984	1.959	1.930
Fe	2.520	2.510	2.576	2.511	2.474	2.553	2.494	2.682	2.645	2.639
Mg	0.456	0.438	0.426	0.459	0.447	0.487	0.432	0.388	0.387	0.408
Mn	0.091	0.080	0.056	0.077	0.088	0.046	0.058	0.047	0.051	0.054
Ca	0.061	0.078	0.071	0.069	0.124	0.070	0.082	0.045	0.049	0.067
Total	3.128	3.106	3.129	3.116	3.133	3.156	3.066	3.162	3.132	3.168
Alm	80.56	80.81	82.33	80.58	78.97	80.89	81.34	84.82	84.45	83.30
Pyr	14.58	14.10	13.61	14.73	14.27	15.43	14.09	12.27	12.36	12.88
Spes	2.91	2.58	1.79	2.47	2.81	1.46	1.89	1.49	1.63	1.70
Gros	1.95	2.51	2.27	2.21	3.96	2.22	2.67	1.42	1.56	2.11
$\frac{Fe}{(Fe+Mg)}$	.847	.851	.858	.845	.847	.840	.852	.874	.872	.866

Table 29, continued. Y33 Garnet Microprobe Analyses.

Alys#	18	19	20	21	22	23	24	25	26	27
SiO_2	36.65	36.36	36.49	36.42	37.03	36.48	36.20	35.91	36.70	35.99
Al_2O_3	20.64	20.46	20.65	20.96	20.29	20.13	20.87	21.36	20.32	20.36
FeO	37.15	36.76	36.96	36.93	36.84	39.02	39.06	39.28	37.26	36.51
MnO	1.02	0.98	1.36	1.03	1.11	0.59	0.58	0.67	0.78	1.16
MgO	3.83	3.38	3.69	3.65	3.60	2.96	3.62	3.12	3.56	3.80
CaO	0.60	1.04	0.83	1.08	0.85	0.48	0.91	0.64	0.89	0.94
Total	99.89	98.98	99.98	100.07	99.72	99.66	101.24	100.98	99.51	98.76
Formulae based on 12 oxygens										
Si	2.970	2.976	2.960	2.943	3.003	2.980	2.954	2.905	2.988	2.955
Al	1.972	1.974	1.974	1.996	1.940	1.938	1.911	2.036	1.950	1.970
Fe	2.518	2.516	2.507	2.495	2.498	2.665	2.665	2.657	2.536	2.507
Mg	0.463	0.412	0.447	0.440	0.435	0.361	0.440	0.376	0.432	0.465
Mn	0.070	0.068	0.094	0.070	0.076	0.041	0.040	0.046	0.054	0.080
Ca	0.052	0.091	0.072	0.094	0.074	0.042	0.080	0.055	0.078	0.052
Total	3.103	3.087	3.120	3.099	3.083	3.109	3.225	3.134	3.100	3.134
Alm	81.15	81.50	80.35	80.51	81.02	85.72	82.64	84.78	81.81	79.99
Pyr	14.92	13.35	14.33	14.20	14.11	11.61	13.64	12.00	13.94	14.94
Spes	2.26	2.20	3.01	2.26	2.47	1.32	1.24	1.47	1.74	2.55
Gros	1.68	2.95	2.30	3.03	2.40	1.35	2.48	1.75	2.52	2.62
$\frac{Fe}{(Fe+Mg)}$	.845	.859	.849	.850	.852	.881	.858	.876	.854	.844

Table 29, continued. Y33 Garnet Microprobe Analyses.

Alys#	28	29	30	31	32	33	34	35	36	37
SiO_2	36.42	37.07	36.54	35.92	36.75	36.11	36.33	35.79	35.87	35.79
Al_2O_3	20.75	21.14	20.44	20.94	20.54	20.77	20.44	20.97	20.94	20.63
FeO	37.76	39.12	37.36	36.87	38.61	36.74	39.17	38.68	36.22	37.09
MnO	0.59	0.27	0.65	0.95	0.67	0.95	0.59	0.85	1.08	1.40
MgO	3.68	2.84	3.30	3.05	3.00	3.50	2.89	3.95	3.99	3.25
CaO	0.64	0.72	0.82	0.89	0.76	0.58	0.40	0.64	0.67	0.64
Total	99.84	101.16	99.11	98.62	100.33	98.65	99.82	100.88	98.77	98.80
Formulae based on 12 oxygens										
Si	2.952	2.971	2.987	2.953	2.980	2.962	2.970	2.896	2.936	2.946
Al	1.983	1.996	1.969	2.029	1.964	2.008	1.969	1.999	2.020	2.001
Fe	2.560	2.621	2.554	2.534	2.618	2.520	2.678	2.617	2.479	2.553
Mg	0.445	0.339	0.402	0.373	0.363	0.428	0.352	0.477	0.487	0.399
Mn	0.040	0.018	0.045	0.066	0.046	0.066	0.041	0.058	0.075	0.098
Ca	0.056	0.062	0.072	0.078	0.066	0.051	0.035	0.056	0.058	0.056
Total	3.101	3.040	3.073	3.051	3.093	3.065	3.106	3.208	3.099	3.106
Alm	82.55	86.22	83.11	83.05	84.64	82.22	86.22	81.58	79.99	82.20
Pyr	14.35	11.15	13.08	12.23	11.74	13.96	11.33	14.87	15.71	12.85
Spes	1.29	0.59	1.46	2.16	1.49	2.15	1.32	1.81	2.42	3.16
Gros	1.81	2.04	2.34	2.56	2.13	1.66	1.13	1.75	1.87	1.80
$\frac{Fe}{(Fe+Mg)}$	.852	.885	.864	.872	.878	.855	.884	.846	.836	.865

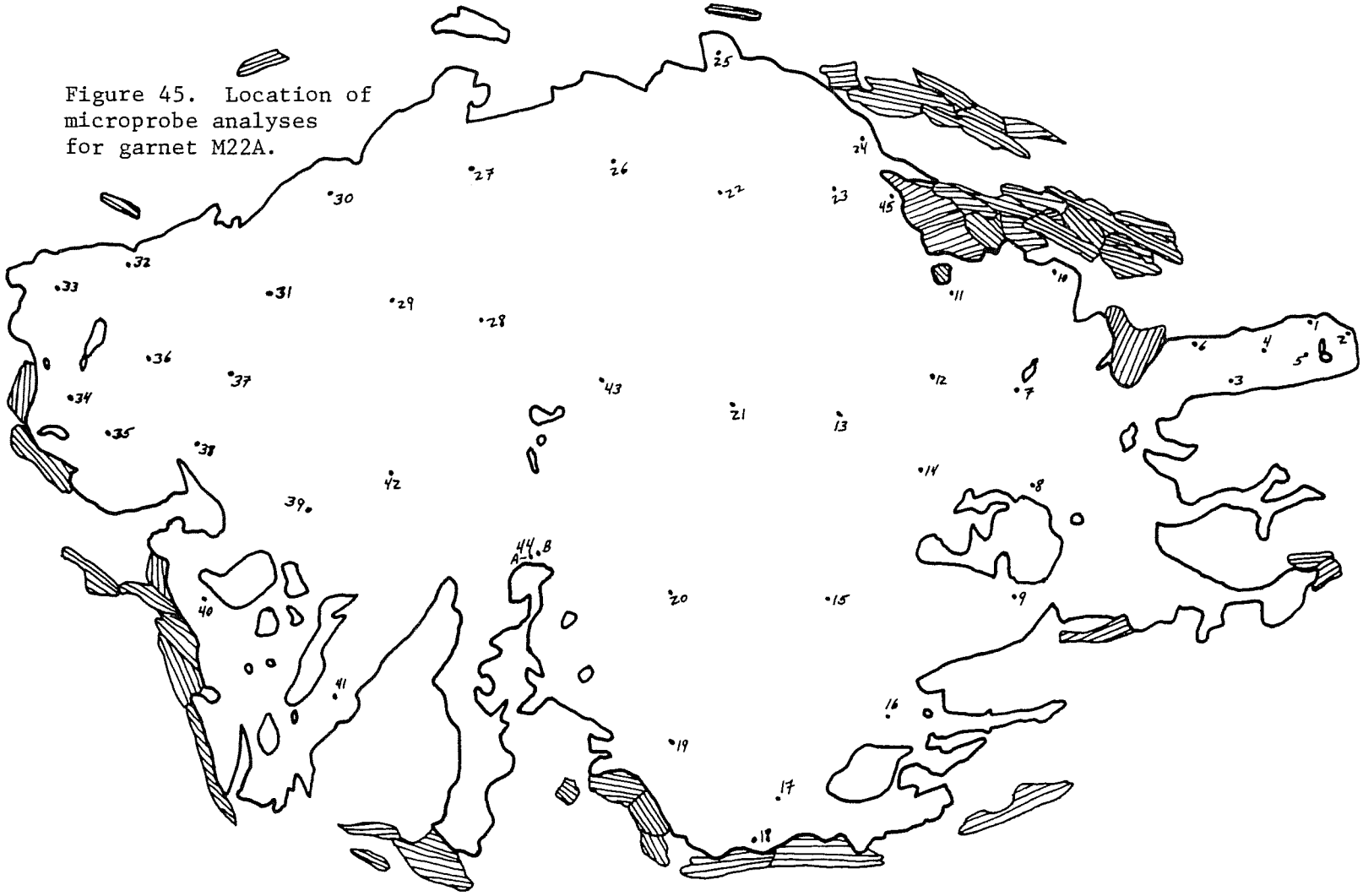

Figure 45. Location of microprobe analyses for garnet M22A.

Table 30. M22A Garnet Microprobe Analyses.

Alys#	1	2	3	4	5	6	7	9	10	11
SiO_2	36.85	36.87	37.32	37.81	37.58	37.18	36.84	37.95	37.11	37.27
Al_2O_3	20.89	21.18	21.53	21.55	21.15	21.58	21.12	21.71	21.51	20.67
FeO	33.37	35.42	31.65	32.31	32.22	31.82	31.65	31.76	35.26	35.67
MnO	0.42	0.35	0.00	0.26	0.27	0.00	0.00	0.32	0.00	0.00
MgO	5.26	4.36	7.59	7.85	5.96	7.54	8.66	7.89	5.16	4.94
CaO	2.20	1.90	1.83	1.37	2.13	1.76	1.43	1.17	2.46	1.40
Total	98.99	100.08	99.92	101.15	99.31	99.88	99.70	100.80	101.50	99.95
Formulae based on 12 oxygens										
Si	2.966	2.957	2.954	2.944	2.989	2.931	2.910	2.949	2.928	2.986
Al	1.981	2.002	1.987	1.977	1.982	2.005	1.966	1.988	2.001	1.952
Fe	2.246	2.376	2.073	2.104	2.142	2.097	2.091	2.064	2.327	2.390
Mg	0.632	0.521	0.886	0.912	0.707	0.886	1.020	0.914	0.608	0.590
Mn	0.029	0.024		0.017	0.018			0.021		
Ca	0.190	0.164	0.154	0.114	0.182	0.148	0.121	0.098	0.208	0.120
Total	3.097	3.085	3.113	3.147	3.049	3.131	3.232	3.097	3.143	3.100
Alm	72.52	77.02	66.59	66.86	70.25	66.98	64.70	66.65	74.04	77.10
Pyr	20.41	16.89	28.46	28.98	23.19	28.30	31.56	29.51	19.34	19.03
Spes	0.94	0.78		0.54	0.59			0.68		
Gros	6.13	5.32	4.95	3.62	5.97	4.73	3.74	3.16	6.62	3.87
$\frac{Fe}{(Fe+Mg)}$	.780	.820	.701	.698	.752	.703	.672	.693	.793	.802

Table 30, continued. M22A Garnet Microprobe Analyses.

Alys#	12	13	14	15	16	17	18	19	20	21
SiO_2	37.60	37.65	37.70	37.34	37.85	37.30	36.86	37.84	37.43	37.38
Al_2O_3	21.75	21.21	21.54	21.98	21.33	21.15	21.57	20.92	21.67	21.95
FeO	31.73	31.15	31.47	30.89	31.21	30.95	34.52	30.95	31.40	30.62
MnO	0.51	0.42	0.30	0.52	0.00	0.22	0.38	0.23	0.00	0.00
MgO	7.99	8.10	8.65	8.54	8.19	7.97	6.85	8.37	8.12	8.50
CaO	1.31	1.35	1.28	1.44	1.34	1.27	1.22	1.29	1.49	1.58
Total	100.89	99.88	100.94	100.71	99.92	98.86	101.40	99.60	100.11	100.03
Formulae based on 12 oxygens										
Si	2.931	2.959	2.928	2.908	2.966	2.953	2.899	2.975	2.933	2.921
Al	1.998	1.964	1.972	2.017	1.969	1.973	2.000	1.939	2.002	2.022
Fe	2.068	2.046	2.043	2.012	2.045	2.049	2.271	2.035	2.058	2.001
Mg	0.929	0.949	1.002	0.992	0.957	0.941	0.803	0.982	0.949	0.991
Mn	0.034	0.028	0.020	0.034		0.014	0.025	0.015		
Ca	0.110	0.113	0.106	0.121	0.113	0.107	0.103	0.108	0.125	0.132
Total	3.141	3.136	3.171	3.159	3.115	3.111	3.202	3.140	3.132	3.124
Alm	65.84	65.24	64.43	63.69	65.65	65.86	70.92	64.81	65.71	64.05
Pyr	29.58	30.26	31.60	31.40	30.72	30.25	25.08	31.27	30.30	31.72
Spes	1.08	0.89	0.63	1.08		0.45	0.78	0.48		
Gros	3.50	3.60	3.34	3.83	3.63	3.44	3.22	3.44	3.99	4.23
$\frac{Fe}{(Fe+Mg)}$	.690	.683	.671	.670	.681	.685	.739	.675	.684	.669

Table 30, continued. M22A Garnet Microprobe Analyses.

Alys#	22	23	24	25	26	27	28	29	30	31
SiO_2	37.18	37.06	37.04	36.68	36.71	37.23	37.35	37.52	37.22	37.83
Al_2O_3	21.47	20.84	21.53	20.92	21.29	21.81	21.82	21.52	21.69	21.52
FeO	31.04	32.05	35.02	34.50	30.80	31.51	31.21	31.27	30.71	30.71
MnO	0.26	0.37	0.00	0.00	0.00	0.00	0.00	0.19	0.00	0.34
MgO	7.92	7.69	5.96	6.35	8.61	8.21	7.98	8.81	8.53	8.00
CaO	1.48	1.29	1.22	1.31	1.55	1.27	1.27	1.53	1.52	1.31
Total	99.35	99.30	100.77	99.76	98.96	100.03	99.63	100.84	99.67	99.71
Formulae based on 12 oxygens										
Si	2.938	2.947	2.931	2.934	2.912	2.917	2.937	2.921	2.915	2.967
Al	1.999	1.953	2.008	1.971	1.990	2.014	2.022	1.974	2.003	1.989
Fe	2.051	2.131	2.318	2.307	2.043	2.064	2.052	2.035	2.012	2.014
Mg	0.933	0.911	0.704	0.757	1.018	0.959	0.936	1.022	0.996	0.935
Mn	0.017	0.025						0.012		0.023
Ca	0.126	0.110	0.104	0.112	0.131	0.106	0.107	0.128	0.128	0.110
Total	3.127	3.177	3.126	3.176	3.192	3.129	3.095	3.197	3.136	3.082
Alm	65.59	67.08	74.15	72.64	64.00	65.96	66.30	63.65	64.16	65.35
Pyr	29.84	28.67	22.52	23.84	31.89	30.65	30.24	31.97	31.76	30.34
Spes	0.54	0.79						0.38		0.75
Gros	4.03	3.46	3.33	3.53	4.10	3.39	3.46	4.00	4.08	3.57
$\frac{Fe}{(Fe+Mg)}$	.687	.701	.767	.753	.667	.683	.687	.666	.669	.683

Table 30, continued. M22A Garnet Microprobe Analyses.

Alys#	32	33	34	35	36	37	38	39	40	41
SiO_2	37.70	37.70	37.18	37.19	37.36	37.50	37.22	38.28	36.53	38.14
Al_2O_3	20.59	20.77	21.40	21.42	21.54	21.22	21.09	21.33	21.22	21.36
FeO	30.82	32.18	31.48	31.73	31.55	30.35	30.31	30.27	32.99	30.64
MnO	0.0	0.0	0.0	0.0	0.0	0.34	0.68	0.69	0.00	0.16
MgO	7.39	7.19	7.32	7.72	7.58	7.85	8.38	8.67	6.73	8.31
CaO	1.57	1.10	1.42	1.30	1.31	1.55	1.22	1.48	1.24	1.24
Total	98.07	99.94	98.80	99.36	99.34	98.81	98.90	100.72	98.71	99.85
Formulae based on 12 oxygens										
Si	3.011	2.963	2.956	2.942	2.952	2.969	2.949	2.970	2.932	2.982
Al	1.937	2.016	2.005	1.997	2.005	1.980	1.969	1.950	2.007	1.967
Fe	2.058	2.115	2.092	2.099	2.084	2.009	2.009	1.963	2.214	2.003
Mg	0.880	0.843	0.868	0.910	0.892	0.927	0.990	1.002	0.805	0.968
Mn						0.023	0.046	0.045		0.011
Ca	0.134	0.092	0.121	0.110	0.111	0.132	0.103	0.123	0.106	0.104
Total	3.072	3.050	3.081	3.119	3.087	3.091	3.148	3.133	3.125	3.086
Alm	66.99	69.34	67.90	67.30	67.51	65.00	63.82	62.66	70.85	64.91
Pyr	28.65	27.64	28.17	29.18	28.90	29.99	31.45	31.98	25.76	31.37
Spes						0.74	1.46	1.44		0.36
Gros	4.36	3.02	3.93	3.53	3.60	4.27	3.27	3.93	3.39	3.37
$\frac{Fe}{(Fe+Mg)}$	.700	.715	.707	.698	.700	.684	.670	.662	.733	.674

Table 30, continued. M22A Garnet Microprobe Analyses.

Alys#	42	43	44A	44B	45
SiO_2	37.37	37.19	37.25	37.28	37.11
Al_2O_3	21.75	21.24	21.02	21.49	20.94
FeO	29.99	30.45	30.67	30.16	36.98
MnO	0.0	0.21	0.39	0.25	0.22
MgO	7.94	8.29	7.95	7.69	4.01
CaO	1.56	1.38	1.41	1.20	1.89
Total	98.61	98.76	98.69	98.07	101.15
Formulae based on 12 oxygens					
Si	2.954	2.948	2.961	2.968	2.962
Al	2.027	1.984	1.968	2.016	1.970
Fe	1.983	2.018	2.038	2.008	2.468
Mg	0.935	0.979	0.941	0.913	0.477
Mn		0.014	0.026	0.017	0.015
Ca	0.132	0.117	0.120	0.103	0.162
Total	3.050	3.128	3.125	3.041	3.122
Alm	65.02	64.51	65.22	66.03	79.05
Pyr	30.66	31.30	30.11	30.02	15.28
Spes		0.45	0.83	0.56	0.48
Gros	4.33	3.74	3.84	3.39	5.19
$\frac{Fe}{(Fe+Mg)}$	.680	.673	.684	.687	.838

Figure 46. Location of microprobe analyses for garnet M21.

Table 31. M21 Garnet Microprobe Analyses.

Alys#	1	2	3	4	5	6	7	8	9	10
SiO_2	35.85	37.29	36.52	37.28	37.23	36.30	37.08	35.53	36.60	36.77
TiO_2	0.0	0.0	0.0	0.0	0.0	0.0	0.0	0.02	0.0	0.0
Al_2O_3	20.84	21.12	21.47	21.28	20.96	20.99	21.10	20.97	21.14	21.08
FeO	33.28	33.61	37.34	35.52	36.89	35.10	34.86	38.18	38.04	38.47
MnO	6.04	5.12	2.47	3.94	3.42	4.92	4.36	1.23	1.19	1.24
MgO	1.13	1.12	1.26	1.28	1.40	1.09	1.02	1.11	1.19	1.32
CaO	3.03	3.01	2.48	2.76	2.43	2.48	2.58	2.73	2.66	2.52
Total	100.17	101.27	101.54	102.06	102.33	100.88	101.00	99.77	100.82	101.40
Formulae based on 12 oxygens										
Si	2.937	2.997	2.943	2.980	2.978	2.952	2.994	2.925	2.966	2.966
Al	2.014	2.002	2.041	2.006	1.978	2.013	2.009	2.036	2.020	2.006
Ti								0.001		
Fe	2.281	2.260	2.518	2.376	2.469	2.389	2.355	2.631	2.580	2.597
Mg	0.138	0.134	0.152	0.152	0.167	0.132	0.123	0.136	0.143	0.159
Mn	0.420	0.349	0.168	0.267	0.232	0.339	0.298	0.086	0.082	0.085
Ca	0.266	0.259	0.214	0.237	0.208	0.216	0.223	0.241	0.231	0.218
Total	3.105	3.002	3.052	3.032	3.076	3.076	2.999	3.095	3.036	3.059
Alm	73.46	75.28	82.50	78.36	80.27	77.67	78.53	85.04	84.98	84.90
Pyr	4.44	4.46	4.98	5.01	5.43	4.29	4.10	4.40	4.71	5.20
Spes	13.53	11.63	5.50	8.81	7.54	11.02	9.94	2.78	2.70	2.78
Gros	8.57	8.63	7.01	7.82	6.76	7.02	7.44	7.79	7.61	7.13
$\frac{Fe}{(Fe+Mg)}$	.943	.944	.943	.940	.937	.948	.950	.951	.947	.942

Table 31, continued. M21 Garnet Microprobe Analyses.

Alys#	11	12	13	14	15	16	17	18	19	20
SiO_2	37.88	37.58	36.61	37.41	36.16	35.08	36.55	37.64	35.51	36.09
TiO_2	0.0	0.0	0.0	0.0	0.0	0.0	0.02	0.0	0.0	0.01
Al_2O_3	20.86	20.32	21.45	20.93	21.37	21.49	20.86	21.00	21.20	21.47
FeO	33.39	35.57	33.27	34.07	34.72	33.63	38.29	38.69	38.14	38.57
MnO	5.83	3.94	5.90	4.95	4.31	5.37	1.37	1.25	1.90	1.18
MgO	1.09	1.43	0.95	1.20	1.26	1.00	1.00	1.18	1.30	1.36
CaO	2.74	2.64	3.19	2.97	2.90	2.97	3.02	2.65	2.25	2.42
Total	101.79	101.48	101.37	101.53	100.72	99.54	101.11	102.41	100.30	101.10
Formulae based on 12 oxygens										
Si	3.029	3.023	2.952	3.002	2.936	2.892	2.964	3.002	2.911	2.925
Al	1.967	1.928	2.039	1.981	2.046	2.089	1.995	1.976	2.049	2.052
Ti							0.001			0.001
Fe	2.234	2.394	2.244	2.288	2.359	2.321	2.599	2.582	2.616	2.615
Mg	0.130	0.172	0.115	0.143	0.153	0.123	0.121	0.140	0.158	0.164
Mn	0.395	0.269	0.403	0.337	0.296	0.376	0.094	0.084	0.132	0.081
Ca	0.235	0.227	0.276	0.256	0.252	0.263	0.263	0.226	0.197	0.210
Total	2.994	3.062	3.038	3.024	3.060	3.083	3.078	3.032	3.103	3.071
Alm	74.62	78.18	73.86	75.66	77.09	75.28	84.47	85.16	84.31	85.18
Pyr	4.34	5.62	3.79	4.73	5.00	3.99	3.93	4.62	5.09	5.34
Spes	13.19	8.79	13.27	11.14	9.67	12.20	3.05	2.77	4.25	2.64
Gros	7.85	7.41	9.08	8.47	8.24	8.53	8.55	7.45	6.35	6.84
$\frac{Fe}{(Fe+Mg)}$	.945	.933	.951	.941	.939	.950	.956	.949	.943	.941

Table 31, continued. M21 Garnet Microprobe Analyses.

Alys#	21	22	23	24	25	26	27	28	29	30
SiO_2	35.23	35.33	37.77	35.26	36.97	36.07	37.05	37.91	38.03	37.59
TiO_2	0.0	0.0	0.0	0.0	0.0	0.0	0.0	0.0	0.0	0.0
Al_2O_3	21.00	20.67	21.58	21.48	21.16	21.15	21.04	20.79	21.10	20.90
FeO	37.30	35.15	33.05	34.87	36.88	37.83	36.33	32.81	35.79	35.23
MnO	1.54	3.44	6.17	4.41	1.97	1.92	2.07	5.97	4.10	3.95
MgO	1.13	1.24	0.93	1.06	1.24	0.90	1.33	1.01	1.26	1.22
CaO	3.10	2.97	2.94	3.02	2.94	3.11	2.96	2.94	2.50	2.90
Total	99.30	98.80	102.44	100.10	101.16	100.98	100.78	101.43	102.78	101.79
Formulae based on 12 oxygens										
Si	2.913	2.932	2.999	2.893	2.979	2.934	2.992	3.037	3.015	3.009
Al	2.047	2.023	2.020	2.079	2.011	2.029	2.003	1.965	1.972	1.973
Ti										
Fe	2.580	2.441	2.196	2.394	2.487	2.576	2.455	2.200	2.374	2.360
Mg	0.140	0.154	0.110	0.130	0.149	0.109	0.160	0.120	0.149	0.145
Mn	0.108	0.242	0.415	0.307	0.135	0.132	0.142	0.253	0.213	0.249
Ca	0.274	0.264	0.250	0.266	0.254	0.271	0.256	0.253	0.213	0.249
Total	3.102	3.101	2.971	3.097	3.025	3.088	3.013	2.826	2.949	3.003
Alm	83.17	78.72	73.91	77.30	82.21	83.42	81.48	73.88	78.82	78.09
Pyr	4.51	4.97	3.70	4.20	4.93	3.53	5.31	4.03	4.95	4.80
Spes	3.48	7.80	13.97	9.91	4.46	4.27	4.71	13.60	9.16	8.87
Gros	8.83	8.51	8.41	8.59	8.40	8.78	8.50	8.50	7.07	8.24
$\frac{Fe}{(Fe+Mg)}$	.949	.941	.952	.948	.943	.949	.939	.948	.941	.942

Table 31, continued. M21 Garnet Microprobe Analyses.

Alys#	31	32	33	34	35	36
SiO_2	36.79	36.80	35.99	37.04	35.56	37.33
TiO_2	0.0	0.0	0.01	0.0	0.0	0.0
Al_2O_3	21.25	21.43	20.73	20.99	20.84	21.07
FeO	37.52	37.85	38.42	37.73	38.24	37.66
MnO	1.60	1.29	1.38	1.28	1.09	1.67
MgO	1.24	1.14	1.00	1.03	0.95	1.21
CaO	2.88	3.24	3.17	3.28	3.17	2.95
Total	101.28	101.75	100.70	101.35	99.85	101.89
Formulae based on 12 oxygens						
Si	2.965	2.955	2.940	2.985	2.929	2.999
Al	2.020	2.030	1.998	1.995	2.024	1.990
Ti			0.001			
Fe	2.531	2.543	2.627	2.545	2.635	2.524
Mg	0.149	0.136	0.122	0.124	0.117	0.145
Mn	0.110	0.088	0.095	0.087	0.076	0.113
Ca	0.249	0.279	0.278	0.283	0.280	0.253
Total	3.039	3.046	3.123	3.039	3.108	3.035
Alm	83.28	83.49	84.14	83.74	84.78	83.16
Pyr	4.90	4.46	3.91	4.08	3.76	4.78
Spes	3.62	2.89	3.04	2.86	2.45	3.72
Gros	8.19	9.16	8.90	9.31	9.01	8.34
$\frac{Fe}{(Fe+Mg)}$	.944	.949	.956	.954	.957	.946